

Piperine biosynthesis in black pepper (*Piper nigrum* L.)

Dissertation

zur Erlangung des akademischen Grades
Doctor rerum naturalium (Dr. rer. nat.)

vorgelegt der
Naturwissenschaftlichen Fakultät I (Biowissenschaften)
der Martin-Luther-Universität Halle-Wittenberg



von Arianne Schnabel
geboren am 22.10.1987 in Dresden

Erstgutachter: PD Dr. Thomas Vogt
Zweitgutachter: Prof. Dr. Milton T. Stubbs II
Drittgutachter: Prof. Dr. Dietrich Ober

Eingereicht am: 30.6.2021
Verteidigung am: 15.11.2021

Table of contents

TABLE OF CONTENTS	1
LIST OF FIGURES	4
LIST OF TABLES	7
LIST OF ABBREVIATIONS	8
1 INTRODUCTION	9
1.1 King of spices - a history on trade and power for pungency	9
1.2 <i>Piper nigrum</i> - the black pepper plant	11
1.3 The flavor of black pepper	14
1.4 The power of piperine and piperamides as bioactive compounds	16
1.5 Piperine synthesis and biosynthesis	17
1.6 Key enzymatic steps of the phenylpropanoid part of piperine biosynthesis	19
1.6.1 CoA ligases.....	19
1.6.2 Acyltransferases	20
1.6.3 Formation of the methylenedioxy group	21
1.7 Aim of this investigation	23
2 MATERIALS AND METHODS	24
2.1 Plant material	24
2.2 Chemicals and substrates	24
2.3 Molecular biology methods	25
2.3.1 RNA isolation and cDNA synthesis	25
2.3.2 RNA-sequencing and data processing	25
2.3.3 RT-qPCR analysis	26
2.3.4 Cloning.....	26
2.4 Biochemical methods	29
2.4.1 Preparation of methanolic extracts from black pepper tissues.....	29
2.4.2 Transient gene expression	29
2.4.3 SDS-PAGE and immunoblotting.....	30

Table of contents

2.4.4	Recombinant protein purification	31
2.4.5	Crystallization	31
2.4.6	Protein preparation of black pepper material	32
2.5	Enzyme activity measurements	33
2.5.1	Extraction of microsomes and following <i>in vitro</i> assays	33
2.5.2	Determination of enzyme activity in transient yeast cell assays	33
2.5.3	Activity measurements of CoA ligases	34
2.5.4	Production of CoA esters on a semi preparative scale	34
2.5.5	Activity measurements of piperine synthase and piperamide synthase	34
2.5.6	Feeding experiments	35
2.6	Analytical methods	35
2.6.1	Spectroscopy	35
2.6.2	High pressure liquid chromatography	35
3	RESULTS	37
3.1	Identification of piperine biosynthetic genes	37
3.1.1	Piperine content in different plant tissues and during fruit development	37
3.1.2	<i>De Novo</i> Assembly of the Black Pepper Transcriptome	38
3.1.3	Identification of candidate genes	40
3.2	Formation of methylenedioxy bridge by CYP719A37	42
3.2.1	Cloning and expression of PnCYP719 and PnCPR	42
3.2.2	PnCYP719 is substrate specific	43
3.2.3	Phylogeny and structural aspects of CYP719A37 and PnCPR	46
3.3	Piperoyl-CoA formation is catalyzed by specific CoA ligase from black pepper fruits ...	49
3.3.1	Piperoyl CoA - synthesis and biosynthesis	49
3.3.2	Functional expression and purification of the enzymes	51
3.3.3	Enzyme activity and substrate specificity of piperoyl-CoA ligase	52
3.4	Piperine biosynthesis by BAHDs	56
3.4.1	Identification, cloning and expression of two putative candidates	56
3.4.1	Purification of recombinant BAHDs	56
3.4.2	Enzyme activity – piperine formation	59
3.4.3	Enzyme activity – substrate specificity	61
3.5	Crystallization	63
3.6	<i>In vivo</i> fermentation of piperine and piperiline	64
3.7	Transcript level of biosynthetic enzymes in piperine biosynthesis	66

3.8	Piperine synthase localization in black pepper fruits.....	67
4	DISCUSSION AND OUTLOOK.....	71
4.1	RNA sequencing and co-expression analysis of the transcriptom data	71
4.2	The activation of piperic acid	74
4.3	Piperine synthase versus Piperamide synthase	75
4.4	methylenedioxy bridges in piperamide sceleton	77
4.5	Additional enzymes involved in piperine biosynthesis	80
4.5.1	Chain elongation – a linkage to fatty acid biosynthesis or flavanol biosynthesis	80
4.5.2	Piperidine biosynthesis	83
4.6	Localization of piperine biosynthesis in black pepper fruits.....	83
5	SUMMARY	88
6	ZUSAMMENFASSUNG	89
7	REFERENCES.....	91
8	APPENDIX	107
9	DANKSAGUNG.....	128
10	EIDESSTÄTTLICHE ERKLÄRUNG	130
11	CURRICULUM VITAE	131

List of Figures

Figure 1-1: Piperine, the pungent principle of black pepper and related "Kunstpfeffer" substances	10
Figure 1-2: The black pepper plant (<i>Piper nigrum</i>).....	11
Figure 1-3: Angiosperm phylogeny with available plant transcriptome and genome datasets	12
Figure 1-4: Different pepper varieties used in traditional cuisine	15
Figure 1-5: The piperamides (Z)-piplartine and 3-chlorosintenpyridone 1 show antifilarial properties .	16
Figure 1-6: Hypothetical biosynthesis of piperine in black pepper	17
Figure 1-7: Different natural products with a piperidine heterocycle and suggested "chiral" model for piperidine biosynthesis	18
Figure 1-8: Specialized metabolites with the methylenedioxy bridge structure element.....	22
Figure 3-1: Detection of piperine and related amides in different black pepper tissues	37
Figure 3-2: Piperine accumulation during fruit development.....	38
Figure 3-3: Quality check of RNA samples for RNA sequencing	39
Figure 3-4: Heatmap of the top 3000 differentially expressed genes, clusters of their biological function and related plant organs.....	40
Figure 3-5: Graphical representation of high abundance transcripts	41
Figure 3-6: Verification of PnCYP719 (1543 bp) and PnCPR (2121 bp) at different levels of Golden Gate cloning (GGC).....	42
Figure 3-7: Putative precursor for methylenedioxy bridge formation in piperine heterocycle	43
Figure 3-8: PnCYP719 catalyzes the methylenedioxy bridge formation within the aromatic part of the piperine molecule.	44
Figure 3-9: Bootstrapped, unrooted cladogram of CYP71 clan families CYP719, CYP77, CYP81 and CYP80 protein sequences obtained using ClustalW.....	46
Figure 3-10: Comparison of amino acid sequences of CYP719As and CYP77As with CYP719A37 ...	48
Figure 3-11: Verification of Piperoyl-CoA ligase and At4CL6 in expression vectors	49
Figure 3-12: Bootstrapped, unrooted cladogram of 4CL and 4CL-like protein sequences obtained using ClustalW.	50
Figure 3-13: Preparation of recombinant piperoyl-CoA ligase (A) and At4CL6 (B) with IMAC	51
Figure 3-14: Photometric measurements of piperoyl-CoA ligase, At4CL6, and At4CL2 activities incubated with different substrates.....	52
Figure 3-15: Identification of piperoyl-CoA and piperic acid by HPLC-UV-ESI-MS	53
Figure 3-16: Identification of piperoyl-CoA and piperic acid by thin layer chromatography	55
Figure 3-17: Verification on BAHD1 and BAHD2 during the cloning procedure	56
Figure 3-18: Preparation of recombinant piperine synthase by IMAC and SEC.....	57
Figure 3-19: Preparation of recombinant piperamide synthase by IMAC and SEC.....	58
Figure 3-20: Analysis of enzyme activity of recombinant and native piperine synthase by HPLC-UV-ESI-MS.	59
Figure 3-21: Isomerisation during piperine synthesis by piperamide synthase	60
Figure 3-22: Metabolic grid of different amides produced by piperine synthase (blue) and piperamide synthase (red).....	62

Figure 3-23: Crystallization of piperamide synthase	63
Figure 3-24: Reaction cascade for the biosynthesis of piperine and piperiline.....	64
Figure 3-25: Analysis of <i>E. coli</i> extracts after feeding piperic acid and piperidine (A) or pyrrolidine (B)	65
Figure 3-26: Organ-specific relative transcript levels of enzymes involved in piperine biosynthesis compared to RNA sequencing results and piperine content.....	66
Figure 3-27: Detection of piperine synthase (PS) and piperamide synthase (PAS) in different black pepper tissues by immunoblotting	67
Figure 3-28: The formation of piperine and 1-piperoylbenzylamide were chosen to determine the activity of piperine and piperamide synthase in black pepper fruits	69
Figure 3-29: Verification of piperine and piperamide synthase in black pepper fruits by activity measurements and immunoblotting.	70
Figure 4-1: Coexpression of annotated genes involved in flavonoid- and fatty acid biosynthesis.....	73
Figure 4-2: Bootstrapped, unrooted cladogram of BAHD protein sequences obtained using ClustalW.	76
Figure 4-3: Piperamides from black pepper.	77
Figure 4-4: Hypothetical pathway of hinokinin and the structure of homolog compounds from black pepper.....	79
Figure 4-5: Enzymes catalyzing chain elongation reactions in plant species	80
Figure 4-6: Different flavonoids and the inversion of benzophenone synthase to a phenylpyrone synthase	82
Figure 4-7: Cross section of a black pepper fruit.....	83
Figure 4-8: Piperine localisation in black pepper fruits.....	84
Figure 4-9: Piperine biosynthesis in black pepper fruits.....	87
Figure 8-1: Structure of piperine and its stereoisomers, isopiperine, chavicine and isochavicine	107
Figure 8-2: The phenylpropanoid biosynthesis and specialized phenylpropanoids of different pathways	108
Figure 8-3: Overview of ANL superfamily members and their possible reactions	109
Figure 8-4: The protein structure of vinorine synthase.....	110
Figure 8-5: RNA integrity determination of RNA preparations	111
Figure 8-6: Golden Gate cloning - entry of PnCYP719 in level 0.....	112
Figure 8-7: Golden Gate cloning - the entry of PnCPR in level 0.....	113
Figure 8-8: Golden Gate cloning - combining PnCYP719 or PnCPR with a galactose inducible promoter and the PGK terminator in level 1.....	114
Figure 8-9: Golden Gate cloning - combining of the expression cassettes of PnCPR (A) or ATR (B) with PnCYP719 in expression level M	115
Figure 8-10: Verification of PnCPR in different vector levels of Golden Gate cloning	116
Figure 8-11: Putative substrates for CYP719A37	117
Figure 8-12: HPLC-analysis of microsomal fraction- and yeast cell assays with C6-C2 substrates...	118
Figure 8-13: HPLC-analysis of microsomal fraction- and yeast cell assays with C6-C1 substrates...	119
Figure 8-14: Detoxification mechanisms in the yeast <i>S. cerevisiae</i>	120

List of Figures

Figure 8-15: Amino acid sequence alignment of PnCPR with ATR1 and ATR2.....	121
Figure 8-16: Preparation of recombinant piperoyl-CoA ligase by IMAC and SEC.....	122
Figure 8-17: Different hydroxycinnamic acid derivates as putative substrates for recombinant CoA ligases.....	123
Figure 8-18: Absorbance spectra of Piperoyl-CoA ligase, At4CL6 and At4CL2 incubated with different substrates	124
Figure 8-19: Absorbance spectra of <i>Piper nigrum</i> 4CL2 incubated with different substrates	125
Figure 8-20: Kinetics of piperoyl-CoA with piperic acid (A) and 5-phenylpentanoic acid (B)	126
Figure 8-21: Specificity of anti-PAS-antibody against different concentrations of recombinant piperamide synthase (A) and recombinant piperine synthase (B)	127

List of Tables

Table 2-1: Primer use for RT-qPCR	26
Table 2-2: Traditional cloning strategy: restriction enzymes and entry-vector	27
Table 2-3: Primer used for cloning and RT-qPCR.....	28
Table 2-4: GenBank accession numbers	29
Table 2-5: Crystallization screening kits	32
Table 2-6: Experimental setup for LC-MS analysis of methanolic plant extracts.....	36
Table 2-7: Experimental setup for LC-MS analysis for <i>in vitro</i> assays of Piperine synthase and Piperamide synthase and for analysis of the feeding experiments	36
Table 2-8: Experimental setup for LC-MS analysis for <i>in vitro</i> assays of CoA ligases	36
Table 2-9: Experimental setup for LC-MS analysis for <i>in vitro</i> CYP719A37 assays with microsomal fractions and transient yeast cell assays	36
Table 3-1: Most abundant transcripts in fruit stage I and II compared to leaves and flowering spadices.	41
Table 3-2: Substrates tested in microsomal and intact yeast assays with heterologous expressed PnCYP719 and reductases, PnCPR or ATR1.....	45
Table 3-3: Substrate specificity of Piperoyl-CoA ligase compared to 5-phenylpentanoic acid/OPDA CoA ligase from <i>A. thaliana</i> (At4CL6).	54
Table 3-4: Apparent kinetic constants of piperine and piperamide synthases using piperoyl-CoA (5-2000 μ M) and piperidine (1-100 mM) as substrate.	60

List of Abbreviations

aa	amino acid
BCIP	5-bromo-4-chloro-3-indolyl phosphate
bp	base pairs
CHS	chalcone synthase
CYP	cytochrome P450 monooxygenases
dpa	days post anthesis
DTT	dithiothreitol
ESI-MS	electrospray ionization mass spectrometry
FDR	false discovery rate
GGC	Golden Gate cloning
HLB	hydrophilic-lipophilic-balanced
HPLC	high performance liquid chromatography
IMAC	immobilized metal ion affinity chromatography
IPB	Leibniz-Institut für Pflanzenbiochemie, Halle
IPTG	isopropyl β -D-1-thiogalactopyranoside
KAS	β -keto-acyl-ACP-synthase
LB-medium	Luria Bertani medium
LFC	log ₂ fold-change
Mbp	mega base pairs
MCS	multi cloning site
MWCO	molecular weight cut-off
NADES	natural deep eutectic solvents
NBT	nitro blue tetrazolium chloride
qRT-PCR	quantitative real time polymerase chain reaction
SEC	size exclusion chromatography
TLC	thin layer chromatography
tpm	transcripts per million reads

1 Introduction

1.1 King of spices - a history on trade and power for pungency

“It is surprising that the use of pepper has come so much into fashion. Commodities as rule attract us by their appearance or utility but the only quality of pepper is its pungency and yet it is for this very undesirable element that we import it in very huge quantities from the first emporium of India, Muziris” – Naturalis Historia by Plinty the Elder (23 – 79 A.D.)

The history of black peppercorns seems as old as the history of human civilisation (Ravindran, 2000). Already the ancient Babylonians were trading with the Malabar Coast, localized in the South-West part of India and represented the very first trading route of black pepper (*Piper nigrum*) and cardamom (*Elettaria cardamomum*). Babylonia was also known for their flourishing sea trade with China and Indonesia. Possibly black pepper was distributed to the Asian countries for the first time in history. First references about black pepper were also found in the Eber’s Papyrus dated around 1550 B.C. and the Egyptian Queen Hatshepsut traded with India around 1000 B.C.. According to the Bible, in 1015-66 B.C. the Queen of Sheba donated spices, including black pepper, to King Solomon of Israel during a royal visit. In ancient Greek, black pepper was well known as “Yavanapriya” - “beloved to the Greeks” (Ummer, 1989). In the *Materia Medica* the Roman physician Dioscordis (40-90 A.D.) described the medical efficacy of black pepper. During the same time, the Indian physician Charaka wrote the *Charaka Samhita*, one of the oldest medical works of ancient India, where he described the use of black pepper for treatment of ear and eye diseases. During the reign of King Solomon, the Jews and Arabs became the dominant spice traders (Rosengarten, 1969). To keep their monopoly, the route to India was a carefully kept secret. After capturing Egypt in the early 1st century, the Romans became a strong competitor. Under the Emperor Claudius (10 B.C. to 54 A.D.) the trade route between Egypt and India was expanded due to the optimal usage of the wind systems of the Indian Ocean (Ummer, 1989). After the fall of Roman Empire in 408 A.D., the Arabs took control over the trade for many centuries. The trade between China and the Malabar Coast flourished and also black pepper plants spread to the South East and Far East (Ummer, 1989). The Venetian merchant Marco Polo mentioned that 10,000 pounds of black pepper arrived daily in the Chinese port Hamgchon in 1298. By the 12 – 13th century the consumption of black pepper in Europe and England strongly increased and in 1345 a consortium of pepperers was founded (Parry, 1962). During this time, the consumption of this spice was still a privilege and black pepper an expensive commodity. The so-called “Pfeffersäcke” were the wealthiest of the merchants. The high prices for black pepper were due to transportation costs and taxes, therefore alternative trade routes were needed. With the discovery of the sea route to India by Portuguese explorer Vasco de Gamas in 1498 the fate of Arab trade was sealed, and the colonialization era began. In 1500, under the command of

Pedro Alvarez Cabral the supremacy of Portugal in India was declared (Rosengarten, 1969). The Portuguese, the Dutch and later the British fought for supremacy in India and the control of the spice trades in several wars. By 1800, the British, represented by the British East India Company, became the supreme power in black pepper trade, while simultaneously production and cultivation techniques of black pepper and cardamom were improved. The United States of America entered the black pepper trade, when Jonatham Carnes sailed from Salem to East India in 1795. The Dutch East Indies improved the pepper production and became the most important producer and exporter of the "black gold" in the world until the outbreak of the Second World War. Black pepper continued to be distributed around the world from India, Brazil (1933), Malaysia, Indonesia, the Malagasy Republic (1938), and Ethiopia (1954).

The pungent principle of black pepper, Piperine was already isolated and characterized in 1820 by the Danish scientist Hans-Christian Ørsted (**Figure 1-1**) (Ørsted, 1820). During the first and second world war entailed by the Continental Blockade, tropical spices were no longer available in Germany. The synthesis of surrogates was promoted. In 1916, the German chemists Hermann Staudinger and the German lawyer Paul Immerwahr developed a mix of compounds called "Kunstpfeffer" (**Figure 1-1**) (Vaupel, 2010). The substances were combined with starch and milled before consuming. It was shown that the methylenedioxy bridge was not essential for pungency. Nevertheless, the final taste of "Kunstpfeffer" was far from being a perfect mimic, since several terpenoids, contributing to the aromatic perception of black pepper, were missing.

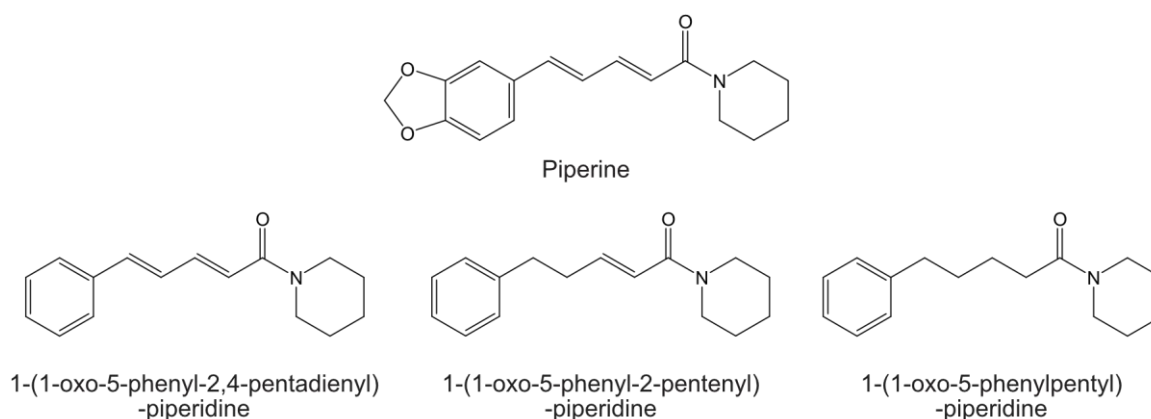


Figure 1-1: Piperine, the pungent principle of black pepper and related "Kunstpfeffer" substances

Piperine is the main alkaloid in black pepper and related to pungency. Provoked by the Continental embargo the chemical synthesis of piperine alternatives was enforced. In 1916, Hermann Staudinger published the synthesis of "Kunstpfeffer", a mix of 1-(1-oxo-5-phenyl-2,4-pentadienyl)-piperidine, 1-(1-oxo-5-phenyl-2-pentenyl)-piperidine and 1-(1-oxo-5-phenylpentyl)-piperidine .

Black pepper is still a sought-after commodity and is an integral part of every kitchen worldwide. In 2019 main producer of black pepper were Ethiopia (374.413 t), Vietnam (264.854 t), Brazil (109.401 t), Indonesia (88.949 t) and India (66.000 t) (Source: Food and 10

Agriculture Organization of the United Nations, 2020). In the same year up to 30.943 t of black pepper were imported to Germany (Statista, 2021).

1.2 *Piper nigrum* - the black pepper plant

Black pepper is a woody evergreen climbing herb and is suggested to be native to Southeast Asia and South Asia (Jaramillo and Manos, 2001) (**Figure 1-2**). Due to the black pepper trades, these plants are nowadays further distributed in Africa, America, and the Pacific Islands. Under cultivation conditions, black pepper can grow up to 4-6 m on poles and up to 20 m on small trees with the help of its aerial roots as anchors (Peter, 2012). The perennial plant has two-ranked leaves with a base sheathing. During plant growth, single adaxial prophylls appear. The plant nodes are trilacunar and swollen (Cole and Hilger, 2016). Upon flowering, pendent spadices appear on side branches opposite of the leaf. They contain several small polygamous flowers, which are reduced to a single ovary and two stamens on the opposite side to the ovary. After self-pollination spherical fruits grow up to one year and can be divided into the fleshy pericarp and the hard and solid perisperm. They can reach up to 7 mm in diameter and contain a single seed. The fruit color changes from unripe, green fruits to ripe fruits, which turn red. Fruit-eating bats are attracted by the essential oils of the ripe fruit and support seed dispersal (Mikich et al., 2003). Interestingly, the oil itself and its impreg-

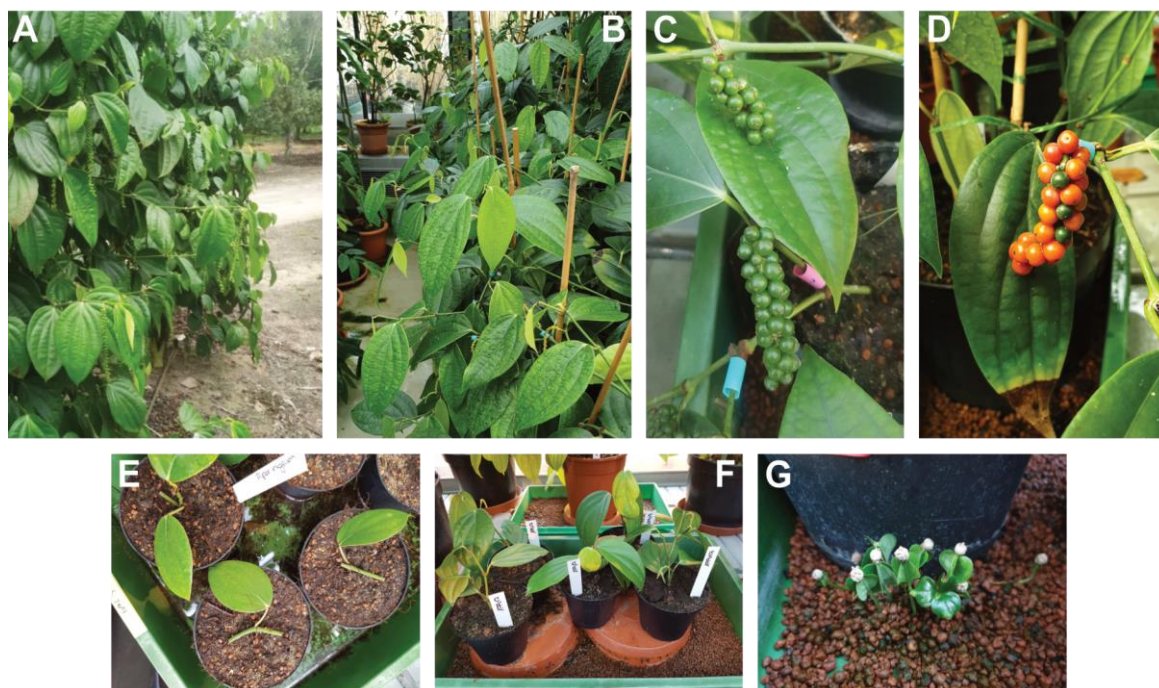


Figure 1-2: The black pepper plant (*Piper nigrum*)

(A) Several black pepper plants are growing on poles on a plantation at São Mateus, Brazil. (The photo was taken by Thomas Vogt) **(B)** Black pepper plants are growing and fruiting in the tropical green-house of the IPB. Shown are unripe black pepper fruits **(C)** and the turning stage between unripe green and ripe red fruits **(D)**. Plants can be easily propagated by cuttings **(E)**. Fresh cuttings from the Vienna Botanical Garden were attached to moist soil and small plants grew after a few months **(F)**. Shoots can also grow from black pepper seeds **(G)**.

nation on other seeds cause such a strong attraction, that bats could be lead to open or degraded forest areas and therefore could be used as a potential tool for forest restoration (Bianconi et al., 2007; Whitehead, Quesada and Bowers, 2016). Normally, cuttings are the easiest and cheapest way in plant propagation and industrial cultivation.

Piper nigrum and more than 2000 other species are part of the genus Piper, one of the most diverse genus among basal angiosperms (Quijano-Abril, Callejas-Posada and Miranda-Esquivel, 2006; Sanderson and Donoghue, 1994) and one of the 20 richest genera of flowering plants (Frodin, 2004) (**Figure 1-3**). With the large sister genus Peperomia and the two smaller

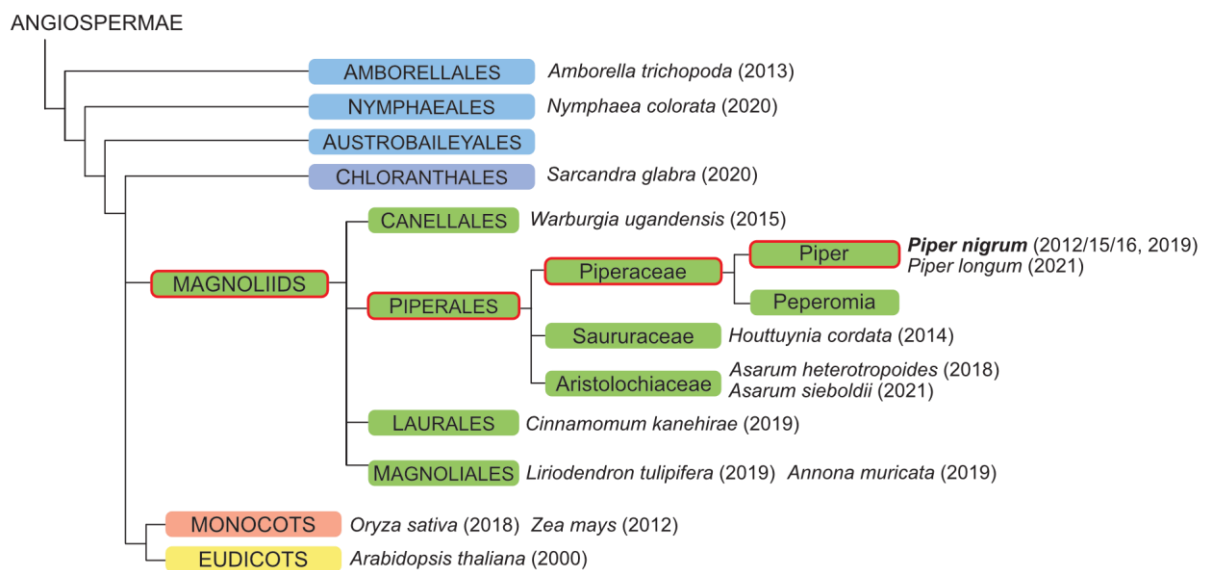


Figure 1-3: Angiosperm phylogeny with available plant transcriptome and genome datasets

Shown are the Angiospermae, the flowering plants with basal angiosperm groups Amborellales, Nymphaeales and Austrobaileyales, and the core angiosperm clades Chloranthales, Magnoliids, Monocots, and Eudicots. The classification of *Piper nigrum* is shown in detail (green with red frame). Several plants with available genome or transcriptome datasets and their release date were added: *Amborella trichopoda*: genome (2013); *Nymphaea colorata*: genome (2020); *Sarcandra glabra*: transcriptome (2020); *Warburgia ugandensis*: transcriptome (2015); *Piper nigrum*: transcriptome datasets (2012, 2015, 2016) and the genome (2019); *Piper longum*: transcriptome (2021); *Houlttuynia cordata*: transcriptome (2014); *Asarum heterotropoides*: transcriptome (2018); *Cinnamomum kanehirae*: genome (2019); *Liriodendron tulipifera*: genome (2019); *Annona muricata*: genome (2019) *Oryza sativa*: genome (2018); *Zea mays*: genome (2012); *Arabidopsis thaliana*: genome (2002). The phylogeny tree was adapted from Cole and Hilger (2016).

genera, Zippelia and Manekia, Piper belongs to the family Piperaceae in the order of Piperales (Wanke et al., 2007). The members of Piperales are characterized by a diverse spectrum of floral morphology, life forms, and specialized metabolites (Doyle and Endress, 2000). All lineages show reduction and several fusions of flower organs, especially in *Piper* and *Peperomia* species (Jaramillo and Manos, 2001; Jaramillo, Manos and Zimmer, 2004). For example, in cubeb pepper (*Piper cubeba*) the flowers and fruits are attached to stalks, whereas in long pepper (*Piper longum*) the flowers and fruits are fused (**Figure 1-4**, E and F).

Due to this high diversity and missing information of the genetic background, it is still difficult to classify all these genera and to elucidate important pathways of bioactive compounds, such as piperine. After the complete annotation of the *Arabidopsis thaliana* genome by a large consortium of scientists in 2000, mainly due to new sequencing technologies, the speed of genome sequencing is rapidly increasing (Delseny et al., 1997; Kaul et al., 2000). In 2013, the first genome of a most basal angiosperm (*Amborella trichopoda*) was annotated and gave a closer look into plant evolution (Albert et al., 2013). Five years later, the genome of five-seeded plume-poppy (*Macleaya cordata*) was sequenced and together with metabolic profiling the biosynthesis of benzylisoquinoline alkaloids, like sanguinarine, reconstructed (Liu et al., 2017). In 2018 and 2019, the genome of three magnoliids, the tulip tree (*Liriodendron tulipifera*) and the soursop (*Annona muricata*) from the order Magnoliales as well as the stout camphor tree (*Cinnamomum kanehirae*) from the order of Laurales were elucidated and completed several evolutionary aspects (Chaw et al., 2018; Chen et al., 2019; Soltis and Soltis, 2019; Strijk et al., 2019). In 2020, the genome of the water lily (*Nymphaea colorata*) was analysed and support the idea of sister lineages of Amborellales and Nymphaeales (Zhang et al., 2020). Among these, the genome of black pepper was elucidated recently, too (Hu et al., 2019). With approximately 761 Mbp it is six-times larger than the *A. thaliana* genome and may now provide insights into common and unique metabolic processes, like piperine biosynthesis. In addition to genome data, transcriptome data are available from many species and provide a more and alternative access to tedious identification of individual enzymatic steps and whole pathways even when no genome information is available (Grabherr et al., 2011). The transcriptome of fish mint (*Houttuynia cordata* Thunb.) was elucidated by Illumina sequencing in 2014 (Wei et al., 2014). The fish mint is a traditional medical herb native to Asian countries and plays an important role in the modulation of the immune system of patients infected with the acute respiratory syndrome (SARS) (Lau et al., 2008). In 2015, the transcriptome of the bark and leaves of Ugandan greenheart (*Warburgia ugandensis*), a medical plant from Africa, was elucidated and in concert with metabolite analysis the pathway of mono- and sesquiterpenoid biosynthesis as well as the biosynthesis of polyunsaturated fatty acids proposed (Wang et al., 2015). In 2018 and 2021, the transcriptome of wild ginger (*Asarum heterotropoides* and *Asarum sieboldii*) were analysed and gave some clues on the biosynthesis of aristolochic acid, a carcinogenic and nephrotoxic alkaloid with an unusual nitro group, and of asarinin, a similar compound to sesamin (Chen et al., 2021; Wang et al., 2018). To answer the question of piperine biosynthesis, independent transcriptome datasets of leaves, fruits and roots were generated, but yet no experimental data related to the biosynthesis of piperine were reported (Gordo et al., 2012; Hao et al., 2016; Hu et al., 2015). Recently the transcriptome of leaves, roots and spikes of *P. longum* were analysed, and again the biosynthesis of piperine was only

theoretically described based on assumptions made by several laboratories in the last decades (Dantu et al., 2021). These examples show the advantage and at the same time a disadvantage of pure transcriptome datasets. They only show a specific moment of active transcripts at a specific time point or a specific plant organ yet require additional knowledge on accumulation and of the metabolite or pathway of interest in order to identify the correct genes or enzymes among small or large gene families, specifically in the biosynthesis of natural products. Among the plethora of transcriptome data published during the last decade, experimental evidence for any of the claims made is often missing in the computational analysis.

1.3 The flavor of black pepper

The name „king of spice” is contributed to the characteristic tastes of black pepper and black pepper varieties (Friedman et al., 2008) (**Figure 1-4**). Unripe black pepper fruits have a spicy and fresh aroma. The woody and floral notes are related to terpenes, like limonene, pinene, α -phellandrene, germacrene and β -caryophyllene or sesquiterpenes, like rotundone, also found in rosemary, grape and wine, located mainly in the pericarp of the fruit (Jirovetz et al., 2002; Siebert et al., 2008). Unripe green fruits can be further processed by drying in the sun for several days. The pericarp shrinks and darkens. The product is called black peppercorn. If the fruits are soaked in water for two weeks, they start to rot, and the periplasm can be removed easily. The final product is known as white peppercorn. Due to the fact of losing the pericarp the white peppercorn flavor differs from the unripe green and black peppercorns (Jagella and Grosch, 1999a, 1999b, 1999c; Lee et al., 2020). If the fruits are not harvested in the unripe state, they turn red, when they are ripe. Unripe green and ripe red peppercorns can be preserved in vinegar or by freeze-drying.

Further prominent pepper varieties used in traditional cuisine are fruits of *P. longum* and *P. cubeba*. Since antiquity long pepper rather than black pepper was the only Piper spice on the market. Starting in the 12th century, black pepper out-competed long pepper and in the 14th century long pepper was completely displaced (Laurieux, 1985). From *P. longum* the unripe and ripe infructescences are used as spice in prickles and curries and have a similar taste like black pepper (Lim, 2012c). Besides usage as spice in traditional dishes, the fruits of *P. cubeba* can be candied and eaten as an aromatic confectionery. It is also used to flavor the Bombay Sapphire gin (Lim, 2012a). The main sesquiterpene cubebol is used as cooling and refreshing agent in chewing gum, drinks and even toothpaste. The common “pink pepper” in mixed spices is not a “real” peppercorn. These fruits belong to the Brazilian pepper tree (*Schinus terebinthifolius*) or the Peruvian pepper tree (*Schinus molle*). Both plants belong to the family Anacardiaceae in the clade of Eudicots and the pungent taste is mostly related to terpenoids.

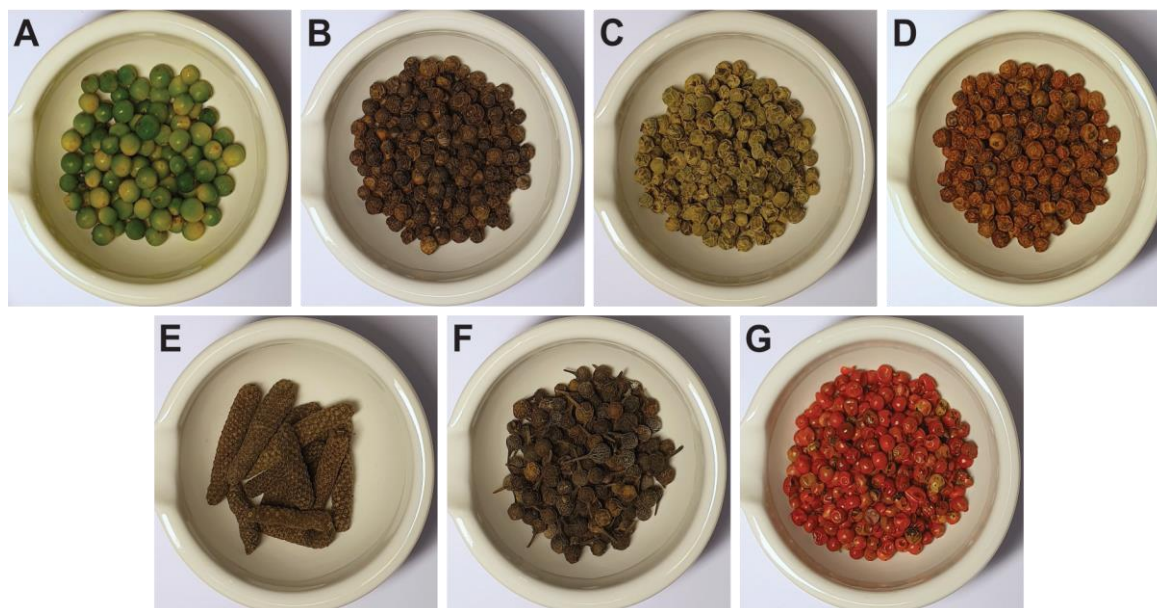


Figure 1-4: Different pepper varieties used in traditional cuisine

Different black pepper varieties and alternative spices are placed in a mortar (\varnothing 7 cm). **(A)** Unripe black pepper, **(B)** dried black pepper, **(C)** and **(D)** freeze-dried unripe black pepper and ripe black pepper (Kampot black pepper), **(E)** fruits of long pepper, **(F)** fruits of cubeb pepper and **(G)** pink pepper of the Brazilian pepper tree. All spices are commercially available from several commercial suppliers. Unripe, green black pepper is from tropical greenhouse grown plants at the IPB.

Besides the aroma, specifically the pungency is characteristic for black pepper and is related to piperine (De Cleyn and Verzele, 1975). Piperine strongly activates the receptor transient receptor potential vanilloid 1 (TRPV1), a non-selective cation channel, which was firstly described by capsaicin activation (Caterina et al., 1997; McNamara, Randall and Gunthorpe, 2005). Interestingly, the binding and resulting response is more effective when caused by piperine as compared to capsaicin (McNamara et al., 2005). Longer aliphatic chains in the piperine derivate do not affect the pungency. A vanilloid structure, like in case of feruperine results in a somewhat reduced activity (Correa et al., 2010). Normally, this channel is activated by thermal and chemical stimuli, like protons, heat, endovanilloids/endocannabinoids as well as pro-inflammatory agents (Palazzo, Rossi and Maione, 2008; Thomas et al., 2012; Tominaga et al., 1998; Zygmunt et al., 1999). The activation of this channel results in a pain sensation for tissue protection (Patapoutian, Tate and Woolf, 2009). Black pepper fruits can lose their pungency in different ways.

Piperine can easily isomerise into its isomers isopiperine, chavicine, or isochavicine (Suppl.: **Figure 8-1**) (Kozukue et al., 2007). This can occur by exposing grinded black pepper to light, long cooking times or extensive storage of black pepper powder. The piperine isomers are nearly tasteless.

1.4 The power of piperine and piperamides as bioactive compounds

Besides the fact that black pepper is used as a spice all over the world, it is used in traditional medicine, in phytochemical compositions as well as in pharmacological applications. Piperine and piperamides have been intensively studied for their biological properties (Meghwal and Goswami, 2013; Salehi et al., 2019). In traditional medicine, mainly the seeds are used to treat gastrointestinal disturbances, headaches, chills and rheumatism, diabetes and epilepsy (Meghwal and Goswami, 2013). Extracts are also used against cold, flu or fevers. Piperine shows numerous health-promoting properties, like anti-microbial, neuroprotective, immunomodulatory, anti-inflammatory, cardioprotective and anticancer effects (Jhanji, Singh and Kumar, 2021; Smilkov et al., 2019; Srinivasan, 2014). The alkaloid is used in topical creams against skin diseases. Piperine loaded lipid carrier suggested a better treatment of atopic dermatitis (Kumar, Sharma and Ashawat, 2021). Piperine increases intestinal absorption, transport, and metabolism of drugs and ions (Smilkov et al., 2019), like the iron uptake (Bioperine®, Sabinsa Corporation, East Windsor, NJ, USA). The bioavailability of Domperidone, an anti-emetic drug with a low oral absorption, can be improved with phytosomes, made of piperine and phosphatidylcholine, up to 79.5 % compared to the pure drug itself (Islam et al., 2021). Piperine itself has a low solubility and therefore low bioavailability. Further combinations of piperine with hydroxypropyl- β -cyclodextrin are discussed to overcome this challenge and further increase the functionality of piperine (Stasiłowicz et al., 2021). Piperine shows a high anti-cancer potential in combinatorial therapies and increases the cytotoxic effect of paclitaxel and topotecan, both chemotherapeutic agents in drug-resistant human ovarian cancer cells (Wojtowicz et al., 2021). Besides piperine, other black pepper amides of different aliphatic chain lengths or decorations like piperlongumine or pellitorine, show various anticancer activities and are therefore discussed as potential anticancer agents (Turrini, Sestili and Fimognari, 2020).

Finally, (Z)-piplartine from *Piper tuberculatum* shows high activity against the epimastigote forms of *Trypanosoma cruzi*, a parasite that causes Chagas` disease (Cotinguiba et al., 2009) The alkaloid 3-chlorosintenpyridone 1 from *Piper pseudoarboreum* showed higher potency against promastigote stages of different *Leishmania* species, than Miltefosine, the common medical application of this disease (**Figure 1-5**) (Flores et al., 2019).

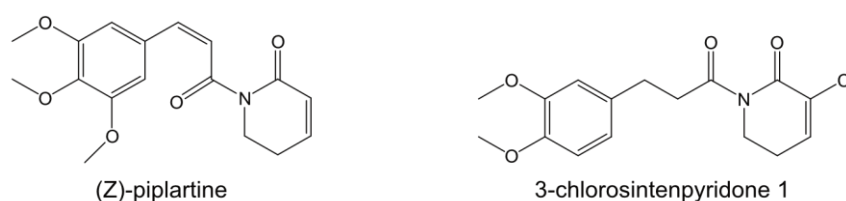


Figure 1-5: The piperamides (Z)-piplartine and 3-chlorosintenpyridone 1 show antifilarial properties

1.5 Piperine synthesis and biosynthesis

Numerous procedures for organic synthesis of piperine and piperamides were developed (Bauer, Nam and Maulide, 2019) since it was first described in 1819 (Ørsted, 1820), whereas the biosynthesis of these amides in most parts is still enigmatic. The piperine structure can be divided into the heterocycle piperidine, a product of lysine metabolism, and an aromatic part piperoyl-CoA, presumably derived from the phenylpropanoid pathway (**Figure 1-6**). The conversion of piperoyl-CoA and piperidine to piperine by a piperine synthase activity was described in a crude plant extract from black pepper shoots (Geisler and Gross, 1990).

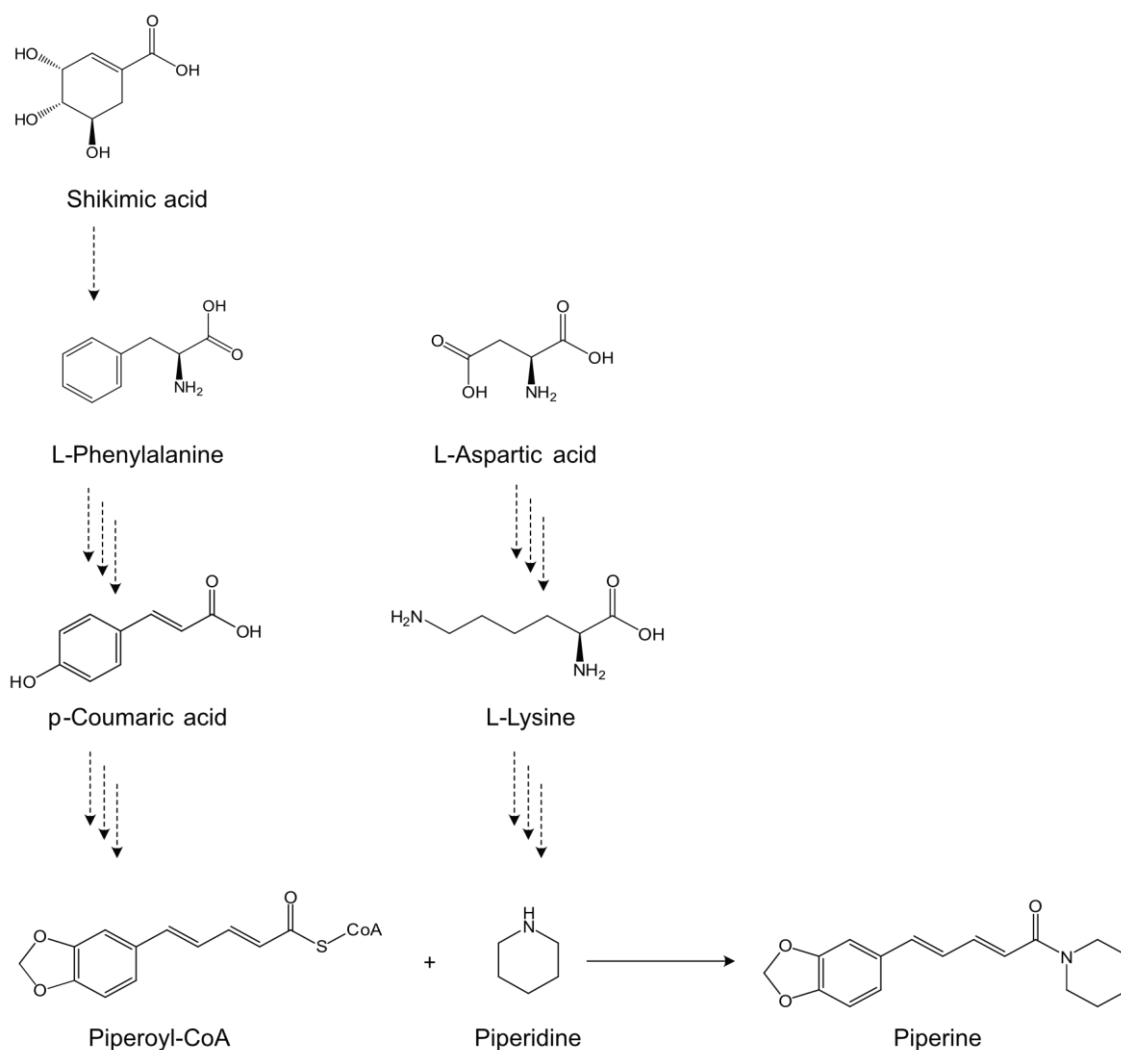


Figure 1-6: Hypothetical biosynthesis of piperine in black pepper

Piperine is synthesized by the condensation of piperoyl-CoA and piperidine. An enzymatic activity was shown in a crude protein extract of black pepper shoots (Geisler and Gross, 1990). Piperidine is suggested to derive from L-lysine with the intermediate cadaverine or pipercolic acid. Piperoyl-CoA is suggested to derive from L-phenylalanine, which is further modified by the phenylpropanoid metabolism.

Piperidine is a common amine in the plant kingdom (**Figure 1-7**, A). Tracer studies with ^{14}C -labeled D- and L-lysine showed that L-lysine is incorporated in alkaloids like sedamine and N-methylpelletierine from *Sedum* species (Crassulaceae) as well as anabesine from

Nicotiana glauca (Solanaceae), whereas pipercolic acid from these plants as well as in *Phaseolus vulgaris* (Fabaceae) is derived from D-lysine (Gupta and Spenser, 1969; Leistner, Gupta and Spenser, 1973). The biosynthesis of coniine from poison hemlock (*Conium maculatum*), famous for poisoning the philosopher Socrates (Puidokait et al., 2016), is still unknown. Within piperidine biosynthesis, cadaverine was identified as an intermediate and the “chiral” model was established (Leistner and Spenser, 1973). This model described the decarboxylation of L-lysine to cadaverine followed by an oxidative deamination to 5-aminopentanal and a spontaneous cyclisation into Δ^1 -piperideine. This hypothesis was confirmed by identification of a lysine/ornithine decarboxylase and a copper amine oxidase from *Lupinus angustifolius* (Fabaceae) in the biosynthesis of lupine alkaloids (**Figure 1-7, B**) (Bunsupa et al., 2011; Frick et al., 2017; Golebiewski and Spenser, 1988). It is assumed that a further reduction of Δ^1 -piperideine leads to piperidine. The incorporation of ^{14}C -labeled L-lysine into piperlongumine emphasises the theory with L-lysine as precursor in piperidine biosynthesis (Prabhu and Mulchandani, 1985).

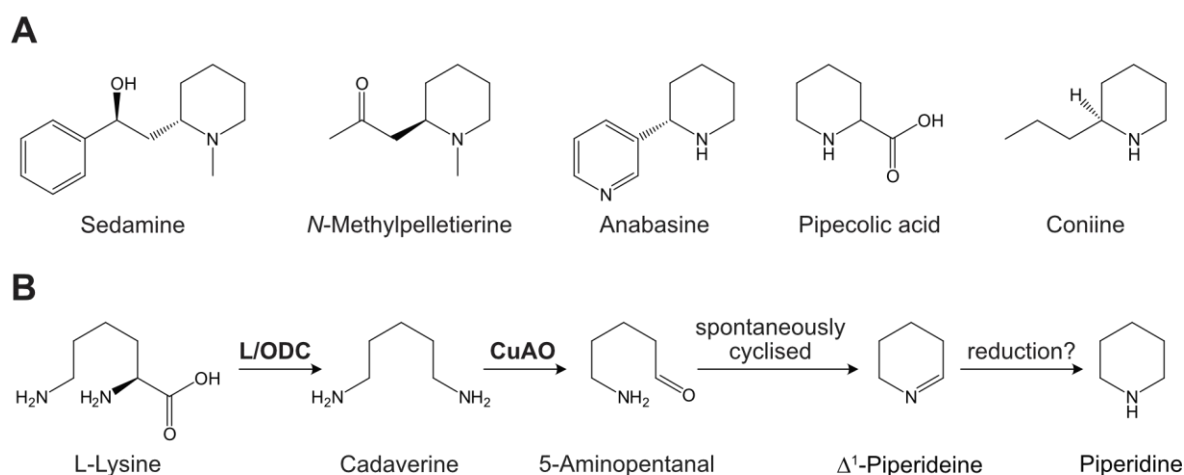


Figure 1-7: Different natural products with a piperidine heterocycle and suggested "chiral" model for piperidine biosynthesis

(A) Different plant natural products with a piperidine heterocycle are shown. Sedamine and N-methylpelletierine in *Crassula* (*Sedum acre*, *Sedum sarmentosum*), anabasine in tobacco plants (*Nicotiana glauca*, *Nicotiana tabacum*) and pipercolic acid in already named plants and common bean (*Phaseolus vulgaris*), coniine from poison hemlock (*Conium maculatum*). (B) Shown is the “chiral” model created by Leistner and Spenser (1973) for the biosynthesis of piperidine. Major steps were confirmed in *Lupinus angustifolius* (Bunsupa et al., 2011; Frick et al., 2017; Golebiewski & Spenser, 1988). L-lysine is decarboxylated to cadaverine by lysine/ornithine decarboxylase (L/ODC). Cadaverine is deaminated by a copper amine oxidase (CuAO). 5-Aminopentanal can spontaneously cyclised into Δ^1 -piperideine. The following reduction to piperidine is only suggested.

Pipercolic acid is a non-protein amino acid in the plant kingdom and accumulates during pathogen infection and is therefore a regulator of plant immunity (Grobbelaar and Steward, 1953; Návarová et al., 2012; Xu et al., 2018; Zacharius, Thompson and Steward, 1952). The decarboxylation of pipercolic acid for piperidine biosynthesis is also discussed.

Besides piperidine, also pyrrolidine and isobutylamine are common amines in *P. nigrum*. The pyrrolidine biosynthesis was partially described in *Nicotiana tabacum* similar to the piperidine biosynthesis and probably starts with L-ornithine instead of L-lysine (Leete, Gros and Gilbertson, 1964). The formation of isobutylamine might be derived from the amino acid L-valine. Up to now no investigation on the biosynthesis of piperidine, pyrrolidine or isobutylamine in *Piper* species were undertaken.

1.6 Key enzymatic steps of the phenylpropanoid part of piperine biosynthesis

The biosynthesis of the aromatic part at a first glance points to the phenylpropanoid pathway. Starting from the shikimate pathway, the decisive step from phenylalanine to C6-C3 aromatic compounds, like cinnamic acid, is initiated by phenylalanine ammonia lyase (PAL). Subsequent hydroxylations, methylations, and acylations result in a series of precursors for a plethora of aromatic metabolites (Hoffmann et al., 2004; Vogt, 2010). In the case of piperine, a C6-C5 instead of a C6-C3 unit is required, and it is unclear, how this extension is catalyzed enzymatically (Jiang, Kim and Suh, 2008). Subsequent reaction may include activation of the resulting acid, formation of the methylenedioxy group, and finally amide bond formation between a CoA-ester and the amine piperidine as suggested from data with crude protein extracts from black pepper shoots (Geisler and Gross, 1990). If this scenario is correct, it remains to be established if the methylenedioxy bridge is formed before CoA-activation or at the level of the ester. In plants, numerous enzymes that are known to perform these reactions have been characterized. They belong to the CoA ligases, cytochrome P450 oxidoreductases, and acyltransferases, providing backbone structures in the case of phenylpropanoids, terpenoids, and alkaloids.

1.6.1 CoA ligases

In plants the subclass of 4-coumarate: CoA ligases (4CLs: EC 6.2.1.12) is well characterized. The enzymes can be annotated as acyl- or aryl-CoA synthetases and require Mg⁺⁺ and ATP as co-factors. Activated CoA-thioesters serve as precursors in the biosynthesis of numerous specialized metabolites of different branch pathways. They are involved in flavonoid as well as lignin polymer biosynthesis and activated different hydroxycinnamic acids, like p-coumaric, ferulic, caffeic and sinapic acids (Suppl.: **Figure 8-2**) (Hamberger and Hahlbrock, 2004; Knobloch and Hahlbrock, 1977; Lavhale, Kalunke and Giri, 2018; Ranjeva, Boudet and Faggion, 1976; Wallis and Rhodes, 1977). The CoA ligases are strictly distinct in their substrate preference (Cukovica et al., 2001; Ehlting et al., 1999; Ehlting, Shin and Douglas, 2001). In many plants multiple isoforms exist, are expressed in different tissues and developmental stages, and show a different biological function (Gui, Shen and Li, 2011; Rastogi et al., 2013; Sun et al., 2013). These kinds of enzymes are not limited to plants. They

are part of the ANL superfamily that, besides the acyland acryl-CoA synthetases (CoA ligases), include the adenylation domains of non-ribosomal peptide synthetases (**N**RPSs) and the firefly **l**uciferases (Suppl.: **Figure 8-3**) (Gulick, 2009; May et al., 2002; Naderi et al., 2021; Wehrs et al., 2019; Zhang et al., 2015). All reactions are characterized by the same mechanism of an enzyme bound AMP-anhydride, that is attacked by phosphopantetheine thiol of CoA, and formed the final CoA-thioester, e.g. p-coumaroyl-CoA, a central precursor of phenylpropanoid metabolism (Vogt, 2010).

1.6.2 Acyltransferases

Subsequent amide formation was assumed as the final step in piperine biosynthesis. The responsible enzyme was described as piperoyl-CoA:piperidine *N*-piperoyltransferase (EC 2.3.1.145) (Geisler and Gross, 1990). This endergonic reaction requires an “energy-rich” acyl donor, like an acyl CoA-thioester usually derived from hydroxycinnamic acids by CoA ligase catalyzed activation. Addition of acyl-groups is a common modification in plant natural product biosynthesis (Bontpart et al., 2015; D'Auria, 2006). Two enzyme families in phenolic metabolism are capable of acylating specialized compounds, BAHD-type acyltransferases (BAHDs) or serine carboxy-peptidase-like acyltransferases (SCPLs) (Bontpart et al., 2015). The use of 1-*O*- β -glucose esters as acyl donor is less common than CoA-activation, but quite abundant in the Brassicaceae, e.g. in the accumulation of sinapate esters in *A. thaliana* (Fraser and Chapple, 2011). BAHDs are named by the first four characterized enzymes, the benzylalcohol *O*-acetyltransferase (**B**EAT) from Brewer's clarkia (*Clarkia breweri*), the anthocyanin *O*-hydroxy-cinnamoyltransferase (**A**HCT) from clustered gentian (*Gentiana triflora*), the *N*-hydroxy-cinnamoyl/benzoyl-transferase (**H**CBT) from clove pink (*Dianthus caryophyllus* L.) and the deacetylindoline 4-*O*-acetyltransferase (**D**AT) from carnation (*Catharanthus roseus*) (Dudareva et al., 1998; Fujiwara et al., 1998; St-Pierre and De Luca, 2000; St-Pierre et al., 1998; Yang et al., 1997). Prominent members participate in the biosynthesis of the alkaloid morphine in opium poppy (*Papaver somniferum*), anthocyanins and the alkaloid vindoline from *C. roseus*, a precursor of the anti-cancer drugs vincristine and vincalucoblastine (Grothe, Lenz and Kutchan, 2001; Nakayama, Suzuki and Nishino, 2003; St-Pierre et al., 1998; Suzuki, Nakayama and Nishino, 2003; Suzuki et al., 2004). Cocaine synthase from young leaves of coca (*Erythoxylon coca*) catalyzes the last step in cocaine biosynthesis by esterification of methylecgonine with benzoic acid (Schmidt et al., 2015). Capsaicin synthase is encoded by the pungency locus (PUN1) in hot pepper cultivars (*Capsicum annuum*, *Capsicum chinense*, and *Capsicum frutescens*) and transfers the acyl group from 8-methyl-6-nonenoyl-CoA to the acyl acceptor vanillylamine (Ogawa et al., 2015; Stewart et al., 2005). Despite progress made in individual cases, the classification of BAHDs is problematic since the enzymes share low amino acid sequence identity (10-30 %) (St-Pierre

and De Luca, 2000). In 2006, D'Auria divided 46 BAHDs into five major clades based on their sequence, other classifications followed (Bontpart et al., 2015; Tuominen, Johnson and Tsai, 2011). Vinorine synthase from Indian snake root (*Rauvolfia serpentina*) catalyzes the reversible acylation of vinorine from 16-epi-vellosimine, a precursor in the biosynthesis ajmaline, a pharmacologically relevant alkaloid. This enzyme was the first example of a successful crystallisation and X-ray diffraction analysis of a BAHD-acyltransferase (Suppl.: **Figure 8-4**) (Ma et al., 2004; Ma et al., 2005). Except for two conserved motifs, HXXXD and DFGWG, the low sequence identity and a very flexible “donut” structure makes it difficult to predict substrate specificity as well as to crystallize and elucidate the structure of unknown BAHDs.

1.6.3 Formation of the methylenedioxy group

Besides common reactions like oxidations and hydroxylations of the carbon skeleton, cytochrome P450 monooxygenases (CYPs) are known for unusual reactions like oxidative C-C bond cleavage, phenol coupling or methylenedioxy bridge formation (Mizutani and Sato, 2011). Up to ~ 7500 CYPs from plants are characterized and play essential roles in modifications of a plethora of specialized metabolites and are classified based on sequence identity and the type of reaction (Nelson, 2018). In general, cytochrome P450 enzymes are heme-dependent monooxygenases. Conserved motifs are the C-terminal heme-binding domain, the K helix and the aromatic binding site. With an N-terminal membrane anchor they are usually associated to the endoplasmic reticulum. The capture “P450” is derived from the absorption maximum of this enzyme in his reduced state (reduction of heme) and in complex with a carbon monoxide. The heme cofactor is essential for the CYP activity. NADPH-cytochrome P450 reductases (CPR) deliver electrons to reduce the iron in heme for further reactions. Therefore, co-expression of CYPs with CPRs is crucial for functionality. For successful heterologous expression and functional characterisation detection by LC-MS or GC-MS in eukaryotic expression systems, either yeast (Scheler et al., 2016), baculovirus infected insect cells (Díaz Chávez et al., 2011), or transient expression in *N. benthamiana* (Pluskal et al., 2019) have been established.

Methylenedioxy group formation is catalyzed by two classes of cytochrome P450 enzymes, the CYP719A and the CYP81Q family. Both CYPs catalyze the closure of aromatic ortho-hydroxymethoxy-substituted ring resulting in a methylenedioxy bridge structure in aromatic skeleton of heterogenous metabolites (**Figure 1-8**). Methylenedioxy bridges are common in isoquinoline alkaloids, like (S)-stylopine, (S)-coptisin or (S)-berberine or other alkaloids like lycorin from different species of Amaryllidaceae or piperine from black pepper (Nakagawa, Uyeo and Yajima, 1956; Phillipson, Roberts and Zenk, 2012). Prominent examples in the case of phenylpropanoids include the phytoalexin pisatin from pea (*Pisum*

sativum), the volatile phenylpropene safrole from the sassafras tree (*Sassafras albidium*), the coumarin ayapin from orchids (*Dendrobium thyrsiflorum*) and the resin of *Cistus* species (Abel, 1997; Perrin and Bottomley, 1962; Vogt, Proksch and Gülz, 1987; Wrigley, 1960). Toxic lignans, like podophyllotoxin from the Himalayan May apple (*Podophyllum peltatum*) or hinokinin in flax (*Linum corymbulosum*) share this characteristic modification of an aromatic ring structure (Lau and Sattely, 2015). In the genus *Piper* the lignin cubebin has been described from *P. cubeba*. Recently, CYP719A26 from the roots of kava pepper (*Piper methysticum*) was shown to convert 11-methoxy-12-hydroxy-dehydrokavain into 5,6-dehydromethysticin, the precursor of methysticin in the biosynthesis of anti-cancerogenic kavalactones (Pluskal et al., 2019). This was the first characterized CYP719A outside the Ranunculales.

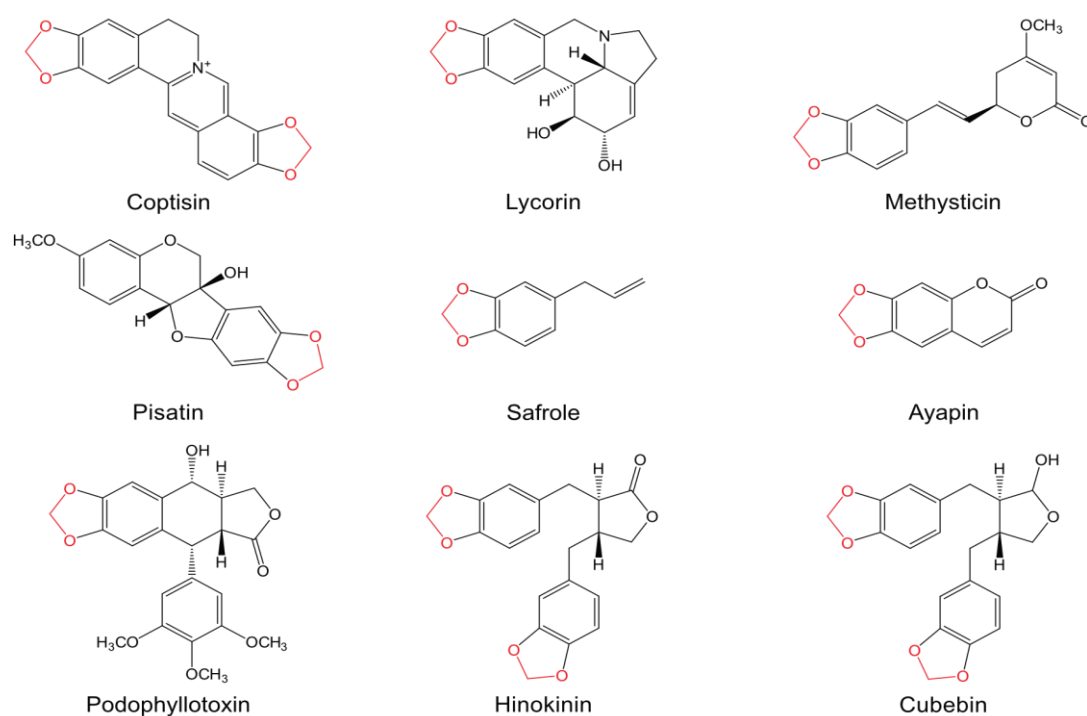


Figure 1-8: Specialized metabolites with the methylenedioxy bridge structure element.

Different plant natural products containing a methylenedioxy bridge (red) are shown. Coptisin in greater celandine (*Chelidonium majus*), lycorin in red spider lily (*Lycoris radiata*), methysticin in kava pepper (*Piper methysticum*), pisatin in pea (*Pisum sativum*), safrole in sassafras tree (*Sassafras albidium*), ayapin in pine cone orchid (*Dendrobium thyrsiflorum*), podophyllotoxin in Himalayan may apple (*Podophyllum peltatum*), hinokinin in hinoki cypress (*Chamaecyparis obtuse*), cubebin in cubeb pepper (*Piper cubeba*).

1.7 Aim of this investigation

Piperine and piperamides show a broad spectrum of biological activities and health-promoting properties. Although the first enzyme activity of the pathway was already discovered three decades ago, the biosynthesis of piperine has not yet been investigated despite the relevance of this spice and its pungent principle for human nutrition and health. As in the case of its biosynthesis, nothing is known about the regulation, as well as compartmentation of the final product.

To address some of these questions, fruiting black pepper plants were established at the IPB in recent years. Based on the hypothesis that piperine formation occurs predominantly in organs where piperine accumulates to high levels, and RNA-abundance of different biosynthesis enzymes followed piperine accumulation, a differential RNA-sequencing approach was initiated comparing RNA from different developmental stages of fruits with RNA isolated from other organs. The approach has been successful several times to identify enigmatic transcripts, genes, and enzymes involved in specialized metabolism and should also facilitated the identification of the decisive steps in piperine biosynthesis. The resulting transcriptome dataset will be computationally compared to public data bases and by this approach, promising candidate genes for individual steps will be identified and functionally expressed in suitable expression systems. Heterologous expressed enzymes will then be further purified and checked for enzymatic activity. Since some substrates are not commercially available, classical organic synthesis in combination with biosynthesis will provide required precursors. Piperine and formation will be monitored by UV-spectroscopy and mass spectrometry coupled with high pressure liquid chromatography. The same technology will be used to identify intermediate compounds and reactions in the pathway. The initial focus of this thesis will be on the presumed final and unique steps in piperine biosynthesis, including methylenedioxy bridge formation of the aromatic ring moiety, activation of piperic acid by an unknown CoA ligase and finally the identification and characterization of a piperine synthase, required for the amide linkage described initially by Geisler and Gross (1990). Finally, some emphasis will also be given to the localisation of piperine and related biosynthetic enzymes *in vivo* in maturing black pepper fruits by immunological methods.

2 Materials and Methods

2.1 Plant material

Piper nigrum plants were obtained from the Botanical Garden of the University of Vienna (Austria). The original plants were collected in 1992 by Dr. R. Samuel in Sri Lanka (IPN No. LK-0-WU-0014181), grown under greenhouse conditions (24 °C at day, 18 °C at night) and with supplemental illumination (R300 NS1-lamps, Valoya, Helsinki, Finland) for 14 hours. The total irradiance was recorded at 150-200 $\mu\text{mol}/\text{m}^2 \times \text{s}$. Individual cuttings of these plants were grown under similar conditions in the tropical green house at the IPB. After a few weeks they started flowering and developing fruits. Plant material was harvested, macerated with a ball mill (Retsch, Germany) and stored at -80 °C.

2.2 Chemicals and substrates

All chemicals were obtained from Carl Roth, Merck, Serva or Duchefa and were of analytical quality. Feruperic acid and feruperine were synthesized by Fernando Cotinguiba (Schnabel et al., 2021b).

2.2.1 Chemical synthesis of piperoyl-CoA

Piperoyl-CoA was synthesized using a modified procedure described in Semler et al. (1987) from 1 g piperic acid (5-(1,3-benzodioxol-5-yl)-2,4-pentadienoic acid). To obtain N-succinimidyl piperate, precipitated N,N-dicyclohexyl urea was repeatedly removed by filtration and subsequently by chromatography on silica gel (0.363–0.2 mm). The filtrate was mixed with silica particles packed on top of a column and fractionated with a mix of petroleum ether:ethyl acetate (ratio 3:2). The fractionation was monitored by TLC (Silica gel 60 F₂₅₄, Merck) with the same solvent mixture. Fractions of 50 mL were analyzed by ESI-MS for the activated ester. After evaporation of the solvent at 30 °C and lyophilization, the resulting N-succinimidyl piperate was crystallized as yellow needles with a melting point of 220-224 °C, subsequently characterized by ¹H- and ¹³C-NMR and stored at -80 °C without noticeable degradation for several months. In a second step, 30 mg of the product was dissolved in dioxane, 36 mg of CoA-SH in 100 mM NaHCO₃ was added, and the resulting CoA ester repeatedly extracted with ethyl acetate. Ammonium acetate (NH₄OAc) was added to the aqueous phase to a final concentration of 4 % w/v. An HLB 20cc (1 g) LP Extraction Cartridge (Waters) was pre-conditioned with 10 volumes of methanol and subsequently with 4 % w/v NH₄OAc. After application, the column was washed with 4 % w/v NH₄OAc and the product was eluted by a stepwise 10 % increase of 100 % MeOH in water. Purification was monitored by TLC (ALUGRAM RP-18W/UV₂₅₄, Macherey-Nagel) with a solvent mixture of aqueous 10 mM NH₄OAc:MeOH (ratio 52:48). The thioester-containing fractions were concentrated by rotary evaporation at 30 °C and lyophilized. Piperoyl-CoA was characterized

by UV absorbance, ESI-MS in positive mode ($m/z = 968.3 [M + H]^+$), $^1\text{H-NMR}$, $^{13}\text{C-NMR}$, and 2D-NMR (Schnabel et al., 2020). Purified piperoyl-CoA was stable for several weeks when stored at $-80\text{ }^\circ\text{C}$, either dry or dissolved in 25 % DMSO.

2.2.2 Chemical synthesis of feruperic acid

Feruperic acid was synthesized from 1 g of coniferyl aldehyde based on the Horner–Wadsworth–Emmons reaction, a modified Wittig reaction (Bazin et al., 2008). Briefly, the aromatic hydroxy group of coniferyl aldehyde was silylated with tertbutyldimethylsilyl trifluoromethanesulfonate and the resulting ester olefinylated by triethylphosphonoacetate in tetrahydrofuran. The reaction was deprotected by tetrabutylammonium fluoride and purified by column chromatography in silica gel (0.363–0.2 mm). The purified ethyl ester was hydrolyzed with LiOH on ice over 24 h, subsequently extracted by ethyl acetate, and concentrated. MS and NMR data are listed in Schnabel et al., (2020).

2.3 Molecular biology methods

2.3.1 RNA isolation and cDNA synthesis

Total RNA was isolated from fruits (20-30 dpa and 40-60 dpa), young leaves and flowering spadices as well as roots with NucleoSpin® RNA Plus (Macherey-Nagel, Germany) using twice the volume of lysis buffer and binding buffer contrary to the manufacturer's instructions. For reversed transcription the Maxima H Minus First Strand cDNA Synthesis Kit (Thermo Fisher, Germany) was used.

2.3.2 RNA-sequencing and data processing

The total RNA from three biological replicates of black pepper spadices, young leaves, fruit stage I (20-30 dpa) and fruit stage II (40-60 dpa) were extracted according to 2.3.1. The RNA was quantified by Nanodrop UV/Vis spectrometer (ThermoFisher). The quality was checked by QIAxcel capillary electrophoresis and the corresponding software (Qiagen). The mRNA-sequencing was carried out by GATC-Biotech and included library preparation using an unstranded protocol, paired-end sequencing with 150 cycles per read, and demultiplexing of the raw data. Illumina HiSeq2000 sequencing was performed. On average 25 million paired-end reads per sample were achieved. The bioinformatic analysis was performed by Benedikt Athmer (IPB) with different software tools and algorithm. Cutadapt was used to remove the sequencing adaptors of the reads and Trimmomatic was used for quality trimming (Bolger, Lohse and Usadel, 2014; Martin, 2011). With the Trinity *de novo* software and further the Trans-ABYSS software the cleaned reads were assembled into 208,308 genes and 540.916 transcripts (Grabherr et al., 2011). Up to 9000 transcripts were classified as full-length transcripts and were annotated by reconciliation with the curated Swiss-Prot database (<https://www.uniprot.org/>). High correlations between replicated groups were confirmed by

hierarchical clustering of sample distances (spearman correlation > 0.95). Further annotation of the dataset was done by the annotation suites Trinotate and BLAST2GO (<https://www.blast2go.com/>). The program CAP3 was used to assemble the contiguous sequences (contigs) to obtain full-length sequences (overlap 200, identity 99 %). BOWTIE2 aligned short sequencing reads to long reference sequences. RSEM was used to quantify the transcript expression levels. For differential gene expression analysis edgeR's exactTest with a $|LFC| > 1$ threshold and a FDR < 0.001 was used. Gene set enrichment analysis (GSEA) was performed on the 3000 most differentially expressed genes clustered by the HOPACH algorithm ($|LFC| > 1$, FDR < 0.001) (Adzima, Bustamam and Aldila, 2019; Van der Laan and Pollard, 2003). The plant-specific MapMan4 functional BIN system was used for refined protein classification and annotation and as input ontology for testing annotated gene clusters with clusterProfiler (Schwacke et al., 2019; Yu, 2018).

2.3.3 RT-qPCR analysis

For RT-qPCR analysis of transcripts in different tissues, 200 ng of total RNA were used for cDNA synthesis and diluted 1:10. The RT-qPCR was run with qPCR Mix Eva Green® No Rox (Bio&Sell GmbH) with 3 µL cDNA and 2 pmol of each primer in a 10 µL reaction and monitored by CFX Connect Real-Time System (Bio-Rad Laboratories, Inc.). The experiments were performed with three technical replicates of three biological independent samples. Primers were listed:

Table 2-1: Primer use for RT-qPCR

	Primer and Sequence
CDC73	qP-RNA-PM-3-for: CCAAGCCCAAGATGCACCTA qP-RNA-PM-3-rev: GAAGACGCCGTCCTCAAGAA
PnCPR	q-CPR-for: TCCCCTCTCCCTGCAGTTTA q-CPR-rev: TCTTGGCTTCGCTAGGTTCCG
CYP719A37	qP3-CYP719-for: GTTTGTGATCGGCGCCA qP3-CYP719-rev: CGCCACCTGCAACTTT
eIF2B	qP-eIF2B-for: CAATGCTTGAAGGGCAGTCG qP-eIF2B-rev: AACACAGATGCAGCTCCCAA
Piperamide synthase	qP-BAHD1-for: GAAAGCGGCAACCTCCTTTG qP-BAHD1-rev: AACTTGGTCCGGGAGTTGAC
Piperine synthase	qP-BAHD2-for: TTGGCGATATCGGAGCACTC qP-BAHD2-rev: CGATCCCGCCGCAAATAAAG

Piperoyl-CoA ligase	qP-TR3893-for: ATTTACCGGTCACTCAGGCC qP-TR3893-rev: ATTGGCATCGGCTAGAGCAA
----------------------------	--

2.3.4 Cloning

2.3.4.1 *Traditional cloning strategy*

The traditional cloning strategy was used in the case of piperine and piperamide synthase as well as piperoyl-CoA ligase. Based on RNA sequencing data selected genes were amplified by gene specific primers (**Table 2-3**) using Phusion polymerase (Thermo Scientific, Germany). Resulting amplicons were purified with Nucleo Spin Clean-up PCR kit (Macherey-Nagel), restricted by restriction enzymes (New England Biolabs), and cloned into MCS of chosen linearized entry-vectors by T4 DNA ligase (Promega) by standard protocols (**Table 2-2**). The recombinant proteins show an N-terminal His₁₀- (piperine and piperamide synthase) or His₆-tag (CoA ligases), respectively.

Table 2-2: Traditional cloning strategy: restriction enzymes and entry-vector

	Restriction enzymes	Entry-vector
At4CL6	BamHI / Sall	pQE30 (Quiagen)
Piperamide synthase	NdeI / BamHI	pET-16b (Novagen)
Piperine synthase	NdeI / BamHI	pET-16b (Novagen)
	BamHI / Sall	pET-Duet - MCS I (Novagen)
Piperoyl-CoA ligase	BamHI / Sall	pQE30 (Quiagen)
	NdeI / XhoI	pET-Duet - MCS II (Novagen)

2.3.4.2 *Golden Gate cloning*

The Golden Gate assembly was used in the case of the cytochrome P450 monooxygenase, and the reductase. From the transcriptome dataset two full length genes encoding CYP719A37 and PnCPR were identified and cloned for expression in yeast by the Golden Gate cloning strategy (Marillonnet and Grützner, 2020). The genes were amplified with gene specific primers (**Table 2-3**). Thereby, internal BsaI and BpiI restriction sites were removed by a silent point mutation in the initial sequence fragments, at level -1. These fragments were assembled into a level 0-entry vector with the full-length sequence of each amplicon. Afterwards assembled amplicons encoding PnCYP719 and PnCPR were combined with the synthetic-galactose-inducible promoter 6 (Gal6) and the tPGK-1 terminator in a level 1 construct. In level M the PnCYP719 cassette was then combined either with the final PnCPR- or ATR1 (alternative reductase gene from *A. thaliana*) expression cassette. The Gal6-promoter, tPGK1-terminator and ATR1-cassette were kindly provided by Alain Tissier and Ulschan Bathe (IPB) (Scheler et al., 2016). Cloning vectors contained an origin of replication for *E. coli* (ColE1) and for *Saccharomyces cerevisiae* (2 μ m ori). The entry-vectors had different

selection markers (kanamycin: level-1; ampicillin: level 1; spectinomycin: level 0 and M). The URA3 gene, encoding orotidine 5-phosphate decarboxylase was used as selection marker for positive yeast transformants. See also **Figure 8-6 – Figure 8-10**.

Table 2-3: Primer used for cloning and RT-qPCR

	Primer and Sequence
At4CL6	4g05160_F1_Bam: TTAATGGATCCATGGAGAAATCCGGCTACGGCAGAG 4g05160_R1_Sal: ATTAATAGTTCGACTCACATCTTGGATCTTACTTGCTGAAC
PnCPR	CPR1-1-for: TTTGGTCTCAACATAATGGAGTCGGGCTCTTCCA CPR1-1-rev: TTTGGTCTCAGCCCGACGAGGAGGGCCGCGGA CPR1-2-for: TTTGGTCTCAGGGCTCGTTGCCGCCCTCGT CPR1-2-rev: TTTGGTCTCAATACAGTGACCTTCCTCTTC CPR1-3-for: TTTGGTCTCAGTATTCTTCGGCACTCAGAC CPR1-3-rev: TTTGGTCTCAACAACCTCATGATCATAAAAATACAA CPR1-4-for: TTTGGTCTCAACATGAGGACTCACGTATTCAAGA CPR1-4-rev: TTTGGTCTCACACCAGTTTCATAATGAAGTC CPR1-5-rev: TTTGGTCTCAACAAAAGCTCACCAGACATCGCGCA
CYP719A37	Cypep1: TTGGTCTCAACATAATGGAGCAAGCTCAATGGGTGCGAC Cypep2: TTGGTCTCAACAACGTGGAAACGTGCCTGCGCCGAAAC Cypep3: TTGGTCTCAACATGAGGACATGAAGCTCCTGGTGAGCGAC Cypep4: TTGGTCTCAACAAAAGCTCATGCACGCGGAACGATTTTGGC Cypep5: TTGGTCTCAACATAATGGCTCATTGGGTCAACCCAGC Cypep6: TTGGTCTCAACAACCTCTTCGTGGAAATGTGCCTGCG Cypep7: TTGGTCTCAACATGAGGACATGAAGCGGTTGGCGAGC Cypep8: TTGGTCTCAACAAAAGCTCATGCACGAGGAACGATCTTGGC
Piper-amide synthase	BAHD1-for: CATCATATGGCTTCTTCTCAGCTCGAATTC BAHD1-rev: CATGGATCCTTACATGCGGGACATGTACCCATG
Piperine synthase	BAHD2-for: CATCATATGGCGCCTTCTTCTCAACTTG BAHD2-rev: CATGGATCCTTACATGCGGGAAAGGTATCCATC
	BAHD2-Duet1-P1-for: TTAATGGATCCGATGGCGCCTTCTTCT BAHD2-Duet1-P1-rev: TATTAATAGTTCGACTTACATGCGGGAAAG
Piperoyl-CoA ligase	TR3893_for1_Bam: TTAATGGATCCATGGAGAAGTCTGGCTATGGAAATG TR3893_rev1_Sal: TATTAATAGTTCGACTTATATCTTTGATCGAACTTTGGCGA
	TR3893-Duet1-P2-for: TTAATCATATGAGAGGATCGCATCACCAT TR3893-Duet1-P2-rev: TATTAATACTCGAGTTATATCTTTGATCGAACTTT

2.3.4.3 *Plasmid preparation and sequencing*

In all cases, 5 mL LB-medium with required antibiotics were inoculated with single colony and incubated overnight at 37 °C. Plasmids were isolated by Nucleospin® plasmid purification kit (Machery-Nagel) and amplicons sequenced by Eurofins Genomics.

2.3.4.4 GenBank accession numbers and RNA sequencing dataset

Identified black pepper enzymes were submitted to the National Center of Biotechnology Information (NCBI, <https://www.ncbi.nlm.nih.gov/genbank>) and have following accession numbers:

Table 2-4: GenBank accession numbers

Enzyme	Accession number
CYP719A37	MT643912
Piperine synthase	QUS53100
Piperamide synthase	QUS53101
Piperoyl-CoA ligase	QGY72664
PnCPR	MT643912
Pn4CL2	Unpublished, available at IPB: bachelor thesis of Raika Milde (2019)

RNA-Seq data were stored in array express and are accessible under the following link: <http://www.ebi.ac.uk/arrayexpress/experiments/E-MTAB-9029>. All publication data are accessible in the public repository RADAR (<https://www.radar-service.eu>) and the access is provided using DOI: 10.22000/400, 10.22000/271, and 10.22000/381.

2.4 Biochemical methods

2.4.1 Preparation of methanolic extracts from black pepper tissues

Frozen tissue of different black pepper compartments was macerated by a ball mill (Retsch) and resuspended in 90 % methanol at a concentration of 100 mg/mL. After sonification for 5 min, the extract was cleared by centrifugation at 20,000 x g for 2 min. Fruit and root extracts were further diluted down to 1 mg/mL or 10 mg/mL. All samples were analysed by HPLC-UV-MS.

2.4.2 Transient gene expression

Piperine - and Piperamide synthase (pET-16b)

The expression plasmids were transformed into *E. coli* LEMO21 cells (New England Biolabs) according to manufacturer specifications. A single colony was used for inoculation 25 mL LB-medium (50 µg/mL ampicillin, 30 µg/mL chloramphenicol) and shaken at 37 °C overnight. The pre-culture was used to inoculate 250 mL LB-medium 1:50 containing both antibiotics and additional 0.2 mM rhamnose. Induction with 1 mM IPTG occurs after the cell density reached 0.7 (OD₆₀₀). The culture was shaken for 12-14 h at 25 °C. Cells were recovered by centrifugation (4,000 x g, 10 min, 4 °C) and stored at -80 °C until reprocessing.

Piperoyl-CoA ligase and At4CL6 (pQE30)

After successful transformation in *E. coli* M15p [Rep4], a single colony was used for inoculation of 25 mL LB-medium (50 µg/mL ampicillin). After incubation overnight at 37 °C, 8 mL of the pre-culture was used to inoculated 400 mL LB-medium. After reaching a cell density of 0.7 OD₆₀₀ the recombinant protein expression was induced by addition of 1 mM IPTG and grown for 20-22 h at 25 °C. Cells were recovered by centrifugation (4,000 x g, 10 min, 4 °C) and stored at -80 °C until reprocessing.

CYP719A37 and PnCPR

The expression plasmids containing CYP719A37 and PnCPR or ATR1 were transformed into yeast strain *S. cerevisiae* INVSc1 (Invitrogen, California) according to the manufacturer specifications. A single yeast colony was used to inoculate 5 mL Ura3-medium with 2 % (w/v) glucose (yeast synthetic drop-out medium without uracil, Sigma-Aldrich) and grown at 30 °C and 170 rpm overnight. The pre-culture was used to inoculate 200 mL Ura3-medium with 2 % (w/v) glucose in a 1 L chicane flask and grown under the same conditions. After 24 h the cells were recovered by centrifugation (4,000 x g, 10 min, 25 °C) and suspended in yeast extract-peptone medium with 2 % (w/v) galactose. After another 24 h of incubation the cells were used for preparation of microsomal fractions or in transient yeast cell assays.

Piperoyl-CoA ligase and piperine synthase (pET-Duet1)

See section 2.5.6.

2.4.3 SDS-PAGE and immunoblotting

SDS-PAGE and Coomassie-Staining

SDS-PAGE and immunoblotting were performed by standard protocols and was performed on a Mini PROTEAN® Tetra Cell unit (Biorad). The gel concentration was always 10 %. For Coomassie staining Roti®-Blue quick solution (Roth) was used and if necessary, the gel bleached with water.

Detection of piperine and piperamide synthase by immunoblotting

Recombinant piperine synthase and piperamide synthase were prepared and 2 mg/each were used for polyclonal antibody production by immunization and following boosts of two New Zealand White rabbits for 51 days. The immunization reaction was performed by ProteoGenixSAS (Schiltigheim, France). Antibodies and pre-immune serum were tested against recombinant piperine and piperamide synthase as well as plant tissue to determine the efficiency.

For Western blot protein fractions were separated by a 10 % SDS-gel and blotted on an activated nitrocellulose membrane (Amersham™ Protran™ Premium 0.2 µm NC, GE Healthcare) by Trans-Blot®Turbo™ (BioRad). The blotted membrane was incubated in 5 % (w/v) milk powder in 1x PBS buffer overnight. The first antibody reaction was performed with 1:5000 dilution of polyclonal rabbit anti-piperamide-synthase-antibody for 2 h with slight shaking at room temperature. After washing with 1x PBS-Tween three times, the membrane was incubated with 1:10000 dilution of goat anti-rabbit-IgG (whole molecule) with coupled alkaline phosphatase for 1 h. After washing three times for 10 min in 1x PBS-tween buffer the membrane was shortly incubated in 100 mM TRIS/HCl (pH 9.5), 100 mM NaCl und 5 mg MgCl₂. The color reaction was performed by adding NBT/BCIP mixture and stopped with water.

2.4.4 Recombinant protein purification

All recombinant proteins except CYP719A37 and PnCPR/ATR1 contained an N-terminal His-tag for purification by ion metal-affinity chromatography. The stored pellets were dissolved in 50 mL buffer (50 mM TRIS-HCl pH 7.5, 150 mM NaCl, 10 % glycerol, EDTA-free protease inhibitor (Roche), some crystals of DNase1 and lysozyme (Roche)). After 20 min incubation on ice, the suspended cells were disrupted twice at 1.3 kbar by French press (device TS 0.75, Constant Systems LTD). The homogenate was centrifuged (10,000 x g, 10 min, 4 °C) and the debris discarded. RNA was precipitated by adding 4 % (w/v) protamine sulfate in a final concentration of 0.05 and discarded by centrifugation at 100,000 x g, 30 min and 4 °C. The cleared supernatant was purified using pre-packed Ni-NTA columns (Macherey-Nagel). His-tagged recombinant protein was eluted with 300-400 mM imidazole in 50 mM TRIS-HCl pH 7.5, 150 mM NaCl, 10 % (v/v) glycerol. The enzyme was concentrated using centrifugal filters (Millipore) with a MWCO of 30.000 Da. Further purification was carried out by size exclusion chromatography. 500 µL of the concentrate were applied to a Sephadex 200 Increase 30/100 column (GE Healthcare) in case of piperine- and piperamide synthase. For CoA ligase purification a HiLoad 16/60 Superdex 200 prep grade column (GE Healthcare) was used. In all cases, all fractions eluting from the column were checked for protein content and for enzymatic activity. Fractions of highest activity were combined and used for subsequent characterization of the enzyme i.e., kinetic constants. The enzymes were stored at -80 °C and were stable for several months

2.4.5 Crystallization

Different concentrations of recombinant monomeric piperamide synthase (2 – 6 mg/mL), with or without 500 µM hexanoyl-CoA or piperoyl-CoA as co-substrate, were combined with different crystallisation screens (Listed in **Table 2-5**). The procedure was performed with an Oryx 8 LCP pipetting robot (Douglas Instruments). Following plates were used for the screening: MRC 2-well (SWISSCI), MRC 3-well (SWISSCI) or EasyXtal 15-Well Tools

(QIAGEN). The incubation temperature was or 20 °C. The screens were checked several times up to 4 months by Rock Imager RI54 (Formulatrix) or manual. Preliminary diffraction data were collected from single crystals using the X-ray diffractometer Synergy-R Micro7HF (Fa. Rigaku-Oxford Diffraction) and the X-ray detector ARC150 (Fa. Rigaku-Oxford Diffraction).

Table 2-5: Crystallization screening kits

Kit	Firma
Crystal Screen HT	Hampton Research
Index HT	Hampton Research
JBScreen Classis 1-4	Jena Bioscience
JBScreen Classis 5-8	Jena Bioscience
JBScreen Classis 9-10	Jena Bioscience
JBScreen JCSG++	Jena Bioscience
JBScreen Wizard	Jena Bioscience
MIDAS	Molecular Dimensions
Morpheus	Molecular Dimensions

2.4.6 Protein preparation of black pepper material

Protein preparation from black pepper fruits based on Geisler and Gross (1990)

Black pepper fruits between 40 – 100 dpa were harvested. Approximately 5 g were grinded per hand and further by precooled ball mill for 30 s with a frequency of 30 s⁻¹ (Retsch). According to Geisler and Gross (1990) a buffer mixture of 44 mL 0.1 M borate buffer (pH 7.5) and 36 mL 1 M TRIS-HCl buffer (pH 8.0) was prepared. The agents 50 mM ascorbic acid, 10 mM (v/v) 2-mercaptoethanol and plant protease inhibitor cocktail (Sigma-Aldrich) were added. The plant powder was mixed with 3 g prewashed PVPP in 50 mL prepared borate/TRIS buffer (pH 7.3) and stirred for 20 min in an ice bath. The cell debris was removed by centrifugation for 10 min, 20.000 x g at 4 °C. The supernatant was further filtrated through two preincubated layers of Miracloth (Millipore). For DNA and RNA precipitation 0.05 % (v/v) protamine sulphate was added. The supernatant was precipitated stepwise with 30 % (w/v) ammonium sulphate and stirred for 15 min in an ice bath. The precipitate was removed by centrifugation for 10 min, 20.000 x g at 4 °C and filtration through two layers of Miracloth. The black pepper piperine synthases were precipitated with 80 % (w/v) ammonium sulphate, which was stepwise added under stirring and incubated for 30 min in an ice bath. After centrifugation (20 min, 20.000 x g, 4 °C) the precipitate was resuspended in 50 mM TRIS/HCl (pH 7.5), 150 mM NaCl, 5 % (v/v) glycerol and 5 mM DTT and desalted by PD-10 desalting column (GE Healthcare) in the same buffer. The protein fraction was concentrated by using centrifugal filters (Millipore) with a MWCO of 30.000 Da and clarified by centrifugation for 10 min,

20.000 x g at 4 °C. The solution was applied on a Sephadex 200 Increase 30/100 column (GE Healthcare) equilibrated in the same buffer. The fractionation was carried out with a flow rate of 0.2 mL/min at an Äkta explorer system (P-900, UV-900; pH/C-900) equipped with UNICORN 5.2 software. 10 µL of each protein fraction were checked for enzymatic activity and analysed by SDS-PAGE with Coomassie staining or immunoblotting.

Small amounts of different plant tissues for immunoblotting (Wessel and Flügge, 1984)

Approximately 200 mg of grinded plant powder was mixed with 1.2 mL PVPP-borate/TRIS buffer, prepared like described before. After sonification for 5 min in a water bath and centrifugation for 10 min, 20.000 x g at 4 °C, 800 µL methanol and 200 µL chloroform were added to 200 µL of the supernatant and mixed vigorously. Afterwards 600 µL water was added and mixed vigorously. After phase separation by centrifugation (10 min, 20.000 x g, 4 °C) the upper phase was discarded and the proteins were precipitate by adding 600 µL methanol and vigorous mixing. The solution was centrifuged for 15 min, 20.000 x g at 4 °C, the supernatant discarded. The dried precipitate was resolved in 10 µL borate/TRIS buffer and 250 µL SDS-sample buffer and boiled for 5 min at 95 °C. Per sample 10 µL were loaded on a gel and separated by SDS-PAGE. The gel was further stained with Coomassie or used for immunoblotting.

2.5 Enzyme activity measurements

2.5.1 Extraction of microsomes and following *in vitro* assays

Microsomal fractions were prepared according to Scheler et al. (2016). Briefly, the yeast cells were centrifuged and crushed with glass beads (Ø 0.25 – 0.5 mm) several times in extraction buffer containing BSA and sorbitol. After centrifugation at 100,000 x g for 2 h at 4 °C, the microsomes were resuspended in 50 mM TRIS/HCl 7.5, 1 mM EDTA and 30 % glycerol. The protein concentration was determined with Bradford reagent (Bio-Rad) and the microsomal fractions were stored at -80 °C for further experiments. For *in vitro* assays 50 – 250 µg crude protein of microsomal fractions were used and with 250 µM of putative substrate, 1 mM NADPH in 50 mM HEPES buffer (pH 7.5) in a total volume of 600 µL incubated for 2 - 24 h at 30 °C and 90 rpm. The reaction was stopped by 20 µL 20 % formic acid and incubated for 10 min on ice. Metabolites were extracted with 600 µL ethyl acetate and the organic phase was concentrated into 100 µL 100 % methanol. Product formation was monitored by HPLC-UV-ESI-MS.

2.5.2 Determination of enzyme activity in transient yeast cell assays

After co-expression of *PnCYP719* with *PnCPR* or *ATR1*, yeast cells were centrifuged and adjusted with 50 mM HEPES (pH 7.5) to a final OD₆₀₀ = 50. For activity measurements 95 µL of the yeast suspension were incubated with 5 µL of 5 mM putative substrate at 30 °C

at 1,000 rpm overnight. The yeast cells were centrifuged at 25,000 x g for 20 min. The supernatant was separated. The yeast cells were resuspended in 100 µL of a mixture with four parts (v/v) methanol one part (v/v) 20 % formic acid and incubated again at 30 °C, 1,000 rpm overnight. The initial supernatants and the methanolic cell extracts were analysed by HPLC-UV-ESI-MS.

2.5.3 Activity measurements of CoA ligases

The activity of CoA ligases was performed in total volume of 100 µL for routine photometric assays. Usually, 1 µg CoA ligase was incubated with 300 µM Coenzyme A, 2.5 mM ATP, 2.5 mM MgCl₂ and 50 µM putative substrate in 50 mM TRIS-HCl buffer (pH 7.5). For inactivation of the enzyme, the protein was boiled for 10 min at 8 °C and stored until usage on ice. The reaction was started by adding the putative substrate and was incubated up to 1 h at 30 °C and 300 rpm. The reaction was stopped by adding 100 µL methanol and after centrifugation (10,000 x g, 5 min, 4 °C) the supernatant was analysed by a spectrophotometer (NanoPhotometer, IMPLEN). The bathochromic wavelength shift was monitored between 290 – 410 nm. For analytical and kinetic measurements, the reactions contained varying concentrations on putative substrate and 0.1 to 1 µg recombinant CoA ligase. The reactions were incubated at 30 °C and 300 rpm for 1 to 5 min for kinetics and up to 3 h for complete substrate turnover. By adding 6.5 µL (v/v) 20 % formic acid the reaction was stopped and afterwards cleared by centrifugation at 20,000 x g for 10 min at 4 °C. All reactions were performed at least in three replicates. Quantitative activity measurements were analysed by HPLC-UV-ESI-MS.

2.5.4 Production of CoA esters on a semi preparative scale

For production of hydroxycinnamoyl-CoA derivatives 50 µg CoA ligase was incubated with 20 mg CoA-SH, 5 mg hydroxycinnamic acid derivative, 50 mg ATP and 10 mg MgCl₂ in 50 mM TRIS/HCl buffer (pH 7.5) for 2 h at 30 °C. The total reaction volume was 10 ml. Additional 50 µg CoA ligase, 25 mg ATP and 10 mg CoA-SH were added after 1h. The reaction was stopped after 1 h with 250 µL 20 % formic acid. Remaining piperic acid was extracted with ethyl acetate 1:1. After adding 4 % (w/v) ammonium acetate to the aqueous solution, it was applied to HLB-solid phase cartridges (Waters) (see also 2.2.1). After washing with 4 % (w/v) ammonium acetate solution and water, the hydroxycinnamoyl-CoA derivative was eluted with a stepwise increasing methanol gradient. The reaction and preparation were monitored by UV-absorption measurements. After evaporation and lyophilisation, the hydroxycinnamoyl-CoA derivative was diluted in 20 % DMSO and the purity was checked by HPLC-UV-ESI-MS.

2.5.5 Activity measurements of piperine synthase and piperamide synthase

All activated CoA esters were produced in a semi-preparative scale by CoA ligases, except for 3,4-(methylenedioxy) cinnamoyl-CoA, which was synthesized chemically (Schnabel

et al., 2020; Semler, Schmidtberg and Gross, 1987). The substrates were dissolved in 25-50 % DMSO and kept in dark tubes, especially piperoyl-CoA to reduce isomerisation. For activity measurements 1 - 2 μg of the purified recombinant enzyme was incubated with 200 μM activated CoA ester, 4 mM amine in a 30 mM TRIS/HCl (pH 8.0) buffer with 1 mM DTT in a total volume of 50 μL up to 30 min. A reaction mix without enzyme acts as negative control and was simultaneously incubated. The reactions were stopped by adding 10 μL of 50 % acetonitrile/ 10 % formic acid mixture. After centrifugation for 10 min, with 20.000 x g at 4 °C the reactions were analysed by HPLC-UV-MS. Every reaction was performed at least in triplicates. Due to the absence of commercial standards, piperine (0.1 μM – 100 μM) was used for MS and UV-based quantification of product formation in the case of all piperamides produced. Kinetic constants for piperine formation were determined in three independent measurements with different enzyme preparations in three technical replicates each. Concentration of substrates were 20 μM - 2000 μM (piperoyl-CoA) and 1 mM – 100 mM (piperidine), with one substrate set ad variable condition and the other one in saturating condition. Between 0.5 μg and 1 μg were used and the incubation time was set to 5 min and 10 min at 30 °C and 50 mM TRIS/HCl pH 8.0 final concentration.

2.5.6 In vivo fermentation

E. coli SOLU BL21 cells (Genlantis) were used for expression of piperine synthase and piperoyl-CoA ligase. As negative control cells transformed with pET-Duet-TR3893 (piperoyl-CoA ligase), pET-Duet-BAHD2 (piperine synthase) or empty vector pET-Duet are used. After inoculation with a single colony, 5 mL LB-culture (50 $\mu\text{g}/\text{mL}$ ampicillin) was shaken at 28 °C overnight. The pre-culture was used to inoculate 5 mL LB-medium to a final $\text{OD}_{600} = 0.2$ and were shaken at 25 °C, 220 rpm. At an $\text{OD}_{600} = 0.4$ the induction with 1 mM IPTG was followed. The cells were incubated at 25 °C, 220 rpm overnight. The cell suspension (1 mL) was incubated with 1 mM piperic acid and 10 mM piperidine or pyrrolidine at 25 °C, 400 rpm for 1 h. The supernatant was collected and extracted 1:1 with ethyl acetate. The organic phase was dried, and the product dissolved in 100 μL 90 % methanol. The reactions were done in triplicates and were analysed by HPLC-UV-ESI-MS.

2.6 Analytical methods

2.6.1 Spectroscopy

For rapid measurements CoA ligase based assays were measured in a NanoPhotometer (IMPLEN) in UV cuvette micro (Brand) from 290 – 410 nm.

2.6.2 High pressure liquid chromatography

All samples were analysed with the Waters Alliance HPLC equipped with the PDA UV-detector and the QDA mass detector. The different experimental setups are listed in the

following tables (**Table 2-6 – Table 2-9**). The data analysis was done with the Empower III software (Waters).

Table 2-6: Experimental setup for LC-MS analysis of methanolic plant extracts

		Gradient		
Column	Nucleosil® RP 100-5 C ₈ , 4 µm, 12,5 cm (Machery-Nagel)	Time (min)	A (%)	B (%)
UV (nm)	220 – 550 nm	0.00	70	30
Mass (m/z)	200 600 m/z; positive mode	10.00	10	90
Flow	0.8 mL/min	10.50	5	95
Solvent A	0.1 % (v/v) formic acid in water	10.80	70	30
Solvent B	acetonitrile	16.00	70	30

Table 2-7: Experimental setup for LC-MS analysis for *in vitro* assays of Piperine synthase and Piperamide synthase and for analysis of the feeding experiments

		Gradient		
Column	Nucleoshell® RP18, 2.7 µm, 5 cm (Machery-Nagel)	Time (min)	A (%)	B (%)
UV (nm)	250 – 500 nm	0.00	70	30
Mass (m/z)	150 – 560 m/z; positive mode	7.00	20	80
Flow	0.6 mL/min	7.50	20	80
Solvent A	0.1 % (v/v) formic acid in water	7.70	70	30
Solvent B	acetonitrile	12.00	70	30

Table 2-8: Experimental setup for LC-MS analysis for *in vitro* assays of CoA ligases

		Gradient		
Column	Nucleosil® RP 120-5 C ₁₈ , 5 µm, 12,5 cm (Machery-Nagel)	Time (min)	A (%)	B (%)
UV (nm)	240 – 400 nm	0.00	95	5
Mass (m/z)	180 – 1000 m/z; positive and negative mode	6.00	5	95
Flow	0.5 mL/min	7.00	5	95
Solvent A	10 mM (w/v) ammonium acetate in water	7.10	95	5
Solvent B	Mixture of 20 % (v/v) isopropanol and 80 % (v/v) acetonitrile	12.00	95	5

Table 2-9: Experimental setup for LC-MS analysis for *in vitro* CYP719A37 assays with microsomal fractions and transient yeast cell assays

		Gradient		
Column	Nucleoshell® RP18, 2.7 µm, 5 cm (Machery-Nagel, Germany)	Time (min)	A (%)	B (%)
UV (nm)	220 – 400 nm	0.00	90	10
Mass (m/z)	100 – 300 m/z; positive mode	7.00	10	90
Flow	0.6 mL/min	7.50	10	90
Solvent A	0.1 % (v/v) formic acid in water	7.70	90	10
Solvent B	100 % acetonitrile	12.00	90	10

2.7 Special software

SigmaPlot 14.0 (Systat Software Inc.) was used for scientific plots and data analysis. Chemical structures were drawn with ChemDraw Professional 17.0 (Perkin Elmer). Affinity Designer 1.9.1.979 (PANTONE® Colours) was used for figure design. EndNote X8.2 (PDF Tron™ Systems Inc.) was used to manage literature, bibliographies and references.

3 Results

3.1 Identification of piperine biosynthetic genes

3.1.1 Piperine content in different plant tissues and during fruit development

Piperine is the predominant metabolite in black pepper fruits. It can be detected easily by UV/Vis-spectroscopy (λ_{\max} = 340 nm) as well as mass spectrometry (m/z = 286.1 [M+H]⁺) (Figure 3-1, B). Different plant tissues from black pepper were harvested, ground and extracted by 90 % methanol. Their piperine content was quantified by HPLC-UV-ESI-MS (Figure 3-1, A). Piperine was the dominant methanol-soluble metabolite in maturing fruits, starting to accumulate in early fruit stages I (20 dpa) and stage II (40 dpa). The small amount of piperine in mature roots is negligible compared to the content in fruits. In leaves and flowering spadices no piperine was detected.

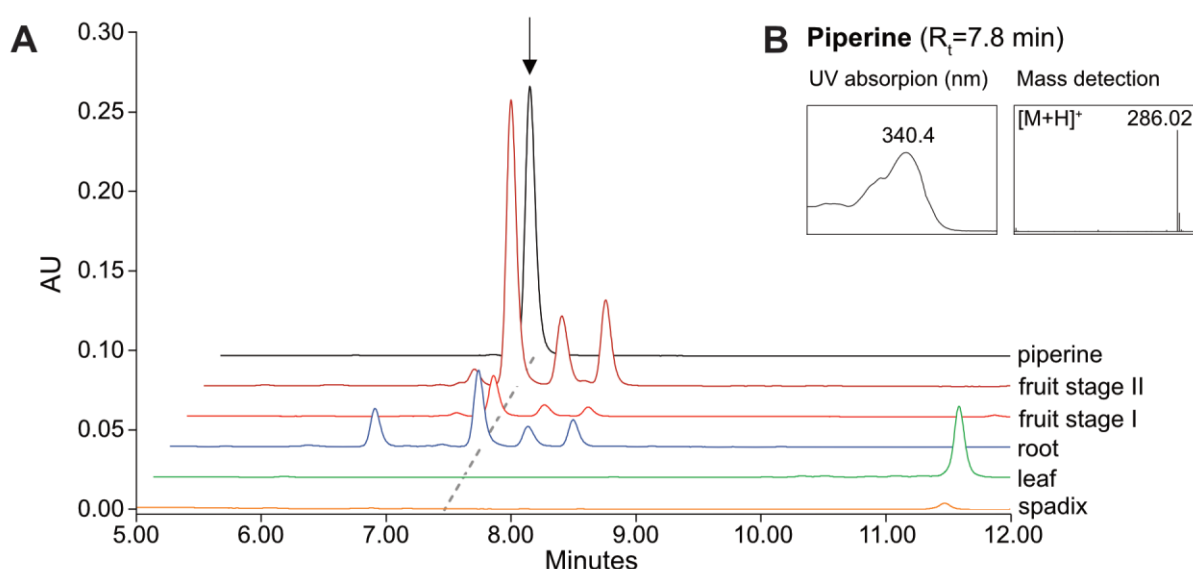


Figure 3-1: Detection of piperine and related amides in different black pepper tissues

Methanolic extracts (90 %) of flowering spadices, leaves, roots and fruits (stage I and II) were analysed by HPLC-ESI-MS and UV/Vis-spectroscopy and were compared to a 500 pmol piperine standard (A). The piperamides were recorded between 320 – 380 nm and piperine was identified with λ_{\max} = 340 nm and m/z = 286.1 [M+H]⁺ (B). Piperine and related amides are absent in flowering spadices and leaves. They occur in low quantities also in mature roots. In fruits piperine is the by far predominant specialized metabolite.

Due to the hypothesis of parallel piperine accumulation and biosynthesis in black pepper fruits, the piperine content during complete fruit development was monitored (Figure 3-2). Spadices of individual plants were marked, and single fruits were harvested at certain time points, the piperine content was measured and compared to a piperine standard. The time course showed that after the lag-phase up to 20 days post anthesis (dpa) piperine could be monitored and was rising constantly. In the following three months the content significantly increased up to 2.5 % piperine per g fresh weight. A stationary phase is reached after around

six months. At about 8 months post anthesis the fruits turn red and subsequently dropped off, and the piperine content dropped.

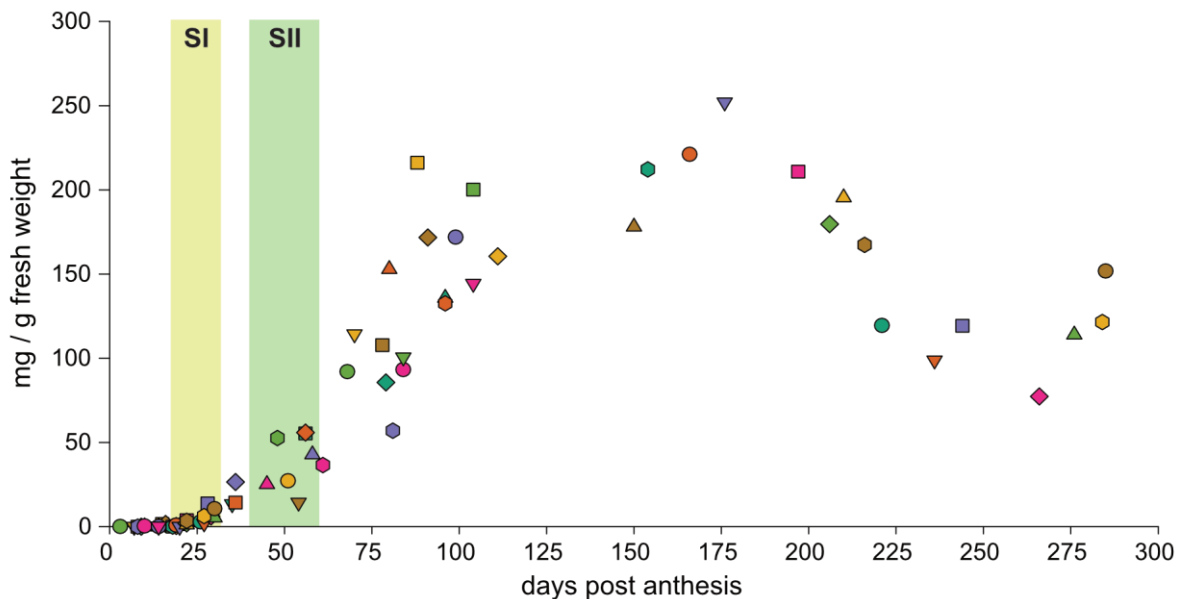


Figure 3-2: Piperine accumulation during fruit development

The piperine contents were quantified from 90 % methanolic extracts of black pepper fruits. Each symbol marks the piperine content of a single fruit from different spadices at different time points. Piperine was detected by UV/Vis ($\lambda_{\max} = 340 \text{ nm}$) and compared to the piperine standard. The piperine content was calculated back to mg per g fresh weight. The fruit stages I (SI : 20 – 30 dpa) and II (SII : 40-60 dpa) were chosen for comparative RNA-sequencing approach and are marked in colored boxes.

3.1.2 De novo assembly of the black pepper transcriptome

We assumed that transcript levels of enzymes preceded piperine biosynthesis and thus the time points fruit stage I (SI: 20 – 30 dpa) and stage II (SII: 40 – 60 dpa) were chosen as optimal candidates for a comparative RNA-sequencing approach. Highest transcript levels were expected shortly before the slope of piperine formation was at its maximum, whereas some transcript should already be present shortly or around the 20-30 dpa, stage I time point. Young leaves and flowering spadices served as negative control. In both organs no, or very low piperine amounts were detected likely consistent with the lack of the transcripts encoding the biosynthetic enzymes (see also **Figure 3-1**). The plant material was harvested, ground and the RNA was extracted. The RNA preparations were checked for RNA quality (**Figure 3-3**). Based on the signal intensity of the detectable bands, especially of 28S (~4718 nt) and 18S (~1874 nt) ribosomal RNA, the RNA integrity was determined (Schröder et al., 2006) (Suppl.: **Figure 8-5**). RNA preparation with a high concentration and an RNA integrity number of 9 or 10, for intact RNA, were chosen and submitted in triplicates (150 ng each) to a commercial enterprise for sequencing and *de novo* RNA-sequencing analysis. Sequencing included library preparation based on an unstranded protocol, paired-end sequencing with 150 cycles per read and the following demultiplexing of the raw data (Grabherr et al., 2011).

Averages of 25 million paired-end reads per sample were received. The dataset was further processed by Benedikt Athmer (IPB). The Trinity and Trans-ABYSS software tools were used

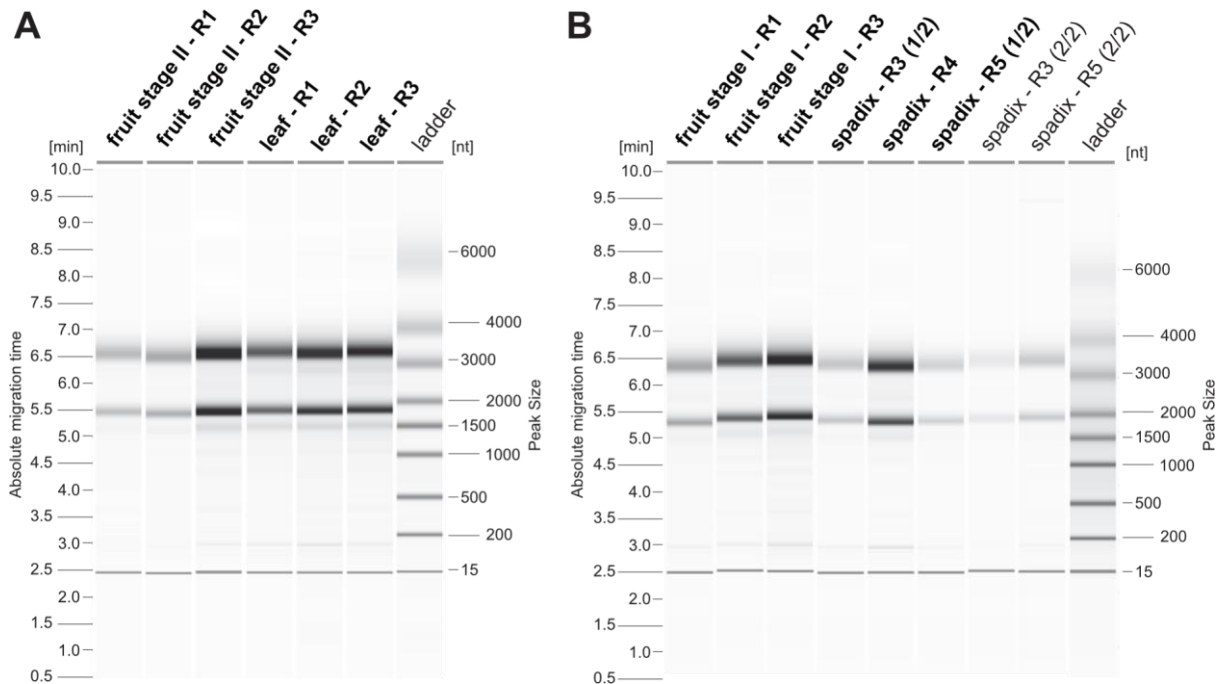


Figure 3-3: Quality check of RNA samples for RNA sequencing

Per lane, 1 μ L each RNA sample were loaded and separated by microcapillary electrophoretic RNA separation (QIAxcel). The RNA pattern was compared to QX RNA Size Marker 200–6000 nt ladder (QIAxcel). For comparability in every samle 1 μ L of QX RNA 15 nt Alignment Marker (QIAxcel) as internal standard was added. Samples were chosen based on a RNA integrity number of 9 or 10 for RNA sequencing (bold; see also Suppl.: **Figure 8-5**).

for *de novo* assembly and the processed reads could be classified in 540.916 transcripts and 208.308 genes. Up to 9000 full-length genes could be annotated by a BLAST search against the Universal Protein Resource database (UniProt). With the HOPACH clustering tool the 3000 most differently expressed genes were identified and summarised in **Figure 3-4**. The heatmap of these unigenes shows varying individual transcript profiles for all plant organs under investigation. The leaf samples show a predominant cluster for photosynthesis, CALVIN-cycle, and carotenoid-biosynthesis. In flowering spadices developmental and regulatory transcripts appear most. The transcripts of fruit stages I and II clearly differ in comparison to leaves and flowering spadices. The early fruit stage I shows transcripts related to cell wall, cytoskeleton biosynthesis and cell cycle. Expression of these genes fits into processes that start the ongoing fruit development. In a highly coordinated way, especially in fruit stage II, transcripts coding for enzymes of plant specialized metabolism, specifically of terpenoid and phenylpropanoid biosynthesis, are over-represented.

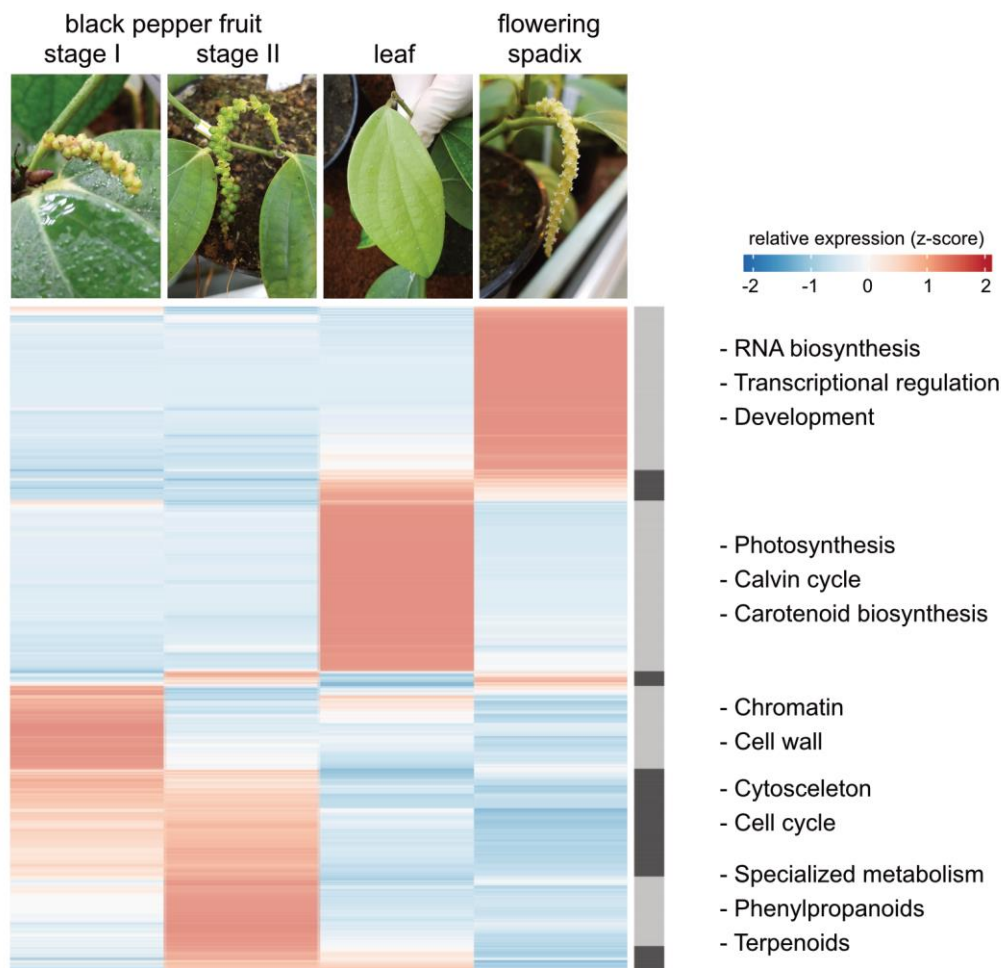


Figure 3-4: Heatmap of the top 3000 differentially expressed genes, clusters of their biological function and related plant organs.

The HOPACH hybrid clustering of the 3000 most significant differentially expressed genes from related plant organs is shown (false discovery rate (FDR) < 0.2, |LFC| > 1). The analysis was performed “first level” clusters. Over-represented categories were exemplified and highlighted (FDR < 0.001). Intensive red color indicates high and blue color low expression. Related biological functions are added.

3.1.3 Identification of candidate genes

The most abundant transcripts in fruit stage I and II encode a series of genes with similarity to genes in specialized metabolism (**Table 3-1**). Within the 20 most abundant hits, annotations for several BAHD-type acyltransferases were detected. They were annotated as acetyl- and benzoyltransferases, termed (Z)-3-hexen-1-ol acetyltransferase- and benzyl alcohol O-benzoyltransferase and were already at this early stage considered as piperine synthase (marked green). Further transcripts were annotated as cheilanthifoline- or (S)-canadine synthase. These CYP719A-type enzymes catalyze the methylenedioxy bridge formation, also a potential step in piperine biosynthesis. These sequences not only match potential candidate genes, but also follow a very similar pattern of transcript abundance (**Figure 3-5**) - low abundance at stage I, higher abundance at stage II, and virtual absence in

flowers and in leaves. This pattern matches the piperine accumulation and therefore, these apparently co-expressed genes seem to represent ideal candidates potentially involved in the biosynthesis of piperine and piperamides.

Table 3-1: Most abundant transcripts in fruit stage I and II compared to leaves and flowering spadices.

Single transcripts were assembled by the Trinity software and annotated by BLAST search against the Universal Protein Resource database (UniProt). The transcripts of fruit stage I and II are ranked beginning with most abundant transcript in fruit development compared to leaves and flowering spadices. The top transcript encodes a BURP-protein of unknown function. The following transcripts are related to specialized metabolism, specifically terpenoid biosynthesis or phenylpropanoid biosynthesis. The first five hits already include two genes encoding BAHD acyltransferases and that might be involved in piperine biosynthesis. Overall, the first 20 transcripts indicate a strong initiation of specialized metabolism consistent with piperine accumulation. Transcripts encoding BAHDs are colored in green. Transcripts encoding CYP-candidates are marked in yellow. (tmp = transcripts/million)

			mean expression (tpm)			
			fruit stage I	fruit stage II	leaf	flowering spadix
Top	TRINITY_DN56430_c3_g3	BURP domain-containing protein 3	14871.2	17784.7	639.1	611.1
1	TRINITY_DN49139_c0_g3	Terpene synthase 10	199.1	1090.8	2.0	5.3
2	TRINITY_DN43391_c4_g4	(Z)-3-hexen-1-ol acetyltransferase	194.2	700.0	6.7	10.9
3	TRINITY_DN48006_c1_g1	Putative lipid-transfer protein DIR1	848.7	636.5	0.2	85.8
4	TRINITY_DN53695_c0_g9	Cheilanthisfoline synthase	157.9	549.4	2.6	12.1
5	TRINITY_DN60552_c4_g3	Chalcone synthase 3	618.0	476.7	45.3	41.0
6	TRINITY_DN43391_c4_g1	Benzyl alcohol O-benzoyltransferase	121.4	464.7	6.6	7.0
7	TRINITY_DN53695_c0_g2	(S)-canadine synthase	127.8	444.4	2.0	9.1
8	TRINITY_DN58395_c1_g1	Acyl-coenzyme A oxidase 4	165.0	411.5	10.9	17.0
9	TRINITY_DN60378_c4_g1	Esterase FUS5	92.6	368.8	0.5	4.0
10	TRINITY_DN53669_c1_g4	Benzyl alcohol O-benzoyltransferase	116.8	352.0	11.4	10.0
11	TRINITY_DN42578_c0_g1	Esterase CG5412	64.2	346.9	0.3	1.6
12	TRINITY_DN43391_c4_g5	Benzyl alcohol O-benzoyltransferase	113.9	333.6	4.7	4.8
13	TRINITY_DN51211_c1_g2	Alpha-terpineol synthase	108.5	328.4	0.5	7.8
14	TRINITY_DN42232_c1_g1	Adenylate isopentenyltransferase 3	336.6	326.7	5.8	34.5
15	TRINITY_DN53669_c1_g1	Benzyl alcohol O-benzoyltransferase	100.7	288.8	8.9	7.4
16	TRINITY_DN60552_c3_g1	Chalcone synthase 3	91.7	282.8	0.6	6.6
17	TRINITY_DN43950_c0_g1	Germin-like protein 8-2	291.7	278.5	11.1	1.6
18	TRINITY_DN52087_c0_g2	Beta-cubebene synthase	98.2	270.4	7.1	12.5
19	TRINITY_DN43083_c1_g1	Germacrene A synthase	157.7	232.5	39.5	18.0
20	TRINITY_DN56875_c1_g1	Triacylglycerol lipase 1	164.2	231.5	12.9	2.7

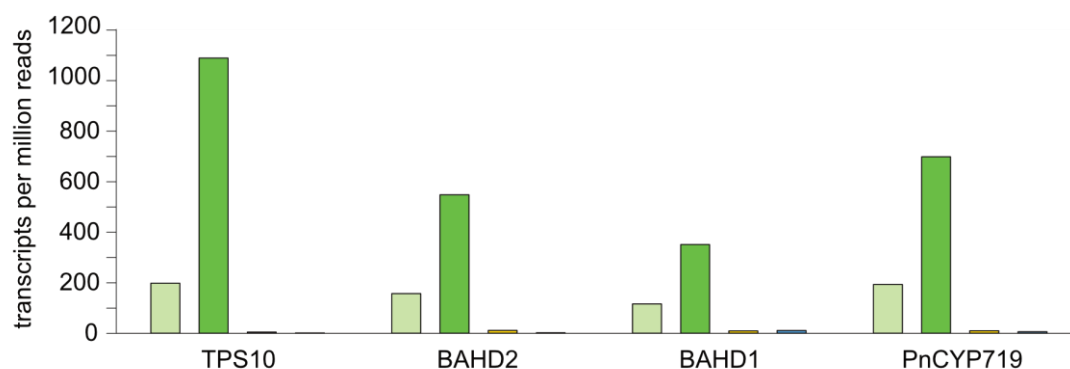


Figure 3-5: Graphical representation of high abundance transcripts

The transcript levels of fruit stage I (light green) and fruit stage II (green) were compared with flowering spadices (yellow) and leaves (blue). TPS10-like terpene synthase was the most abundant transcript of specialized metabolism followed by two transcripts encoding BAHD-like enzymes and one transcript encoding CYP719 homolog.

3.2 Formation of a methylenedioxy bridge by PnCYP719

3.2.1 Cloning and expression of PnCYP719 and PnCPR

A single full-length sequence could be obtained from the RNA sequencing fragments 4 and 7 (listed in **Table 3-1**). The full-length sequence showed a high similarity to genes encoding cheilanthifoline and S-canadine synthases. Both enzymes catalyze the formation of a methylenedioxy bridge in isoquinoline biosynthesis (Bauer and Zenk, 1991; Ruffer and Zenk, 1994). The assembled transcript of 1512 bp encoded a protein of 56 kDa (PnCYP719), which is consistent with the expected molecular size of plant CYP719A enzymes (**Figure 3-6**) (Díaz Chávez et al., 2011; Ikezawa et al., 2003; Pluskal et al., 2019; Yahyazadeh et al., 2017).

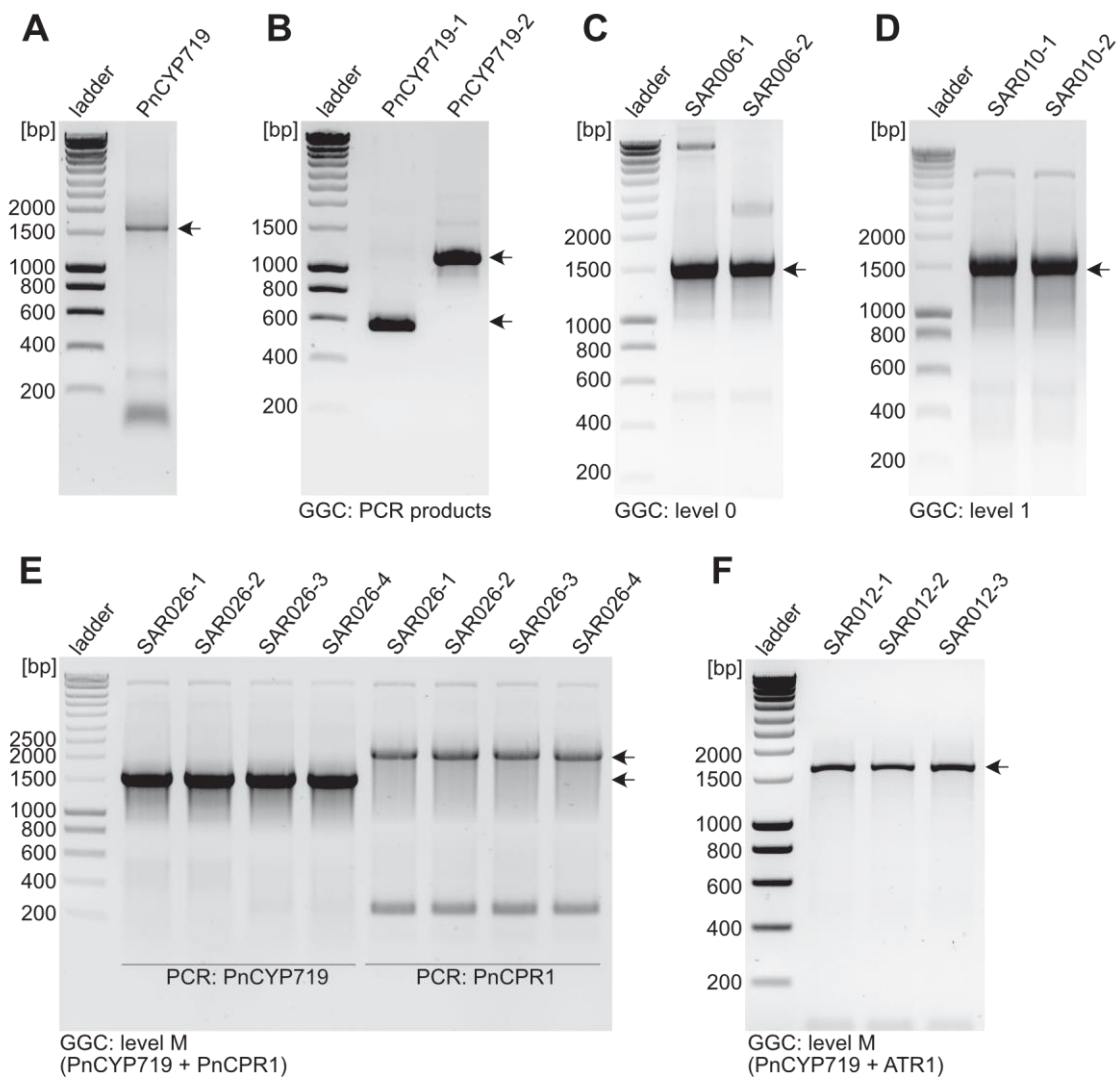


Figure 3-6: Verification of PnCYP719 (1543 bp) and PnCPR (2121 bp) at different levels of Golden Gate cloning (GGC)

Every step in Golden Gate cloning was verified by a PCR reaction, analysed in a 1 % agarose gel and stained with ethidium bromide: (A) PnCYP719 from cDNA of black pepper fruit stage II; (B) GGC fragments PnCYP719-1 (514 bp) and -2 (1059 bp) from cDNA of black pepper fruit stage II; (C) verification of PnCYP719 in level 0 vector; (D) verification of PnCYP719 in level 1 vector; (E) verification of PnCYP719 and PnCPR in level M vector; (F) verification of PnCYP719 in level M vector with ATR1. Expected amplicon is marked with an arrow. The vectors are named SARXXX, consistent with the GGC strategy (see also Suppl.: **Figure 8-6 - Figure 8-10**)

Transcripts coding for cytochrome P450 enzymes from the CYP81Q clade were not observed. A single full-length transcript (2154 bp) encoded a NADPH-dependent cytochrome P450 reductase (PnCPR). To isolate and clone the corresponding genes from fruits, total RNA from fruit stage II was extracted and cDNA synthesized. The sequences encoding the newly identified PnCYP719 and PnCPR genes were amplified and cloned using the modular Golden Gate cloning system (**Figure 3-6**, see also for cloning strategy Suppl.: **Figure 8-6 – Figure 8-10**) (Marillonnet and Grützner, 2020). The gene encoding the alternative reductase, ATR1 from *A. thaliana* was kindly provided by Alain Tissier and Ulschan Bathe (IPB).

ER-localized cytochrome P450 enzymes and cytochrome P450 reductases were already successfully characterized by heterologous expression in yeast (Sauveplane et al., 2009; Scheler et al., 2016; Yahyazadeh et al., 2017), thus the genes encoding PnCYP719 combined with the amplicons encoding either PnCPR, or alternatively ATR1, were simultaneously expressed in the yeast *S. cerevisiae*.

3.2.2 PnCYP719 is substrate specific

Substrates with the essential aromatic vanilloid structure but differences in length of the aliphatic carbon chain were selected as potential substrates (Suppl.: **Figure 8-11**) and fed directly to intact yeast cells or added to isolated yeast microsomal fractions to determine the activity of PnCYP719. The most plausible precursors were ferulic acid, feruperic acid, and feruperine (**Figure 3-7**), the latter ones were kindly synthesized by our collaboration partner Fernando Cotinguiba (Federal University of Rio de Janeiro, Brazil) during a sabbatical at the IPB Halle (Schnabel et al., 2021b). Feruperine can be also found in small amounts in black pepper (Inatani, Nakatani and Fuwa, 1981).

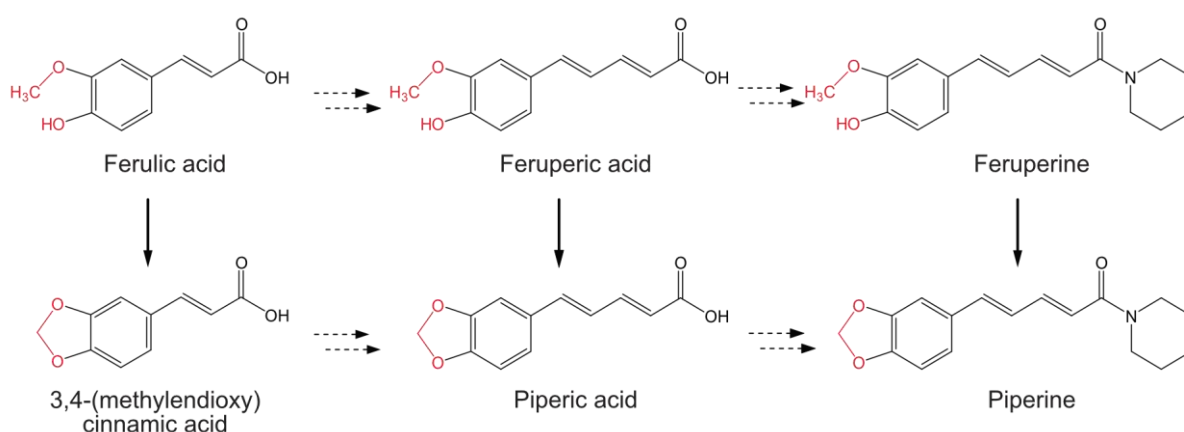


Figure 3-7: Putative precursor for methylenedioxy bridge formation in piperine heterocycle

The three most plausible precursors for introduction of an 3,4-methylenedioxy bridge in the piperine heterocycle are shown (bold arrow). Further unknown steps in piperine biosynthesis are marked with dashed arrows.

After heterologous co-expression of PnCYP719:PnCPR, PnCYP719:ATR1 or cells transformed with empty vector, microsomal fractions of these yeast cells were prepared. Substrates at a final concentration of 250 μ M were added, and extracted to monitor the product formation by HPLC-UV-ESI-MS. The products were identified based on commercially available or synthesized standards, UV-spectra and/or expected product mass. Feruperic acid was the only substrate, which was converted into piperic acid, a methylenedioxy bridge containing compound (**Figure 3-8, A**).

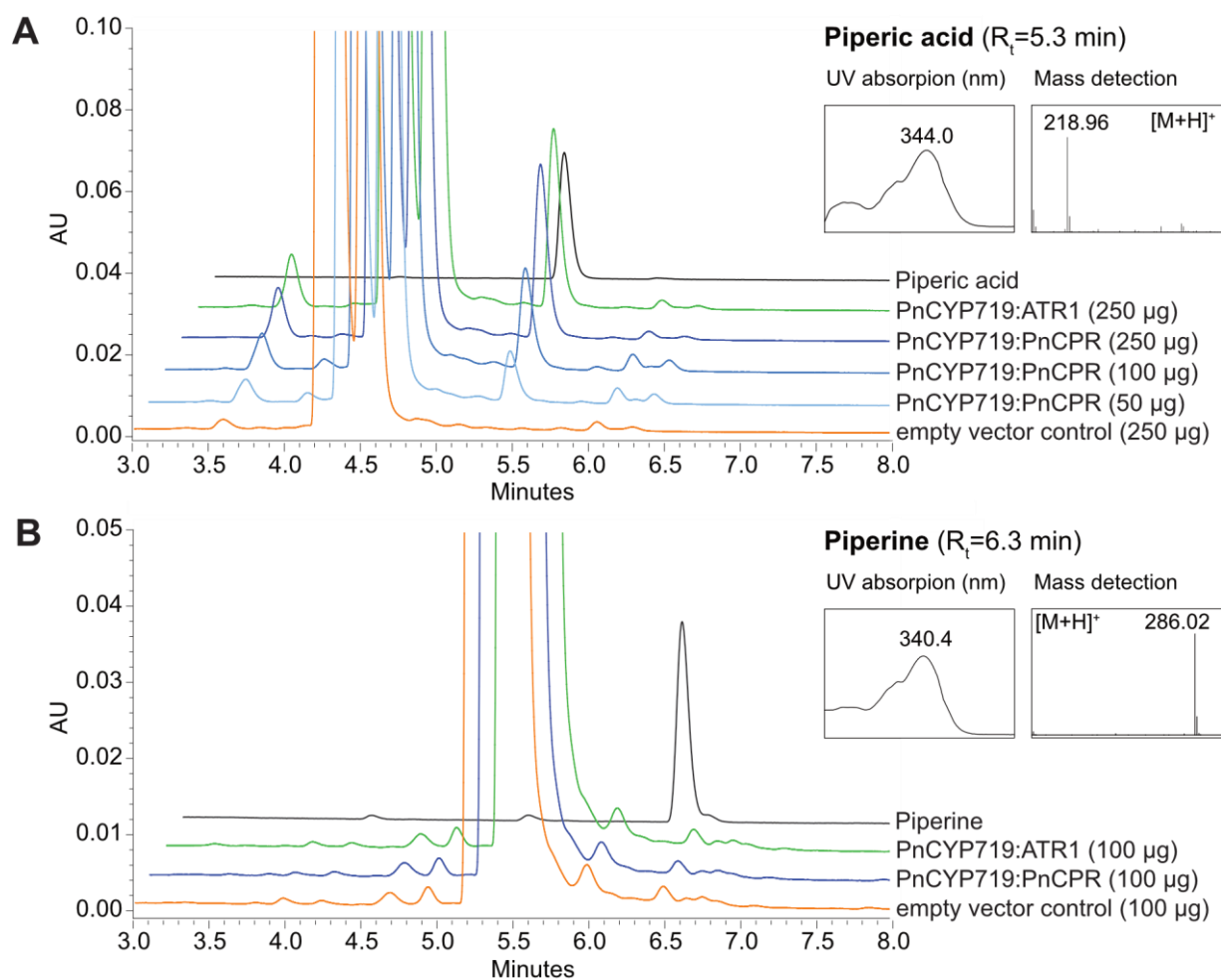


Figure 3-8: PnCYP719 catalyzes the methylenedioxy bridge formation within the aromatic part of the piperine molecule.

PnCYP719 and PnCPR or ATR1 were heterologous expressed in *S. cerevisiae*. Microsomal fractions were isolated and incubated with 250 μ M feruperic acid (**A**) for 2 h or feruperine (**B**) for 24 h. After extraction with ethyl acetate, the organic phase was dissolved in methanol and the product formation was analyzed by HPLC-UV-ESI-MS. Different amounts of microsomes with PnCYP719:PnCPR (light blue, blue, dark blue) or PnCYP719:ATR1 (green) were used. As controls the empty vector control (orange) and 10 pmol piperic acid (black) or 10 pmol feruperine (black) as standards are shown. For feruperic acid as substrate the UV signals were monitored at 344 nm. Piperic acid was confirmed by corresponding single mass ion ($m/z = 219.1$, [M+H]⁺). By adding feruperine the UV signals were monitored by 340 nm and the single mass recorded by $m/z = 286.1$ [M+H]⁺.

The product peak showed an UV maximum at 344 nm and a mass signal of $m/z = 219.1$ $[M+H]^+$ and was confirmed by a commercial standard as piperic acid. A steady increase of product formation from 50 μg to 250 μg total protein amount underline the protein-dependence. For proton-supply it was irrelevant if PnCPR or ATR1 were co-expressed with the CYP719 candidate. No product formation was observed with microsomes isolated from wildtype or cells transformed with the empty vector. In all other cases, no product formation with a methylenedioxy bridge was monitored (Suppl.: **Figure 8-12**, **Figure 8-13**), especially not by adding feruperine as a substrate, even with prolonged incubation times of 24 h (**Figure 3-8**, B). This experiment confirmed, consistent with previous assumptions, that the methylenedioxy group is introduced into the piperine skeleton before amide bond formation (Geisler and Gross, 1990). The maximum activity of the newly identified PnCYP719 was calculated as 0.92 ± 0.05 pkat/mg crude microsomal protein (**Table 3-2**).

Several detoxification products of phenolic compounds were observed by adding C6-C3 or C6-C1 substrates in intact yeast cell assays (Suppl.: **Figure 8-13**, **Figure 8-14**). Coniferyl alcohol was converted into vanillic acid ($m/z = 171.1$ $[M+H]^+$) and ferulic acid ($m/z = 195.1$ $[M+H]^+$). Coniferyl aldehyde was oxidized into ferulic acid. The analysis of yeast cell assays fed with ferulic acid showed a product peak at $R_t = 5.2$ min and a single mass of $m/z = 151.1$ $[M+H]^+$, which was tentatively identified as 2-methoxy-4-vinylphenol. This compound is also detected in assays with coniferyl aldehyde as well as coniferyl alcohol in smaller amounts. Vanillyl alcohol and vanillyl aldehyde were oxidized into vanillic acid. These products were reported previously from yeast assays (Wang et al., 2016) and were synthesized by endogenous reductases and dehydrogenases as detoxification mechanisms in yeast cells (Suppl.: **Figure 8-14**).

Table 3-2: Substrates tested in microsomal and intact yeast assays with heterologous expressed PnCYP719 and reductases, PnCPR or ATR1

All substrates showed an aromatic vanilloid moiety but different length in the aliphatic carbon chain. PnCYP719 enzyme catalyzes the oxidation and cyclization of the ortho-hydroxymethoxy groups resulting in a methylenedioxy bridge. This reaction is exclusive for feruperic acid (green) and resulted in the formation of piperic acid. Putative substrates and their products with expected masses ($[M+H]^+$) are listed and the activities of PnCYP719 determined (Schnabel et al., 2021b).

Substrate [m/z]	Product [m/z]	Activity [pkat/ mg crude protein]
Feruperic acid [221.1]	Piperic acid [219.1]	0.92 \pm 0.05
Feruperine [288.1]	Piperine [286.1]	n.d. ²
Ferulic acid [195.1]	3,4-(methylenedioxy) cinnamic acid [193.1]	n.d.
Coniferyl aldehyde [179.1]	3,4-(methylenedioxy) cinnamyl aldehyde ¹ [177.1]	n.d.
Coniferyl alcohol [181.1]	3,4-(methylenedioxy) cinnamyl alcohol ¹ [179.1]	n.d.
Vanillic acid [168.1]	Piperonylic acid [166.1]	n.d.
Vanillyl aldehyde [153.1]	Piperonal ¹ [151.1]	n.d.
Vanillyl alcohol [155.1]	Piperonyl alcohol [153.1]	n.d.

¹ reference was not available, identification was based on expected mass signals; ² n. d. – not detected

3.2.3 Phylogeny and structural aspects of CYP719A37 and PnCPR

Only a single full-length transcript was detected in the whole RNA sequencing dataset, which encoded a methylenedioxy bridge-catalyzing enzyme. When analysed by amino acid sequence, PnCYP719 shows 95 % identity to CYP719A26, a recently published cytochrome P450 enzyme from the *Piper methysticum* rhizome (Pluskal et al., 2019). CYP719A26 introduces a methylenedioxy bridge into the kavalactone skeleton. As an orthologue of CYP719A26, David Nelson (<http://drnelson.utmem.edu/CytochromeP450.html>, University of Tennessee, Memphis, U.S.A.) classified this *P. nigrum* CYP719, as CYP719A37, since it shows a similar sequences but a different substrate specificity as compared to CYP719A26 (Nelson, 2009). A corresponding phylogenetic tree shows representatives of the families CYP719, CYP77, and CYP81, all members of the CYP71 clan (**Figure 3-9**). CYP719A37 and CYP719A26 share 50 % identity to several classified CYP719A and CYP719B enzymes.

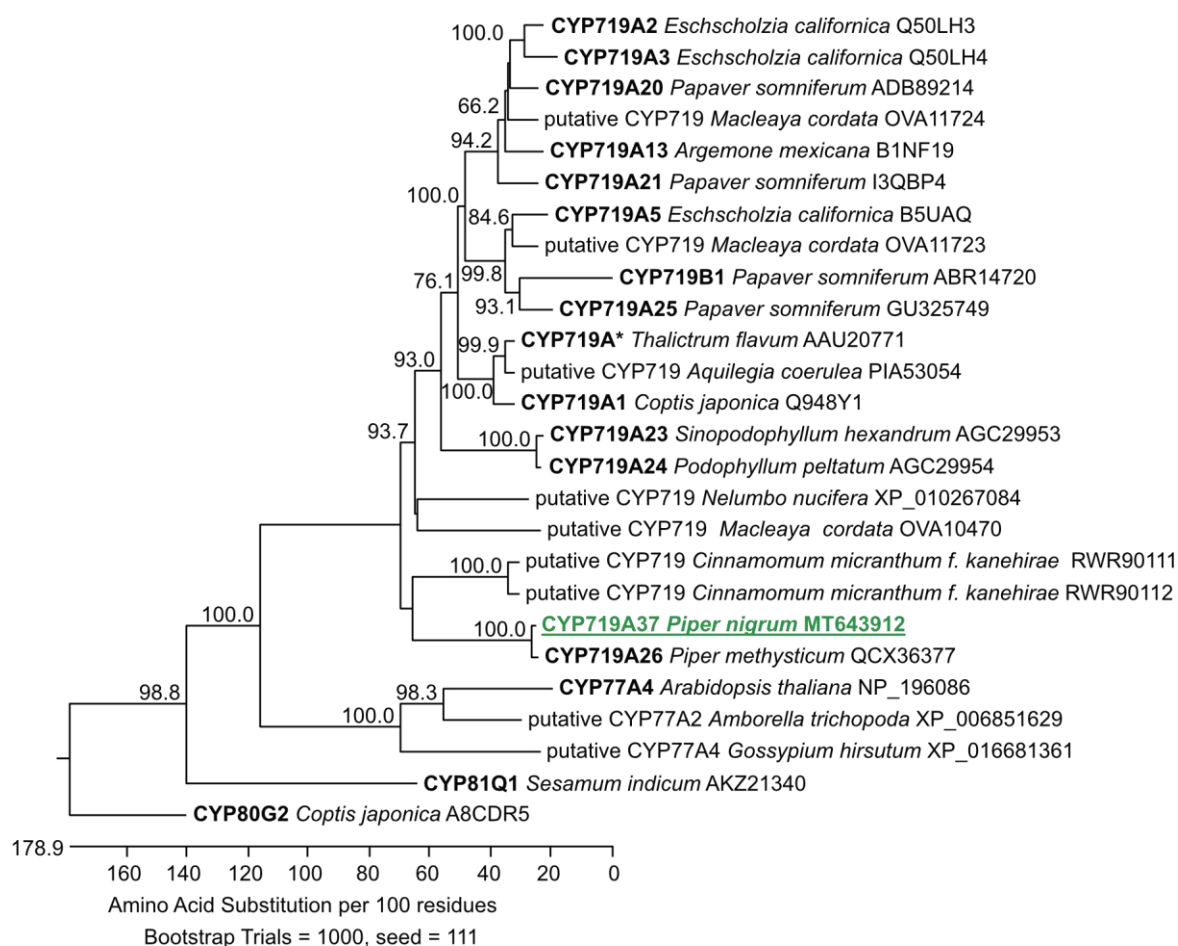


Figure 3-9: Bootstrapped, unrooted cladogram of CYP71 clan families CYP719, CYP77, CYP81 and CYP80 protein sequences obtained using ClustalW.

Shown are cytochrome P450 enzymes, related plant species and NCBI accession numbers. Bold – functional characterized enzymes; asterisks – without unique number given by Dr. David Nelson. *Piper nigrum* CYP719A37 is shown in green and underlined.

CYP719A members catalyze steps in benzyloquinoline alkaloid biosynthesis, like cheilanthifoline, (S)-canadine and stylophine synthases from opium poppy (*Papaver somniferum*) or prickly poppy (*Argemone mexicana*) (Díaz Chávez et al., 2011; Rüffer and Zenk, 1994; Yahyazadeh et al., 2017), all functionally characterized including the first enzyme of this clade tetrahydroberberine synthase from japanese goldthread (*Coptis japonica*) (Ikezawa et al., 2003). CYP719B1 from prickly poppy is the only C-C phenol-coupling enzyme in the whole clade (Gesell et al., 2009). Apparently, the sequence for a C-C coupling enzyme is hardly distinguishable from methylenedioxy group formation. CYP719A37 and CYP719A26 are localized in a distinct subclade with highest identity to unknown enzymes from stout camphor tree (*Cinnamomum micranthum f. kanehirae*).

Interestingly, members of CYP81, represented by CYP81Q1, are clearly distinct from the CYP719 clade although in principle the same type of reaction is catalyzed. CYP81Q1 from sesame (*Sesamum indicum*) catalyzes the methylenedioxy bridge in the sesamin biosynthesis (Ono et al., 2006). Outside the CYP719 clade, CYP719A37 shows highest identity to CYP77A4 from *A. thaliana*. This enzyme is involved in epoxidation of fatty acids in the primary metabolism (Sauveplane et al., 2009).

CYP719A37 shows typical cytochrome P450 features, like the C-terminal heme-binding domain, the K helix and the aromatic binding site (**Figure 3-10**). A hydrophobic membrane anchor on the N-terminus predicts an ER-localization. Like all members of the CYP719A clade, CYP719A37 contains two characteristic substitutions, Gly300Leu and Thr304Ser.

The identified PnCPR showed a high identity with already characterized oxidoreductases, like ATR1 (63 %) and ATR2 (68 %) from *A. thaliana*. Classical features of cytochrome P450 oxidoreductases, like FMN-PP_i-, FMN-isoallozazine-, FAD-PP_i-, NADPH-ribose- and substrate binding domains are conserved and highlighted (Suppl.: **Figure 8-15**).

membrane-anchored region										
CYP719A37 (Pni)	-----M	EQAQWVDPAL	FSAFVSIIEF	FLGMFLGRIS	LGVGKGAAPR	SPSSTEWHDG				
CYP719A26 (Pme)	-----M	EQAQWVDPTL	LPAFVGIIEF	FLGMFFGRSS	LGAGKGAAPR	STSSTEWHDG				
CYP719A1 (Cja)	-----MEMN	PLLVCATVAI	VFATTTIIRI	LF-----	-----SSS	SLPQMKWHSK				
CYP719A5 (Eca)	-----M	EESLWVVVAT	VVVVFVIAKL	LK-----	-----KSS	SISTMEWHSK				
pCYP77A2 (Atr)	-----	-MALLYLFSI	LSALLFCYLF	LS-----	-----SR	KTKALKLHPG				
CYP77A4 (Ath)	MFPLISFSPT	SLDFTFFFAI	ISGFVFIITR	WN-----	-----SN	SKKRLNLHPG				
							:	:	:	*

CYP719A37 (Pni)	PPKLPPIIGNL	HQLNKGGLV	HHKLAKLAQS	YDRAMTIWVG	SWGPMIVVSD	ADLAWEVLVV				
CYP719A26 (Pme)	PPKLPPIIGNL	HQLNKGGLV	HHLAKLAQS	YDRAMTIWVG	SWGPMIVVSD	ADLAWEVLVV				
CYP719A1 (Cja)	PRKLPPIIGNL	HQLG--DDVL	HVALAKLAKV	HGSVMTIWIG	SWRPVIVISD	IEKAWEVLVN				
CYP719A5 (Eca)	PKKLPPIIGNL	HQLG--GEAF	HVVLANLAKI	HGTVMTIWVG	AWRPVIVISD	IDKAWEVLVN				
pCYP77A2 (Atr)	PKGWFPLVGNL	LQIARSGKPF	VFIVNELSQK	YGPIFTLKM	AR-TLIVISS	AELAHEALIQ				
CYP77A4 (Ath)	PPGWVVGVLN	FQFARSGKPF	FEYAEDLKK	YGPIFTLRMG	TR-TMILISD	ATLVHEALIQ				
	*	*:*:*	*	:	:	:	:	:	:	*

CYP719A37 (Pni)	KSPDFAGRVL	SKLS-HLFNA	DYNTVVAYDA	GPQWQSLRRG	LQHGPLGPAH	VSAQARFHEE				
CYP719A26 (Pme)	KSPDFAGRVL	SKLS-HLFNA	NYNTVVAYDA	GPQWQSLRRG	LQHGPLGPAH	VSAQARFHEE				
CYP719A1 (Cja)	KSADYGARDM	PEIT-KIASA	SWHTISTSDA	GSFWQNVKRG	LQSGAMGPLN	VAAQNVYQER				
CYP719A5 (Eca)	KSSDYAGRDF	PEIT-KIIISA	NWKNISCSDS	GPWFQNLKRG	LQGGALPLN	VISQVQLQER				
pCYP77A2 (Atr)	KGQTFANRPA	ETPTRAIFSS	HKKTVNSAEY	GPLWRSLLRN	MVQGLMTPAK	LRAFRPIRKK				
CYP77A4 (Ath)	RGALFASRPA	ENPRTIFSC	NKFTVNAAKY	GPVRSLLRN	MVQNLMSSTR	LKEFGKLRQS				
	:	:	:	:	:	:	:	:	:	:

CYP719A37 (Pni)	DMKLLVSDMM	RAAKKGGNNG	VVEPLAYVRR	ATIRFLSRLC	FGEAFNDEAF	VEGMDEAVEE				
CYP719A26 (Pme)	DMKLLVSDMM	RAAQKGGNSG	VVEPLAYVRR	ATIRFLSRLC	FGEAFNDEAF	VEGMDEAVEE				
CYP719A1 (Cja)	DMKRLIKAMS	DEAAN--NNG	IVKPLDHKK	NTVRLRLRLI	FGQAFDDNKF	IESMHHYEID				
CYP719A5 (Eca)	DMKNLITSMQ	EKASK--NNG	ILKPLDYLKE	ETIRLLSRLI	FGQSFNDENF	VKGVHLALDD				
pCYP77A2 (Atr)	ALDKLVERLA	AESKS---G	LVRVLSNCRF	TVFRILLCMC	FGVEMDENMI	EKVDSVLKVV				
CYP77A4 (Ath)	AMDKLIERIK	SEARDN--DG	LIWVLKNARF	AAFCILLEM	FGIEMDEETI	EKMDEILKTV				
	:	:	:	:	:	:	:	:	:	:

CYP719A37 (Pni)	TIRATG----	HARILDAFYF	TRHLPIIRRS	FMNTVAAKKK	IESLVRPLLS	---RPAPPG				
CYP719A26 (Pme)	TIGATG----	HARILDAFYF	TRHLPIIRRS	FIDTVNAKKK	IESLVRPLLS	---RPAPPG				
CYP719A1 (Cja)	IIRISG----	YARLAEAFYF	AKYLPSHKKA	EREAFVVKCR	VEELVRPLLS	---SKPPTN				
CYP719A5 (Eca)	LVRISG----	YASLADAFKF	CENLPSHKKS	IREVHEVNRR	VVNLVKPYLV	---KNPPTN				
pCYP77A2 (Atr)	LITLEPRIDD	LPIPLQAIWF	KKVAHAHVH	KEQLETLPL	IRSRKKTQON	---AMSAP				
CYP77A4 (Ath)	LMTVDPRIDD	YLPIAPFFS	KERKRALEVR	REQVDVVGV	IERRRAIQN	PGSDKTASSF				
	:	:	:	:	:	:	:	:	:	:

CYP719A37 (Pni)	SYLHFLSSTD	AP-----E	SMIIFRIFEV	YLGVDSIAS	TTTWALAFVL	SNQQAQEKLH				
CYP719A26 (Pme)	SYLHFLSSTD	AP-----E	NMIIFRIFEV	YLGVDSIAS	TTTWALAFVL	SNQQAQEKLH				
CYP719A1 (Cja)	SYLYFLNSQN	FE-----E	EVIIFCIFEL	YLGVDSISS	TTTWALAYLI	REQQAQEKLY				
CYP719A5 (Eca)	TYLYFLNSQK	FS-----D	EVIIISAVLE	YLGVDSIAS	TAVWALTFLV	REPRVQEKLY				
pCYP77A2 (Atr)	AYIDSLFDLD	MG--QGPPSE	DMLVTLCAEF	LNSTDTAT	AVEWAMAHLV	ADSEIQRVR				
CYP77A4 (Ath)	SYLDTLFDLK	IEGRKTPSN	EELVTLCESE	LNSTDTAT	AIEWGIAQLI	ANPEIQSRLY				
	:	:	:	:	:	:	:	:	:	:

K helix										
CYP719A37 (Pni)	NELAQCASQ	NNQNIKAEDV	GKLSYLLGVV	KETMRMKPIA	PLAVPHKTLK	ETMLDGKRVA				
CYP719A26 (Pme)	NELAQCASQ	NNQIIKADDV	GKLSYLLGVV	KETMRMKPIA	PLAVPHKTLK	ETMLDGKRVA				
CYP719A1 (Cja)	QDIRMTLGDV	D--LVKIEDV	NKLKYLQGVV	KETMRMKPIA	PLAIPHKTAK	ETTLMGTKVA				
CYP719A5 (Eca)	KEIIDLTTGE	R--SVKVEDV	SKLHYLQAVM	KETMRMKPIA	PMAIPHKTSR	DTSLMGKQVN				
pCYP77A2 (Atr)	AEIDR-VSPD	H--RVNDEDV	EKMHYLQAFV	KETLRKHPPPT	YFLLTHAVTE	KSTLGGYDIP				
CYP77A4 (Ath)	DEIKSTVGDD	R--RVDEKDV	DKMVFQAFV	KELLRKHPPPT	YFSLTHAVME	TTTTLAGYDIP				
	:	:	:	:	:	:	:	:	:	:

aromatic region				heme-		
CYP719A37 (Pni)	AGTTVVVNLV	AVHYNPKLWP	EPEQFRPERF	VIGASGGNGG	GSSEYMLQSY	IPFGGGMRC
CYP719A26 (Pme)	AGTTVVVNLV	AVHYNPKLWP	EPEQFRPERF	VVGASGGNGG	GSSEYMLQSY	IPFGGGMRC
CYP719A1 (Cja)	KGTRIMVNLY	ALHHNQNIWP	DPYKFMPERF	LEG---ETGT	AYNKAMEQSF	IPFSAGMRC
CYP719A5 (Eca)	KGTSIMVNLY	AIHHNPKVFP	EPYKFIPERF	LQQG---ESKY	GDIKEMEQSL	IPFSAGMRC
pCYP77A2 (Atr)	EGVNVDFYTP	SISDDPKLWG	DPERFRPERF	VDRMDGDDDA	DLTGKVGKVM	MPPFGVGRIC
CYP77A4 (Ath)	AGVNVVEYLP	GISEDPRIWN	NPKKFDPRF	MLGKE---DA	DITGISGKVM	IPFGVGRIC
	*	:	:	:	:	*

binding domain						
CYP719A37 (Pni)	AGMEVGKLQV	AMVVANLVMS	FKWLPEAEGK	MPDLAEDMTF	VLMMKPLAA	KIVPRA--
CYP719A26 (Pme)	AGMEVGKLQV	AMVVANLVMA	FKWLPEEEGK	MPDLAEDMTF	VLMMKPLAA	KIVPRA--
CYP719A1 (Cja)	AGMDLGLKQF	AFALANLVNA	FKWSCVEEGK	LPDMGEELSF	VLLMKTPLA	RIAGRNV-
CYP719A5 (Eca)	AGMELGKLQY	GFSLASLVEA	FKWTCVADGK	LPDLSSEDFC	ILLMKNPLA	RITPRTQL
pCYP77A2 (Atr)	PGLGLGMLHI	SLMVATMVQQ	FEWLNPVAVP	RVDMSEKFEF	TVLMKTPLA	IAQPRKHK
CYP77A4 (Ath)	PGLAMATIHV	HLMLARMVQE	FEWCAHPPGS	EIDFAGKLEF	TVMKNPLRA	MVKPRI--
	:	:	:	:	:	:

Figure 3-10: Comparison of amino acid sequences of CYP719As and CYP77As with CYP719A37. Shown are characteristic features of cytochrome P450 enzymes (frames) as well as specific substitutions in the CYP719A clade (black boxes and dashed line). CYP719A26: *Piper methysticum* (MK058499.1); CYP719A1: *Coptis japonica* (Q948Y1.1); CYP719A5: *Eschscholzia californica* (B5UAQ8.1) putative CYP77A2: *Amborella trichopoda* (XP_006851629); CYP77A4: *Arabidopsis thaliana* (NP_196086). The protein sequences were aligned using CLUSTAL 2.1 Multiple Sequence Alignments. The similarity is indicated by: asterix – full conserved region; colon – strong similarity; period – weak similarity.

3.3 Piperoyl-CoA formation is catalyzed by a specific CoA ligase from black pepper fruits

3.3.1 Piperoyl-CoA - synthesis and biosynthesis

Initial efforts to synthesize piperoyl-CoA, the crucial substrate for the reported piperine synthase reaction, starting from piperic acid and coenzyme A based on a published method by Semler et al. (1987) and performed in collaboration with Bernhard Westermann and Angela Schaks (IPB) were successful. However, purification of the resulting CoA ester from the large amounts of dicyclohexyl urea, a side product of the reaction, was tedious. Therefore, a search for an alternative production of this CoA ester, that is not commercially available, was undertaken. A CoA ligase based biosynthesis seemed to be a suitable approach and has been reported in the literature (Beuerle and Pichersky, 2002). At that time of the project our own RNA-sequencing data was not yet available, but an RNA-sequencing dataset from black pepper fruits was analysed for putative CoA ligase candidate genes, who could activate piperic acid (Afgan et al., 2016; Hu et al., 2015). A promising query was a sequence corresponding to *A. thaliana* OPDA- and 5-phenylpentanoic acid CoA ligase (At4CL6: *At4g05160*), which activates oxylipids, precursors of the phytohormone jasmonic acid and similar compounds (Kienow et al., 2008; Schneider et al., 2005). One of its substrates, 5-phenylpentanoic acid, shows high structural similarity to piperic acid. A single sequence of the black pepper fruits transcriptome showed 60 % sequence identity to *At4g05160* at amino acid level and was selected as a promising candidate.

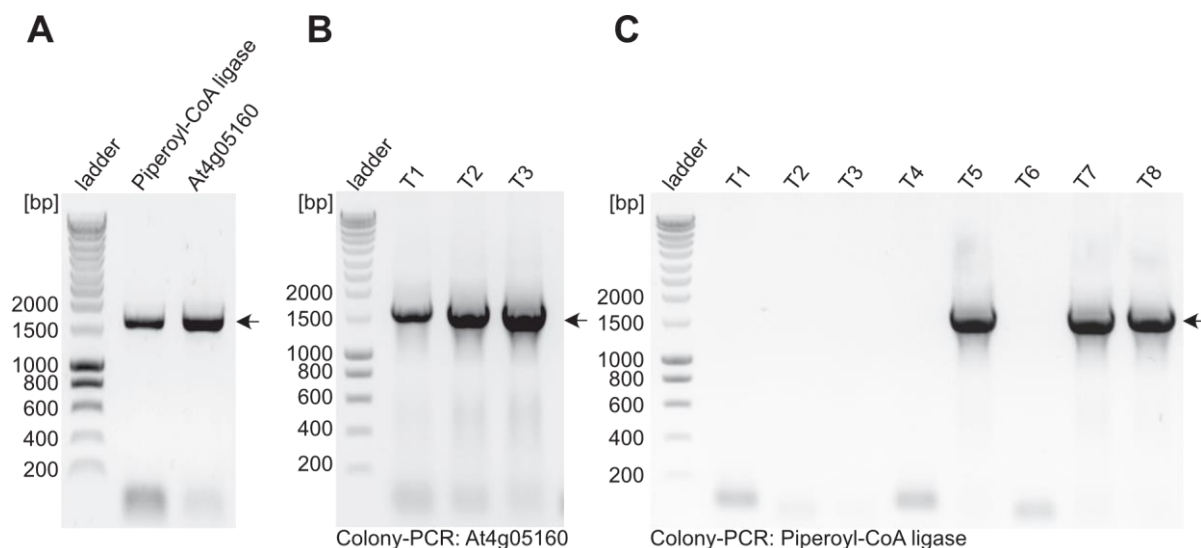


Figure 3-11: Verification of Piperoyl-CoA ligase and At4CL6 in expression vectors

Every step in the cloning procedure was verified by a PCR reaction, analysed in a 1 % agarose gel and stained with ethidium bromide: **(A)** *At4g05160* (1635 bp) from cDNA of *A. thaliana* flower buds and piperoyl-CoA ligase (1647 bp) from cDNA of black pepper fruit stage II; **(B)** single *E. coli* M15 [Rep4] transformants (TX) were tested for *At4g05160*; **(C)** single *E. coli* M15 [Rep4] transformants (TX) were tested for piperoyl-CoA ligase. Expected amplicon is marked with an arrow.

Total RNA was extracted from green black pepper fruits and *A. thaliana* flower buds and transcribed into cDNA. A full-length gene for a CoA ligase was obtained in black pepper fruits, which matches the suggested gene to 99 %. The corresponding genes, encoding Piperoyl-CoA ligase and At4CL6 encoded by *At4g05160* were cloned into an expression vector (**Figure 3-11**).

The full-length piperoyl-CoA ligase sequence showed highest similarity to a subgroup of characterized short-chain CoA ligase At4CL4 and putative CoA ligases of unknown function from other species (**Figure 3-12**). This subclass is clearly distinct from the classical 4CLs such as At4CL1 and At4CL2 from *A. thaliana*. Approximately 60 % sequence identity at the amino acid level was observed compared to the original At4CL6. The piperoyl-CoA ligase has a similarity of 69 % and 67 % to XP_010267197 from *N. nucifera* and OVA06957 from *M. cordata*

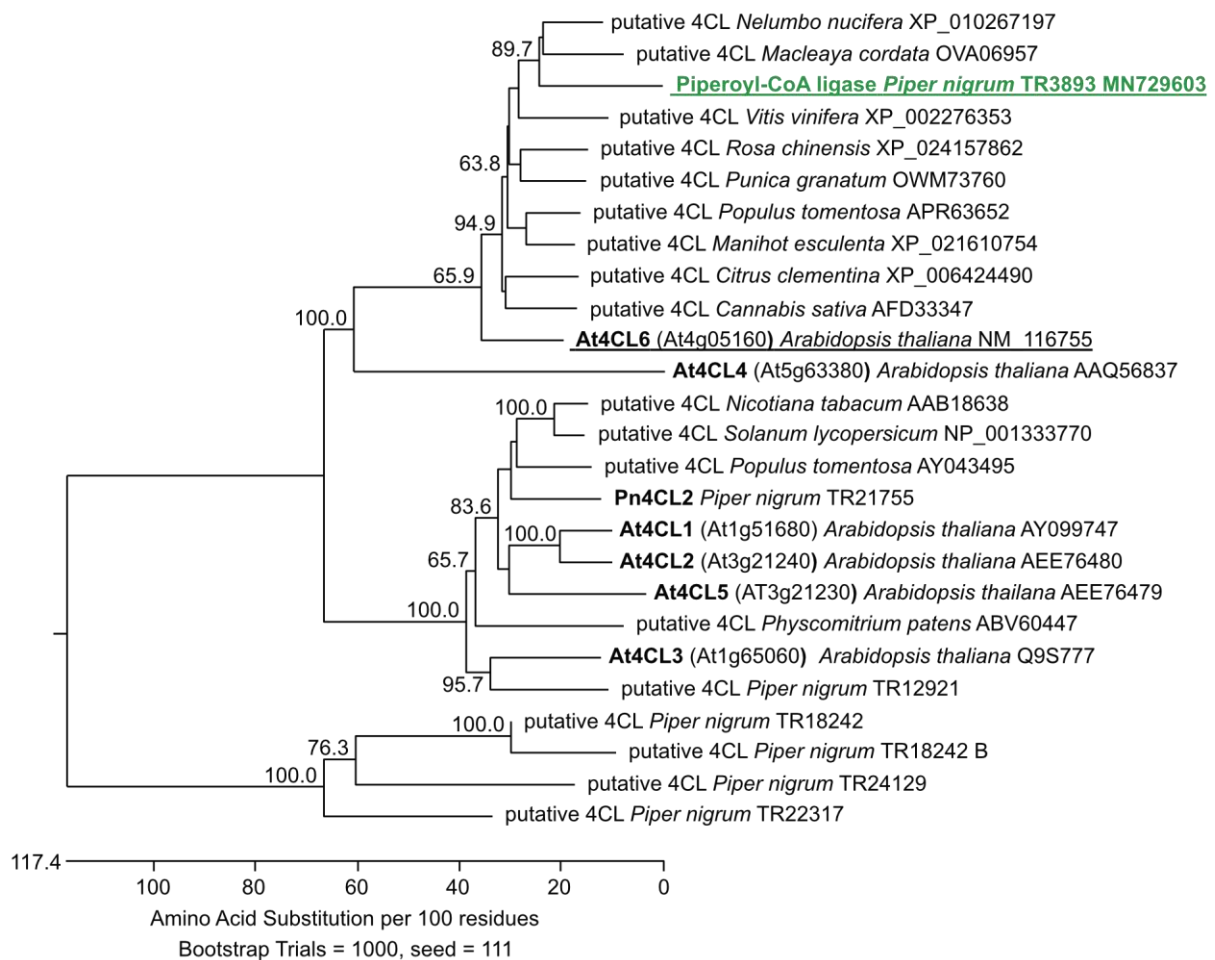


Figure 3-12: Bootstrapped, unrooted cladogram of 4CL and 4CL-like protein sequences obtained using ClustalW.

Amino acid sequences include CoA ligases from *Piper nigrum* fruit transcriptome SRX890122 (Hu et al., 2015), characterized members of At4CL ligase family and putative CoA ligases from different taxa. Piperoyl-CoA ligase and At4CL6 (At4g05160) are underlined. Sequences of characterized CoA ligases are marked in bold. The plant species, NCBI accession numbers and TAIR IDs for corresponding *Arabidopsis thaliana* genes are shown.

(NCBI blast). In case of annotated genomes of these non-model taxa, no information about the function as well as substrate preference of the CoA ligases are known. Other candidate sequences, from the black pepper transcriptome like TR21755 and TR12921 showed highest similarity to At4CL1 and At4CL2, both phenylpropanoid i.e. p-coumaric acid activating enzymes (Hu et al., 2015). TR21755 was characterized by Raika Milde in her bachelor thesis in our group in 2019 at the IPB and the corresponding CoA ligase, termed Pn4CL2, was identified as an At4CL2 homolog. Further *P. nigrum* sequences (TR18242, TR24129, TR22317) showed a high homology to genes coding for putative acyl-activating enzymes and could be associated to fatty acid metabolism, although they are clearly distinct from corresponding fatty acid CoA ligases in *A. thaliana*.

3.3.2 Functional expression and purification of the enzymes

Arabidopsis 4CL-like CoA ligases are localized in peroxisomes (database SUBA4) but can be prepared as soluble enzymes (Hamberger and Hahlbrock, 2004; Hooper et al., 2017). The N-terminally His₆-tagged piperoyl-CoA ligase from *P. nigrum* and also the amplicon derived from *At4g05160* from *A. thaliana* were expressed in *E. coli* cells as soluble proteins and purified by immobilized metal affinity chromatography (IMAC) (**Figure 3-13**).

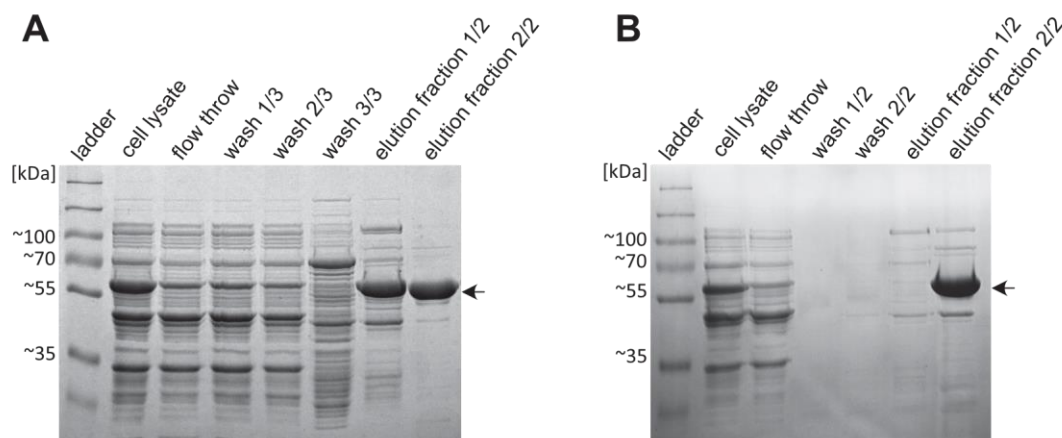


Figure 3-13: Preparation of recombinant piperoyl-CoA ligase (A) and At4CL6 (B) with IMAC

After cell lysis of *E. coli* M15 [Rep4] cells expressing recombinant piperoyl-CoA ligase or At4CL6, both with N-terminal His₆-tag and ~ 61 kDa, the cell lysate was applied on a Protino Ni-NTA column (1 ml). The column was washed with a buffer containing 50 mM imidazole and unbound proteins were removed. The recombinant protein was eluted with a buffer containing 300 mM imidazole. Collected samples were separated by SDS-PAGE and stained with Coomassie Blue. Fractions with recombinant CoA ligase were combined, desalted and used for enzymatic activity measurements or stored by -80 °C. The expected protein mass is marked with an arrow.

The piperoyl-CoA ligase was further purified by size exclusion chromatography and showed active as monomeric enzyme (Suppl.: **Figure 8-16**). Piperoyl-CoA ligase and At4CL6 were stable for 3 days at 4 °C and at least several months at -80 °C in a neutral buffer with 15 % glycerol at a final concentration of 1 mg/mL of protein.

3.3.3 Enzyme activity and substrate specificity of piperoyl-CoA ligase

Active piperoyl-CoA ligase is a monomeric enzyme *in vitro* with a calculated mass of 59.8 kDa (His₆-tagged: 61.2 kDa). The isoelectric point is approximately 7.83 (His₆-tagged: 8.03). The substrate specificity of recombinant piperoyl-CoA ligase was compared to *A. thaliana* 5-phenylpentanoic acid/OPDA CoA ligase (At4CL6) and At4CL2. The enzymes were incubated with 50 μ M of different hydroxycinnamic acid derivatives for 1 h (**Figure 8-17**). For a rapid result, the bathochromic shift of 20-25 nm in UV-absorbance caused by product formation was measured photometrically (**Figure 3-14**).

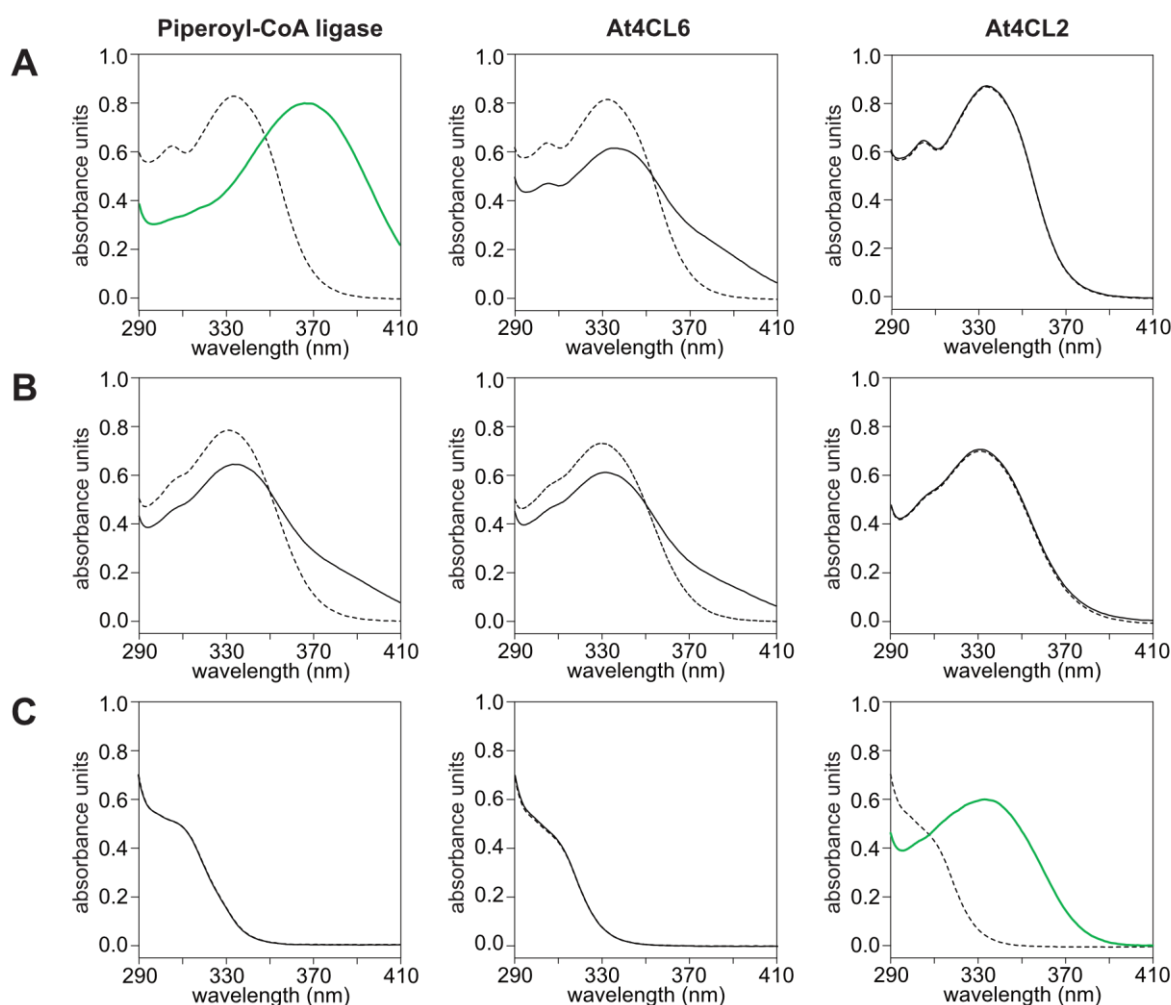


Figure 3-14: Photometric measurements of piperoyl-CoA ligase, At4CL6, and At4CL2 activities incubated with different substrates.

The enzymes were incubated with different hydroxycinnamic acids (**A**) piperic acid, (**B**) feruperic acid or (**C**) p-coumaric acid at a concentration of 50 μ M for 1 h at 30 °C. The reactions were analyzed photometrically recording the absorbance between 290 – 410 nm. A bathochromic shift of approximately 25 nm indicated CoA ester formation (green). Solid line indicates active and dashed line indicates inactive enzyme. The original figure was slightly modified (Schnabel et al., 2020).

An absorbance shift from 330 nm for piperic acid to 365 nm for piperoyl-CoA could be detected in the reaction with piperoyl-CoA ligase (**Figure 3-14, A**). Only a shoulder was

detected by the *A. thaliana* OPDA CoA ligase encoded by *At4g05160*, whereas At4CL2 was completely inactive. As expected, At4CL2 activates p-coumaric acid, shown by the bathochromic shift of 20 nm, whereas this substrate was not accepted by the piperoyl-CoA ligase and At4CL6 (**Figure 3-14, C**). Interestingly, the structural similar substrate feruloyl-CoA with respect to piperoyl-CoA could not be activated by piperoyl-CoA ligase and all other chosen CoA ligases (**Figure 3-14, B**).

Additional hydroxycinnamic acids were tested as putative substrates (Suppl.: **Figure 8-18**). All combinations of the substrates ferulic acid, caffeic acid, 3,4-(methylenedioxy) cinnamic acid and sinapic acid with the CoA ligases showed no activation, besides At4CL2, which also catalyzes CoA formation with caffeic acid. The characteristic enzymatic activities of AT4CL2 and At4CL6 are consistent with former publications (Hamberger and Hahlbrock, 2004; Kienow et al., 2008; Schneider et al., 2003).

For quantitative determination of the enzymatic activity the reactions were analysed by HPLC-UV-ESI-MS. Detection of hydroxycinnamoyl-CoA derivatives by reversed-phase LC are challenging due the tailing effect of the product during elution using standard methanol- or acetonitrile-based gradients in reversed phase chromatography. Alternative methods work with the indirect measurement of the ATP-consumption, that is sometimes misleading due to the two step reaction (Dippe et al., 2019). This tailing was successfully reduced by elution of the CoA ester with an isopropanol/acetonitrile gradient. Piperoyl-CoA was clearly separated from piperic acid without any overlap in retention times (**Figure 3-15**).

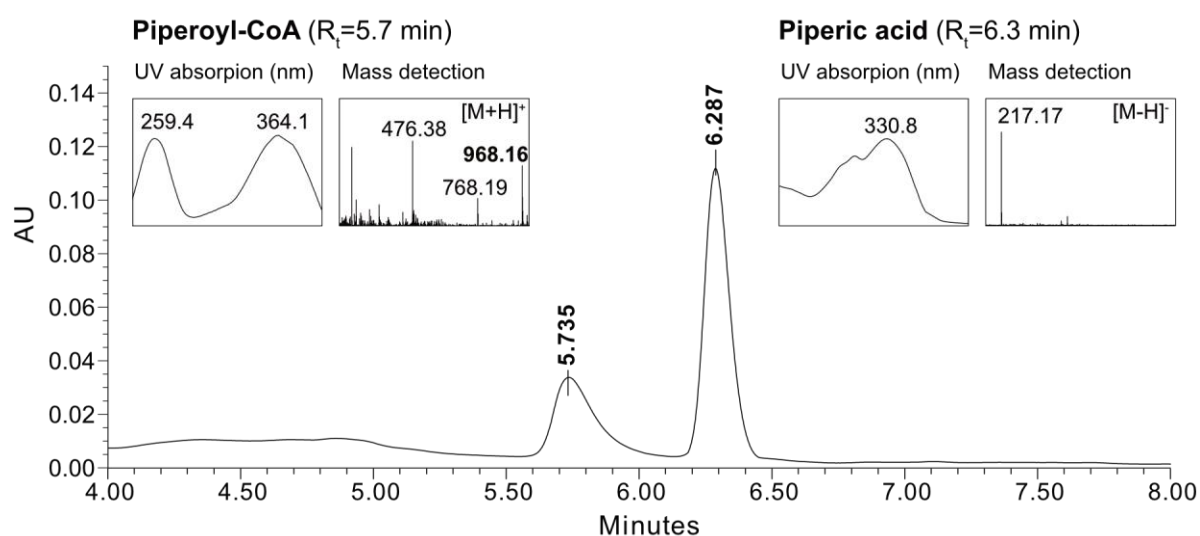


Figure 3-15: Identification of piperoyl-CoA and piperic acid by HPLC-UV-ESI-MS

Piperoyl-CoA and piperic acid could be nicely separated by an isopropanol/acetonitrile mixture as elution solvent. UV-spectra, mass signals and retention times are shown.

For kinetic parameter, piperoyl-CoA ligase was compared to At4CL6. The piperoyl-CoA ligase only activates piperic acid and the synthetic 5-phenylpentanoic acid, last one surprisingly with higher efficiency than At4CL6. The apparent K_M was calculated between 10 – 60 μM of piperic acid or 5-phenylpentanoic acid for the piperoyl-CoA ligase based on Michaelis-Menten- and Lineweaver-Burk calculations (Suppl.: **Figure 8-20**). Piperoyl-CoA ligase shows a K_M of 43.3 +/- 4.7 μM for piperic acid and 24.3 +/- 0.8 μM for 5-phenylpentanoic acid. The catalytic efficiency was 19.6 +/- 7.4 nkat/mg protein for piperic acid versus 27.9 +/- 1.4 nkat/mg protein for 5-phenylpentanoic acid. With a molecular mass of 61 kDA, the turnover rates were approximately 1.1 s^{-1} for piperic acid and 4.2 s^{-1} for 5-phenylpentanoic acid. The kinetic efficiencies (k_{cat}/K_M) were 26.000 $\text{s}^{-1}\text{M}^{-1}$ for piperic acid and 68.000 $\text{s}^{-1}\text{M}^{-1}$ for 5-phenylpentanoic acid. The efficiency of piperoyl-CoA ligase for activation of 5-phenylpentanoic acid was three times higher than the activation of piperic acid. All substrate specificities are listed in the following table.

Table 3-3: Substrate specificity of Piperoyl-CoA ligase compared to 5-phenylpentanoic acid/OPDA CoA ligase from *A. thaliana* (At4CL6).

(Slightly modified after Schnabel et al., 2020)

Substrate	Piperoyl-CoA ligase Activity [nkat/mg protein]	At4CL6
Piperic acid	19.6	0.5
Feruperic acid	n.d.	n.d.
3,4-(Methylenedioxy) cinnamic acid	n.d.	n.d.
5-Phenylpentanoic acid	27.9	4.9
p-Coumaric acid	n.d.	n.d.
Ferulic acid	n.d.	n.d.
Caffeic acid	n.d.	n.d.
Sinapic acid	n.d.	n.d.

n.d. – no enzyme activity detected

Piperoyl-CoA ligase was used for activation of piperic acid and also production of piperoyl-CoA on a semi preparative scale (Materials and methods section 2.5.4). After the CoA ligase reaction was completed, the corresponding CoA ester was concentrated by solid phase extraction and residual piperic acid removed by chromatography with a LH20 matrix. The purification was monitored by thin layer chromatography (TLC) (**Figure 3-16**). For piperoyl-CoA biosynthesis a recovery of 50 % based on the concentration of piperic acid was achieved. Pn4CL2 could be used in similar assays for the biosynthesis of p-coumaroyl-, feruloyl-, 5-aminocinnamoyl- and caffeoyl-CoA (Suppl.: **Figure 8-19**). Products were purified with the same procedure.

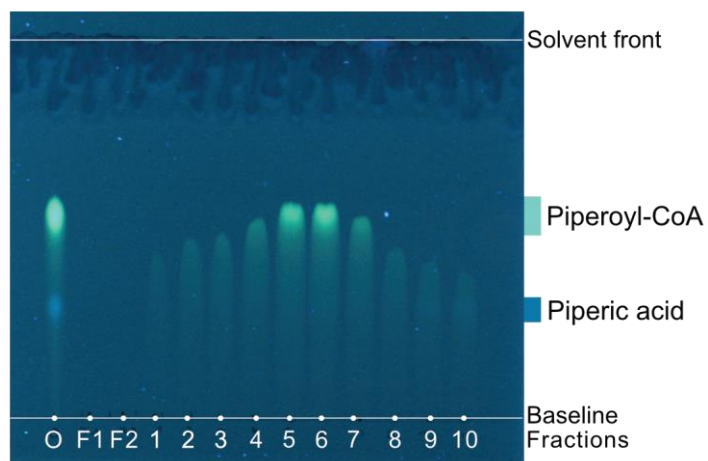


Figure 3-16: Identification of piperoyl-CoA and piperic acid by thin layer chromatography

Piperoyl-CoA could be separated from piperic acid by chromatography on LH20-silica gel (0.363 - 0.2 mm). The fractions were checked by TLC. Per fraction 10 μ L were applied on an ALUGRAM[®] RP-18W/UV₂₅₄ sheet (Macherey-Nagel) and run in a mixture of 10 mM ammonium acetate:100 % methanol (52:48). Piperoyl-CoA is shown in light green and piperic acid in blue. Both substances were confirmed with HPLC-UV-ESI-MS.

3.4 Piperine biosynthesis by BAHDs

3.4.1 Identification, cloning and expression of two putative candidates

After the production of piperoyl-CoA was established successfully, investigation of the decisive enzymatic step, the production of piperine from piperoyl-CoA and piperidine, could be started. From the RNA-sequencing dataset generated at the IPB, the two most prominent transcripts coding for a hexen-1-ol-acetyltransferase and benzoyl-benzoate acyltransferase (see also **Table 3-1**) were selected. Both transcripts were highly abundant in fruit stage II in comparison with fruit stage I and were nearly absent in flowering spadices as well as in leaves. Both full length transcripts were extracted from the GALAXY platform by the Trans-ABYSS software and briefly annotated as members of the BAHD superfamily, known to catalyze amide formation. RNA from fruit stage II was extracted, cDNA synthesized, and corresponding genes amplified with gene-specific primers (**Figure 3-17**).

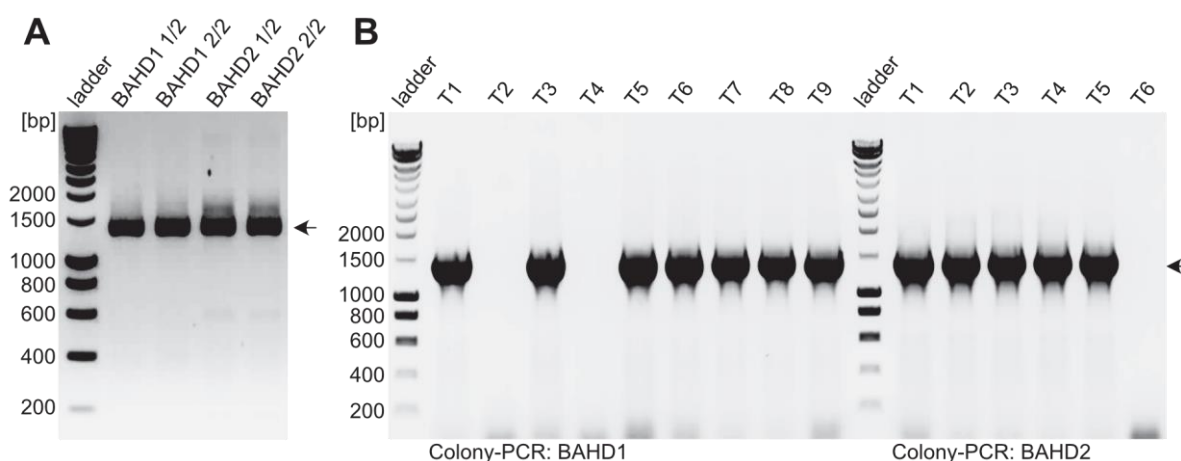


Figure 3-17: Verification on BAHD1 and BAHD2 during the cloning procedure

Every step during cloning was verified by a PCR reaction, analysed in a 1 % agarose gel and stained with ethidium bromide: **(A)** BAHD1 (1383 bp) and BAHD2 (1386 bp) from cDNA of black pepper fruit stage II; **(B)** single *E. coli* LEMO21 transformants were tested for BAHD1 and BAHD2. Expected amplicon is marked with an arrow.

The full-length cDNAs encoded two proteins, BAHD1 (461 aa) and BAHD2 (462 aa), with a calculated mass of 51 kDa each. The amplicons were cloned into pET16b expression vectors and were functional expressed with an N-terminal His₁₀-tag in *E. coli* LEMO21 cells.

3.4.1 Purification of recombinant BAHDs

After expression at 25 °C, both enzymes remained soluble and were purified by IMAC (**Figure 3-18, A**; **Figure 3-19, A**). The recombinant His₁₀-tagged enzymes were separated by SDS-PAGE and were displayed at ~55 kDa. The slightly higher anticipated molecular mass on SDS-PAGE was also observed for other BAHDs and is not solely due to the His₁₀-tag (D'Auria, Chen and Pichersky, 2002). Size exclusion chromatography (SEC) was chosen as the second purification step. To reduce enzyme aggregation, DTT was added.

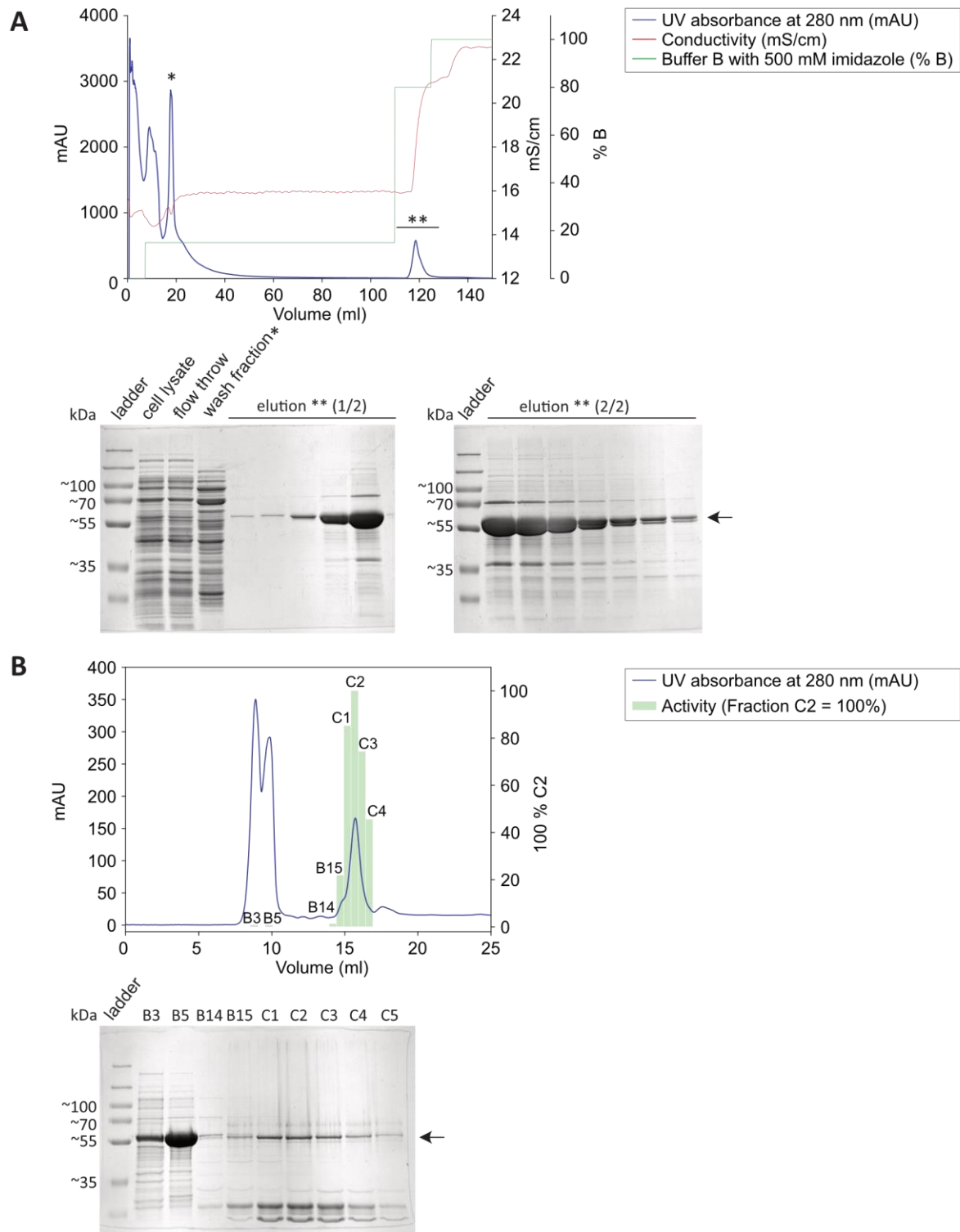


Figure 3-18: Preparation of recombinant piperine synthase by IMAC and SEC

(A) The elution profile of the IMAC and the corresponding SDS-PAGE with selected samples are shown. Elution fractions containing piperine synthase are marked with ** and the expected size with an arrow. (B) The elution profile of the SEC and the corresponding SDS-PAGE with selected samples are shown. Different fractions were tested for enzymatic activity. The highest activity was set 100 % and belongs to fraction C2. The fractions were analyzed by SDS-PAGE and the expected mass is marked with an arrow. The UV absorption was measured at 280 nm (blue). The conductivity is marked in red. The increase of buffer B is marked with a green line. The activity is shown as bars of corresponding fractions. The SDS-PAGE was stained with Coomassie Blue.

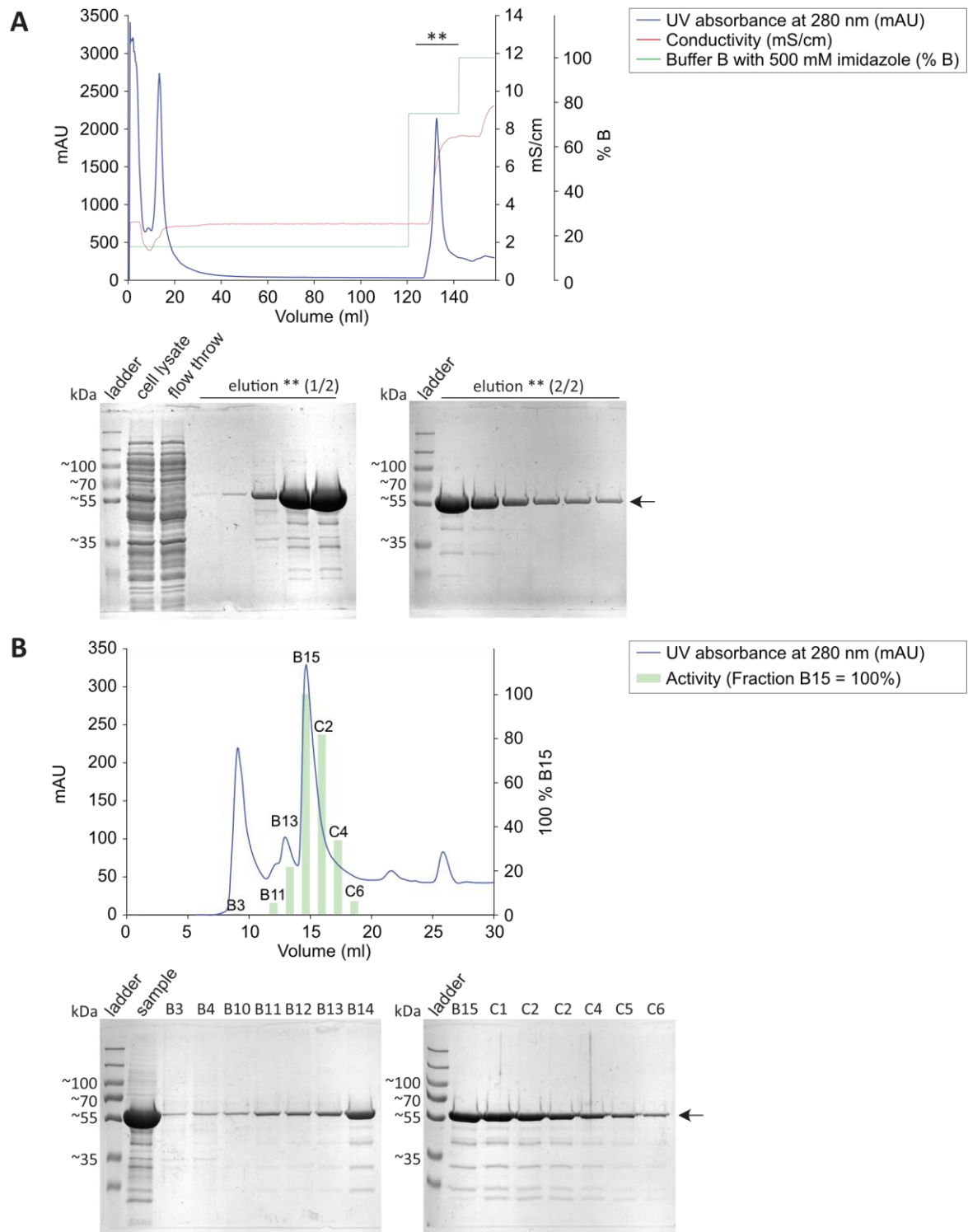


Figure 3-19: Preparation of recombinant piperamide synthase by IMAC and SEC

(A) The elution profile of the IMAC and the corresponding SDS-PAGE with selected samples are shown. Elution fractions containing piperamide synthase are marked with ** and the expected size with an arrow. (B) The elution profile of the SEC and the corresponding SDS-PAGE with selected samples are shown. Different fractions were tested for enzymatic activity. The highest activity was set 100 % and belongs to fraction B15. The fractions were analyzed by SDS-PAGE and the expected mass is marked with an arrow. The UV absorption was measured at 280 nm (blue). The conductivity is marked in red. The increase of buffer B is marked with a green line. The activity is shown as barres of corresponding fractions. The SDS-PAGE was stained with Coomassie Blue.

In both cases only fractions containing monomeric enzyme showed activity (**Figure 3-18, B; Figure 3-19, B**). The prepared enzymes were stable for several weeks at -80 °C in a neutral buffer containing 15 % glycerol. Total protein yields ranged from <1 mg/L in the case of piperine synthase up to 5 mg/L fermentation broth for piperamide synthase.

3.4.2 Enzyme activity – piperine formation

The enzyme activities were tested with the substrates piperoyl-CoA and piperidine. Product formation was analysed by HPLC-UV-ESI-MS. Only purified BAHD2 catalyzed the efficient formation of piperine and was therefore termed **piperine synthase (Figure 3-20)**. For the reaction no additional co-factors were required.

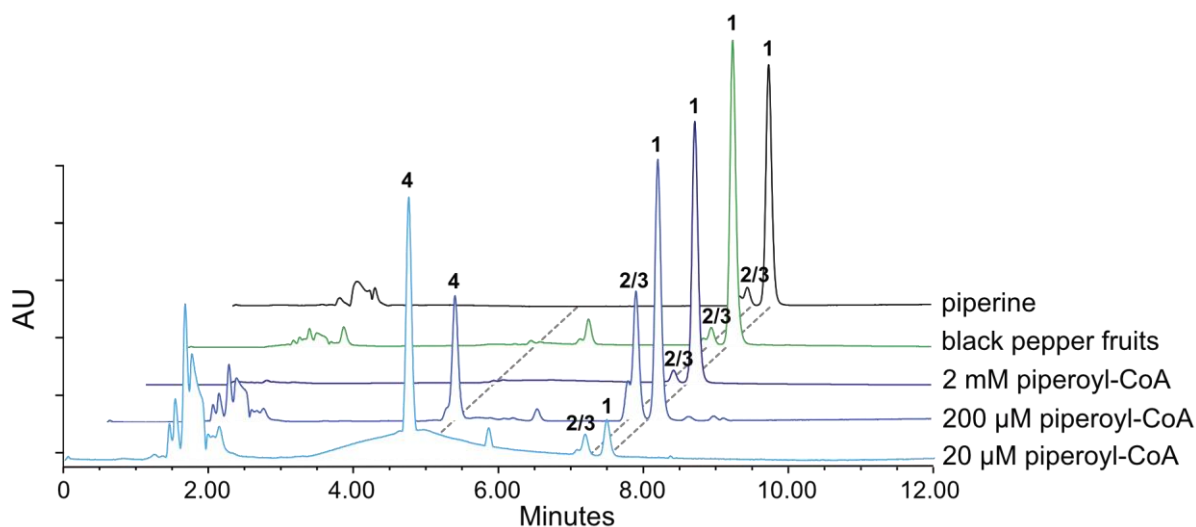


Figure 3-20: Analysis of enzyme activity of recombinant and native piperine synthase by HPLC-UV-ESI-MS.

Representative chromatograms display the formation of piperine at different concentrations of piperoyl-CoA by recombinant piperine synthase (blue), by partly purified native piperine synthase activity from black pepper fruits (green), and a piperine standard (black). Besides the product piperine (**1**), side products like piperine stereoisomers (**2/3**) and piperic acid (**4**) were detected. UV-absorption was measured between 280-380 nm. The original figure was slightly modified (Schnabel et al., 2021a).

The pH optimum was at 8.0 in a TRIS/HCl-based buffer. At low μM concentrations of piperidine, piperine formation was poor and prominent piperic acid formation ($m/z = 219 [M+H]^+$) was recorded. In minor quantities also stereoisomers of piperine were identified with identical masses, but slightly different UV absorbance maxima compared to piperine. If the concentrations of piperoyl-CoA and piperidine were increased, preferentially piperine was synthesized. In parallel, the concentrations of piperic acid and piperine isomers were reduced. A crude protein extract was prepared from young black pepper fruits (stage II) and the activity was compared to the activity of the recombinant piperine synthase. In the crude, native protein mixture of the fruits the exclusive formation of piperine and only minor levels of piperic acid and piperine stereoisomers was observed at comparably high substrate concentrations.

The second enzyme identified in the RNA sequencing dataset, was also cloned, expressed, purified, and was initially termed BAHD1. This enzyme preferentially synthesizes a mix of piperine isomers, rather than piperine (**Figure 3-21**). The reaction products showed identical masses but different UV-absorbance spectra and shifted retention times. Piperine was synthesized as a side product, unaffected by substrate concentrations. Whether isomerization takes place during binding of the CoA ester, during the enzymatic reaction or during the release of the product remains a mystery.

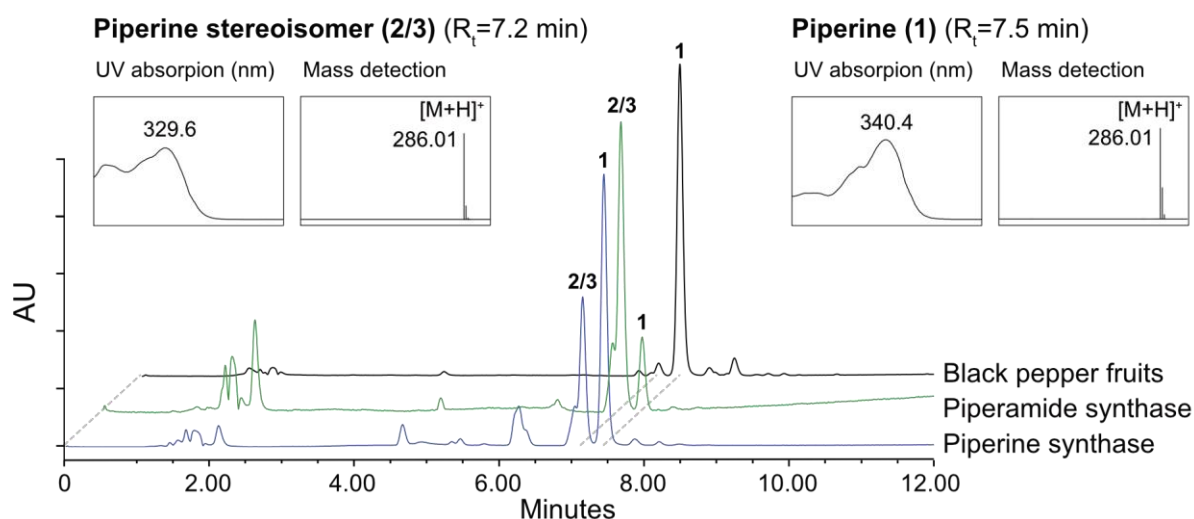


Figure 3-21: Isomerisation during piperine synthesis by piperamide synthase

Representative chromatograms display the formation of piperine by recombinant piperine synthase (blue) and piperamides synthase (green) and a methanolic extract from black pepper fruit (Kampot pepper) (black). The piperine (**1**) and piperine stereoisomers (**2/3**) were detected in different ratio depending on the catalytic enzyme. UV-absorption was measured between 320-380 nm.

Piperine synthase showed an apparent K_M of 0.34 ± 0.06 mM for piperoyl-CoA and 7.6 ± 0.5 mM for piperidine based on classical Michaelis-Menten kinetics (**Table 3-4**). The catalytic efficiency k_{cat} for piperoyl-CoA was 1.01 ± 0.12 s⁻¹ and for piperidine 0.47 ± 0.11 s⁻¹ based on total product formation, including piperine and stereoisomers. The kinetics constants

Table 3-4: Apparent kinetic constants of piperine and piperamide synthases using piperoyl-CoA (5-2000 μ M) and piperidine (1-100 mM) as substrate.

(Slightly modified after Schnabel et al., 2021)

	Apparent K_M [mM]	Apparent K_{cat} [s ⁻¹]	K_{cat}/K_M [s ⁻¹ M ⁻¹]
Piperine synthase			
Piperoyl-CoA	0.342 ± 0.060	1.01 ± 0.12	2953
Piperidine	7.6 ± 0.5	0.47 ± 0.11	16.2
Piperamide synthase			
Piperoyl-CoA	0.196 ± 0.009	0.35 ± 0.01	1786
Piperidine	8.69 ± 3.6	0.27 ± 0.02	31.1

of BAHD1 are comparable to piperine synthase in the case of piperoyl-CoA and piperidine as substrates.

3.4.3 Enzyme activity – substrate specificity

Piperine synthase showed a preference for piperine formation, but not an exclusive specificity to piperoyl-CoA and piperidine. The amines pyrrolidine and isobutylamine are also suitable acyl-acceptors, although with a lower activity of 40 % and 15 %, respectively compared to piperidine. The corresponding amides of piperoyl-CoA and pyrrolidine or isobutylamine, identified by HPLC-UV-ESI-MS, were also detected in minor quantities in commercially available dried peppercorns from several suppliers. More bulky amines like vanillylamine or dopamine were not accepted. As an acyl-donor, piperine synthase also accepted 3,4-(methylenedioxy) cinnamoyl-CoA, but with reduced catalytic activities. Benzoyl-CoA was not accepted as substrate.

BAHD1 showed much broader substrate specificity compared to piperine synthase (BAHD2). Besides piperoyl-CoA BAHD1 accepted 3,4-(methylenedioxy) cinnamoyl-CoA with similar and benzoyl-CoA with lower activity. Production of amides was observed in several combinations of CoA esters and amines, e.g. vanillylamine and dopamine (**Figure 3-22**). Both enzymes showed significant product formation with medium-chain aliphatic CoA esters, like hexanoyl- or octanoyl-CoA. Again, a higher activity was observed with BAHD1. It is obvious that BAHD1 is highly promiscuous and accepts a broad range of acyl-donors and acyl-acceptors resulting in efficient amide production. Therefore, the enzyme was named **piperamide synthase**.

In summary, piperine- and piperamide synthase produce many amides with diverse pharmacological, therapeutical, and protective properties. Several of these amides are covered by recent patent applications, like 1-benzoylpiperidine as inhibitor of GLUD1/2 in cancer cell lines (US20160068610A1), 1-3,4-(methylenedioxy) cinnamoyl-piperidine for therapeutical applications of neurological conditions (US20100179130A1) or general alkamide patents (US20200290950A1), but are all chemically synthesized. Besides the production of piperine, piperamide and piperine synthase can produce these compounds in a microbial system.

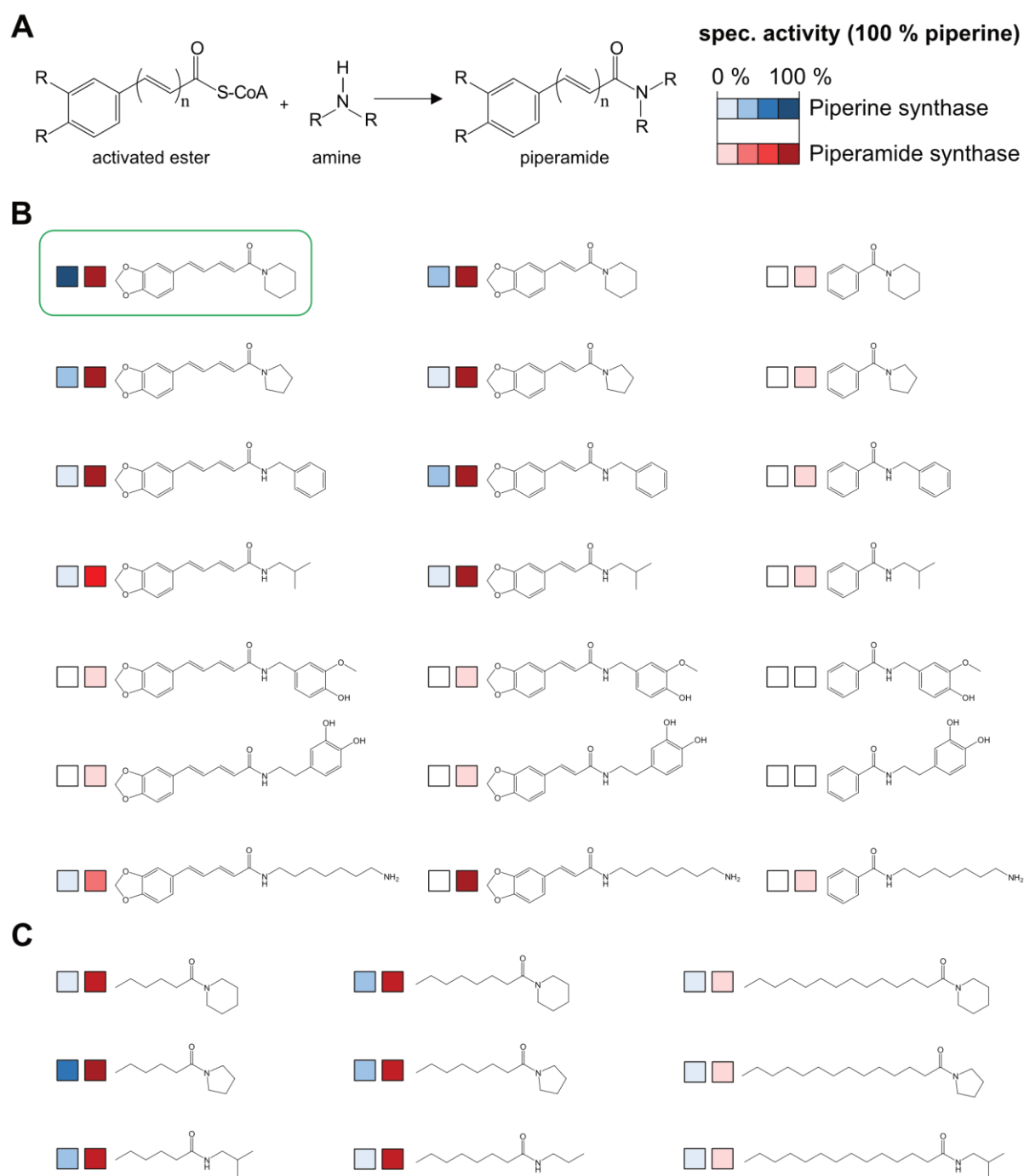


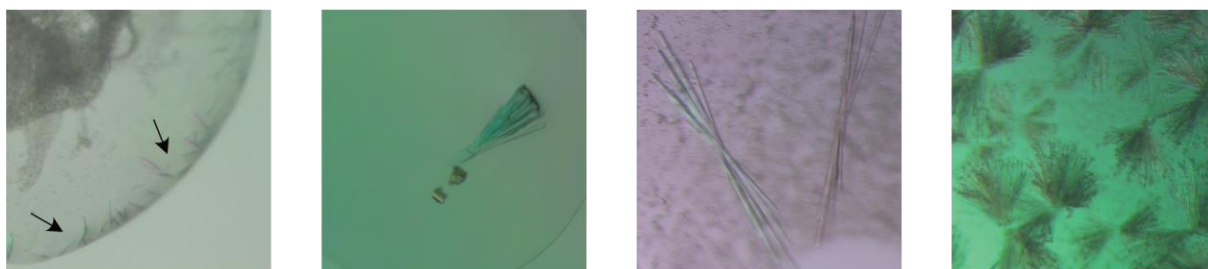
Figure 3-22: Metabolic grid of different amides produced by piperine synthase (blue) and piperamide synthase (red).

(A) The activity of piperine and piperamide synthase were tested with different CoA esters and amine combinations. The color intensity is related to the relative enzyme activity for CoA ester and amine to 100 % piperine formation. The products were analysed by HPLC-UV-ESI-MS. Due to the lack of available standards and individual ionization intensities of each product, more relative than absolute values can currently be provided with confidence. Different CoA esters and amines were combined and resulted in a large array of amides: aromatic amides (B) and aliphatic amides (C). (Slightly modified after Schnabel et al., 2021a)

3.5 Crystallization

Piperine and Piperamide synthase share 62 % identity on amino acid level, catalyzing the same reaction but clearly differ in their substrate specificity. For a better understanding of the mode of action and for further manipulation of the substrate specificity, we decided to go for protein crystallisation and structure elucidation. Piperamide synthase, with a yield of up to 5 mg/L fermentation broth, seemed a suitable candidate. In a pre-screening with different conditions of nine commercial crystallization screens 2 – 6 mg/mL monomeric piperamide synthase were combined with or without piperoyl- or hexanoly-CoA as substrate. Besides precipitation reactions, various crystals, especially different needle variations, appeared (**Figure 3-23, A**).

A



B



C

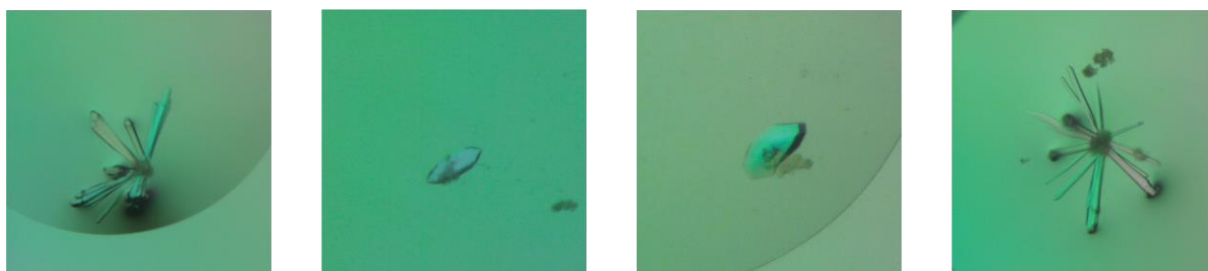


Figure 3-23: Crystallization of piperamide synthase

Representative crystals from first crystallisation trials of recombinant piperamide synthase are shown. The size of the crystal was always $\leq 200 \mu\text{m}$. (**A**) In various conditions crystals of different size and variety appear, predominant were needle structures. (**B**) In two conditions of the JBScreen JCSG++ (D6, D7) hexagonal crystal structures appear after 2-3 d. Unfortunately, the crystals started to dissolve after ~ 5 d. (**C**) It was not possible to reproduce the hexagonal crystals, shown in **B**, in a further experiment. Nevertheless after 3 months defined crystals appeared and showed a diffraction pattern with a resolution of 7-10 Å.

In one trial with 6 mg/mL piperamide synthase and 500 μ M hexanoyl-CoA hexagonal crystals appeared after 2-3 d (**Figure 3-23**, B). However, the crystals started to dissolve after 5 d. It was not possible to reproduce these crystals in a second trial. Nevertheless, after 3 months defined piperamide synthase crystals appeared and showed a protein diffraction pattern with a resolution of 7-10 Å (**Figure 3-23**, C).

3.6 *In vivo* fermentation of piperine and piperiline

For biotechnological approaches, the production of amides from CoA esters is far too expensive. The scenario changes when amides can be produced from free acids. As a pilot project for a combinatorial approach, the production of piperine and piperiline (1-piperoylpyrrolidine) was performed by feeding piperic acid and either piperidine or pyrrolidine to cell cultures expressing the piperoyl-CoA ligase and piperine synthase (**Figure 3-24**).

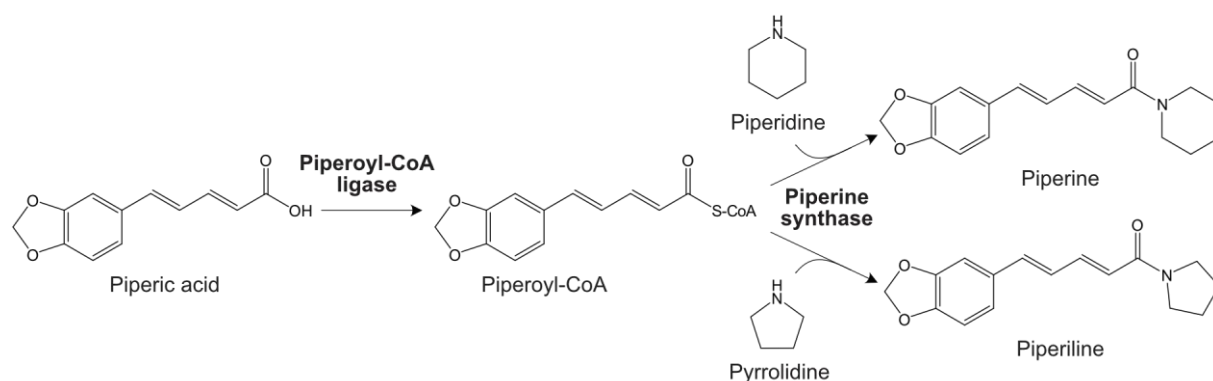


Figure 3-24: Reaction cascade for the biosynthesis of piperine and piperiline.

Piperic acid is activated by piperoyl-CoA ligase. Piperine synthase catalyzes the amide formation of piperoyl-CoA and the amine piperidine to piperine or piperoyl-CoA and the amine pyrrolidine to piperiline.

E. coli SOLU BL21 cultures that simultaneously expressed piperoyl-CoA ligase and piperine synthase or one of both under identical conditions were incubated with 1 mM piperic acid and 10 mM amines, piperidine or pyrrolidine for 1 h. The products were extracted and analysed by HPLC-UV-ESI-MS. In both cases, only in combination of piperoyl-CoA ligase and piperine synthase the final products piperine (**Figure 3-25**, A) and piperiline (**Figure 3-25**, B) were synthesized. No side products occurred and underlined the specificity of this enzyme combination.

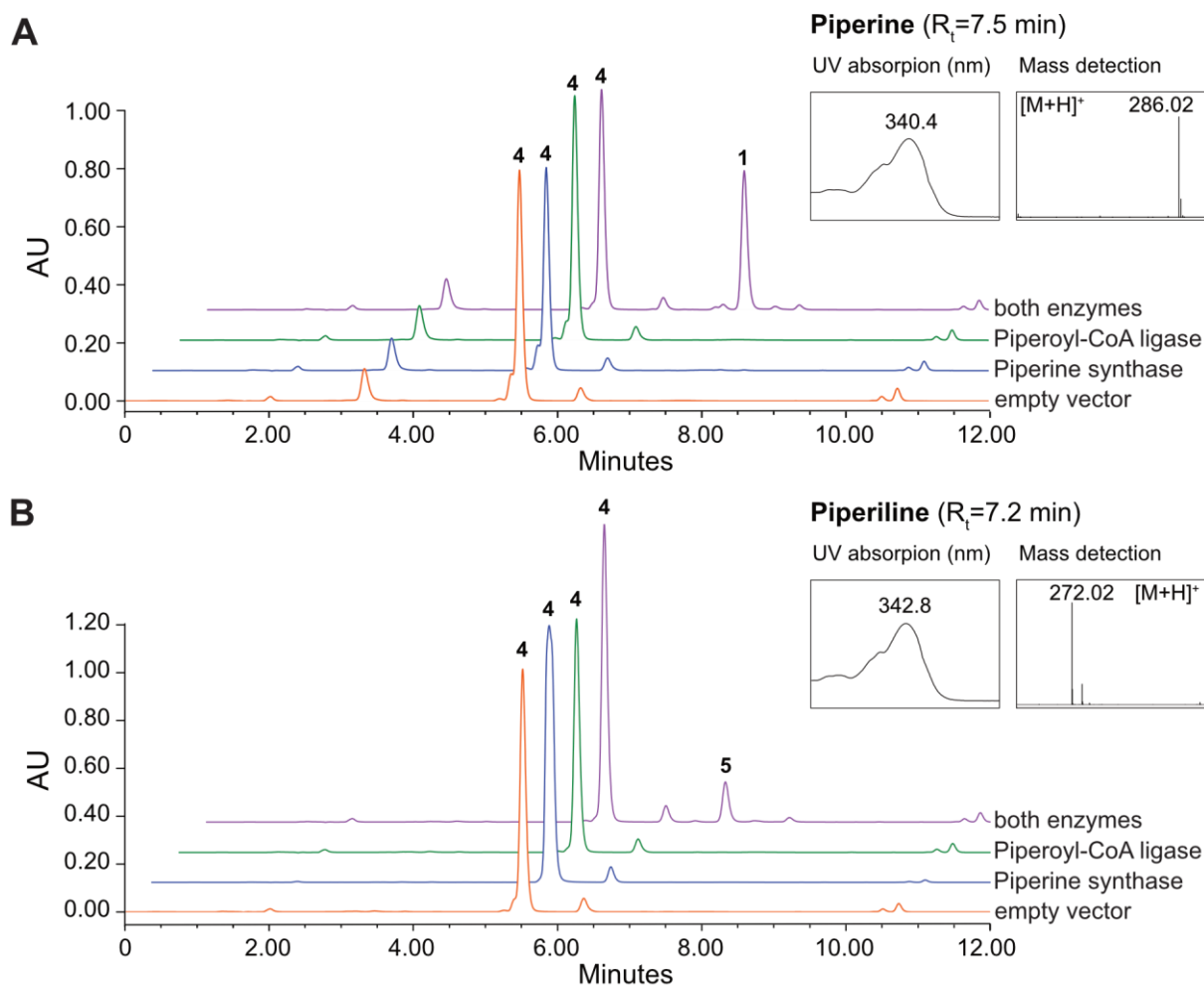


Figure 3-25: Analysis of *E. coli* extracts after feeding piperic acid and piperidine (A) or pyrrolidine (B)

Cells expressing the empty vector (orange), piperine synthase (blue), piperoyl-CoA ligase (green) or both enzymes (both - violet) were incubated with 1 mM piperic acid (**4**) and 10 mM piperidine or pyrrolidine at 25 °C, 400 rpm for 1 h. The supernatant was collected, and the product was extracted with ethyl acetate, then concentrated, and finally dissolved in 90 % methanol. Product formation was monitored between 300 – 360 nm and piperine (**1**) was identified with $\lambda_{max} = 340$ nm and $m/z = 286.1$ $[M+H]^+$ and piperiline (**5**) was identified with $\lambda_{max} = 342$ nm and $m/z = 272.0$ $[M+H]^+$.

3.7 Transcript level of biosynthetic enzymes in piperine biosynthesis

The RNA sequencing dataset already suggested that transcript abundance of piperine synthase and piperamide synthase were highest in fruits around 40-60 days post anthesis. To corroborate these data, expression profiles of piperine biosynthesis, related genes in different black pepper organs were generated by RT-qPCR and compared to piperine content of each organ (**Figure 3-26**). Transcript levels of piperamide synthase, piperine synthase, piperoyl-CoA ligase as well as CYP719A37 and PnCPR show higher expression levels in fruit stage II compared to fruit stage I and minor amounts in leaves and spadices. At the time point of sample collection for RNA-sequencing, root material was not available. Mature root material from two-year-old plants was analysed by RT-qPCR and piperine content was measured. Like in the case of spadices, only low levels of transcripts were detected, the same holds true for piperine levels. Overall, the piperine content is in line with the transcript profiles and genes of the pathway appear co-expressed, which should facilitate the discovery of additional and unsolved steps in the biosynthesis of piperine.

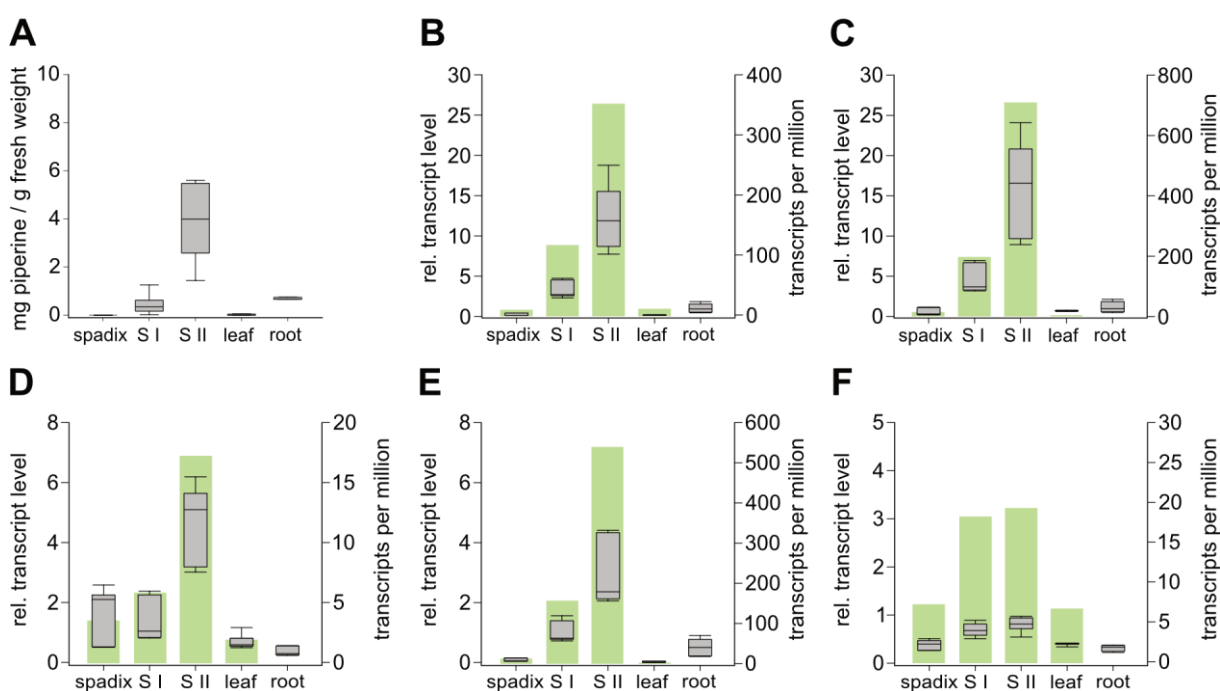


Figure 3-26: Organ-specific relative transcript levels of enzymes involved in piperine biosynthesis compared to RNA sequencing results and piperine content.

Flowering spadices, fruit stage I and II, leaves, and roots were analyzed. (**A**) The piperine content of chosen organs is shown. Plant material ($n > 6$) was ground and piperine extracted with 90 % methanol. The content was quantified by HPCL-UV-ESI-MS compared to piperine standard. (**B-F**) Plant material was ground, and RNA extracted. Synthesized cDNA was used as template for RT-qPCR and related transcript levels of (**B**) piperamide synthase, (**C**) piperine synthase, (**D**) piperoyl-CoA ligase, (**E**) CYP719A37 and (**F**) PnCPR were amplified by gene specific primers (grey boxes; $n = 9$). Elongation factor 2b (eIF2b) was selected as reference (Schnabel et al., 2020). This data was compared visually with corresponding predictions from RNA-sequencing shown by appearance of transcript per million reads (green). At the time point of sample collection for RNA-sequencing, black pepper roots were not available.

3.8 Piperine synthase localization in black pepper fruits

To detect the presence of piperine and piperamide synthases in black pepper fruits, polyclonal antibodies were produced in New Zealand White rabbits that were infected with recombinant piperine synthase or recombinant piperamide synthase. Initially, the resulting antiserum was tested against different concentrations of purified or partly purified recombinant piperine synthase and piperamide synthase. One polyclonal anti-piperamide synthase-antibody (anti-PAS-AB) showed a detection limit of 5 ng for piperamide synthase as well as 2.5 ng for piperine synthase (Suppl.: **Figure 8-21**).

This antibody was chosen to verify piperine and piperamide synthase in black pepper tissue. A total protein extract from spadix, black pepper fruit (70 d), shoots without nodes, leaves and roots was prepared slightly modified according to Wessel and Flügge, 1984.

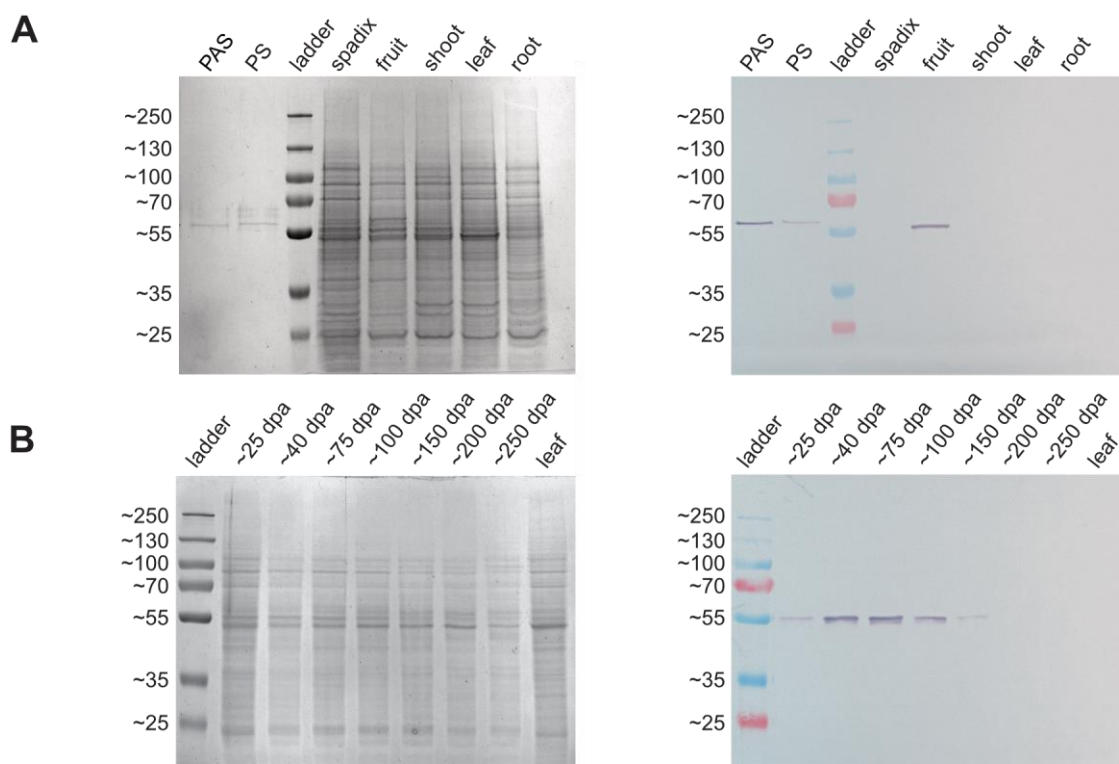


Figure 3-27: Detection of piperine synthase (PS) and piperamide synthase (PAS) in different black pepper tissues by immunoblotting.

Total protein of different black pepper tissues was prepared and analysed by SDS-PAGE combined with Coomassie-staining (left) or immunoblotting with polyclonal anti-PAS-AB (1:5000, 10 min, right). **(A)** Total protein of different black pepper organs compared to recombinant piperine and piperamide synthase is shown. Comparable amounts of total proteins in all tissues were observed. In the immunoblots, clear signals for recombinant piperine and piperamide synthase were observed in the case of recombinant proteins as well as in crude protein preparations from fruit tissues. **(B)** Total protein at different developmental stages of black pepper fruits was analyzed and showed comparable amounts at all stages after Coomassie-staining. In the corresponding immunoblot, piperine and piperamide synthase signals were detected between 25 and 100 dpa with a maximum at 75 dpa. No signal was observed beyond 150 dpa and in leaves. The immunodetection of piperine and piperamide synthase was part of the master thesis from Luise Jäckel and was performed in our group (IPB).

Total protein of 200 mg per tissue was precipitated, was resolved in a low salt- and SDS-sample buffer and was separated on a 10 % gel per SDS-PAGE (**Figure 3-27, A**). A second gel, run in parallel was used for immunodetection of piperine and piperamide synthesis with anti-PAS-AB. As a control, 10 ng of recombinant piperine synthase and piperamide synthase were used. The Coomassie-stained gel showed a broad range of precipitated proteins of different sizes, a good separation, and comparable amounts of protein each tissue. The data from the corresponding Western blot shows a high specificity of anti-PAS-AB for a protein band at the same molecular mass as piperine as well as piperamide synthase, and the exclusive detection of this band in fruit tissue. In spadix, shoot, leaf, and root tissue no signals could be detected.

With the same precipitation method total protein of different developmental stages of black pepper fruits was prepared and checked for precipitation efficiency and immunoreaction with anti-PAS-AB (**Figure 3-27, B**). As a negative control, total protein of leaf tissue was used. Signals were only observed in fruit tissue of ~25 - ~150 dpa and are absent in old fruits (200 - 250 dpa) and in leaves. The strongest signal is observed for approximately 75 dpa old fruits. This accumulation pattern up to 75 days is consistent with rising piperine content during fruit stages I (20 – 30 dpa), stage II (40 – 60 dpa) and up to 100 – 125 dpa (see also **Figure 3-2**). The virtual lack of any signal also seems to be in line with a stationary phase of piperine content between 120-150 dpa old fruits and the decrease after 150 dpa old fruits, simply due to the lack of any biosynthetically functional piperine synthase.

In freshly extracted black pepper fruits and commercially available peppercorns we never detected a high content of piperine isomers, piperine was by far the dominant peak e.g. in the Kampot variety (see also **Figure 3-21**). It was always puzzling, why piperamide synthase that is highly expressed *in vivo*, synthesizes *in vitro* piperine isomers, which have not been found *in vivo*. Due to the similar molecular mass of piperine and piperamide synthase and the overlapping detection of piperine synthase and piperamide synthase by the polyclonal antibodies a clear identification and separation of both activities appears difficult. To differentiate between piperine and piperamide synthase activity in black pepper fruits, and to detect hints that this enzyme actually exists in the mature fruit as an active protein, total protein was prepared from 40 – 80 dpa old black pepper fruits according to Geisler and Gross, 1990. The protein extract was separated by size exclusion chromatography and single fractions were tested for piperine and piperamide synthase activity. Whereas piperine and piperamide synthase both catalyze the piperine formation, piperamide synthase preferentially catalyzes the formation of 1-piperoylbenzylamide *in vitro* and therefore this activity should be detectable also *in vivo* (**Figure 3-28**). After size exclusion chromatography, piperine formation was detected in fractions B13-C6 with highest activity in fraction C1 (**Figure 3-29, A**). The retention

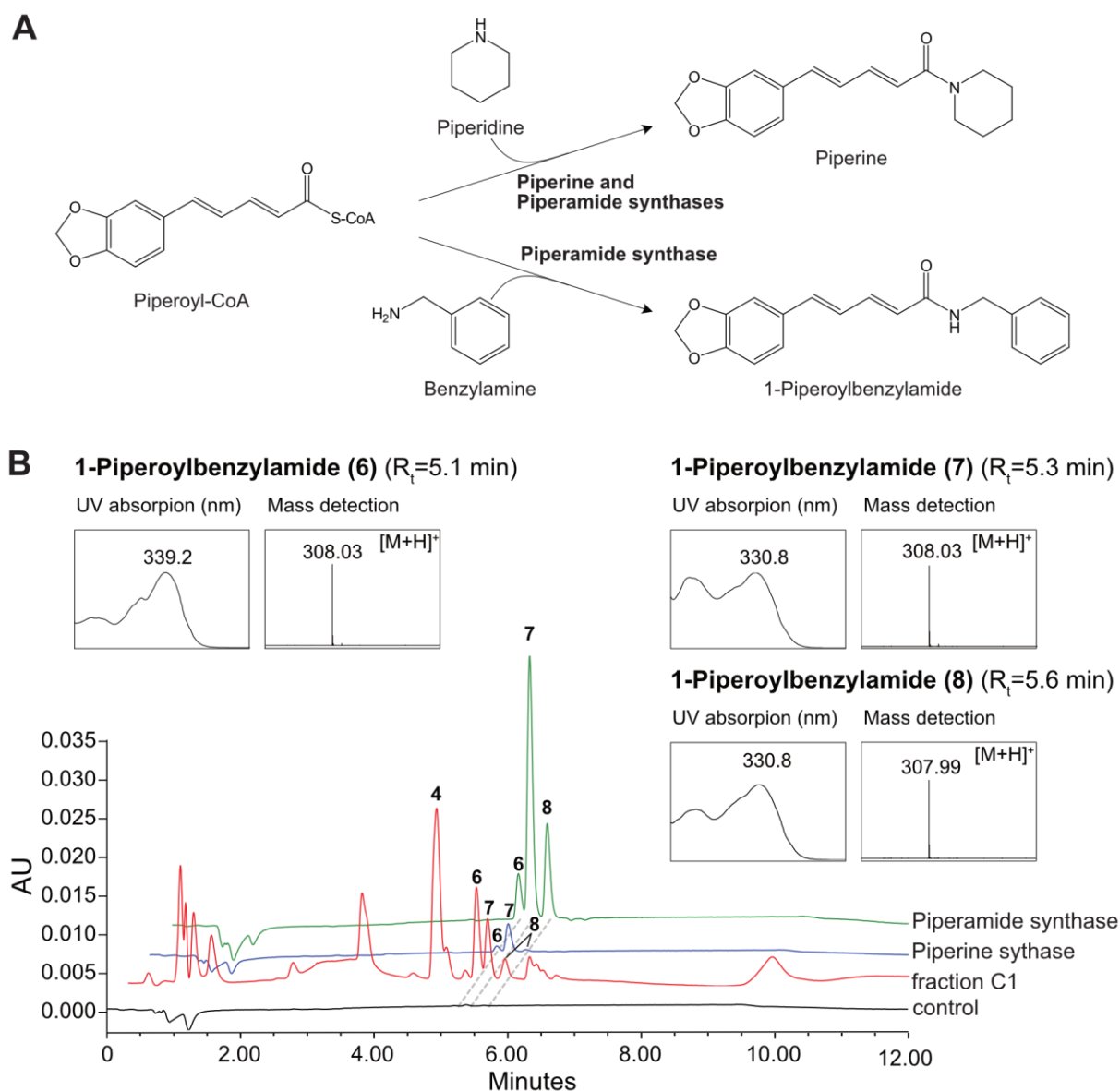


Figure 3-28: The formation of piperine and 1-piperoylbenzylamide were chosen to determine the activity of piperine and piperamide synthase in black pepper fruits

(A) Reaction scheme. (B) Representative chromatograms display the formation of 1-piperoylbenzylamide by fraction C1 (partly purified native piperine synthase activity from black pepper fruits, red), by recombinant piperine synthase (blue) and by recombinant piperamide synthase (green). The control-reaction without enzyme, is shown in black. The reaction time was 10 min. Three variants of 1-piperoylbenzylamide (**6**, **7**, **8**) and piperic acid (**4**) were detected. UV-absorption was measured between 320-380 nm. Due to low intensity of fraction C1, the chromatogram was aligned for comparison with the others.

volume of approximately 16 mL at C1 is consistent with monomeric enzymes of recombinant piperine and piperamide synthase. The formation of 1-piperoylbenzylamide ((2E,4E)-5-(1,3-Benzodioxol-5-yl)-N-(phenylmethyl)-2,4-pentadienamide), the product of piperamide synthase reaction, can be detected. Although it is only 20 % compared to piperine formation, it overlaps with the active fractions of piperine formation. This result corroborates the presence and the activity of both monomeric acyltransferases, piperine and piperamide

synthase in mature fruits and suggests that both activities are present. The total protein solution and selected fractions were further analysed by SDS-PAGE and stained with Coomassie-Blue or used for immunoreaction with anti-PAS-AB. A clear color signal was observed in the active fractions and validated this presumption (**Figure 3-29, B**).

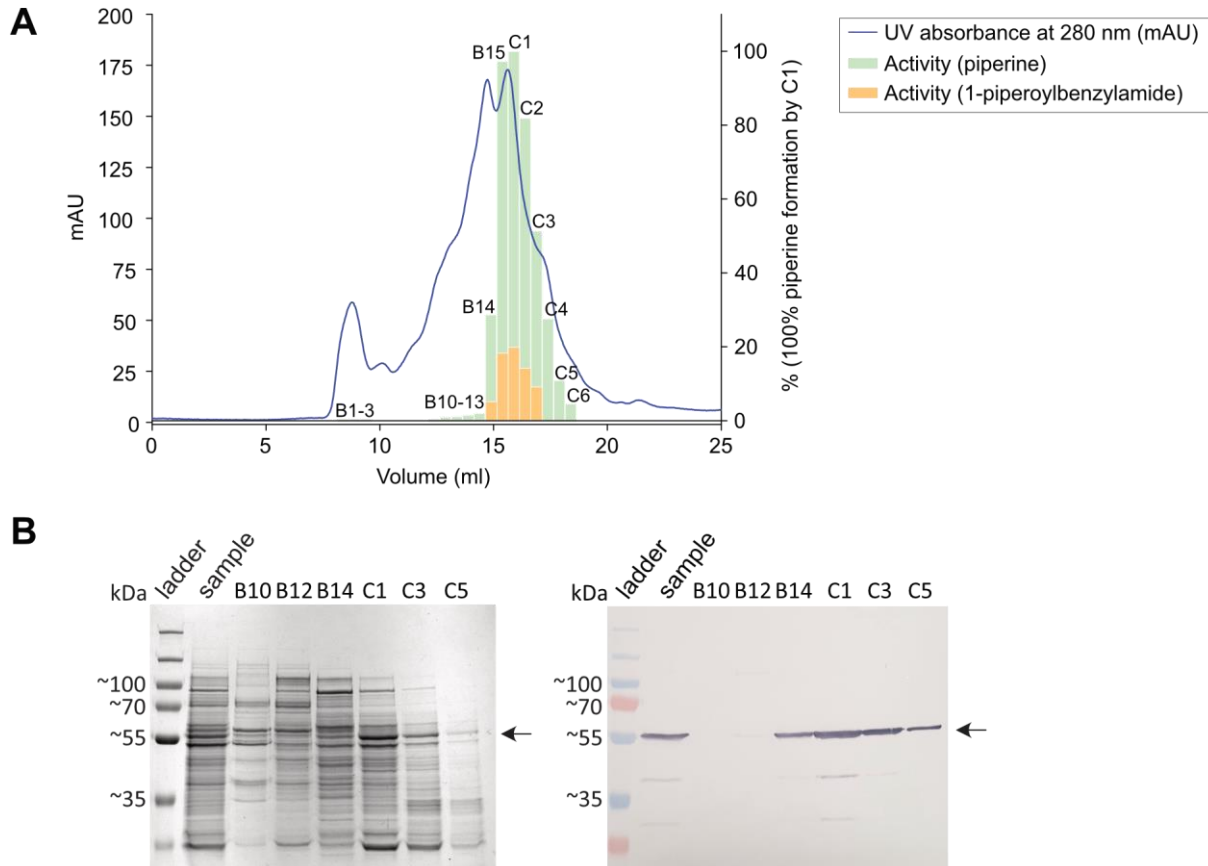


Figure 3-29: Verification of piperine and piperamide synthase in black pepper fruits by activity measurements and immunoblotting.

(A) Total protein of 40-80 dpa old fruits was prepared according to Geissler and Gross (1990) and separated by SEC on a Sephadex 200 Increase 30/100 column (GE Healthcare). The UV absorption at 280 nm was monitored (blue). Selected fractions were checked for piperine formation (green) or 1-piperoylbenzylamide formation (orange) and the fraction C1 with the highest content in piperine formation was set to 100 %. (B) Selected fractions were also applied on a 10 % gel and separated by SDS-PAGE and stained with Coomassie-Blue (left) or used for immunoblotting with anti-PAS-AB (right). Only fractions with a piperine activity showed a color signal in the immunoblot (antibody dilution 1:5000, detection time 1 min). Piperine synthase and piperamide synthase were marked with an arrow. The immunodetection of piperine and piperamide synthase was part of the master thesis from Luise Jäckel and was performed in our group (IPB).

In summary, all data corroborate that the band detected in the crude protein extracts by the anti-PAS-AB recognizes piperine and piperamide synthase with high sensitivity and quite high specificity. It can therefore be used in future experiments to detect the localization of these enzymes in black pepper fruits and are currently performed in our laboratory by Luise Jäckel (master thesis) in collaboration with Gerd Hause (Biocenter, Martin-Luther-University, Halle-Wittenberg).

4 Discussion and Outlook

In contrast to the work on various other alkaloids over several decades, the biosynthesis of piperine in black pepper was virtually untouched by scientists (Pluskal et al., 2019). Black pepper certainly is not a model plant species and only advanced synthesis and analytics of ^{14}C - or tritium labelled precursors efforts successfully predicted the biosynthetic origin of the piperine molecule, which most likely derived from phenylpropanoid biosynthesis and lysine metabolism (Leistner et al., 1973; Leistner and Spenser, 1973; Prabhu and Mulchandani, 1985). Based on the synthesis of CoA-activated esters and ^{14}C -labelling, both the method of choice in the late 1980s, an enzymatic reaction of piperoyl-CoA and the amine piperidine to piperine by a unstable 'piperoyl-CoA: piperidine N-piperoyltransferase' (EC 2.3.1.145) was described from black pepper shoots (Geisler and Gross, 1990). Nowadays, bioactive compounds from black pepper and other *Piper* species are of considerable pharmaceutical interest and bring the biosynthesis of such compounds back into focus (Nayaka et al., 2021; Salehi et al., 2019; Zhu et al., 2021). In addition, technology driven molecular approaches, first used for a few model species like *A. thaliana*, now became routine and the wealth of genetic information collected over the last decades seem overwhelming. The genome of black pepper and different transcriptome datasets of different black pepper tissues were published in the literature and the piperine biosynthesis was, at least hypothetically, elucidated. Numerous possible enzyme candidates were proposed to participate in the biosynthesis (Dantu et al., 2021; Gordo et al., 2012; Hao et al., 2016; Hu et al., 2015; Hu et al., 2019). However, experimental evidence was missing from a merely bioinformatics guided data collection. Chemical, biochemical, and molecular tools are required to verify the various assumptions made.

4.1 RNA sequencing and co-expression analysis of the transcriptome data

Whereas piperine is nearly exclusively detected in black pepper fruits, in some cases also minor levels are detected in leaves or roots (**Figure 3-26**). At the beginning of this work it was only a vague speculation that piperine biosynthesis takes place in the fruits, specifically since Geisler and Gross (1990) reported the enzyme activity from shoots. The localization of biosynthesis and storage of specialised metabolites, mainly alkaloids in plants is quite diverse. Some specialised metabolites like nicotine from *Nicotiana tabacum* are synthesized in roots and are further transported to the leaves, presumably as a defence mechanism against generalist herbivores (Zenkner, Margis-Pinheiro and Cagliari, 2019). Others, like the tropane alkaloid cocaine from coca (*Erythroxylon coca*) is synthesized and stored in the leaves (Nathanson et al., 1993; Schmidt et al., 2015). The first step in the biosynthesis of pyrrolizidine alkaloids in rattlepods (*Crotalaria* species), is exclusively expressed in the root nodules after infection by rhizobial bacteria. The alkaloids were further transported into the leaves (Irmer et

al., 2015). These pyrrolizidine alkaloids are responsible for the intoxication of grazing animals and the induced effect is known as hepatic veno-occlusive disease. In lesser periwinkle (*Vinca minor*) the biosynthetic relevant enzymes of monoterpene indole alkaloids like the vasodilator vincamine were identified again in the leaves by gene co-expression analysis based on transcriptome data and functionally validated by heterologously expression and activity tests (Stander et al., 2020).

Based on the by far highest content of piperine in black pepper fruits, we speculated early on that piperine biosynthesis and its storage are co-localized. Therefore young fruit stages at the onset of the increase in piperine content were chosen as optimal candidates for RNA sequencing co-expression analysis and comparison to non piperine tissues – young leaves and flowering spadices. The quality of the RNA-dataset is highly dependent on the quality of the RNA send for sequencing (Weber, 2015). The combination of the correct time points with an optimization of the RNA-preparation resulted in 300 million paired end raw reads, that could be obtained totally and assembled by the TRINITY or Trans-ABYSS software which enable transcriptome assembly without a reference genome (Grabherr et al., 2011; Robertson et al., 2010). The combination of several software tools that analyse the sequences under different aspects and therefore result in different annotations and classifications provided the information required for optimal annotation, before the first experiments were performed in the “wet lab” at the bench. E.g. Blast algorithms analyzed the pure sequence information, whereas Mapman classified individual signatures into so-called *bins* and fits a specific data with lower or higher significance, shown by a color (Schwacke et al., 2019). The high-quality classification of the datasets by the individual tools and the overall quality of the reads and reproducibility of individual triplicates in a heat map, facilitate organ specific transcript clustering and in the case of black pepper clearly associate co-expressed genes with different metabolic pathways. Transcripts of two pathways of specialised metabolism, terpenoid metabolism and, as shown in this thesis, piperine biosynthesis, were highly abundant in developing fruits, consistent with the abundance of resulting compounds for the specific “taste” and aroma of the fruits. The confidence in the myriads of data generated, therefore, was extremely high. Since black pepper is not well investigated, the transcript data also provided surprising results on the sideline to us. E.g. among two highly expressed CHS-encoding transcripts, one was co-expressed with piperine biosynthesis genes and also fatty acid biosynthesis (discussed later), whereas the other one was expressed during very early stages of fruit development, both apparently belong to two different pathways (**Figure 4-1**).

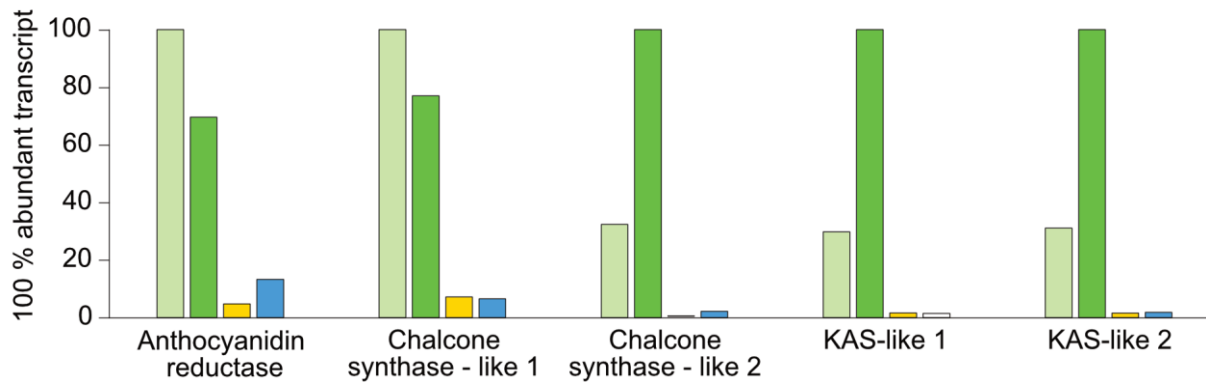


Figure 4-1: Coexpression of annotated genes involved in flavonoid- and fatty acid biosynthesis

Anthocyanidin reductase and two chalcone synthases are related to flavonoid biosynthesis. KAS-like enzymes (β -keto-acyl-ACP-synthase) are essential in fatty acid synthesis and catalyzing the elongation step. The organs are colored: fruit stage I (light green), fruit stage II (green), flowers (yellow), leaves (blue).

The cluster of photosynthesis genes, that are highly abundant in leaves, have low expression levels in green fruits. Yet, the pericarp of green black pepper fruits is green and contains chlorophyll, which was confirmed with expected red fluorescence under a microscope (see also **Figure 3-4**). So, why are the photosynthesis genes expressed at low levels? This certainly is an aspect worth investigating in future studies. During our investigation of CoA ligase candidates our dataset showed an extreme and high expression of a single CoA ligase only in the flowers. This CoA ligase has no similarity to any other CoA ligase present in the databases. This expression was also confirmed by qPCR, so what does it do? Obviously, many questions are raised by the RNA sequencing dataset that need experimental answers.

For this investigation on piperine biosynthesis, the initial examination of the RNA sequencing dataset provided more inspiring support than we ever expected. Among the highest number of transcripts specifically in 40-60 day old fruits, two BAHD-type acyltransferases popped up, annotated as benzoyl-CoA benzoyl transferases, and in addition this unknown PnCYP719, annotated as cheilantifoline- as well as (S)-canadine synthase, all highly abundant and highly expressed exactly at the developmental stage, shortly before the slope of piperine accumulation reached its maximum (**Figure 3-2**). BAHD acyltransferases use CoA-ester activated precursors and catalyze the formation of esters and amides (D'Auria et al., 2002), whereas the cheilantifoline and (S)-canadine synthase encode cytochrome P450 enzymes catalyzing methylenedioxy bridge formation in an isoquinoline alkaloid substructure (Rüffer and Zenk, 1994; Yahyazadeh et al., 2017). So, the dataset seemed to guide us directly to the set of genes we were interested in. Among other transcripts, a PnCPR, a cytochrome P450 reductase, followed the trend, although at lower abundance, too. This trend was also seen in the case of piperoyl-CoA ligase, which activates piperic acid and was identified and characterized prior to the availability of our transcriptome data (Schnabel et al., 2020). When

the genome dataset that was published with a set of transcriptome data of black pepper was monitored, the same trend of co-expression was observed and plausible suggestions of piperine formation in black pepper were in line with our data (Hu et al., 2019).

Since root material was low, we could not include the root transcriptome data in the RNA sequencing data. Already in 2012, Gordo et al. pointed out the relevance of transcriptome data analyzing the black pepper root transcriptome after infection with pathogens, *Phytophthora capsici* and *Fusarium solani*. No emphasis was given to plant specialized metabolites and any relevance to piperine was missing. Therefore, the root transcriptome contained transcripts for piperine biosynthesis remained unclear. When we analyzed roots by qRT-PCR, it became clear that none of the transcripts for piperine formation were abundant in roots, and therefore, this organ neither accumulates considerable levels of piperine nor is responsible for its biosynthesis. Thus, the biosynthesis of the phenylpropanoid moiety and most likely that of piperidine seems fruit specific.

4.2 The activation of piperic acid

Piperoyl-CoA ligase was discovered an educated guess. The similarity search was not limited to classical p-coumaroyl-CoA ligases (Jin et al., 2020), which may be present in black pepper, but could also be involved in lignin formation, but for an enzyme that has a specificity for a longer carbon chain length, like the 5-phenylpentanoic acid/OPDA CoA ligase from *A. thaliana* (Kienow et al., 2008). The precursor piperoyl-CoA in the final piperine formation was not commercially available. Therefore an enzyme able to provide the CoA-activated precursor (Beuerle and Pichersky, 2002) proved very useful for the characterization of piperine synthase, by producing the required substrate. Whereas this CoA ligase was discussed initially as a CoA-producing enzyme (Schnabel et al., 2020), the subsequent identification of remaining enzymatic steps showed that this enzyme is essential for the piperine biosynthesis in black pepper fruits. It could also be useful to replenish the pool of piperoyl-CoA, when piperine synthase may produce piperic acid in case of low piperidine concentrations (Schnabel et al., 2021a). The CoA ligases identified by Jin et al. (2020) in parallel from black pepper also encoded CoA ligases, but the screen was based on classical Arabidopsis 4-CLs. These resulted in transcripts that were not preferentially expressed in fruits, and encoded proteins with a broader specificity, like Pn4CL3 which activates caffeic acid, piperonylic acid, 3,4-(methylenedioxy) cinnamic acid, and piperic acid, the latter with a lower turnover. PnCL3 is interesting in terms of the product profile and promising for biotechnological production of diverse CoA esters, but is clearly not associated to piperine biosynthesis.

4.3 Piperine synthase versus Piperamide synthase

Two BAHDs were highly abundant in young black pepper fruits and catalyze the formation of piperine or piperine stereoisomers. The piperine synthase shows a high preference and specificity for piperine formation, whereas the piperamide synthase showed a higher promiscuity to different acyl-donor and acyl-acceptor. Also, the piperamide synthase catalyzed the formation of stereoisomers of piperine. This unusual product profile of piperamide synthase is inconsistent with the product profile of fresh fruits from the IPB green house and in dried peppercorns or the activity in total protein preparation of young fruits. The biological relevance remains obscure, although piperamide synthase is highly expressed in black pepper fruits, piperoyl-CoA and piperidine as *in vivo* substrates are questionable. Interestingly, isomer formation is similar to observations with *A. thaliana* coumarin synthase (COSY) (Vanholme et al., 2019). This BAHD catalyzes the intramolecular acyl transfer and lactonization in coumarin biosynthesis after active isomerization of 6-*ortho*-hydroxy-transferuloyl-CoA to 6-*ortho*-hydroxy-cis-feruloyl-CoA. This isomerization was suggested to occur spontaneously. A similar mechanism in piperamide synthase could be plausible, but requires further investigations, more specific elucidation of the structure and site directed mutagenesis that may reveal the relevant amino acids. Nevertheless, the high promiscuity of piperamide synthase makes it a very interesting candidate for production of bioactive relevant substances (Eudes et al., 2016). Piperine synthase and piperamide synthase share 62 % amino acid sequence identity and contain the characteristic HXXXD motif, whereas the DFGWG motif is slightly modified. The *Piper* DWGWG seems to be unique for *Piper* BAHDs. This motif plays a general role in conformational changes during the reaction. Among hundreds of BAHD-like sequences the highest sequence identity of 42 % is shown compared with two enzymatically characterized BAHDs, the benzylalcohol *O*-benzoyltransferase (BEBT) from *Clarkia breweri* flowers and hexen-1-ol acetyltransferase from *A. thaliana* leaves. Both enzymes are *O*-acyltransferases and accept aliphatic alcohols as acyl-acceptors. In contrast to the unique correlation of classification and properties of CoA ligases or cytochrome P450 enzymes, the BAHD classification gives virtually no information about the enzymatic activity. This is intensified by only a handful characterized BAHDs and *N*-acyltransferases, that are present in nearly all BAHD clades based on sequence identity (D'Auria, 2006; Tuominen et al., 2011). Less than 22 % amino acid identity of *Piper* BAHDs is observed in *N*-acyltransferases, like the capsaicin synthase (Pun1) from *Capsicum annum* or spermidine hydroxycinnamoyl transferase (SHT) and disinapoyl/dicoumaroyl transferase (SDT) from *A. thaliana*. Although it is apparent from the rare crystal data that BAHDs all share a similar protein fold (Suppl.: **Figure 8-14**), it is extremely difficult to identify residues, that are important for substrate specificity, or simply to distinguish between *N*- and *O*-acylation. Therefore, only a successful protein crystallization and structure elucidation of piperine synthase or piperamide synthase

will shed light on the usual isomerization and will reveal the amino acids that determine the substrate specificity and the mechanism of both enzymes.

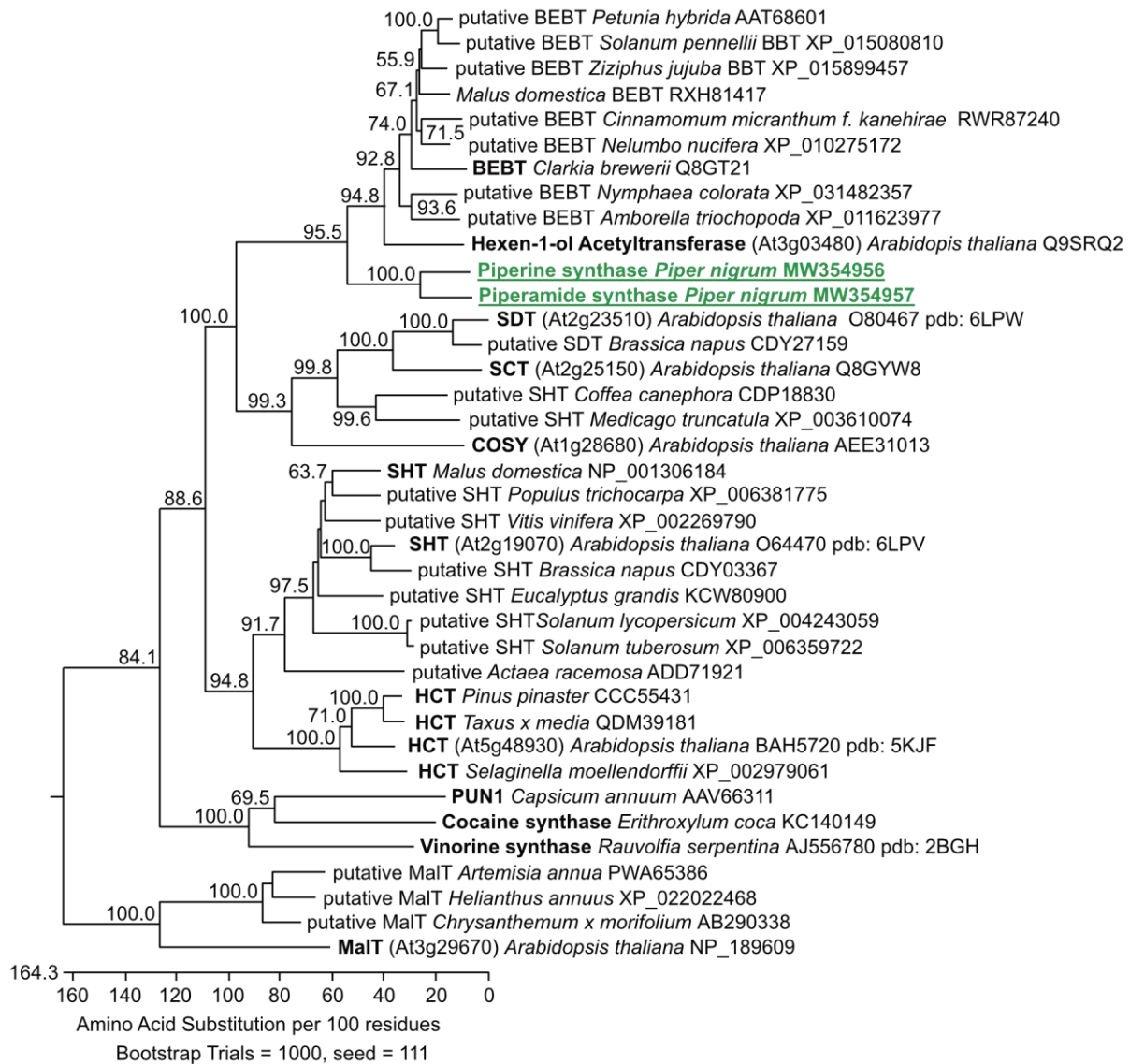


Figure 4-2: Bootstrapped, unrooted cladogram of BAHD protein sequences obtained using ClustalW.

Piperine synthase and closely related piperamide synthase from black pepper (bold, underlined, green) were compared to representative BAHDS from all five clades (D'Auria, 2006). Functionally characterized benzoyl-CoA benzoate transferases (BEBTs) and (Z)-hexen-1-ol acetyltransferase from *Arabidopsis thaliana* represent clade V of BAHD-like acyltransferases but are distinct from piperine and piperamide synthases. Clusters harboring capsaicin synthase, vinorine synthase, malonyltransferases, cocaine synthase, hydroxycinnamoyltransferases (HCTs), and spermidine hydroxycinnamoyl transferases (SHTs, SDTs and SCT) share <25 % amino acid sequence identity to piperine and piperamide synthase, respectively. Either NCBI accession numbers, *Arabidopsis thaliana* gene entries (www.tair.org), and/or the pdb-accession number of crystallized and functionally characterized synthases are shown. (Slightly modified after Schnabel et al., 2021a.)

4.4 Methylenedioxy bridges in piperamide skeleton

By RNA sequencing a single fruit specific transcript of a cytochrome P450 enzyme with a high similarity to cheilanthilfoine and canadine-synthases was annotated. PnCYP719 was identified as CYP719A37 and exclusively converts feruperic acid into piperic acid by methylenedioxy bridge formation. The enzyme belongs to the class of CYP719A clade, containing several alkaloid biosynthesis enzymes of high substrate and even regiospecificity. In the genome of early diverged angiosperms (ANA-clade) like *Amborella* (*Amborella trichopoda*) or the water lily (*Nymphaea cordata*) CYP719-like genes and related products are missing (Albert et al., 2013; Zhang et al., 2020). In the recently published black pepper genome, in the genome of sacred lotus (*Nelumbo nucifera*), as well as in the transcriptome dataset of kava pepper (*Piper methysticum*) only a single CYP719 gene is present. All three species belong to the Magnoliids (Hu et al., 2019; Ming et al., 2013; Pluskal et al., 2019). The CYP719 clade could, therefore, be developed from a CYP719-ancestor after diversification of magnoliids, eudicots, and monocots from this ANA-clade. In the genome of *Aristolochia spec.*, also closely related to *Piper* and able to synthesize hepatotoxic aristolochic acid, that besides an unusual aromatic nitro-group also contains a methylenedioxy bridge, at least one CYP719 must be detectable. Diversification, probably by gene or genome duplication of the CYP719 family, may have occurred several times independently during subsequent evolution of the eudicots, and resulted in a whole CYP719 gene family detected in recently published genomes from the Papaveraceae five-seede plume-poppy (*Macleaya cordata*), or the stout camphor tree (*Cinnamomum kanehirae*), from the Lauraceae family, encoding enzymes of benzylisoquinoline biosynthesis (Chaw et al., 2018; Liu et al., 2017). CYP719A26 from kava pepper and CYP719A37 from black pepper share 95 % of amino acid sequence and could be derived from a common ancestor. Although they have a high similarity, they catalyze the reaction on different skeletons in different organs, one in piperine and the other in kavalacton skeleton, a psychoactive polyketide. CYP719A26 was predominantly found in roots (Pluskal et al., 2019).

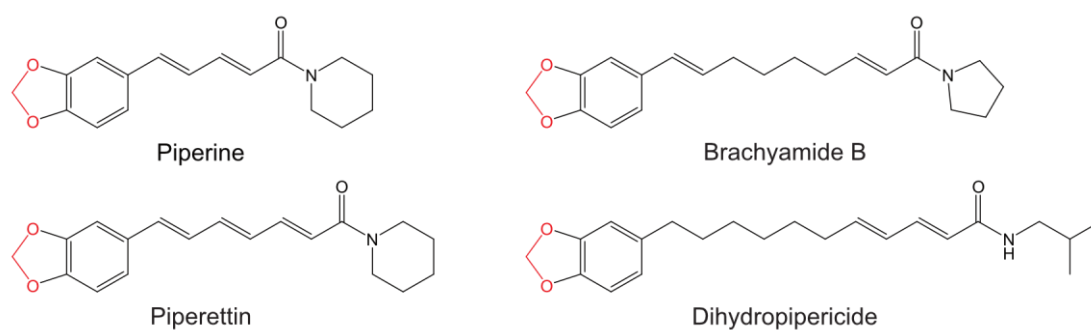


Figure 4-3: Piperamides from black pepper.

Besides piperine, further methylenedioxy bridge containing piperamides were detected in black pepper (Parmar et al., 1997). As examples brachyamide B, piperettin and dihydropipericide are shown.

Further methylenedioxy bridge-containing piperamides occur in black pepper, although in smaller quantities. It seems that the two double bonds or a chain of four in the aliphatic chain are a minimum for methylenedioxy bridge formation since piperine is the smallest molecule with a methylenedioxy bridge in black pepper. Further piperamides with a methylenedioxy bridge have a longer even numbered chain (**Figure 4-3**). This raises the question if piperic acid is the starter molecule for all elongated piperamides or CYP719A37 accepts elongated substrates originating from ferulperic acid.

Methylenedioxy bridge-containing lignans like (S)-sesamin and (S)-pinoresinol were extracted from other *Piper* species, whereas they were not reported in black pepper so far (**Figure 4-4**). Instead black pepper and cubeb pepper, contain (R)-cubebin and derivatives (Lim, 2012b; Rezende et al., 2016). These compounds are similar to the lignan hinokinin, a dibenzoylbutyrolactone from hinoki cypress (*Chamaecyparis obtuse*). Hinokinin has anti-inflammatory properties and a high activity against *Trypanosoma cruzi*, the pathogen of Chagas' disease (Marcotullio, Pelosi and Curini, 2014). The lignan biosynthesis starts with pinoresinol synthase, which couples two molecules of coniferyl alcohol. It is suggested that (S)-pinoresinol as precursor is reduced by pinoresinol-lariciresinol reductase into (S)-secoisolariciresinol and in further steps, including methylenedioxy bridge formation, catalyzed into (R)-hinokinin (Bayindir, Alfermann and Fuss, 2008) (**Figure 4-4**).

Interestingly, transcripts coding for pinoresinol-lariciresinol reductase (PLR) and pinoresinol reductase as well as secoisolariciresinol dehydrogenase (SDH) like enzymes are also present in our RNA dataset but are more abundant in leaves. Similar biosynthetic steps in cubebin biosynthesis are realistic. Nevertheless, a cytochrome P450 catalyzing the methylenedioxy bridge in hinokin skeleton is not characterized yet and CYP81Q was only shown to be involved in sesamin biosynthesis. Furthermore, a transcript for CYP81Q or a homolog is also missing in our transcriptome data. However, since there is only one member of the CYP719 family present in our dataset of black pepper, it remains to be experimentally verified if a CYP81Q homolog or an unknown cytochrome P450 enzyme catalyzes the methylenedioxy bridge in the cubebin biosynthesis. The high diversity of methylenedioxy bridge-containing piperamides and lignans call for more than one enzyme for formation. One should not forget that the transcriptome dataset do not cover the transcripts to 100 %, so the existence of a 2nd gene could be tested in the genome data (Hu et al., 2019).

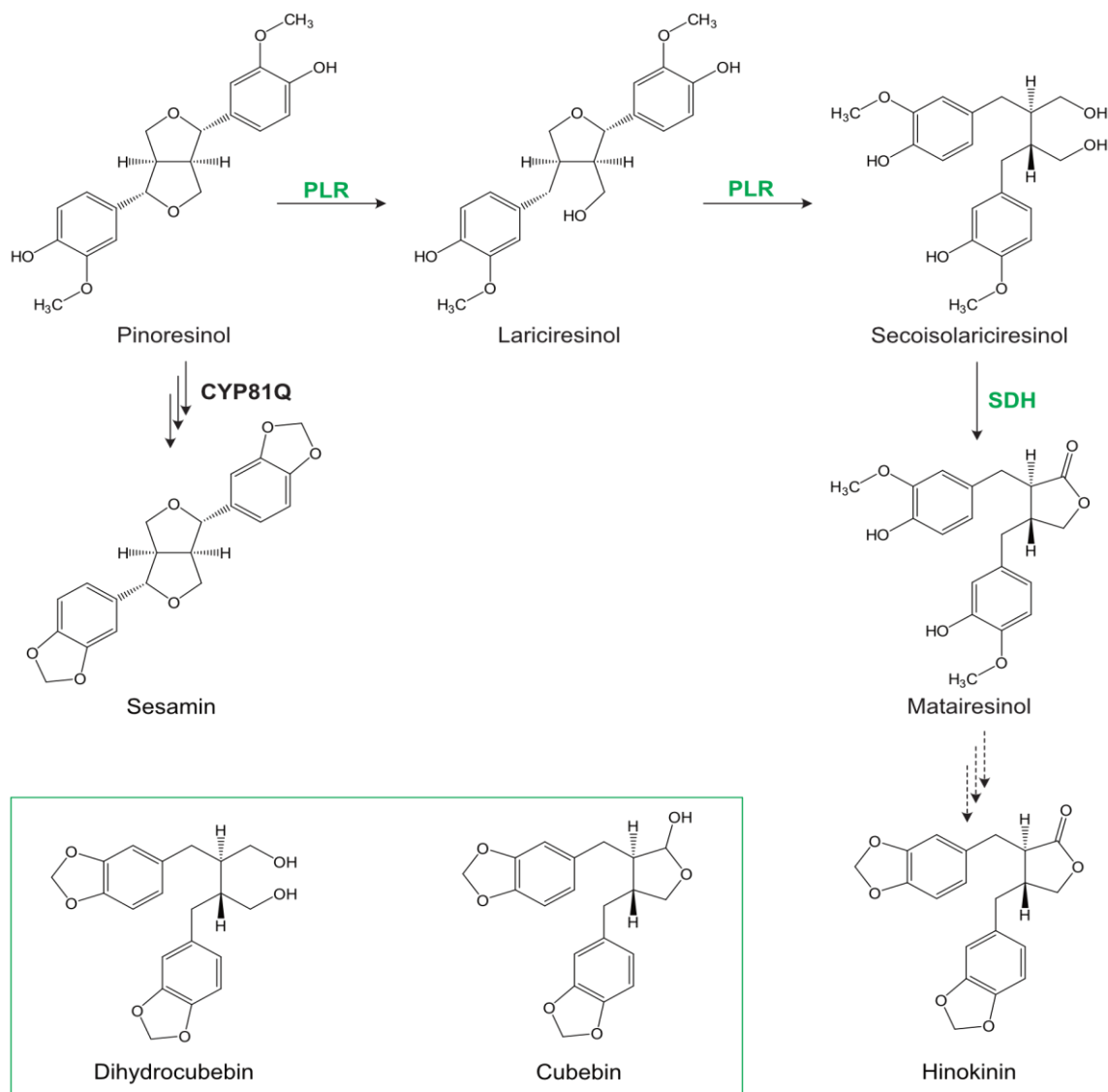


Figure 4-4: Hypothetical pathway of hinokinin and the structure of homolog compounds from black pepper

The hypothetical pathway of hinokinin in *Linum corymbulosum* in comparison to sesamin biosynthesis is shown (Bayindir et al., 2008). Pinoresinol is reduced twice to secoisolariciresinol by pinoresinol-lariciresinol reductase (PLR). Matairesinol is formed by secoisolariciresinol dehydrogenase (SDH). In further steps methylenedioxy bridges were introduced into the matairesinol skeleton, resulting in hinokinin. Dashed lines indicate unknown steps. Enzymes, which were also found in our black pepper transcriptome, are marked green. Dihydrocubebin and cubebin from black and cubeb pepper are shown in the green frame.

4.5 Additional enzymes involved in piperine biosynthesis

4.5.1 Chain elongation – a linkage to fatty acid biosynthesis or flavanol biosynthesis

Besides piperine, black pepper and other *Piper* species show a variety on medium chain, often unsaturated amides (Strunz, 2000). Several of these compounds incorporate an aromatic group, like piperine or coumaperine. Further all have in common an even number of carbon atoms in the side chain and often differ only in the incorporated amine. Based on our knowledge and numerous data on structure analysis of *Piper* amides, a chain elongation by fatty acid synthesis is proposed (Gómez-Calvario and Rios, 2019; Strunz, 2000).

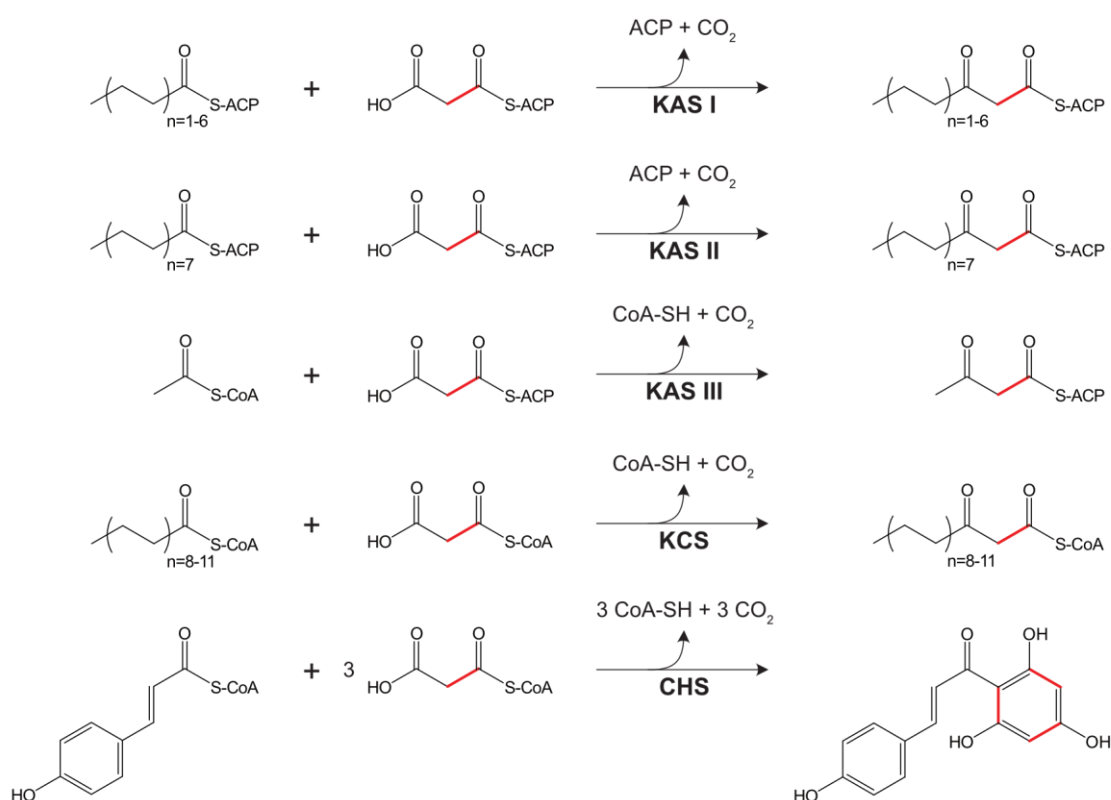


Figure 4-5: Enzymes catalyzing chain elongation reactions in plant species

The β -keto-acyl-ACP-synthases (KASI, KASII and KASIII) are involved in the general fatty acid biosynthesis and differ in the chain length. The 3- ketoacyl-CoA synthase (KCS) is involved in wax biosynthesis. Chalcone synthases (CHS) add C2 units in the polyketide biosynthesis. Incorporated C2 unit is marked red. Figure is slightly modified after Jiang et al., 2008)

In plants, different C-C elongating enzymes are known (Jiang et al., 2008) (**Figure 4-5**). One possibility is the chain elongation mediated by the acyl carrier proteins (ACP) dependent fatty acid synthase type II system (FAS). This complex consists of four distinct monofunctional enzymes: the β -keto-acyl-ACP-synthase, the β -ketoacyl-ACP-reductase, the β -hydroxyacyl-ACP dehydrogenase and enoyl-ACP reductase. Each enzyme is encoded by one gene, whereas in mammals one multi-enzyme protein with all four catalytic sites (FAS Type I) catalyzes the whole reaction (Smith, Witkowski and Joshi, 2003). The β -keto-acyl-ACP-

synthases KAS I and KAS II, both localised in the plastids, are catalyzing the chain elongation step by adding a C2 unit, derived from malonyl-ACP to a growing fatty acid chain (von Wettstein-Knowles et al., 2000; Yasuno, von Wettstein-Knowles and Wada, 2004). KASI and related *de novo* fatty acid synthesis play an essential role in the embryo development in *A. thaliana*. A deficiency in KASI causes a change in the lipid composition and a followed disrupted embryo development (Wu and Xue, 2010). Besides KASI and KAS II, also KASIII plays an important role in fatty acid biosynthesis, initiating the first elongation step from C2 to C4 (Tsay et al., 1992), but can be also involved in specialized metabolism (Nofiani et al., 2019). Some KASIII proteins show unusual catalytic functions, like head-to head condensation to form a lactone structure, formation of tetronate rings, esterification or amidation reactions (Nofiani et al., 2019). They use acyl-CoA and some acyl-ACP as substrate. A fourth member, the 3-ketoacyl-CoA synthase (KCS) is especially involved in wax biosynthesis and their storage in seeds (Blacklock and Jaworski, 2006). In our black pepper RNA dataset transcripts, annotated as KASI like from *A. thaliana* (63 %) or KASIII like from Korean perilla (*Perilla frutescens*, 90 %) and from sun sunflower (*Helianthus annuus*, 72 % identity) are highly abundant in the black pepper fruits (see also **Figure 4-1**) (González-Mellado et al., 2010). Functional characterisations of KASIII enzymes in plants besides *A. thaliana* are rare and some conclusions about piperamide elongation could be misleading. Nevertheless, FAS type I multicomplex protein from rat liver and mammary glands also accepted phenylacetyl-CoA and the substrate can be elongated up to phenyldodecanoic acid (Smith and Stern, 1983) and a KASIII like enzyme from bacterium *Streptomyces pactum* transfers a 6-methylsalicylyl moiety in the biosynthesis of pactamycin, a protein synthesis inhibitor (Abugrain et al., 2017). Benzoyl-ACP and cinnamoyl-ACP are also accepted, but with a reduced activity. If there are similar properties in plant KAS enzymes, especially KASIII, is unknown.

Besides classical fatty acid synthesis, polyketidsynthases/chalcone synthases can catalyze a decarboxylative condensation, (aldol condensation). Chalcone synthases (CHS) are substrate specific and add C2 units by utilizing malonyl-CoA, regulate the number of elongation steps, and further cyclize the intermediate into the final polyketides (Jiang et al., 2008). Typical polyketides are chalcones, stilbenes and phloroglucinols (**Figure 4-6**, A). Transcripts for CHS are highly abundant and one is virtually co-expressed with piperine biosynthesis genes during fruit development (see also **Figure 4-1**). Transcripts show a high identity to classical naringenin chalcone synthases (Raharjo et al., 2004; Zheng et al., 2001), whereas another transcript shows high identity to styrylpyrone synthase from kava pepper (95 %), which exclusively synthesizes the triketide lactone bisnoryangonin instead the naringenin chalcone (Pluskal et al., 2019). In black pepper fruits, up to 13 µg/g fresh weight of naringenin chalcone can be extracted with 80 % methanol (Lackova et al., 2017). The flavones apigenin and quercetin also occur in black pepper fruits (Chandra et al., 2015). A linkage between flavonoid content in

black pepper fruits and high levels of chalcone synthase-like transcripts to flavonoid biosynthesis is most likely (see also **Figure 4-1**). Underlined is this hypothesis by the conservation of the CHN triad, amino acid residues essential for the mechanism of elongation and cyclisation of polyketides (Jiang et al., 2008). Nevertheless, a single amino acid substitution can change the product formation. In shrubby St. John's Wort (*Hypericum androsaemum*) the substitution T135L in benzophenone synthase changes the enzyme to a phenylpyrone synthase (**Figure 4-6, B**) (Klundert et al., 2009).

After all, whether either fatty acid synthases, like KAS III, or chalcone synthases are involved in the elongation step of piperine biosynthesis is still enigmatic. From our RNA sequencing KAS like enzymes and also one CHS follow the coexpression pattern of piperine biosynthetic enzymes and are suggested (see also **Figure 4-1**). Nevertheless, in both cases, an efficient stop is required after only one elongation step of a previously synthesized phenylpropanoid starter, most likely ferulic acid.

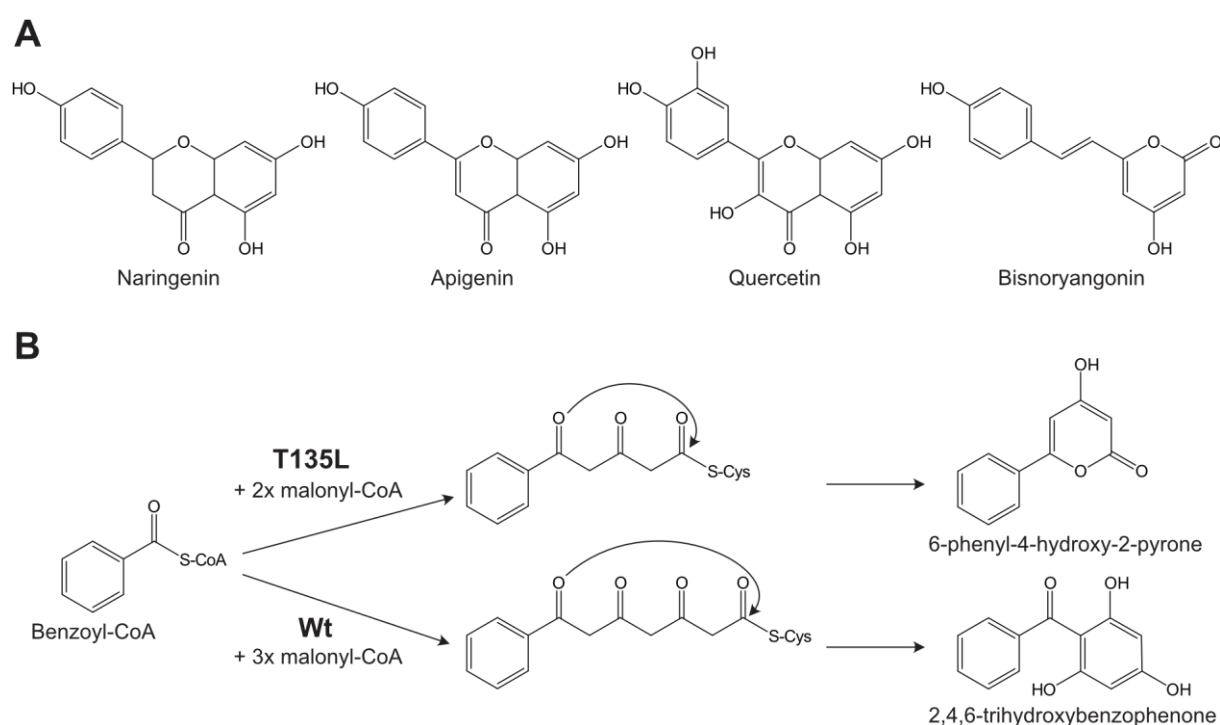


Figure 4-6: Different flavonoids and the inversion of benzophenone synthase to a phenylpyrone synthase

(A) Different flavonoids are shown: naringenin, a flavanone in grapefruit (*Citrus x paradise*); apigenin, a flavanone from parsley (*Petroselinum crispum*) and celery (*Apium graveolens*); quercetin, a wide distributed flavonol named by the oak tree (*Quercus*) and bisnoryangonin, a styrene from kava pepper (*Piper methysticum*). **(B)** The T135L substitution in benzophenone synthase changes the enzyme in a phenylpyrone synthase in shrubby St. John's Wort (*Hypericum androsaemum*). Part B is slightly modified after Klundert et al., 2009.

4.5.2 Piperidine biosynthesis

The biosynthesis of the amine piperidine is still unclear. Based on different tracer studies with ^{14}C -labeled L-lysine in Crassulaceae, Solanaceae, Fabaceae and in *P. longum*, the incorporation of L-lysine in the piperidine molecule and in further experiments cadaverine as intermediate were identified (Gupta and Spenser, 1969; Leistner and Spenser, 1973; Prabhu and Mulchandani, 1985). The model of decarboxylation of L-lysine to cadaverine and the oxidative deamination to 5-aminopental was already confirmed in the biosynthesis of lupine alkaloids (see also **Figure 1-7**) (Bunsupa et al., 2011; Frick et al., 2017). Only the reduction of Δ^1 -piperideine to piperidine is unclear. A high expression of a lysine/ornithine decarboxylase and an aliphatic diamine oxidase in fruit stage II, virtually co-expressed with piperine biosynthesis genes encoding CYP719A37 and piperine synthase support this biosynthesis also in black pepper. An imine reductase for the last step in piperidine biosynthesis is still missing, was also not specifically identified from the genome dataset (Hu et al., 2019), and needs further investigations. Maybe, a simple, constitutively expressed, and non-specific general reductase is sufficient.

4.6 Localization of piperine biosynthesis in black pepper fruits

The black pepper fruit is surrounded by an epidermis with a cuticula and contained two major compartments, the pericarp and the perisperm (**Figure 4-7**) (Mangalakumari, Sreedharan and Mathew, 1983). Both are separated by a pigment layer, characterized by the high content of flavonols (Mangalakumari et al., 1983). Polyphenols were detected by bis-diazotized benzidine in the pericarp. Less is known about the distribution of piperine during fruit development, possible storage capacities and the localisation of biosynthetic relevant enzymes.

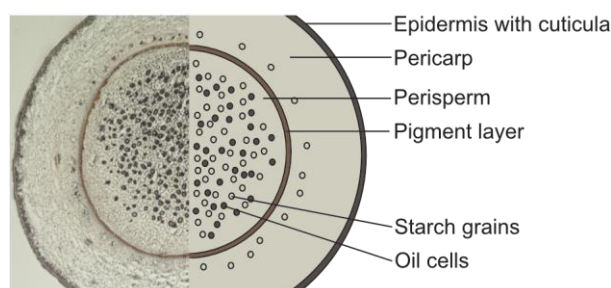


Figure 4-7: Cross section of a black pepper fruit

A thin section (15 μm) of a 70 dpa old black pepper fruit was prepared by the cryotom CM1950 (Leica) and a light image was taken with an axioskop 2 (ZEISS). The image was halved and combined with a simplified scheme, designed with Affinity Designer software. Different fruit compartments and specialised cells were marked. The captions are based on Mangalakumari et al. (1983).

In 2005 Schulz et al. performed a Raman mapping on mature black pepper fruits. Piperine was determined in the perisperm. In a preliminary test, single cells from perisperm

and pericarp from a 70 dpa old black pepper fruit were collected by laser capture microdissection and the piperine content was measured. The highest piperine concentration was contributed to the perisperm. To get a closer look into piperine distribution in different developmental stages we used MS-imaging in a preliminary experiment. Microscopic sections (15 μm) of three developmental fruit stages were prepared and the piperine localization recorded by MALDI-imaging (Alexandrov et al., 2013). Normally coating is required, especially for weak ionizable molecules, but in case of piperine no matrix was needed. It can easily be

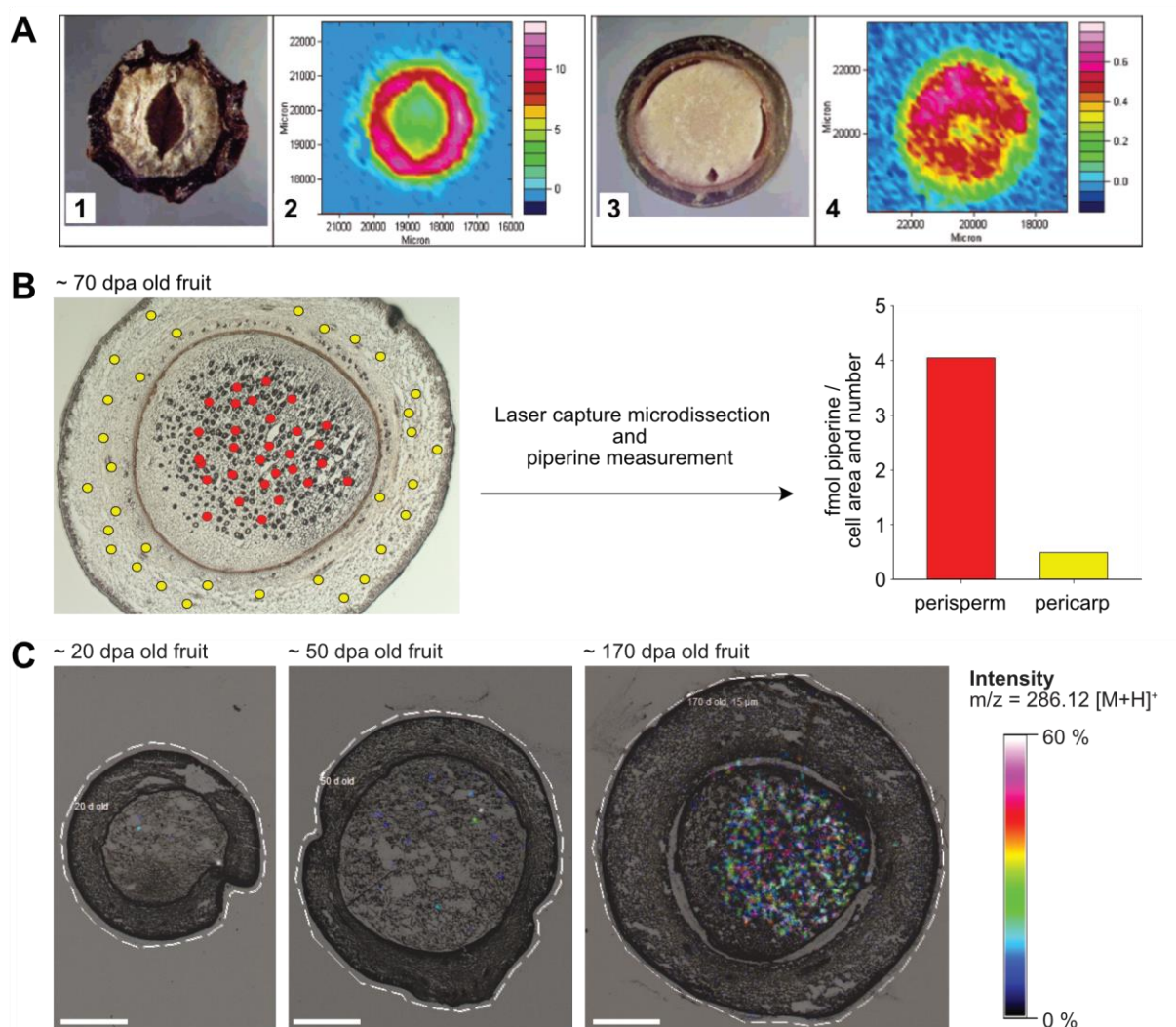


Figure 4-8: Piperine localisation in black pepper fruits

(A) Microscopic images of a dried black peppercorn (1) and a mature green pepper fruit (3) as well as the related Raman maps (2, 4) showing the distribution of piperine in the plant tissue. The relative concentration of piperine was determined according to the intensity in the frequency range between 1547 and 1659 cm^{-1} . (Slightly modified after Schulz et al., 2005). (B) From a 70 dpa fruit thin sections were cut and single cells of the pericarp and perisperm were collected by laser capture microdissection. The piperine content was measured by HPLC-UV-ESI-MS. (C) Sections (15 μm) of three developmental stages (~ 20 d, ~ 50 dpa and ~ 170 dpa) were analyzed by MS-imaging. The mass signal of $m/z = 286 [M+H]^+$ was recorded. The light image of the section is shown in a grey scale whereas the mass signal intensity is colored. The scanning frame is shown as white dashed lines. The white scale corresponds to 1 mm.

ionized and can be detected by MS at $m/z = 286$ $[M+H]^+$ up to 10 fmol. After scanning the section, the intensity of the selected mass signal and the incident light image of the section were combined (**Figure 4-8**). The mass signal of $m/z = 286$ $[M+H]^+$ is clearly distributed to the perisperm and only a few spots with lower intensity are shown in the pericarp. The signal intensity and the signal number increased during fruit development. This observation can be underlined by combining microscopy with fluorescence detection. Piperine, as an aromatic compound can be excited by low wavelength UV, similar to caffeic or ferulic acid and shows a specific emission spectrum based on different solvents (Debnath and Mishra, 2020). All data indicate up to now that piperine is stored in specific cells, rather than distributed equally all over the place.

The piperine content in mature black pepper fruits is up to 2-8 % of the dry weight and seems to require specialized storage capacities (Kanaki et al., 2008). It could mean, that molar concentrations are stored in these specialized cells. How does a plant manage that? Anthocyanins can make up to 30 % of the dry weight, like rutin in the flowers of sophora (*Sophora japonica*), and are stored in specific structures, termed anthocyanoplasts or vacuolar structures (Chanoca et al., 2015; Knudsen et al., 2020; Pecket and Small, 1980). This is a concentration that is 12-fold higher than in aqueous solutions. The concentration of vanillin glucoside from mature *Vanilla planifolia* pods can be stored up to 4 M in phenyloplasts (Brillouet et al., 2014; Gallage and Møller, 2015). The microscopic findings in case of piperine suggested rather a whole cell storage capacity, comparable to resin ducts or heads of glandular trichomes than specialized chloroplasts. In such cases, natural deep eutectic solvents (NADES) as liquid storage capacities are currently discussed as one solution to explain this high concentrations (Dai et al., 2013). NADES are highly viscous liquids based on sugars, amino acids, organic acids, choline or urea, with only very limited water content and were shown to be excellent solvents for weakly soluble natural products like vanillin glycoside or the anthocyanin rutin (Dai et al., 2013; González et al., 2018; Knudsen et al., 2020). They might stabilize metabolons of biosynthetic enzymes and improve their activity. For example, the biosynthesis of dhurrin, a cyanogenic glycoside in the plant defense of sorghum (*Sorghum bicolor* L.), was stabilized and performed in a NADES solution of glucose:tartrate, even better than in a standard buffer solution (Knudsen et al., 2020). As `liquid crystal` some NADES combinations are discussed to stabilize specific natural products with established hydrogen bonds between the NADES substances, the water molecules, and the natural products in a high coordinated system. Solubility and accumulation of high amounts of natural products without any isomerization seems therefore plausible. Amines, as in the case of betaine and choline could act as NADES substances (Bartels and Sunkar, 2005). Is it possible, that piperidine serves as a component or partner of NADES itself? No real saturation of

piperine and piperamide synthase activity was observed even at extremely high piperidine concentrations of up to 100 mM. To check for these arbitrarily high concentrations, one needs to analyse the metabolomics content of the cells, which seem to contain large amounts of piperine by untargeted LC-MS data combined with laser microdissection. If piperidine is a compound of a NADES solution in black pepper and inhibiting the isomerization of piperine in case of piperamide synthase reaction is intriguing, although still speculative and should be further investigated.

Black pepper plants are difficult to transform. Therefore localization studies with GFP reporter lines like in *A. thaliana* is not possible (Grunewald et al., 2020). With the specific anti-PAS-antibody in our hands (see also **Figure 3-27**), we can now look for the localization of piperine- and piperamide synthase in black pepper organs and cells. With a second anti-rabbit-LgG antibody coupled to Alexa Fluor™-488 the localization of biosynthetic enzymes can be determined potentially down to cell organelle level. Furthermore, the transcripts coding for biosynthetic enzymes are highly abundant in the black pepper fruits and increase between stage I and stage II (**Figure 3-26**). With an *in situ*-PCR it is possible to localize abundant transcripts in tissue sections (Andersen et al., 2017). All together, diverse microscopical techniques allow us to get a closer look at piperine and piperine biosynthesis in black pepper fruits.

4.7 Piperine biosynthesis in black pepper fruits – conclusive statement

The biosynthesis of piperine was enigmatic for decades. Advances in the synthesis of potential precursors and tracer experiments on the biosynthesis of piperlongumine performed in *P. longum* (Prabhu and Mulchandani, 1985) combined with data from Leistner and Spencer (1973) on piperidine biosynthesis in *S. acre* provided initial evidence that piperamide biosynthesis is based on phenylalanine and lysine biosynthesis, thus combining a phenylpropanoid moiety with the piperidine heterocycle. It took 20 years to provide the first enzymatic evidence for a piperine synthase reaction by Geisler and Gross (1990) and additional 30 years for a more precise annotation of the three piperine biosynthesis specific genes and enzymes described now in this thesis. Advances in computational and molecular, specifically sequencing tools combined with established organic synthesis, enzyme assays and product detection by HPLC-ESI-MS not only enabled characterisation of individual reaction, but also suggested a plausible order of the late reactions in piperine and piperamide formation and last but not least provided evidence that the biosynthesis and storage of the products in the case of piperine is localized in the same organ, or even cells (**Figure 4-9**). In addition, all functional characterized enzymes appear highly specific to black pepper fruits. The wealth of data obtained by the RNA-Seq approach should allow to unravel the remaining enzymatic steps, either presumed chain elongation of heterocycle or formation of the

heterocycle in due course. But even when this pathway is completely solved numerous fascinating questions on regulation as well as product accumulation and storage remain. Potential biotechnological applications are not only limited to the production of relevant compounds in microbial hosts but may be extended towards producing the complete biosynthetic pathway in pro- and eukaryotic hosts by newly developed modular cloning techniques (Grützner and Marillonnet, 2020).

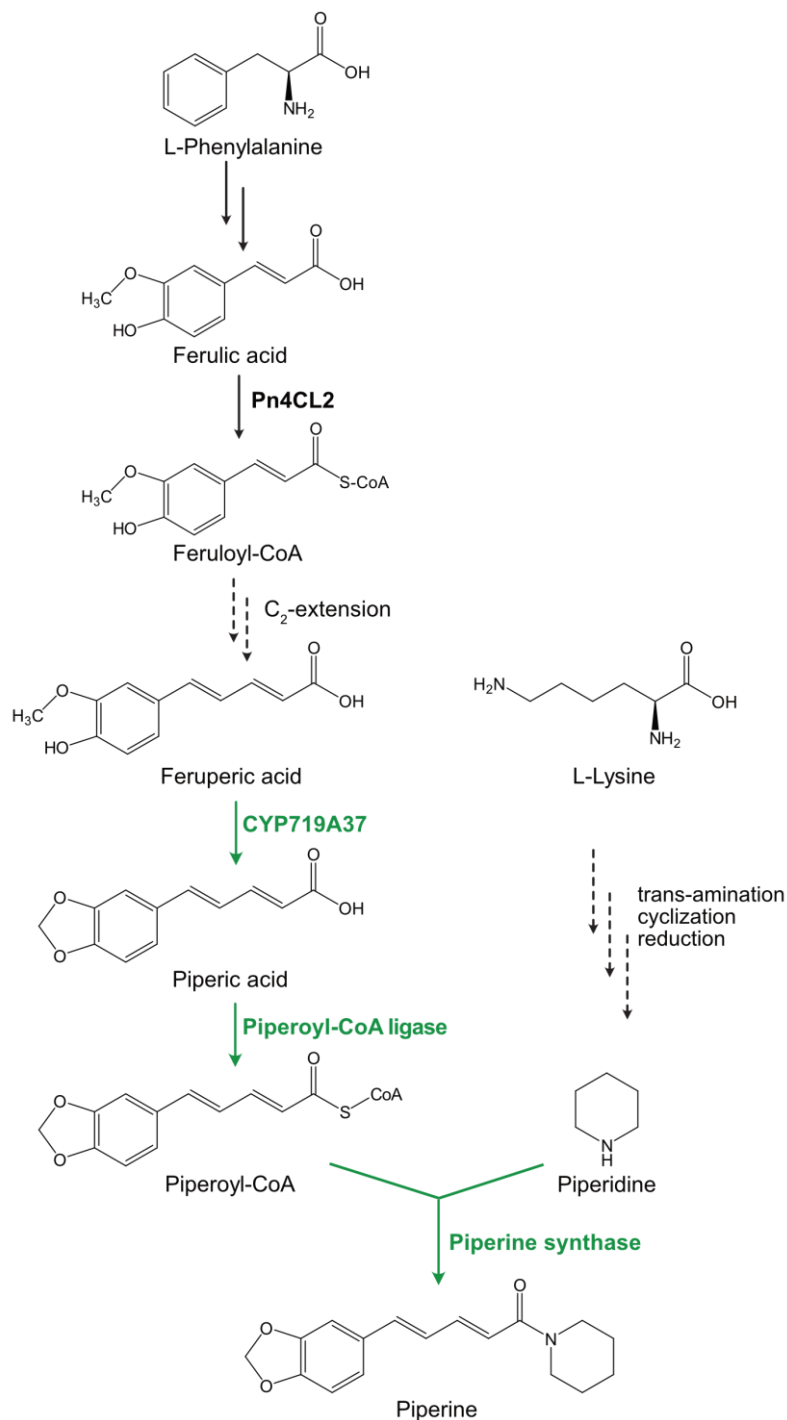


Figure 4-9: Piperine biosynthesis in black pepper fruits

Three final fruit steps have been described in this thesis (green). Pn4CL2 likely catalyzes the activation of ferulic acid. C₂-extension and piperidine formation require enzymatic and molecular evidence.

5 Summary

Black pepper (*Piper nigrum* L.) is the king of spices and has been used over centuries in traditional as well as in modern medicine. Most bioactivities are related to piperine (1-piperoyl-piperidine), an amide and likewise an alkaloid essentially derived from the amino acids, phenylalanine, and lysine. Due to the high content of piperine in black pepper fruits, it was suggested that piperine biosynthesis is localized in the fruits and thus, identification of genes encoding piperine biosynthesis related enzymes could be facilitated by a differential RNA-sequencing approach comparing organs with and without piperine formation. Therefore, piperine accumulation was monitored during fruit development. Based on these data, two developmental stages, 20 to 30 days post anthesis, and 40 to 60 days post anthesis that show the either initiation or the strongest increase in piperine formation, respectively were chosen for a differential RNA-sequencing approach. Candidate genes were selected by expression analysis of transcripts compared to RNA-Sequencing data from young leaves and flowering spadices. Among a series of putative candidates that might encode enzymes catalyzing individual steps in piperine formation, one candidate showed highest similarity to CYP719A enzymes, known to be involved in methylenedioxy bridge formation. The gene was heterologously co-expressed with a reductase in yeast. Yeast microsomal fractions only catalyzed methylenedioxy bridge formation in the case of feruperic acid to piperic acid and the enzyme was subsequently classified as CYP719A37. A candidate for the presumed piperoyl-CoA formation was selected by high similarity to At4CL6 (*At4g05160*), a CoA ligase that activates 5-phenylpentanoic acid in *A. thaliana*. The CoA ligase expressed heterologously in *E. coli* showed a high specificity towards piperic acid. Structurally related hydroxycinnamic acids were not accepted. In combination with the specific expression in black pepper fruits, this enzyme can be described as a piperoyl-CoA ligase, essential to produce the precursor for the subsequent piperine synthase reaction. Consistent with earlier reports in enzyme activity, piperine synthase was identified from black pepper fruits and annotated as a BAHD-acyltransferase with highest similarity to benzoyl:benzoate transferase from *Clarkia brewerii*. Piperine synthase catalyzes the piperine formation from piperoyl-CoA and piperidine. Piperine synthase is among a small gene family detected in black pepper fruits. A second, highly expressed gene, encoding another BAHD-like enzyme, was termed piperamide synthase, since it showed more promiscuous substrate specificity, accepting different CoA esters and aromatic as well as aliphatic amines. Further it preferentially produces piperine stereoisomers from piperidine and piperoyl-CoA. As expected, all identified enzymes related to piperine biosynthesis are co-expressed in immature black pepper fruits, suggesting that additional biosynthesis genes may be identified based on this co-expression pattern. To identify the critical amino acids determining different enzymatic properties of piperine synthase and piperamide synthase, crystallization trials of both enzymes have been initiated.

6 Zusammenfassung

Schwarzer Pfeffer (*Piper nigrum* L.) als König der Gewürze, wird seit Jahrhunderten sowohl in der traditionellen als auch in der modernen Medizin verwendet. Seine Wirksamkeit bezieht sich meist auf Piperin (1-Piperoylpiperidin), ein Amid und Alkaloid, das im Wesentlichen von den Aminosäuren Phenylalanin und Lysin abgeleitet wird. Aufgrund des hohen Piperingehalts in Früchten des schwarzen Pfeffers lag die Vermutung nahe, dass die Piperinbiosynthese ebenfalls in Früchten lokalisiert sein könnte. Um die Identifizierung von Genen, welche für die Piperinbiosynthese relevanten Enzymen kodieren, zu erleichtern wurde ein differentieller RNA-sequencing Ansatz vorgeschlagen, welcher auf dem Vergleich von Transkripten aus Pflanzenorganen mit und ohne Piperin beruht. Die Piperinakkumulation wurde über die gesamte Fruchtentwicklung aufgezeichnet. Basierend auf diesen Daten wurden zwei Entwicklungsstadien, 20 bis 30 Tage und 40 bis 60 Tage nach der Blüte, welche die Initiation bzw. die stärkste Zunahme der Piperinbildung zeigten, für einen differentiellen RNA-Sequenzierungsansatz ausgewählt. Unter einer Reihe von möglichen Kandidaten, codierend für Piperinbiosynthese spezifische Enzyme, zeigte ein Kandidat eine hohe Ähnlichkeit zu CYP719A, ein Cytochrom P450 Enzym, welches an der Bildung von Methyldioxybrücken beteiligt ist. Das Gen wurde zusammen mit einem Transkript, codierend für eine NADPH-Cytochrom-P450-Reduktase, heterolog in Hefe exprimiert. Die aus Hefe isolierten Mikrosomen katalysierten anschließend eine Methyldioxybrücke im Fall der Feruperinsäure und Piperinsäure wurde gebildet. Das Enzym wurde als CYP719A37 klassifiziert. Ein weiterer Kandidat zeigte eine hohe Ähnlichkeit zu At4CL6, welche 5-Phenylpentansäure in *A. thaliana* aktiviert. Die Aktivierung der Piperinsäure und die Herstellung von Piperoyl-CoA wurden vermutet. Die rekombinant in *E. coli* exprimierte CoA-Ligase zeigte eine hohe Spezifität gegenüber Piperinsäure während strukturell verwandte Hydroxyzimtsäuren nicht akzeptiert wurden. Das Enzym wurde als Piperoyl-CoA ligase klassifiziert und ist essenziell für die Synthese der Vorstufe für die nachfolgende Piperin-Synthese-Reaktion. Desweiteren wurde, wie in vorangegangenen Arbeiten vermutet, die Piperinsynthese aus schwarzen Pfefferfrüchten identifiziert. Mit einer hohen Ähnlichkeit zu Benzoyl:Benzoat-Transferase aus *Clarkia breweri* wird sie den BAHD-Acyltransferasen zugeordnet. Die Piperinsynthese katalysiert die Piperinbildung aus Piperoyl-CoA und Piperidin und gehört zu einer kleinen Genfamilie, die in Früchten des schwarzen Pfeffers nachgewiesen werden konnte. Ein zweites, stark exprimiertes Gen, das ebenfalls für ein BAHD-ähnliches Enzym kodiert, wurde Piperamid-Synthase genannt. Dieses Enzym zeigte eine promiskuitivere Substratspezifität und akzeptierte verschiedene CoA-Ester als auch aromatische sowie aliphatische Amine. In der Piperinsynthese werden jedoch bevorzugt die Stereoisomere von Piperin gebildet. Um die kritischen Aminosäuren zu identifizieren, die die unterschiedlichen enzymatischen Eigenschaften von Piperinsynthase und Piperamidsynthase bestimmen, wurde die

Kristallisation beider Enzyme initiiert. Alle identifizierten Enzyme der Piperinbiosynthese waren in unreifen Früchten des schwarzen Pfeffers co-exprimiert. Es ist daher sehr wahrscheinlich, dass zusätzliche Biosynthesegene basierend auf diesem Coexpressionsmusters identifiziert werden können.

7 References

Abel, G. (1997) Safrole – *Sassafras albidum*. In *Adverse Effects of Herbal Drugs* pp. 123-127. Springer.

Abugrain, M.E., et al. (2017) A highly promiscuous β -ketoacyl-*acp* synthase (KAS) III-like protein is involved in pactamycin biosynthesis. *ACS Chemical Biology* 12: 362-366.

Adzima, K.R., et al. (2019) The implementation of k-means partitioning algorithm in HOPACH clustering method. In *IOP Conference Series: Earth and Environmental Science* p. 012073. IOP Publishing.

Afgan, E., et al. (2016) The Galaxy platform for accessible, reproducible and collaborative biomedical analyses: 2016 update. *Nucleic Acids Research* 44: W3-W10.

Albert, V.A., et al. (2013) The *Amborella* genome and the evolution of flowering plants. *Science* 342: 1241089.

Alexandrov, T., et al. (2013) MALDI-imaging segmentation is a powerful tool for spatial functional proteomic analysis of human larynx carcinoma. *Journal of Cancer Research and Clinical Oncology* 139: 85-95.

Andersen, T.B., et al. (2017) Localization and in-vivo characterization of *Thapsia garganica* CYP76AE2 indicates a role in Thapsigargin biosynthesis. *Plant Physiology* 174: 56-72.

Bartels, D., et al. (2005) Drought and salt tolerance in plants. *Critical Reviews in Plant Sciences* 24: 23-58.

Bauer, A., et al. (2019) A short, efficient, and stereoselective synthesis of piperine and its analogues. *Synlett* 30: 413-416.

Bauer, W., et al. (1991) Two methylenedioxy bridge forming cytochrome P-450 dependent enzymes are involved in (S)-stylophine biosynthesis. *Phytochemistry* 30: 2953-2961.

Bayindir, Ü., et al. (2008) Hinokinin biosynthesis in *Linum corymbulosum* Reichenb. *The Plant Journal* 55: 810-820.

Bazin, M.-A., et al. (2008) Synthesis of new avenalamic carboxamide derivatives in the ferulic series. *Synthetic Communications* 38: 3947-3959.

Beuerle, T., et al. (2002) Enzymatic synthesis and purification of aromatic coenzyme A esters. *Analytical Biochemistry* 302: 305-312.

Bianconi, G.V., et al. (2007) Attraction of fruit-eating bats with essential oils of fruits: A potential tool for forest restoration. *Biotropica* 39: 136-140.

Blacklock, B.J., et al. (2006) Substrate specificity of *Arabidopsis* 3-ketoacyl-CoA synthases. *Biochemical and Biophysical Research Communications* 346: 583-590.

Bolger, A.M., et al. (2014) Trimmomatic: a flexible trimmer for Illumina sequence data. *Bioinformatics* 30: 2114-2120.

Bontpart, T., et al. (2015) BAHD or SCPL acyltransferase? What a dilemma for acylation in the world of plant phenolic compounds. *New Phytologist* 208: 695-707.

Brillouet, J.-M., et al. (2014) Phenol homeostasis is ensured in vanilla fruit by storage under solid form in a new chloroplast-derived organelle, the phenyloplast. *Journal of Experimental Botany* 65: 2427-2435.

Bunsupa, S., et al. (2011) An acyltransferase-like gene obtained by differential gene expression profiles of quinolizidine alkaloid-producing and nonproducing cultivars of *Lupinus angustifolius*. *Plant Biotechnology* 28: 89-94.

Caterina, M.J., et al. (1997) The capsaicin receptor: a heat-activated ion channel in the pain pathway. *Nature* 389: 816-824.

Chandra, P., et al. (2015) Quantitative determination of chemical constituents of *Piper* spp. using UPLC–ESI–MS/MS. *Industrial Crops and Products* 76: 967-976.

Chanoca, A., et al. (2015) Anthocyanin vacuolar inclusions form by a microautophagy mechanism. *The Plant Cell* 27: 2545-2559.

Chaw, S.-M., et al. (2018) Stout camphor tree genome fills gaps in understanding of flowering plant genome and gene family evolution. *BioRxiv*: 371112.

Chen, C., et al. (2021) Full-length transcriptome analysis and identification of genes involved in asarinin and aristolochic acid biosynthesis in medicinal plant *Asarum sieboldii*. *Genome* 99: 1-15.

Chen, J., et al. (2019) *Liriodendron* genome sheds light on angiosperm phylogeny and species-pair differentiation. *Nature Plants* 5: 18-25.

Cole, T.C.H., et al. (2016) Angiosperm phylogeny poster–flowering plant systematics.

Correa, E.A., et al. (2010) *In vitro* TRPV1 activity of piperine derived amides. *Bioorganic & Medicinal Chemistry* 18: 3299-3306.

Cotinguiba, F., et al. (2009) Piperamides and their derivatives as potential anti-trypanosomal agents. *Medicinal Chemistry Research* 18: 703-711.

Cukovica, D., et al. (2001) Structure and evolution of 4-coumarate: coenzyme A ligase (4CL) gene families. *Biological Chemistry* 382: 645-654.

- D'Auria, J.C. (2006) Acyltransferases in plants: a good time to be BAHD. *Current Opinion in Plant Biology* 9: 331-340.
- D'Auria, J.C., et al. (2002) Characterization of an acyltransferase capable of synthesizing benzylbenzoate and other volatile esters in flowers and damaged leaves of *Clarkia breweri*. *Plant Physiology* 130: 466-476.
- Dai, Y., et al. (2013) Natural deep eutectic solvents as new potential media for green technology. *Analytica Chimica Acta* 766: 61-68.
- Dantu, P.K., et al. (2021) Elucidating biosynthetic pathway of piperine using comparative transcriptome analysis of leaves, root, and spike in *Piper longum* L. *BioRxiv*: 2021.2001.2003.425108.
- De Cleyn, R., et al. (1975) Constituents of peppers. *Chromatographia* 8: 342-344.
- Debnath, S., et al. (2020) Understanding the intrinsic fluorescence of piperine in microheterogeneous media: partitioning and loading studies. *New Journal of Chemistry* 44: 8317-8324.
- Delseny, M., et al. (1997) The *Arabidopsis thaliana* genome project. *Comptes Rendus de l'Académie des Sciences-Series III-Sciences de la Vie* 320: 589-599.
- Díaz Chávez, M.L., et al. (2011) Characterization of two methylenedioxy bridge-forming cytochrome P450-dependent enzymes of alkaloid formation in the Mexican prickly poppy *Argemone mexicana*. *Archives of Biochemistry and Biophysics* 507: 186-193.
- Dippe, M., et al. (2019) Coenzyme A-conjugated cinnamic acids—enzymatic synthesis of a CoA-ester library and application in biocatalytic cascades to vanillin derivatives. *Advanced Synthesis & Catalysis* 361: 5346-5350.
- Doyle, J.A., et al. (2000) Morphological phylogenetic analysis of basal angiosperms: comparison and combination with molecular data. *International Journal of Plant Sciences* 161: 121-153.
- Dudareva, N., et al. (1998) Acetyl-CoA: benzylalcohol acetyltransferase—an enzyme involved in floral scent production in *Clarkia breweri*. *The Plant Journal* 14: 297-304.
- Ehlting, J., et al. (1999) Three 4-coumarate: coenzyme A ligases in *Arabidopsis thaliana* represent two evolutionarily divergent classes in angiosperms. *The Plant Journal* 19: 9-20.
- Ehlting, J., et al. (2001) Identification of 4-coumarate: coenzyme A ligase (4CL) substrate recognition domains. *The Plant Journal* 27: 455-465.
- Eudes, A., et al. (2016) Exploiting members of the BAHD acyltransferase family to synthesize multiple hydroxycinnamate and benzoate conjugates in yeast. *Microbial Cell Factories* 15: 1-16.

- Flores, N., et al. (2019) An unprecedented chlorine-containing piperamide from *Piper pseudoarboreum* as potential leishmanicidal agent. *Fitoterapia* 134: 340-345.
- Fraser, C.M., et al. (2011) The phenylpropanoid pathway in *Arabidopsis*. *The Arabidopsis Book* 9.
- Frick, K.M., et al. (2017) Quinolizidine alkaloid biosynthesis in lupins and prospects for grain quality improvement. *Frontiers in Plant Science* 8: 87.
- Friedman, M., et al. (2008) Analysis by HPLC and LC/MS of pungent piperamides in commercial black, white, green, and red whole and ground peppercorns. *Journal of Agricultural and Food Chemistry* 56: 3028-3036.
- Frodin, D.G. (2004) History and concepts of big plant genera. *Taxon* 53: 753-776.
- Fujiwara, H., et al. (1998) cDNA cloning, gene expression and subcellular localization of anthocyanin 5-aromatic acyltransferase from *Gentiana triflora*. *The Plant Journal* 16: 421-431.
- Gallage, N.J., et al. (2015) Vanillin - bioconversion and bioengineering of the most popular plant flavor and its *de novo* biosynthesis in the vanilla orchid. *Molecular Plant* 8: 40-57.
- Geisler, J.G., et al. (1990) The biosynthesis of piperine in *Piper nigrum*. *Phytochemistry* 29: 489-492.
- Gesell, A., et al. (2009) CYP719B1 is salutaridine synthase, the CC phenol-coupling enzyme of morphine biosynthesis in opium poppy. *Journal of Biological Chemistry* 284: 24432-24442.
- Golebiewski, W.M., et al. (1988) Biosynthesis of the lupine alkaloids. II. Sparteine and lupanine. *Canadian Journal of Chemistry* 66: 1734-1748.
- Gómez-Calvario, V., et al. (2019) ¹H and ¹³C NMR data, occurrence, biosynthesis, and biological activity of *Piper* amides. *Magnetic Resonance in Chemistry* 57: 994-1070.
- González-Mellado, D., et al. (2010) The role of β -ketoacyl-acyl carrier protein synthase III in the condensation steps of fatty acid biosynthesis in sunflower. *Planta* 231: 1277-1289.
- González, C.G., et al. (2018) Application of natural deep eutectic solvents for the “green” extraction of vanillin from vanilla pods. *Flavour and Fragrance Journal* 33: 91-96.
- Gordo, S.M.C., et al. (2012) High-throughput sequencing of black pepper root transcriptome. *BMC Plant Biology* 12: 1-9.
- Grabherr, M.G., et al. (2011) Full-length transcriptome assembly from RNA-Seq data without a reference genome. *Nature Biotechnology* 29: 644–652.

Grobbelaar, N., et al. (1953) Pipecolic acid in *Phaseolus vulgaris*: evidence on its derivation from lysine. *Journal of the American Chemical Society* 75: 4341-4343.

Grothe, T., et al. (2001) Molecular characterization of the salutaridinol 7-O-acetyltransferase involved in morphine biosynthesis in opium poppy *Papaver somniferum*. *Journal of Biological Chemistry* 276: 30717-30723.

Grunewald, S., et al. (2020) The tapetal major facilitator NPF2. 8 is required for accumulation of Flavonol glycosides on the pollen surface in *Arabidopsis thaliana*. *The Plant Cell* 32: 1727-1748.

Gui, J., et al. (2011) Functional characterization of evolutionarily divergent 4-coumarate: coenzyme A ligases in rice. *Plant Physiology* 157: 574-586.

Gulick, A.M. (2009) Conformational dynamics in the acyl-CoA synthetases, adenylation domains of non-ribosomal peptide synthetases, and firefly luciferase. *ACS Chemical Biology* 4: 811-827.

Gupta, R.N., et al. (1969) Biosynthesis of the piperidine nucleus: the mode of incorporation of lysine into pipecolic acid and into piperidine alkaloids. *Journal of Biological Chemistry* 244: 88-94.

Hamberger, B., et al. (2004) The 4-coumarate: CoA ligase gene family in *Arabidopsis thaliana* comprises one rare, sinapate-activating and three commonly occurring isoenzymes. *Proceedings of the National Academy of Sciences* 101: 2209-2214.

Hao, C., et al. (2016) *De novo* transcriptome sequencing of black pepper (*Piper nigrum* L.) and an analysis of genes involved in phenylpropanoid metabolism in response to *Phytophthora capsici*. *BMC Genomics* 17: 1-14.

Hoffmann, L., et al. (2004) Silencing of hydroxycinnamoyl-coenzyme A shikimate/quinic acid hydroxycinnamoyltransferase affects phenylpropanoid biosynthesis. *The Plant Cell* 16: 1446-1465.

Hooper, C.M., et al. (2017) SUBA4: the interactive data analysis centre for *Arabidopsis* subcellular protein locations. *Nucleic Acids Research* 45: 1064-1074.

Hu, L., et al. (2015) *De novo* assembly and characterization of fruit transcriptome in black pepper (*Piper nigrum*). *PLOS ONE* 10: e0129822.

Hu, L., et al. (2019) The chromosome-scale reference genome of black pepper provides insight into piperine biosynthesis. *Nature Communications* 10: 1-11.

Ikezawa, N., et al. (2003) Molecular cloning and characterization of CYP719, a methylenedioxy bridge-forming enzyme that belongs to a novel P450 family, from cultured *Coptis japonica* cells. *Journal of Biological Chemistry* 278: 38557-38565.

- Inatani, R., et al. (1981) Structure and synthesis of new phenolic amides from *Piper nigrum* L. *Agricultural and Biological Chemistry* 45: 667-673.
- Irmer, S., et al. (2015) New aspect of plant-rhizobia interaction: alkaloid biosynthesis in *Crotalaria* depends on nodulation. *Proceedings of the National Academy of Sciences* 112: 4164-4169.
- Islam, N., et al. (2021) Piperine phytosomes for bioavailability enhancement of domperidone. *Journal of Liposome Research*: 1-9.
- Jagella, T., et al. (1999a) Flavour and off-flavour compounds of black and white pepper (*Piper nigrum* L.) I. Evaluation of potent odorants of black pepper by dilution and concentration techniques. *European Food Research and Technology* 209: 16-21.
- Jagella, T., et al. (1999b) Flavour and off-flavour compounds of black and white pepper (*Piper nigrum* L.) II. Odour activity values of desirable and undesirable odorants of black pepper. *European Food Research and Technology* 209: 22-26.
- Jagella, T., et al. (1999c) Flavour and off-flavour compounds of black and white pepper (*Piper nigrum* L.) III. Desirable and undesirable odorants of white pepper. *European Food Research and Technology* 209: 27-31.
- Jaramillo, M.A., et al. (2001) Phylogeny and patterns of floral diversity in the genus *Piper* (Piperaceae). *American Journal of Botany* 88: 706-716.
- Jaramillo, M.A., et al. (2004) Phylogenetic relationships of the perianthless Piperales: reconstructing the evolution of floral development. *International Journal of Plant Sciences* 165: 403-416.
- Jhanji, R., et al. (2021) Antibacterial potential of selected phytomolecules: an experimental study. *Microbiology and Immunology*.
- Jiang, C., et al. (2008) Divergent evolution of the thiolase superfamily and chalcone synthase family. *Molecular Phylogenetics and Evolution* 49: 691-701.
- Jin, Z., et al. (2020) 4-Coumarate: coenzyme A ligase isoform 3 from *Piper nigrum* (Pn4CL3) catalyzes the CoA thioester formation of 3, 4-methylenedioxycinnamic and piperic acids. *Biochemical Journal* 477: 61-74.
- Jirovetz, L., et al. (2002) Aroma compound analysis of *Piper nigrum* and *Piper guineense* essential oils from Cameroon using solid-phase microextraction-gas chromatography, solid-phase microextraction-gas chromatography-mass spectrometry and olfactometry. *Journal of Chromatography A* 976: 265-275.
- Kanaki, N., et al. (2008) A rapid method for isolation of piperine from the fruits of *Piper nigrum* Linn. *Journal of Natural Medicines* 62: 281-283.

- Kaul, S., et al. (2000) Analysis of the genome sequence of the flowering plant *Arabidopsis thaliana*. *Nature* 408: 796-815.
- Kienow, L., et al. (2008) Jasmonates meet fatty acids: functional analysis of a new acyl-coenzyme A synthetase family from *Arabidopsis thaliana*. *Journal of Experimental Botany* 59: 403-419.
- Klundt, T., et al. (2009) A single amino acid substitution converts benzophenone synthase into phenylpyrone synthase. *Journal of Biological Chemistry* 284: 30957-30964.
- Knobloch, K.-H., et al. (1977) 4-Coumarate: CoA ligase from cell suspension cultures of *Petroselinum hortense* Hoffm. partial purification, substrate specificity, and further properties. *Archives of Biochemistry and Biophysics* 184: 237-248.
- Knudsen, C., et al. (2020) Stabilization of dhurrin biosynthetic enzymes from *Sorghum bicolor* using a natural deep eutectic solvent. *Phytochemistry* 170: 112214.
- Kozukue, N., et al. (2007) Kinetics of light-induced cis-trans isomerization of four piperines and their levels in ground black peppers as determined by HPLC and LC/MS. *Journal of Agricultural and Food Chemistry* 55: 7131-7139.
- Kumar, P., et al. (2021) Topical creams of piperine loaded lipid nanocarriers for management of atopic dermatitis: development, characterization, and *in vivo* investigation using BALB/c mice model. *Journal of Liposome Research*: 1-9.
- Lackova, Z., et al. (2017) Anticarcinogenic effect of spices due to phenolic and flavonoid compounds - *in vitro* evaluation on prostate cells. *Molecules* 22: 1626.
- Lau, K.M., et al. (2008) Immunomodulatory and anti-SARS activities of *Houttuynia cordata*. *Journal of Ethnopharmacology* 118: 79-85.
- Lau, W., et al. (2015) Six enzymes from mayapple that complete the biosynthetic pathway to the etoposide aglycone. *Science* 349: 1224-1228.
- Lauriou, B. (1985) Spices in the medieval diet: A new approach. *Food and Foodways* 1: 43-75.
- Lavhale, S.G., et al. (2018) Structural, functional and evolutionary diversity of 4-coumarate-CoA ligase in plants. *Planta* 248: 1063-1078.
- Lee, J.-G., et al. (2020) Comparative study of the bioactive compounds, flavours and minerals present in black pepper before and after removing the outer skin. *Food Science and Technology* 125: 109356.
- Leete, E., et al. (1964) Biosynthesis of the pyrrolidine ring of nicotine: Feeding experiments with N15-labeled ornithine-2-C14. *Tetrahedron Letters* 5: 587-592.

Leistner, E., et al. (1973) General method for the determination of precursor configuration in biosynthetic precursor-product relations. Derivation of pipercolic acid from D-lysine, and of piperidine alkaloids from L-lysine. *Journal of the American Chemical Society* 95: 4040-4047.

Leistner, E., et al. (1973) Biosynthesis of the piperidine nucleus. Incorporation of chirally labeled [1-³H]-cadaverine. *Journal of the American Chemical Society* 95: 4715-4725.

Lim, T.K. (2012a) *Piper cubeba*. In *Edible Medicinal And Non-Medicinal Plants* pp. 311-321. Springer.

Lim, T.K. (2012b) *Piper nigrum*. In *Edible Medicinal And Non-Medicinal Plants* pp. 322-350. Springer.

Lim, T.K. (2012c) *Piper retrofractum*. In *Edible Medicinal And Non-Medicinal Plants* pp. 351-357. Springer.

Lin, F., et al. (2015) Isofunctional enzymes PAD1 and UbiX catalyze formation of a novel cofactor required by ferulic acid decarboxylase and 4-hydroxy-3-polyprenylbenzoic acid decarboxylase. *ACS Chemical Biology* 10: 1137-1144.

Liu, X., et al. (2017) The genome of medicinal plant *Macleaya cordata* provides new insights into benzyloisoquinoline alkaloids metabolism. *Molecular Plant* 10: 975-989.

Ma, X., et al. (2004) Vinorine synthase from *Rauvolfia*: the first example of crystallization and preliminary X-ray diffraction analysis of an enzyme of the BAHD superfamily. *Biochimica et Biophysica Acta (BBA) - Proteins and Proteomics* 1701: 129-132.

Ma, X., et al. (2005) Crystal structure of vinorine synthase, the first representative of the BAHD superfamily. *Journal of Biological Chemistry* 280: 13576-13583.

Mangalakumari, C.K., et al. (1983) Studies on blackening of pepper (*Piper nigrum* Linn) during dehydration. *Journal of Food Science* 48: 604-606.

Marcotullio, M.C., et al. (2014) Hinokinin, an emerging bioactive lignan. *Molecules* 19: 14862-14878.

Marillonnet, S., et al. (2020) Synthetic DNA assembly using golden gate cloning and the hierarchical modular cloning pipeline. *Current Protocols in Molecular Biology* 130.

Martin, M. (2011) Cutadapt removes adapter sequences from high-throughput sequencing reads. *EMBnet. journal* 17: 10-12.

May, J.J., et al. (2002) Crystal structure of DhbE, an archetype for aryl acid activating domains of modular nonribosomal peptide synthetases. *Proceedings of the National Academy of Sciences* 99: 12120-12125.

- McNamara, F.N., et al. (2005) Effects of piperine, the pungent component of black pepper, at the human vanilloid receptor (TRPV1). *British Journal of Pharmacology* 144: 781-790.
- Meghwal, M., et al. (2013) *Piper nigrum* and piperine: an update. *Phytotherapy Research* 27: 1121-1130.
- Mikich, S.B., et al. (2003) Attraction of the fruit-eating bat *Carollia perspicillata* to *Piper gaudichaudianum* essential oil. *Journal of Chemical Ecology* 29: 2379-2383.
- Ming, R., et al. (2013) Genome of the long-living sacred lotus (*Nelumbo nucifera* Gaertn.). *Genome Biology* 14: 1-11.
- Mizutani, M., et al. (2011) Unusual P450 reactions in plant secondary metabolism. *Archives of Biochemistry and Biophysics* 507: 194-203.
- Naderi, S., et al. (2021) Inhibition of neovascularisation in human endothelial cells using anti NRP-1 nanobody fused to truncated form of diphtheria toxin as a novel immunotoxin. *Immunopharmacology and Immunotoxicology* 43: 230-238.
- Nakagawa, Y., et al. (1956) The double bond in lycorine. *Chemistry & Industry* 42: 1238-1239.
- Nakayama, T., et al. (2003) Anthocyanin acyltransferases: specificities, mechanism, phylogenetics, and applications. *Journal of Molecular Catalysis B: Enzymatic* 23: 117-132.
- Nathanson, J.A., et al. (1993) Cocaine as a naturally occurring insecticide. *Proceedings of the National Academy of Sciences* 90: 9645-9648.
- Návarová, H., et al. (2012) Pipecolic acid, an endogenous mediator of defense amplification and priming, is a critical regulator of inducible plant immunity. *The Plant Cell* 24: 5123-5141.
- Nayaka, N.M.D.M.W., et al. (2021) *Piper betle* (L.): Recent review of antibacterial and antifungal properties, safety profiles, and commercial applications. *Molecules* 26: 2321.
- Nelson, D.R. (2009) The cytochrome P450 homepage. *Human Genomics* 4: 1-7.
- Nelson, D.R. (2018) Cytochrome P450 diversity in the tree of life. *Biochimica et Biophysica Acta (BBA)-Proteins and Proteomics* 1866: 141-154.
- Nofiani, R., et al. (2019) 3-ketoacyl-ACP synthase (KAS) III homologues and their roles in natural product biosynthesis. *Medicinal Chemistry Communications* 10: 1517-1530.
- Ogawa, K., et al. (2015) Evidence of capsaicin synthase activity of the Pun1-encoded protein and its role as a determinant of capsaicinoid accumulation in pepper. *BMC Plant Biology* 15: 1-10.

- Ono, E., et al. (2006) Formation of two methylenedioxy bridges by a *Sesamum* CYP81Q protein yielding a furofuran lignan,(+)-sesamin. *Proceedings of the National Academy of Sciences* 103: 10116-10121.
- Ørsted, H.C. (1820) Über das Piperin, ein neues Pflanzenalkaloid. *Journal of Chemical Physics* 29: 80-82.
- Palazzo, E., et al. (2008) Role of TRPV1 receptors in descending modulation of pain. *Molecular and Cellular Endocrinology* 286: 79-83.
- Parmar, V.S., et al. (1997) Phytochemistry of the genus *Piper*. *Phytochemistry* 46: 597-673.
- Parry, J.W. (1962) Spices: their Morphology, Histology and Chemistry. *Spices: their Morphology, Histology and Chemistry*.
- Patapoutian, A., et al. (2009) Transient receptor potential channels: targeting pain at the source. *Nature Reviews Drug Discovery* 8: 55-68.
- Pecket, R.C., et al. (1980) Occurrence, location and development of anthocyanoplasts. *Phytochemistry* 19: 2571-2576.
- Perrin, D.R., et al. (1962) Studies on phytoalexins. V. The structure of pisatin from *Pisum sativum* L. *Journal of the American Chemical Society* 84: 1919-1922.
- Peter, K.V. (2012) Handbook of herbs and spices. Elsevier.
- Phillipson, J.D., et al. (2012) The chemistry and biology of isoquinoline alkaloids. Springer Science & Business Media.
- Pluskal, T., et al. (2019) The biosynthetic origin of psychoactive kavalactones in kava. *Nature Plants* 5: 867-878.
- Prabhu, B.R., et al. (1985) Biosynthesis of piperlongumine. *Phytochemistry* 24: 2589-2591.
- Puidokait, M., et al. (2016) γ -Conicein und Coniin aus Geflecktem Schierling: Zwei Pseudoalkaloide töten Sokrates. *Chemie in unserer Zeit* 50: 382-391.
- Quijano-Abril, M.A., et al. (2006) Areas of endemism and distribution patterns for Neotropical *Piper* species (Piperaceae). *Journal of Biogeography* 33: 1266-1278.
- Raharjo, T.J., et al. (2004) Cloning and over-expression of a cDNA encoding a polyketide synthase from *Cannabis sativa*. *Plant Physiology and Biochemistry* 42: 291-297.
- Ranjeva, R., et al. (1976) Phenolic metabolism in petunia tissues. IV. - Properties of p-coumarate: coenzyme A ligase isoenzymes. *Biochimie* 58: 1255-1262.

- Rastogi, S., et al. (2013) 4-Coumarate: CoA ligase partitions metabolites for eugenol biosynthesis. *Plant and Cell Physiology* 54: 1238-1252.
- Ravindran, P.N. (2000) Black pepper: *Piper nigrum*. CRC Press.
- Rezende, K.C.S., et al. (2016) Antibacterial activity of (-)-cubebin isolated from *Piper cubeba* and its semisynthetic derivatives against microorganisms that cause endodontic infections. *Revista Brasileira de Farmacognosia* 26: 296-303.
- Robertson, G., et al. (2010) *De novo* assembly and analysis of RNA-seq data. *Nature Methods* 7: 909-912.
- Rosengarten, F.J. (1969) The book of spices. *The Book of Spices*.
- Rüffer, M., et al. (1994) Canadine synthase from *Thalictrum tuberosum* cell cultures catalyses the formation of the methylenedioxy bridge in berberine synthesis. *Phytochemistry* 36: 1219-1223.
- Salehi, B., et al. (2019) *Piper* species: A comprehensive review on their phytochemistry, biological activities and applications. *Molecules* 24: 1364.
- Sanderson, M.J., et al. (1994) Shifts in diversification rate with the origin of angiosperms. *Science* 264: 1590-1593.
- Sauveplane, V., et al. (2009) *Arabidopsis thaliana* CYP77A4 is the first cytochrome P450 able to catalyze the epoxidation of free fatty acids in plants. *FEBS journal* 276: 719-735.
- Scheler, U., et al. (2016) Elucidation of the biosynthesis of carnosic acid and its reconstitution in yeast. *Nature Communications* 7: 12942.
- Schmidt, G.W., et al. (2015) The last step in cocaine biosynthesis is catalyzed by a BAHD acyltransferase. *Plant Physiology* 167: 89-101.
- Schnabel, A., et al. (2021a) Identification and characterization of piperine synthase from black pepper, *Piper nigrum* L. *Communications Biology* 4: 1-10.
- Schnabel, A., et al. (2021b) *Piper nigrum* CYP719A37 catalyzes the decisive methylenedioxy bridge formation in piperine biosynthesis. *Plants* 10: 128.
- Schnabel, A., et al. (2020) A piperic acid CoA ligase produces a putative precursor of piperine, the pungent principle from black pepper fruits. *The Plant Journal* 102: 569-581.
- Schneider, K., et al. (2003) The substrate specificity-determining amino acid code of 4-coumarate: CoA ligase. *Proceedings of the National Academy of Sciences* 100: 8601-8606.

- Schneider, K., et al. (2005) A new type of peroxisomal acyl-coenzyme A synthetase from *Arabidopsis thaliana* has the catalytic capacity to activate biosynthetic precursors of jasmonic acid. *Journal of Biological Chemistry* 280: 13962-13972.
- Schröder, A., et al. (2006) The RIN: an RNA integrity number for assigning integrity values to RNA measurements. *BMC Molecular Biology* 7: 1-14.
- Schwacke, R., et al. (2019) MapMan4: a refined protein classification and annotation framework applicable to multi-omics data analysis. *Molecular Plant* 12: 879-892.
- Semler, U., et al. (1987) Synthesis of piperoyl coenzyme A thioester. *Zeitschrift für Naturforschung C* 42: 1070-1074.
- Siebert, T.E., et al. (2008) Determination of rotundone, the pepper aroma impact compound, in grapes and wine. *Journal of Agricultural and Food Chemistry* 56: 3745-3748.
- Smilkov, K., et al. (2019) Piperine: old spice and new nutraceutical? *Current Pharmaceutical Design* 25: 1729-1739.
- Smith, S., et al. (1983) The effect of aromatic CoA esters on fatty acid synthetase: biosynthesis of ω -phenyl fatty acids. *Archives of Biochemistry and Biophysics* 222: 259-265.
- Smith, S., et al. (2003) Structural and functional organization of the animal fatty acid synthase. *Progress in Lipid Research* 42: 289-317.
- Soltis, D.E., et al. (2019) Nuclear genomes of two magnoliids. *Nature Plants* 5: 6-7.
- Srinivasan, K. (2014) Antioxidant potential of spices and their active constituents. *Critical Reviews in Food Science and Nutrition* 54: 352-372.
- St-Pierre, B., et al. (2000) Origin and diversification of the BAHD superfamily of acyltransferases involved in secondary metabolism. *Recent Advances in Phytochemistry* 34: 285-315.
- St-Pierre, B., et al. (1998) The terminal O-acetyltransferase involved in vindoline biosynthesis defines a new class of proteins responsible for coenzyme A-dependent acyl transfer. *The Plant Journal* 14: 703-713.
- Stander, E.A., et al. (2020) Identifying genes involved in alkaloid biosynthesis in *Vinca minor* through transcriptomics and gene co-expression analysis. *Biomolecules* 10: 1595.
- Stasiłowicz, A., et al. (2021) Combinations of piperine with hydroxypropyl- β -cyclodextrin as a multifunctional system. *International Journal of Molecular Sciences* 22: 4195.
- Stewart, C.J., et al. (2005) The *Pun1* gene for pungency in pepper encodes a putative acyltransferase. *The Plant Journal* 42: 675-688.

Strijk, J.S., et al. (2019) The soursop genome and comparative genomics of basal angiosperms provide new insights on evolutionary incongruence. *BioRxiv*: 639153.

Strunz, G.M. (2000) Unsaturated amides from *Piper* species (Piperaceae). In *Studies in Natural Products Chemistry* pp. 683-738. Elsevier.

Sun, H., et al. (2013) Analysis of five rice 4-coumarate: coenzyme A ligase enzyme activity and stress response for potential roles in lignin and flavonoid biosynthesis in rice. *Biochemical and Biophysical Research Communications* 430: 1151-1156.

Suzuki, H., et al. (2003) Proposed mechanism and functional amino acid residues of malonyl-CoA: anthocyanin 5-O-glucoside-6-O-malonyltransferase from flowers of *Salvia splendens*, a member of the versatile plant acyltransferase family. *Biochemistry* 42: 1764-1771.

Suzuki, H., et al. (2004) Identification and characterization of a novel anthocyanin malonyltransferase from scarlet sage (*Salvia splendens*) flowers: an enzyme that is phylogenetically separated from other anthocyanin acyltransferases. *The Plant Journal* 38: 994-1003.

Thomas, K.C., et al. (2012) Contributions of TRPV1, endovanilloids, and endoplasmic reticulum stress in lung cell death *in vitro* and lung injury. *American Journal of Physiology-Lung Cellular and Molecular Physiology* 302: 111-119.

Tominaga, M., et al. (1998) The cloned capsaicin receptor integrates multiple pain-producing stimuli. *Neuron* 21: 531-543.

Tsay, J.-T., et al. (1992) Isolation and characterization of the beta-ketoacyl-acyl carrier protein synthase III gene (fabH) from *Escherichia coli* K-12. *Journal of Biological Chemistry* 267: 6807-6814.

Tuominen, L.K., et al. (2011) Differential phylogenetic expansions in BAHD acyltransferases across five angiosperm taxa and evidence of divergent expression among *Populus* paralogues. *BMC Genomics* 12: 1-17.

Turrini, E., et al. (2020) Overview of the anticancer potential of the “king of spices” *Piper nigrum* and its main constituent piperine. *Toxins* 12: 747.

Ummer, C. (1989) Indian spices-from the leaves of history. *Spice fair commemorative volume. Spices Board, Cochin*: 27-40.

Van der Laan, M.J., et al. (2003) A new algorithm for hybrid hierarchical clustering with visualization and the bootstrap. *Journal of Statistical Planning and Inference* 117: 275-303.

Vanholme, R., et al. (2019) COSY catalyses *trans-cis* isomerization and lactonization in the biosynthesis of coumarins. *Nature Plants* 5: 1066-1075.

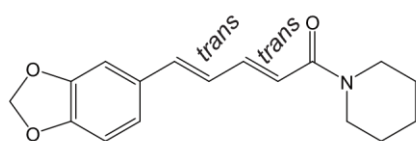
- Vaupel, E. (2010) Hermann Staudinger und der Kunstpfeffer. Ersatzgewürze. *Chemie in unserer Zeit* 44: 396-412.
- Vogt, T. (2010) Phenylpropanoid biosynthesis. *Molecular Plant* 3: 2-20.
- Vogt, T., et al. (1987) Epicuticular flavonoid aglycones in the genus *Cistus*, Cistaceae. *Journal of Plant Physiology* 131: 25-36.
- von Wettstein-Knowles, P., et al. (2000) Molecular aspects of β -ketoacyl synthase (KAS) catalysis. Portland Press Ltd.
- Wallis, P.J., et al. (1977) Multiple forms of hydroxycinnamate: CoA ligase in etiolated pea seedlings. *Phytochemistry* 16: 1891-1894.
- Wang, X., et al. (2018) Deep sequencing and transcriptome analysis to identify genes related to biosynthesis of aristolochic acid in *Asarum heterotropoides*. *Scientific Reports* 8: 1-14.
- Wang, X., et al. (2016) Identification and functional evaluation of the reductases and dehydrogenases from *Saccharomyces cerevisiae* involved in vanillin resistance. *BMC Biotechnology* 16: 1-9.
- Wang, X., et al. (2015) *De novo* transcriptome analysis of *Warburgia ugandensis* to identify genes involved in terpenoids and unsaturated fatty acids biosynthesis. *PLOS ONE* 10: e0135724.
- Wanke, S., et al. (2007) Evolution of Piperales - *matK* gene and *trnK* intron sequence data reveal lineage specific resolution contrast. *Molecular Phylogenetics and Evolution* 42: 477-497.
- Weber, A.P.M. (2015) Discovering new biology through sequencing of RNA. *Plant Physiology* 169: 1524-1531.
- Wehrs, M., et al. (2019) Sustainable bioproduction of the blue pigment indigoidine: Expanding the range of heterologous products in *R. toruloides* to include non-ribosomal peptides. *Green Chemistry* 21: 3394-3406.
- Wei, L., et al. (2014) Transcriptome analysis of *Houttuynia cordata* Thunb. by Illumina paired-end RNA sequencing and SSR marker discovery. *PLOS ONE* 9: e84105.
- Wessel, D.M., et al. (1984) A method for the quantitative recovery of protein in dilute solution in the presence of detergents and lipids. *Analytical Biochemistry* 138: 141-143.
- Whitehead, S.R., et al. (2016) Chemical tradeoffs in seed dispersal: defensive metabolites in fruits deter consumption by mutualist bats. *Oikos* 125: 927-937.

- Wojtowicz, K., et al. (2021) Piperine targets different drug resistance mechanisms in human ovarian cancer cell lines leading to increased sensitivity to cytotoxic drugs. *International Journal of Molecular Sciences* 22: 4243.
- Wrigley, T.C. (1960) Ayapin, scopoletin and 6, 7-dimethoxycoumarin from *Dendrobium thysiflorum* (Reichb. f.). *Nature* 188: 1108-1108.
- Wu, G.-Z., et al. (2010) *Arabidopsis* β -ketoacyl-[acyl carrier protein] synthase I is crucial for fatty acid synthesis and plays a role in chloroplast division and embryo development. *The Plant Cell* 22: 3726-3744.
- Xu, B., et al. (2018) Insights into pipercolic acid biosynthesis in *Huperzia serrata*. *Organic Letters* 20: 2195-2198.
- Yahyazadeh, M., et al. (2017) Cloning and characterization of cheilanthifoline and stylopine synthase genes from *Chelidonium majus*. *Plant and Cell Physiology* 58: 1421-1430.
- Yang, Q., et al. (1997) Characterization and heterologous expression of hydroxycinnamoyl/benzoyl-CoA: anthranilate N-hydroxycinnamoyl/benzoyltransferase from elicited cell cultures of carnation, *Dianthus caryophyllus* L. *Plant Molecular Biology* 35: 777-789.
- Yasuno, R., et al. (2004) Identification and molecular characterization of the β -ketoacyl-[acyl carrier protein] synthase component of the *Arabidopsis* mitochondrial fatty acid synthase. *Journal of Biological Chemistry* 279: 8242-8251.
- Yu, G. (2018) clusterProfiler: universal enrichment tool for functional and comparative study. *BioRxiv*. 256784.
- Zacharius, R.M., et al. (1952) The detection, isolation and identification of (-)-pipercolic acid as a constituent of plants. *Journal of the American Chemical Society* 74: 2949-2949.
- Zenkner, F.F., et al. (2019) Nicotine biosynthesis in *Nicotiana*: a metabolic overview. *Tobacco Science* 56: 1-9.
- Zhang, K., et al. (2015) Coupling binding to catalysis: using yeast cell surface display to select enzymatic activities. In *Yeast Surface Display* pp. 245-260. Springer.
- Zhang, L., et al. (2020) The water lily genome and the early evolution of flowering plants. *Nature* 577: 79-84.
- Zheng, D., et al. (2001) Molecular and biochemical characterization of three aromatic polyketide synthase genes from *Rubus idaeus*. *Plant Molecular Biology* 46: 1-15.
- Zhu, P., et al. (2021) Overview of piperlongumine analogues and their therapeutic potential. *European Journal of Medicinal Chemistry*. 113471.

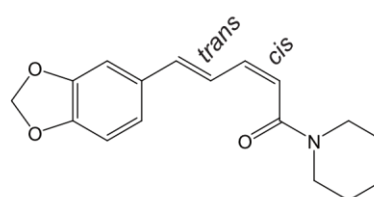
References

Zygmunt, P.M., et al. (1999) Vanilloid receptors on sensory nerves mediate the vasodilator action of anandamide. *Nature* 400: 452-457.

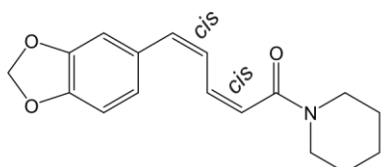
8 Appendix



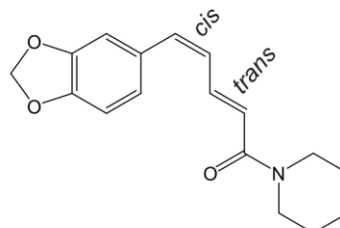
Piperine
E,E-(trans-trans)-piperine



Isopiperine
Z,E-(cis-trans)-piperine



Chavicine
Z,Z-(cis-cis)-piperine



Isochavicine
E,Z-(trans-cis)-piperine

Figure 8-1: Structure of piperine and its stereoisomers, isopiperine, chavicine and isochavicine

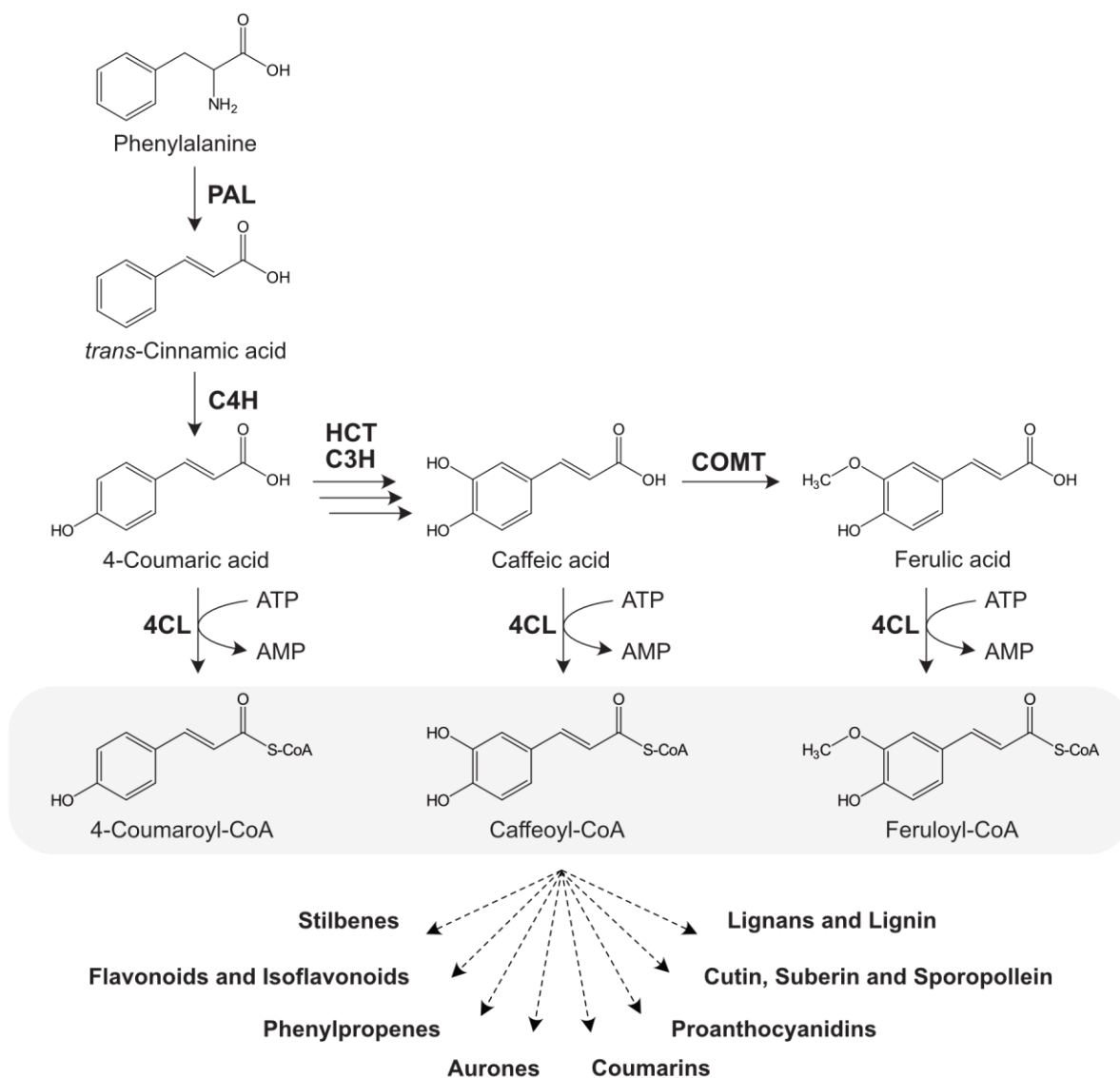
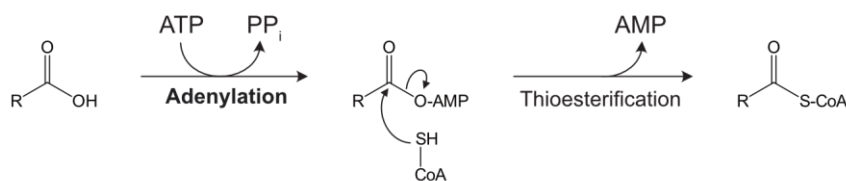
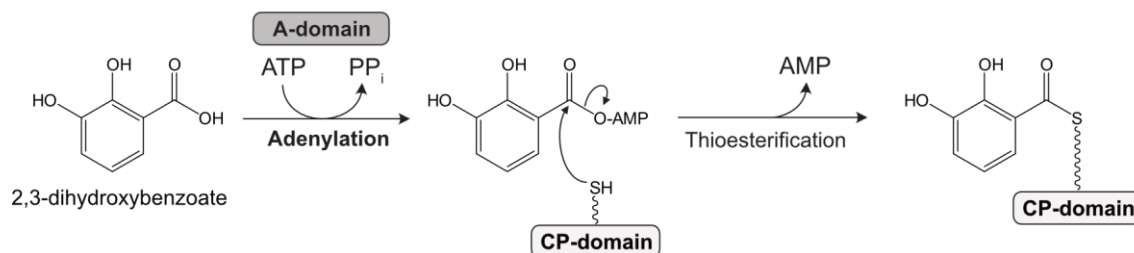
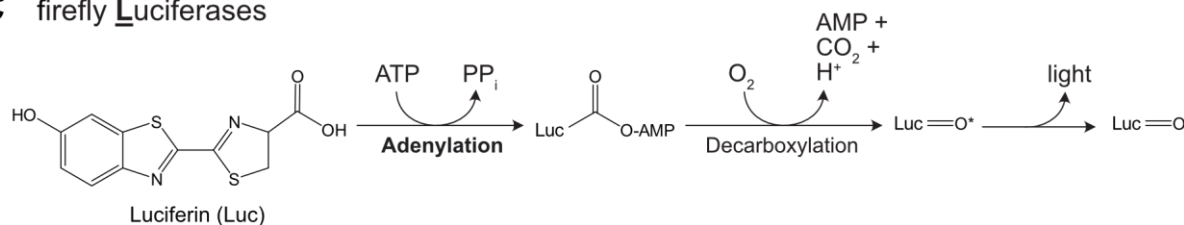


Figure 8-2: The phenylpropanoid biosynthesis and specialized phenylpropanoids of different pathways

The phenylpropanoid biosynthesis starts with the molecule phenylalanine, derived from shikimate pathway. The deamination of phenylalanine is catalyzed by phenylalanine ammonia lyase (PAL) result in formation of *trans*-cinnamic acid. Further hydroxylations by cinnamate 4-hydroxylase (C4H), activation by hydroxycinnamoyltransferase (HCT), and subsequent hydroxylations by *p*-coumarate 3-hydroxylase (C3H), and O-methylations by caffeic acid O-methyltransferase (COMT) results in *p*-coumaric acid, caffeic acid or ferulic acid. Different 4-coumarate-CoA ligases (4CL) catalyze the activation of this hydroxycinnamic acid derivative. This activated CoA thioesters (grey) serve as precursors in the biosynthesis of numerous specialized metabolites of different branch pathways. Adapted from Hoffmann et al. (2004) and Vogt (2010).

A Acy- and acryl synthetases**B** NRPS Adenylation Domains (example: adenylation and thioesterification by DhbE)**C** firefly Luciferases**Figure 8-3: Overview of ANL superfamily members and their possible reactions**

(A) The general reaction of acyl- and acryl synthetases is shown. In a first step the adenylation and in a second step the thioesterification are catalyzed by the synthetase. **(B)** The adenylation domains of non-ribosomal peptide synthetases (NRPSs) catalyzes the formation of hydroxycinnamate-AMP. In this case the DhbE adenylation domain (a-domain, blue) catalyzes the adenylation of 2,3-dihydroxybenzoate. The DhbE carrier protein domain (CP-domain) catalyzes the thioesterification in a second step. **(C)** The firefly luciferase the adenylation and decarboxylation of luciferin to generate oxyluciferin and light. In all three cases the first step, the adenylation is conserved.

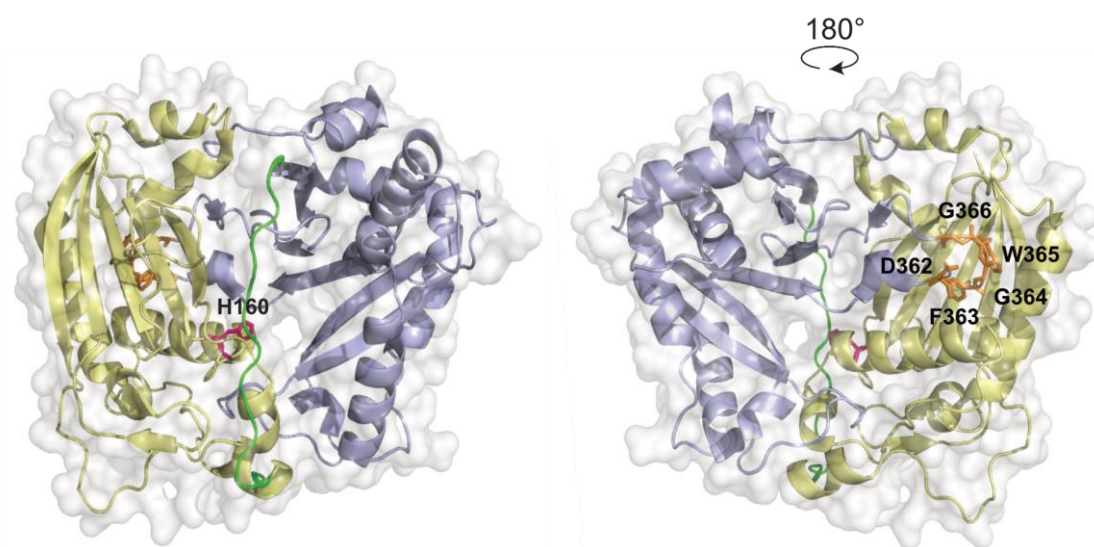


Figure 8-4: The protein structure of vinorine synthase

(A) and **(B)** represent the structure of vinorine synthase from both sites of the channel as secondary structure and protein surface (gray). (Ma et al., 2004; Ma et al., 2005) (pdb: 2bgh). The N-terminal domain (residues 1-197, yellow) and the C-terminal domain (residue 214-421, blue) are connected by a loop (residue 198-213, green). Both domains have a nearly equal size with a β -sheet core flanked with α -helices. Two motifs are highly conserved in the BAHDs superfamily: the HXXXD and the DFGWG. **(A)** The catalytic active histidine 160 (sticks, magenta) from the HXXXD motif is in the interface and is accessible from both sites of the channel. **(B)** The DFGWG motif (residue 362-366, sticks, orange) is located on the outside of the N-terminal domain and play a structural role.

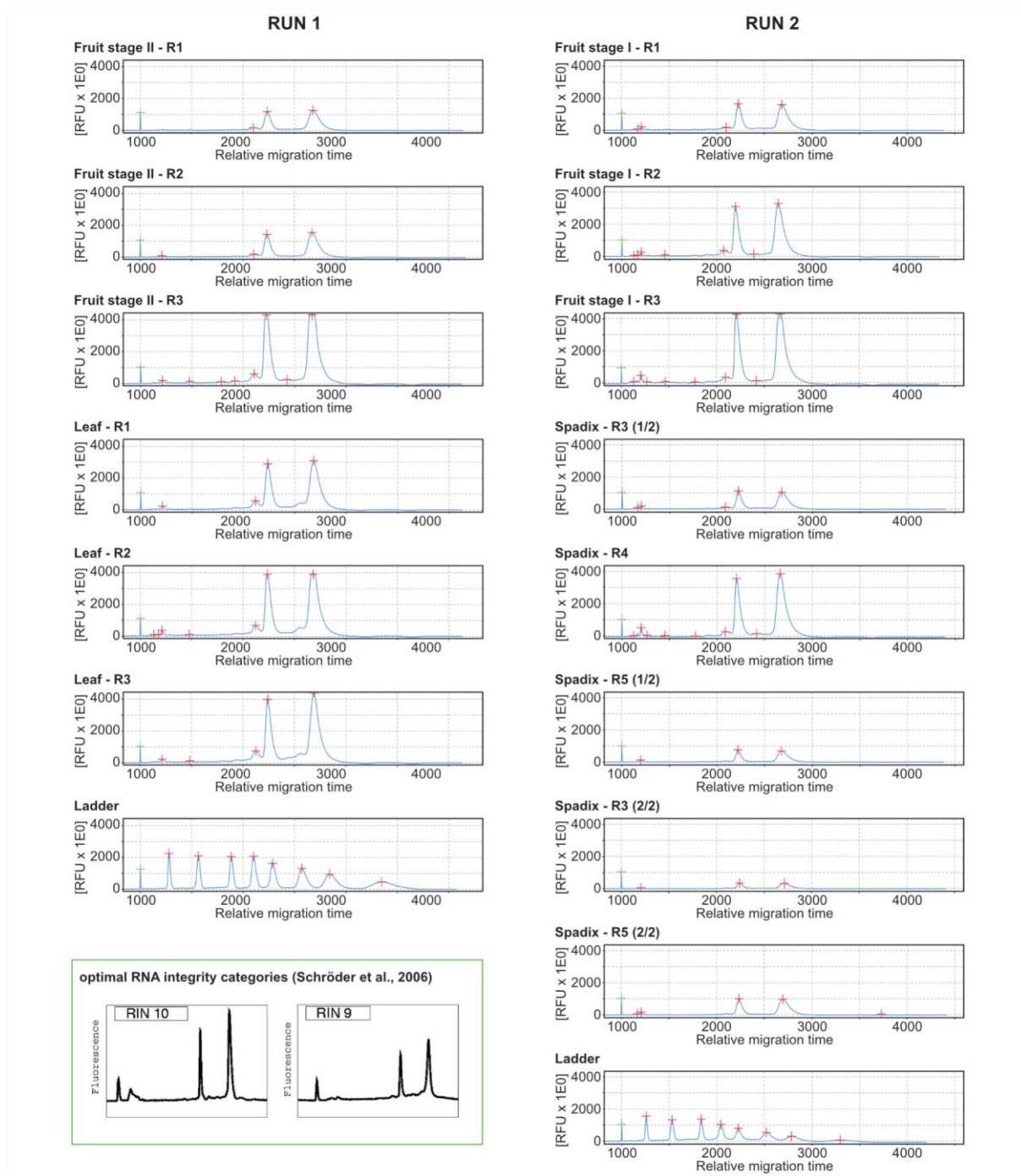


Figure 8-5: RNA integrity determination of RNA preparations

Based on the RNA separation by microcapillary electrophoretic RNA separation (QIAxcel) the fluorescence signals were compared. RNA preparation were chosen based on RNA integrity numbers 9 or 10 (RIN, green frame) and a high signal intensity for RNA sequencing (Schröder et al., 2006). The data were recorded by QIAxcel ScreenGel 1.1.0.

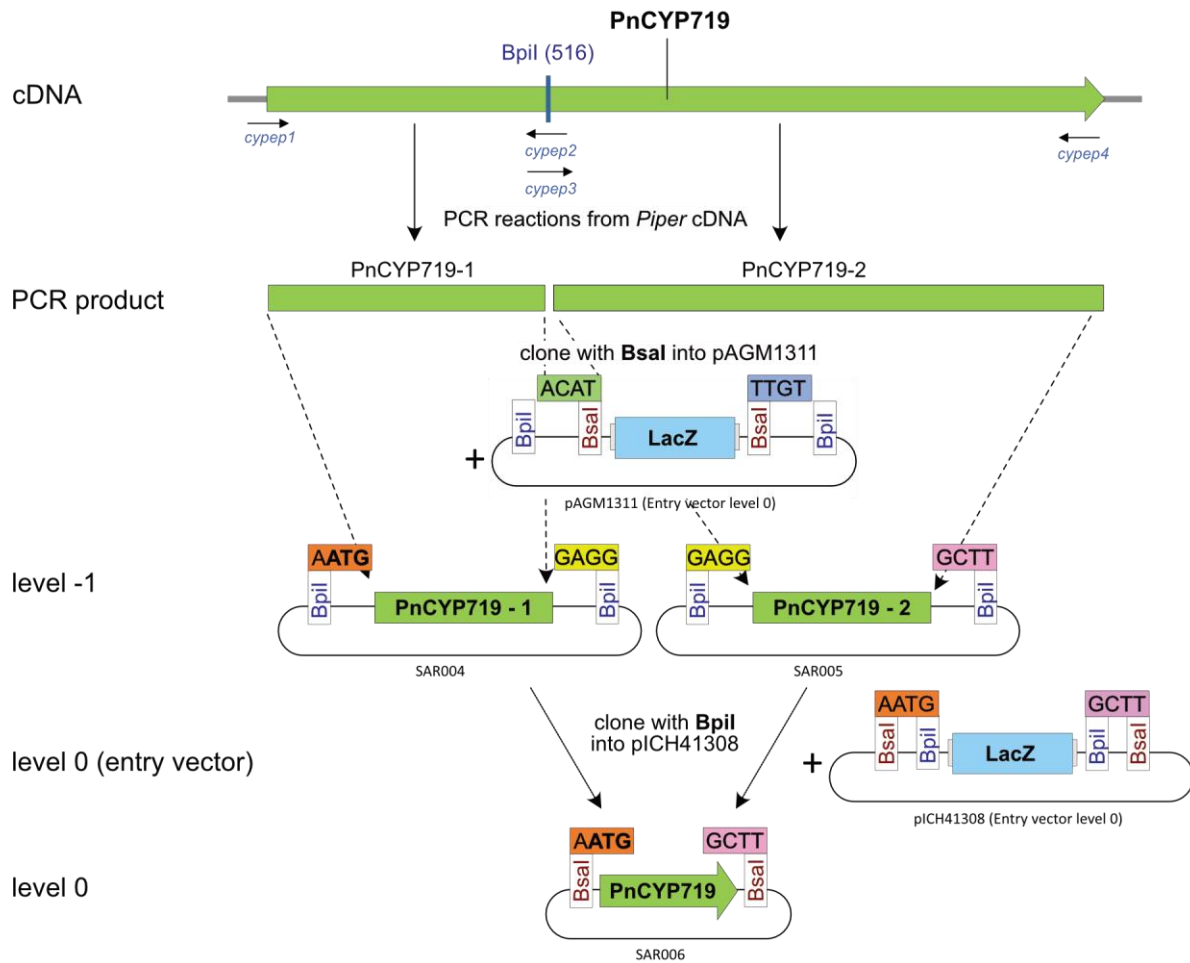


Figure 8-6: Golden Gate cloning - entry of PnCYP719 in level 0

RNA from black pepper fruit stage II was extracted, transcribed, and two PCR fragments were amplified. The primer (cysep 1-4) adds a Bsal cleavage site with compatible four base overhangs. Additionally, the primer cysep2 and 3 introduce a silent point mutation to remove the internal Bpil cleavage site. Each amplicon is cloned into entry vector level -1 (kanamycin resistance). Both amplicons were combined position specific into entry vector level 0 (spectinomycin resistance).

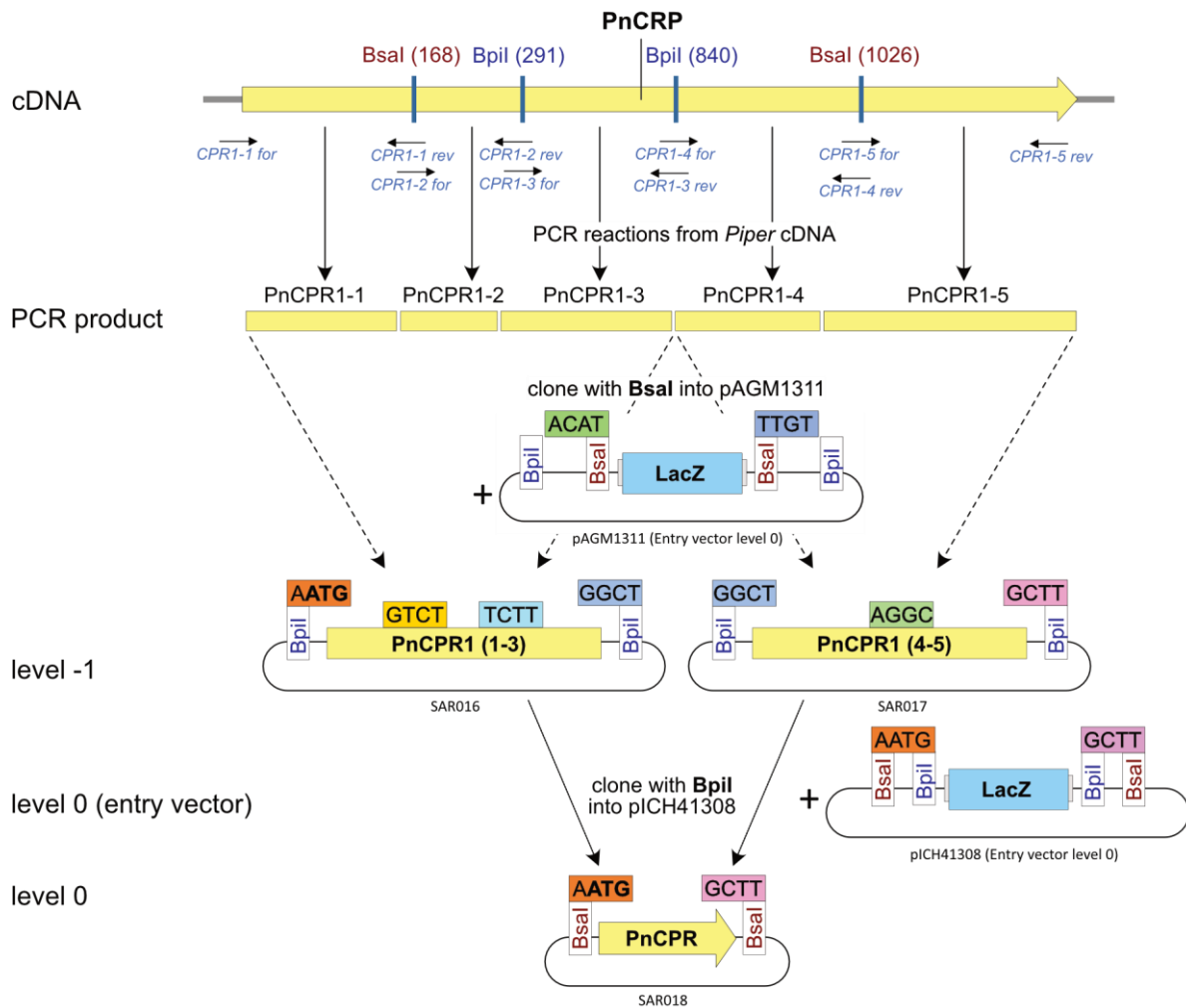


Figure 8-7: Golden Gate cloning - the entry of PnCRP in level 0

RNA from black pepper fruit stage II was extracted, transcribed and five PCR fragments were amplified. The primer (CPR1-1 for – CPR 1-5 rev) adds a Bsal cleavage sites with compatible four base overhangs. Additionally, the internal primer introduce silent point mutations to remove internal Bsal and Bpil cleavage sites. Amplicon 1-3 and amplicon 4-5 are cloned into entry vector level -1 (kanamycin resistance). Both fragments were combined into position specific into entry vector level 0 (spectinomycin resistance).

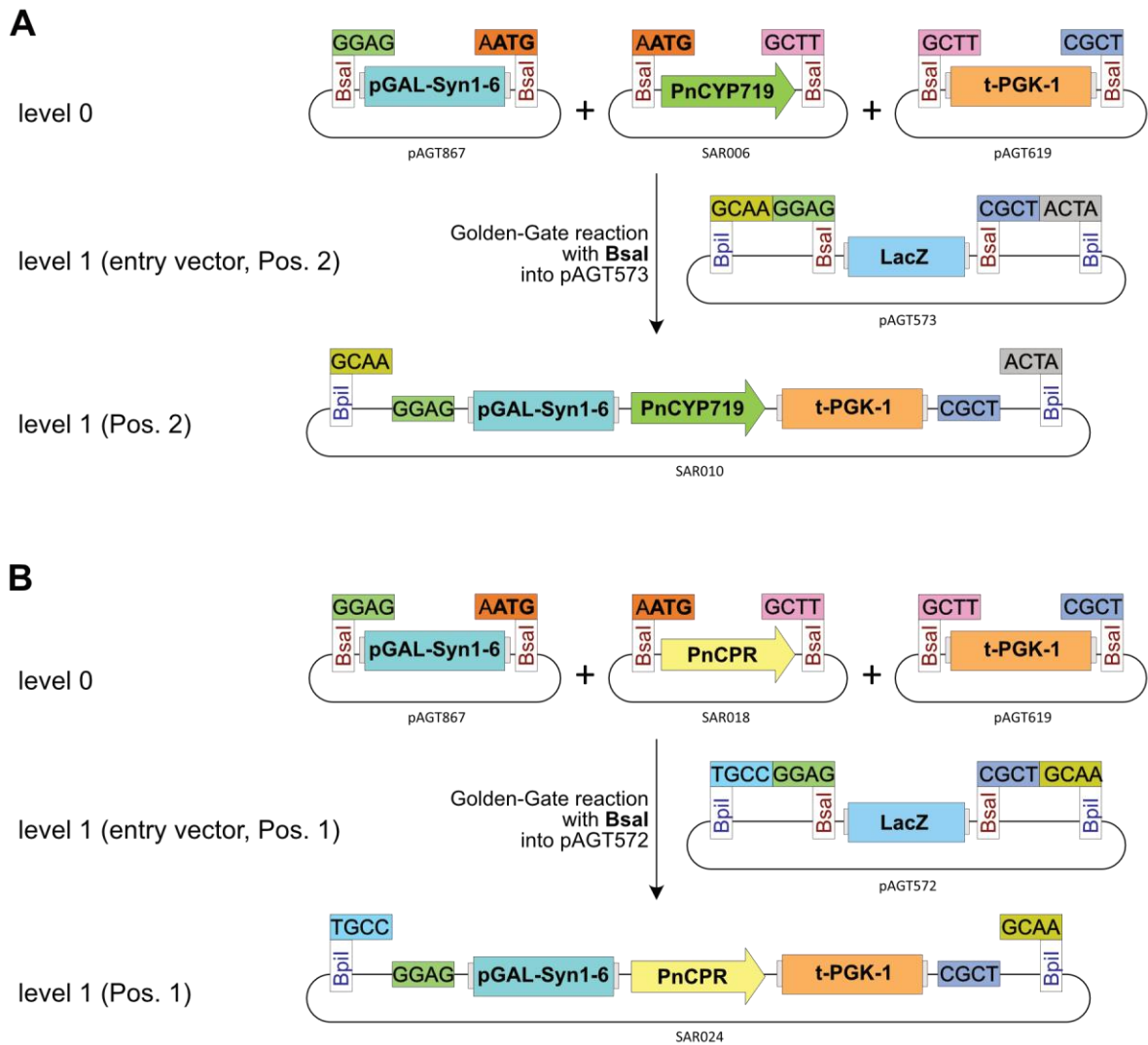


Figure 8-8: Golden Gate cloning - combining PnCYP719 or PnCPR with a galactose inducible promoter and the PGK terminator in level 1

PnCYP719 (**A**) or PnCPR (**B**) were cloned with a galactose-inducible promoter 6 and the PGK terminator into level 1 vector (carbenicillin resistance). The single units were ligated in a specific orientation based on their overhangs. Furthermore, level 1 vectors determine the position in the next level.

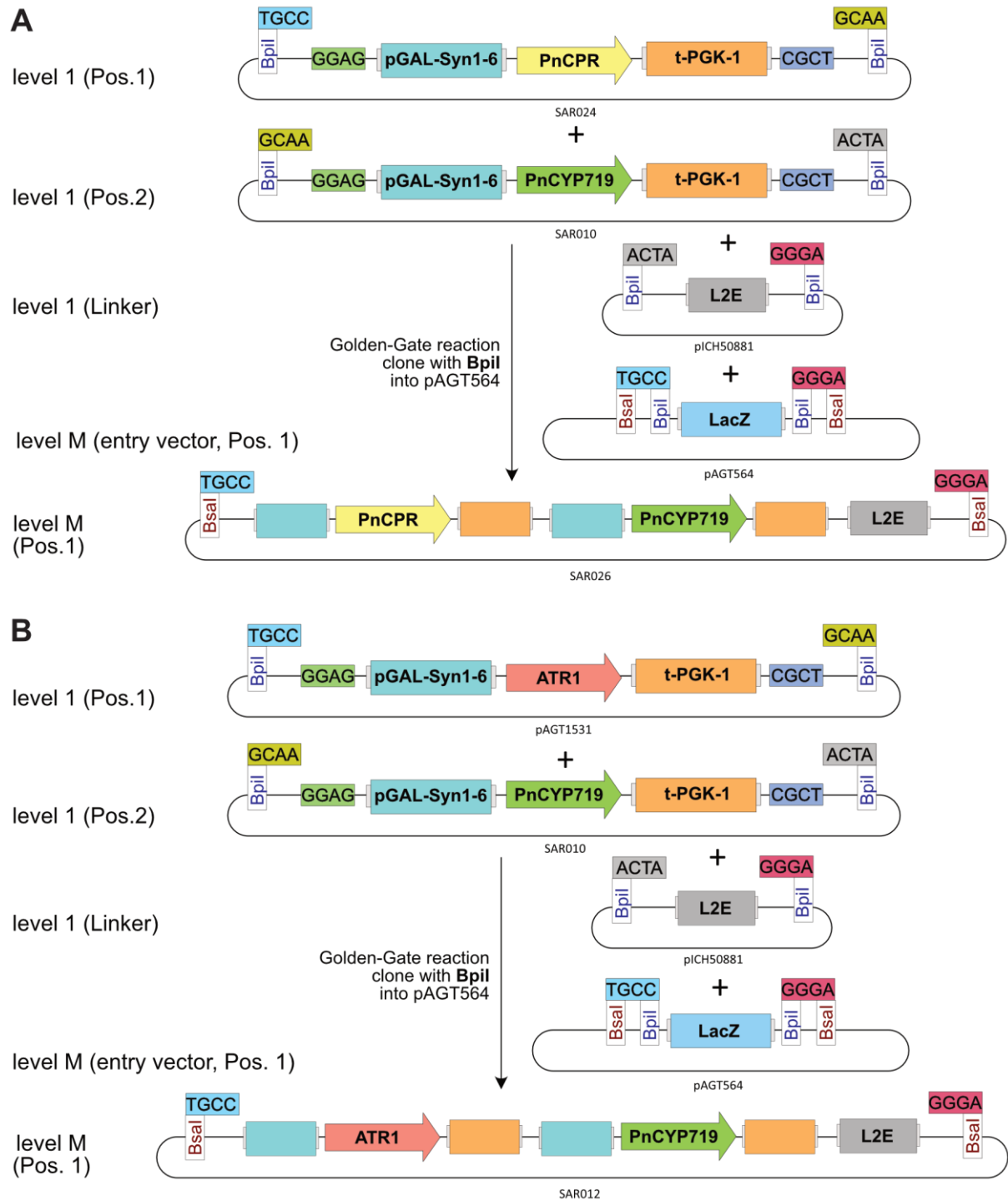


Figure 8-9: Golden Gate cloning - combining of the expression cassettes of PnCPR (A) or ATR (B) with PnCYP719 in expression level M

In a final Golden Gate reaction both expression cassettes were cloned into a level M destination vector (spectinomycin, URA3). This construct was used for heterologous expression in *S. cerevisiae*.

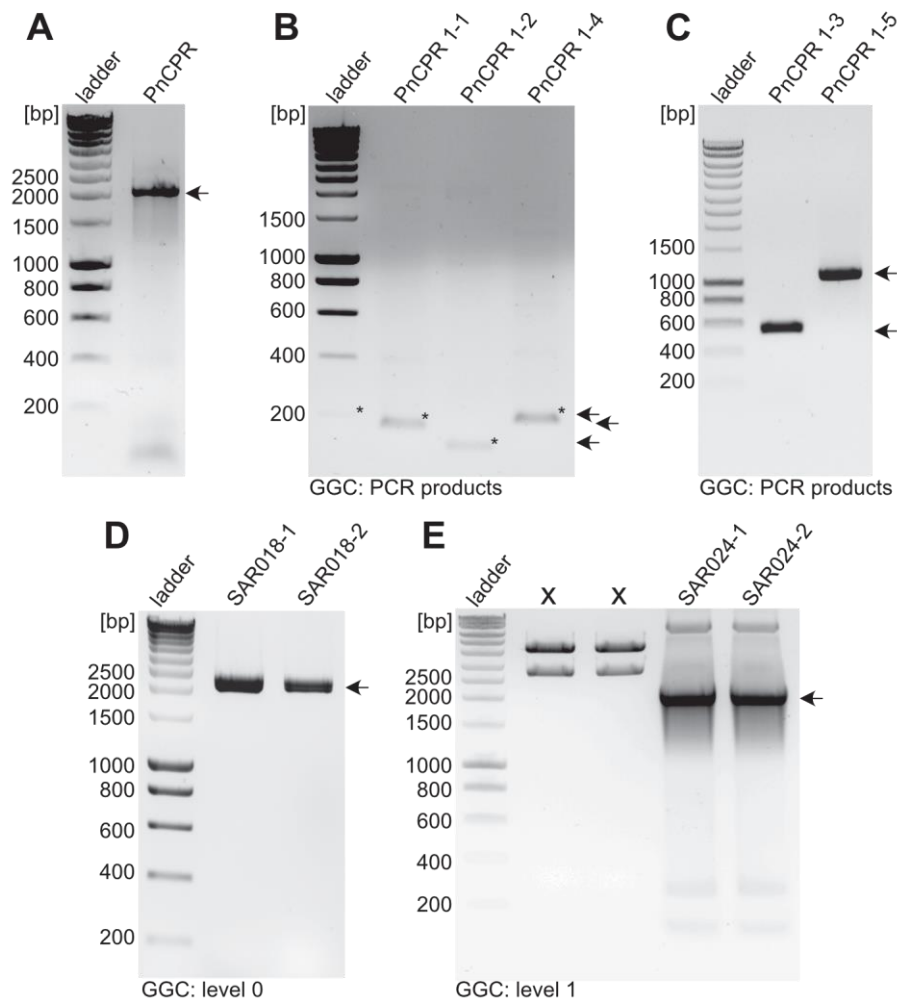


Figure 8-10: Verification of PnCPR in different vector levels of Golden Gate cloning

Every step in Golden Gate cloning was verified by a PCR reaction, analyzed in a 1 % agarose gel and stained with ethidium bromide: (A) PnCPR from cDNA of black pepper fruit stage II; (B) and (C) GGC fragments PnCPR 1-1 – 1-5 from cDNA of black pepper fruit stage II; (D) verification of PnCPR in level 0 vector; (E) verification of PnCPR in level 1 vector; Expected amplicon is marked with an arrow. The vectors are named consecutively, SARXXX, consist with the GGC strategy (see also Suppl.: **Figure 8-6 – 8-9**)

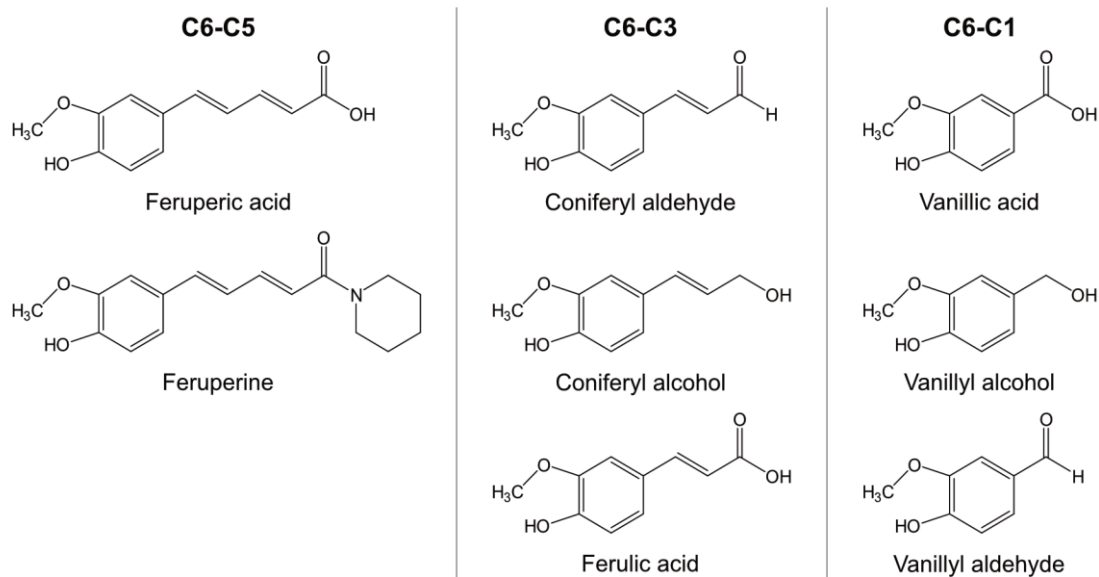


Figure 8-11: Putative substrates for CYP719A37

Different substrates with an aromatic vanilloid moiety were chosen and classified by their length of the carbon chain in C6-C5 (feruperic acid and feruperine), C6-C3 (coniferyl aldehyde, coniferyl alcohol and ferulic acid) and C6-C1 (vanillic acid, vanillyl alcohol and vanillyl aldehyde). The substrates were added to intact yeast cells or microsomal fractions to determine the activity of CYP719A37 co-expressed with PnCPR or ATR1.

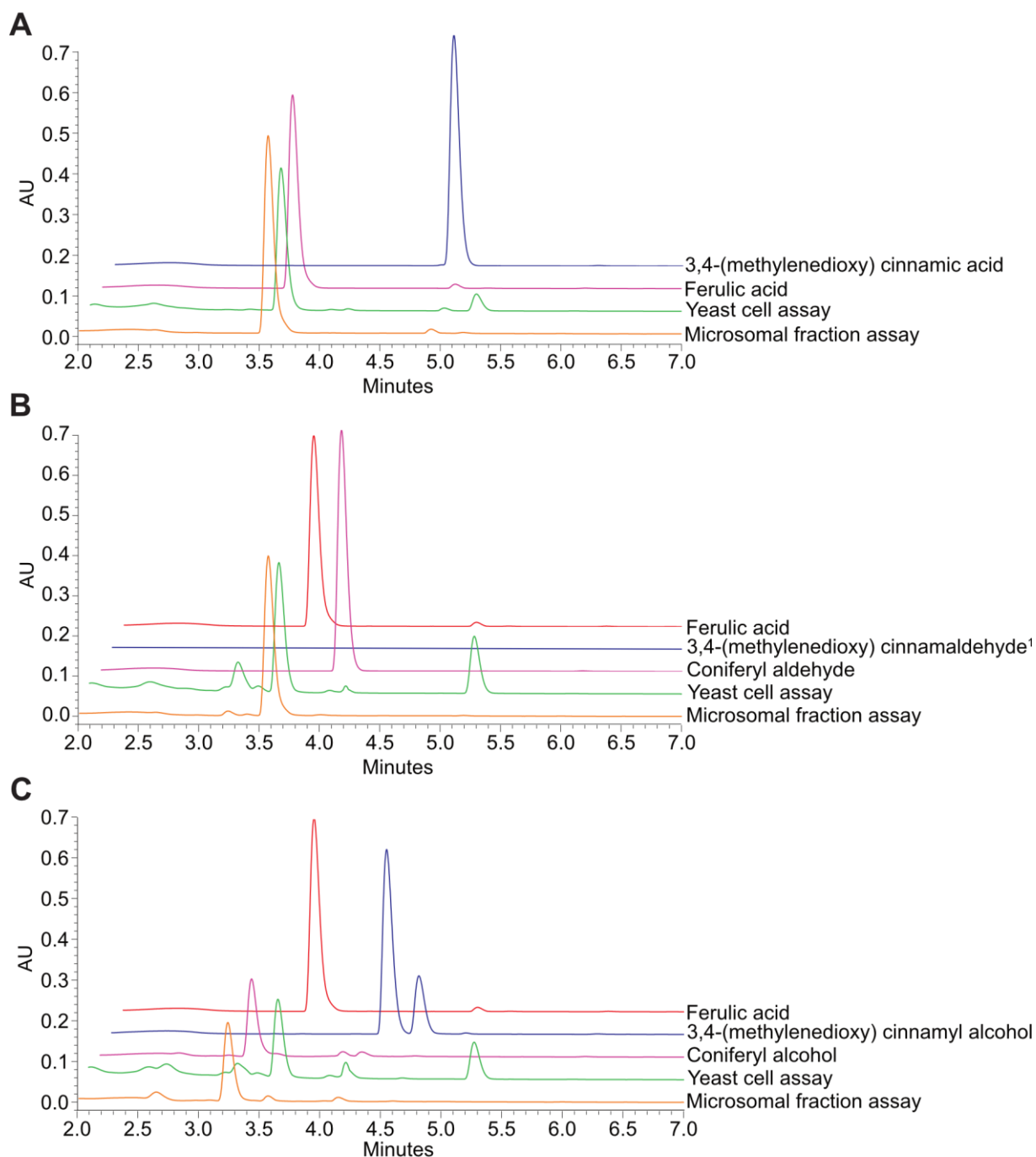


Figure 8-12: HPLC-analysis of microsomal fraction- and yeast cell assays with C6-C2 substrates

CYP719A37 and PnCPR were heterologously expressed in *S. cerevisiae*. Yeast cells or microsomal fractions were incubated with ferulic acid (A), coniferyl aldehyde (B) or coniferyl alcohol (C) for 24 h and the product formation was monitored. In the case of the microsomal assay the products were extracted with ethyl acetate, concentrated, re-dissolved in methanol, and analyzed by HPLC-UV-ESI-MS (orange). The supernatant from yeast cell assays was directly analyzed (green). The UV signal was monitored between 225 – 400 nm and the masses between $m/z = 100 - 300 [M+H]^+$. Substrates are shown in magenta, products with a methylenedioxy bridge in blue, whereas unexpected products are marked in red. (¹ – Reference was not available)

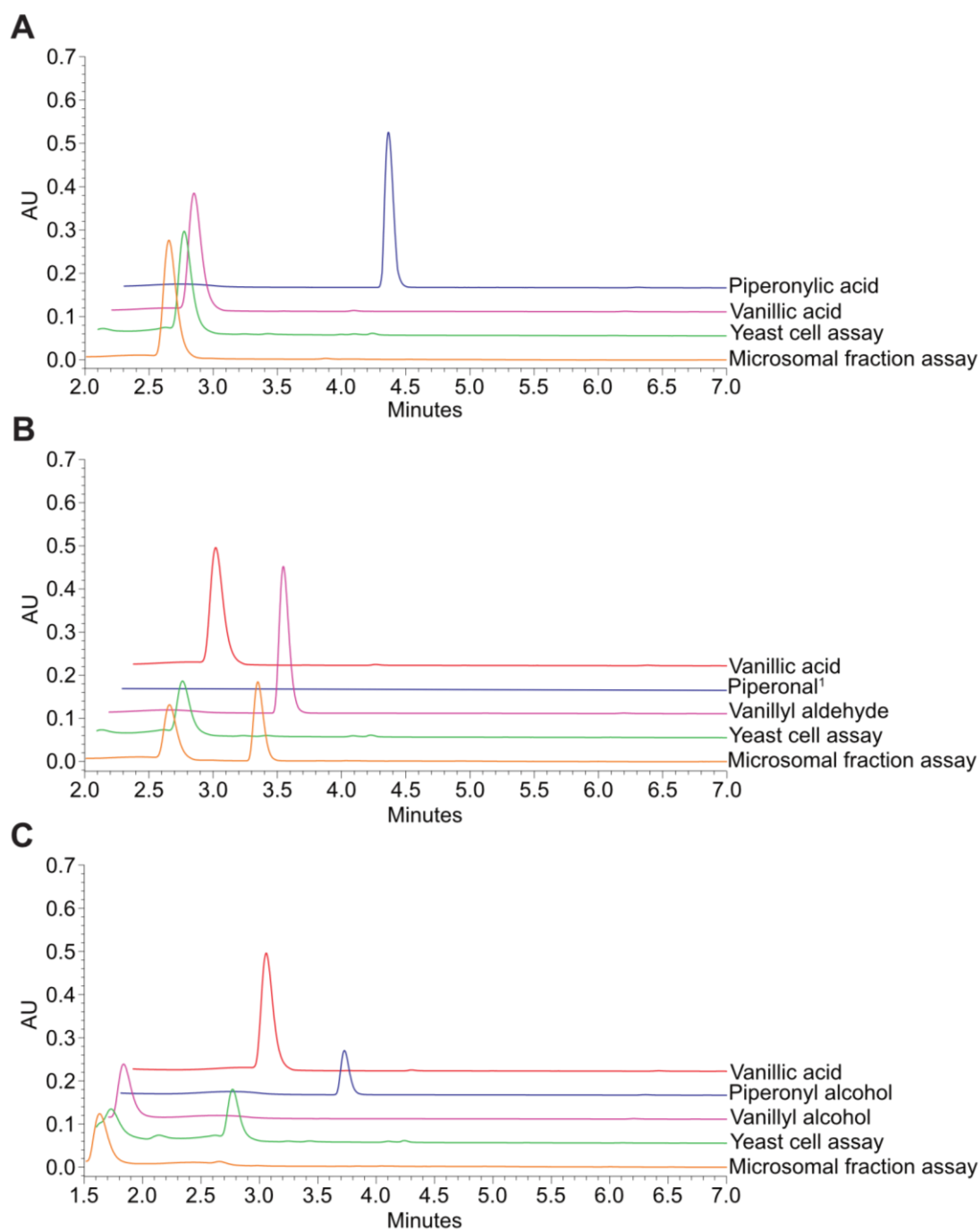


Figure 8-13: HPLC-analysis of microsomal fraction- and yeast cell assays with C6-C1 substrates

CYP719A37 and PnCPR were heterologously expressed in *S. cerevisiae*. Yeast cells or microsomal fractions were incubated with vanillic acid (**A**), vanillyl aldehyde (**B**) or vanillyl alcohol (**C**) for 24 h and the product formation was monitored. In the case of microsomal fractions, products were extracted with ethyl acetate, concentrated, re-dissolved in methanol and were analyzed by HPLC-UV-ESI-MS (orange). The supernatant from yeast cell assays was directly analyzed (green). The UV-signal was monitored between 225 – 400 nm and the masses between $m/z = 100 - 300 [M+H]^+$. Substrates are shown in magenta, products with a methylenedioxy bridge in blue, whereas unexpected products are marked in red. (¹ – Reference was not available)

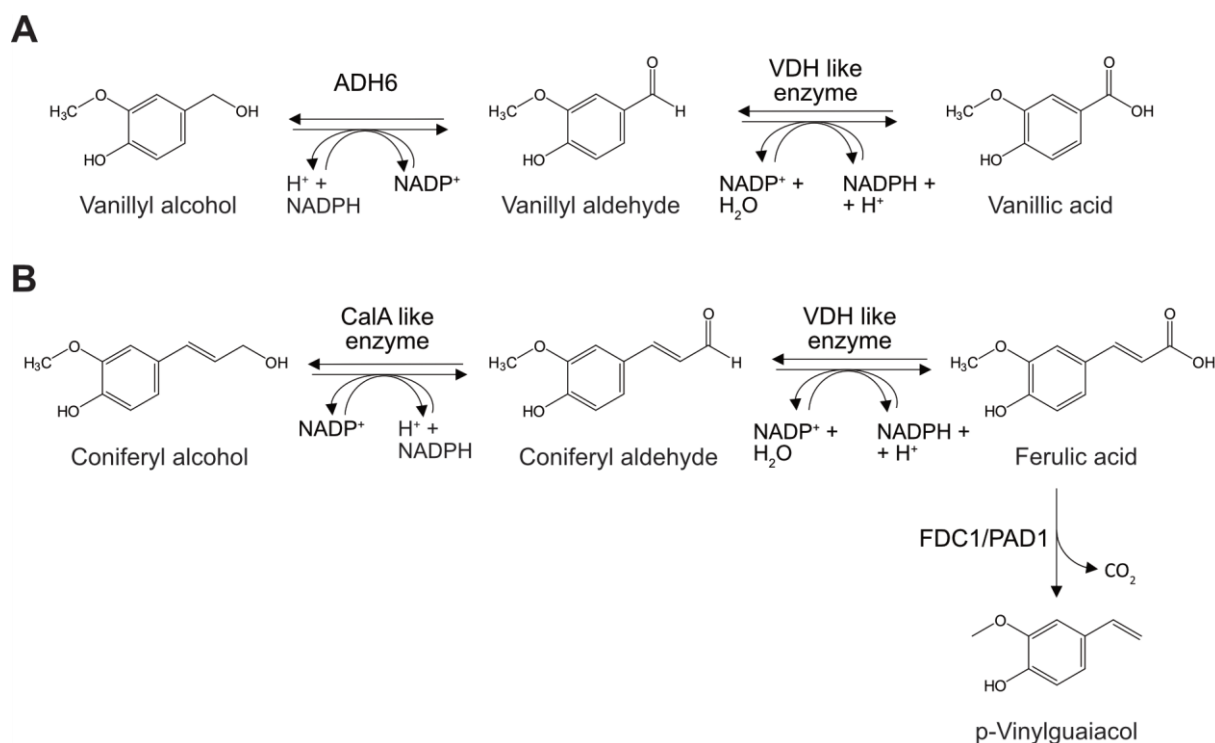


Figure 8-14: Detoxification mechanisms in the yeast *S. cerevisiae*

S. cerevisiae convert toxic phenolic compounds, especially vanillyl aldehyde or coniferyl aldehyde, into less cell inhibitory compounds. Aldehydes show a high chemical reactivity by forming Schiff bases and can inhibit enzymatic activities, which may result in toxic effects. **(A)** Vanillyl alcohol can be dehydrogenated by ADH6 (alcohol dehydrogenase) into reactive vanillyl aldehyde. A vanillin dehydrogenase like enzyme further oxidized vanillyl aldehyde into vanillic acid. **(B)** Coniferyl alcohol can be dehydrogenated by CalA like enzyme (*Candida antarctica* lipase A) into reactive coniferyl aldehyde, which is further oxidized. Ferulic acid can decarboxylated into p-vinylguaiacol by FDC1 (ferulic acid decarboxylase) (Lin et al., 2015).

CPR	(Pni)	MESGSSIDL	PLDLVAAILQ	G-----	KADASSLLSL	TRSTVSDNG	DLLVLLATSA
ATR1	(Ath)	-----	-----	---MTSALY	ASDLFKQLKS	IMGTDSLDD	VVLVIATSTL
ATR2	(Ath)	MSSSSSSSTS	MIDLMAAIK	GEPVIVSDPA	NASAYESVAA	ELSSMLIENR	QFAMIVTTSI
					::: .: .:	..: .: .:**	
FMN-PP_i-bs							
CPR	(Pni)	ALLVGLVAAL	VWRRSAAAR-	TAEPPKPLLA	KKEAEPE---	-VDDGKRV	VFFGTQTGTA
ATR1	(Ath)	ALVAGFVLL	WKKTADRSG	ELKPLMIPKS	LMAKDEDDL	DLGSGKTRV	IFFGTQTGTA
ATR2	(Ath)	AVLIGCIVML	VWRRSGSUNS	KRVEPLKPLV	IKPREE---	-IDDGRKRV	IFFGTQTGTA
		::: * .: *	: .:	: :	: :	: .: *	:****:
CPR	(Pni)	EGFAKAFAGE	AKARYEKAFF	RILDLDYYAA	DDDEYEEKMK	EETLAFFFLA	TYGDGPEPTDN
ATR1	(Ath)	EGFAKALSEE	IKARYEKAFF	KVIDLDYYAA	DDQYEEKK	KETLAFFFCVA	TYGDGPEPTDN
ATR2	(Ath)	EGFAKALGEE	AKARYEKTRF	KIVDLDYYAA	DDDEYEEKK	KEDVAFVFLA	TYGDGPEPTDN
		****:.*	*****:.	:::*****	****:.*	*:.*:*	:****:
FMN-isoallozazine bs							
CPR	(Pni)	AARFYKWFEE	GKDTGNFEEK	MQYGVFGLGN	ROYEHFNKIA	KVVDELLAEQ	GAKRLVPLGL
ATR1	(Ath)	AARFSKWFTE	ENERDIKLOQ	LAYGVFALGN	ROYEHFNKIG	IVLDEELCKK	GAKRLIEVGL
ATR2	(Ath)	AARFYKWFTE	GNDRGEWLKN	LKYGVFGLGN	ROYEHFNKVA	KVDDILLVEQ	GAQRLVQVGL
		*** **:*	::: .: .:	: ***:**	*****:.	*:*:*	::: **:*:*
substrate-bs							
CPR	(Pni)	GDDQCIEDD	FTAWRELIWP	ELDQLLRNED	DVSGASATYT	AAIPEYRVV	YDHEDSRIQE
ATR1	(Ath)	GDDQSIEDD	FNAWKESLWS	ELDKLLKDED	DKSVATP-YT	AVIPEYRVV	HDPR--FTTQ
ATR2	(Ath)	GDDQCIEDD	FTAWREALWP	ELDTILREEG	DTAVATP-YT	AAVLEYRVS	HDSEDAKEND
		****:****	*.*:*:	::: ***	:*:*:*	*: .: **	*: .: ****
CPR	(Pni)	KKNANGYANG	HASYDIQHPC	LANVAVRREL	HTPASDRSCT	HLEFDVSLGL	LHYETGDHVG
ATR1	(Ath)	KSMESNVANG	NTTIDIHPC	RVDVAVQKEL	HTHESDRSCI	HLEFDISRFG	IYETGDHVG
ATR2	(Ath)	ITLAN--GNG	YTVFDAQHPY	KANVAVKREL	HTPESDRSCI	HLEFDIAGSG	LTMKLGHDVG
		. . .*	: * :*	.:*:*:*	** *****	*****: *	: : *****
CPR	(Pni)	VYAENCIETV	EKAECLLGLS	PATIFSHTD	QVDGTPSLGS	FLPPFPSPC	SLRTALAKYA
ATR1	(Ath)	VYAENHVEIV	EEAGKLLGHS	LDLVFSIHAD	KEDGSPLESA	VPPP-FPGPC	TLGTGLARYA
ATR2	(Ath)	VLCDNLSETV	DEALRLDMS	PDTYFSLHAE	KEDGTPISSS	LPPP--FPPC	NLRTALTRYA
		* .:* *	::* **.*	*:*:*:	:::***:..:	* ** *	* .:*:***
CPR	(Pni)	DLSSPKKAA	LVALASYASE	PSEAKRLQFL	ASPSGKDEYS	QWIVANQRL	LEVMAEFPSPA
ATR1	(Ath)	DLNPPRKA	LVALAAYATE	PSEAEKRLHL	TSPDGKDEYS	QWIVASQRL	LEVMAEFPSPA
ATR2	(Ath)	CLSSPKKSA	LVALAAHASD	PTEAERLKL	ASPAGKDEYS	KWVVSQRSL	LEVMAEFPSPA
		*.:.**	*****:.*:	*:*:*:*	** *****	:*.*	***** *
FAD-PP_i-bs							
CPR	(Pni)	KPPLGVFFGA	IAPRLQPRYY	SISSPKVAP	TRIHVTCALV	YEPTPTGRIH	KGVCSTWMKN
ATR1	(Ath)	KPPLGVFFAA	IAPRLQPRYY	SISSQDWAP	SRVHVTALV	YGPTPTGRIH	KGVCSTWMKN
ATR2	(Ath)	KPPLGVFFAG	VAPRLQPRFY	SISSPKIAE	TRIHVTCALV	YEKPTGRIH	KGVCSTWMKN
		*****:.	:*****:*	*****:.	* .:*** ** *	*****	***** **
NADPH-ribose-bs (NRB)							
CPR	(Pni)	AVPQEESNC	SS-APISVRQ	SNFKLPMDS	LPVIMIGPGT	GLAPFRGFLQ	ERLALDAGF
ATR1	(Ath)	AVPAEKSHC	SG-APIFIRA	SNFKLPSMPS	TPVIMVGPPT	GLAPFRGFLQ	ERMALKEDGE
ATR2	(Ath)	AVPYEKSEKL	FLGRPIFVRQ	SNFKLPSDESK	VPIIMIGPGT	GLAPFRGFLQ	ERLALVESGV
		** *:* :	*:*	*****:	.: .:***	*****	**:*:
NRB							
CPR	(Pni)	NLGPVLFPG	CRNRKMDFIY	ENELNEFVEA	GVLSDLIVAF	SREGPTKEYV	CHKMAEKAVD
ATR1	(Ath)	ELGSSLLFFG	CRNRQMDFIY	EDELNNFVDQ	GVISELIMAF	SREGAQKEYV	CHKMMEKAAQ
ATR2	(Ath)	ELGPSVLFFG	CRNRMDFIY	EEELQRFVES	GALAEVAF	SREGPTKEYV	CHKMMDKASD
		:**::***	****:*****	*:*:*:*	*:***	:** *****	*** *:* :
NRB							
CPR	(Pni)	IWNMISQGGY	VYVCGDAKGM	ARDVHRALHT	IVQEQGSMDS	SKVESYVKNL	QMEGRYLDRV
ATR1	(Ath)	VWDLIKEEGY	LYVCGDAKGM	ARDVHRTLHT	IVQEQGVSS	SEAEAVKKL	QTEGRYLDRV
ATR2	(Ath)	IWNMISQGAY	LYVCGDAKGM	ARDVHRSHT	IAQEQGSMDS	TKAEGFVKNL	QTSGRYLDRV
		::*:.*	:*****	*****:***	*.***	.:*	:::. *:* *
CPR	(Pni)	W					
ATR1	(Ath)	W					
ATR2	(Ath)	W					
		*					

Figure 8-15: Amino acid sequence alignment of PnCPR with ATR1 and ATR2.

Boxes show conserved domains of eukaryotic cytochrome P450 oxidoreductases, like FMN-PP_i-, FMN-isoallozazine-, substrate-, FAD-PP_i-, and NADPH-ribose binding sites (bs). The protein sequences were aligned using CLUSTAL 2.1 Multiple Sequence Alignments. CPR: *Piper nigrum* (QQS74307); (ATR1: *Arabidopsis thaliana* (X66016); ATR2: *Arabidopsis thaliana* (X66017). The similarity is indicated by: asterisk – full conserved region; colon – strong similarity; period – weak similarity.

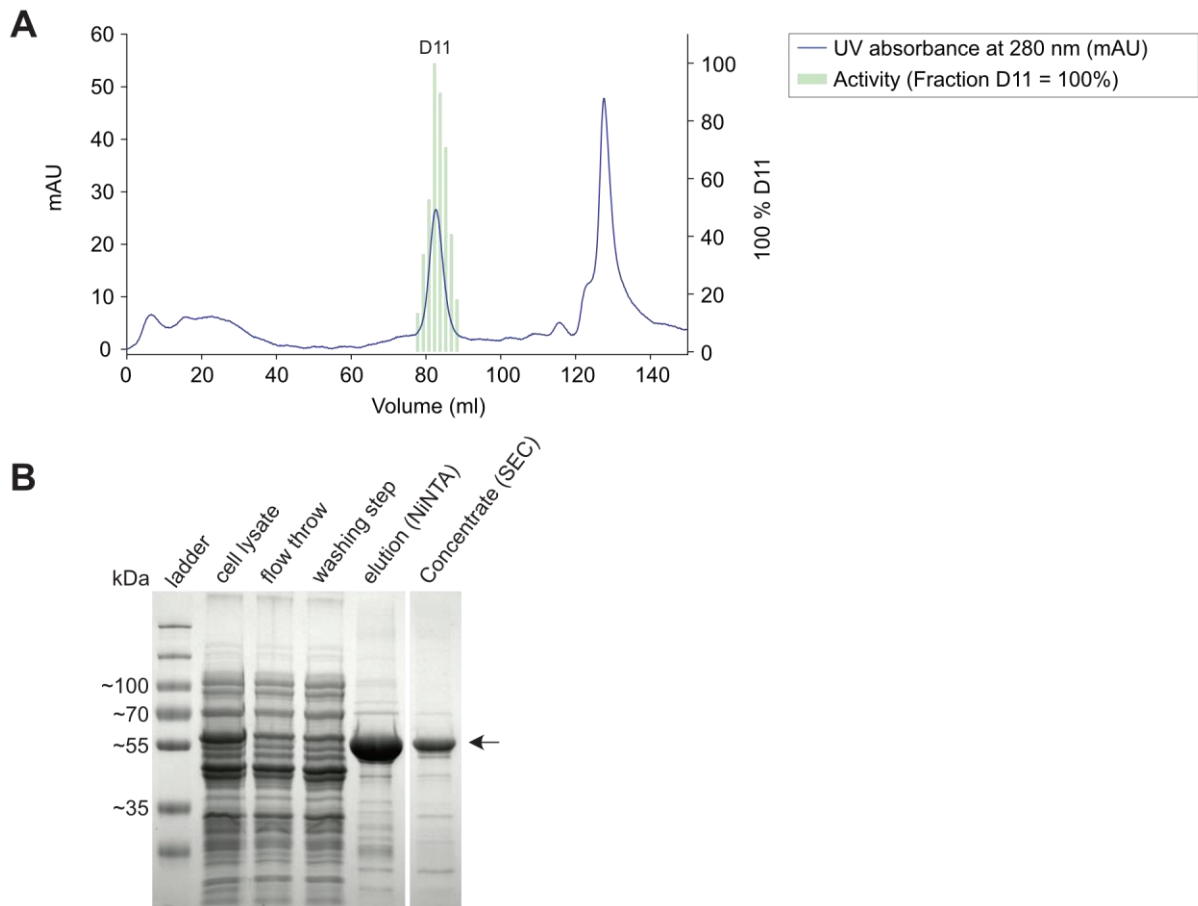


Figure 8-16: Preparation of recombinant piperoyl-CoA ligase by IMAC and SEC

The IMAC was done with a manual pump without a UV detector. Nevertheless, elution fractions were combined and applied on a HiLoad 16/60 Superdex 200 prep grade column (GE Healthcare). The elution profile of the SEC (**A**) and the corresponding SDS-PAGE (**B**) with selected samples are shown. Different fractions were tested for enzymatic activity. The highest activity was set 100% and is localized in fraction D11. The UV-absorption was measured at 280 nm (blue). The conductivity is marked in red. The increase of buffer B is marked with a green line. The activity of the corresponding fractions is shown in green bars. The cell lysate, the flow throw, and washing step of the IMAC, the elution of the IMAC and the combined fractions with high activity of the SEC were analyzed by SDS-PAGE, stained with Coomassie-Brilliant Blue and the expected protein size is marked with an arrow.

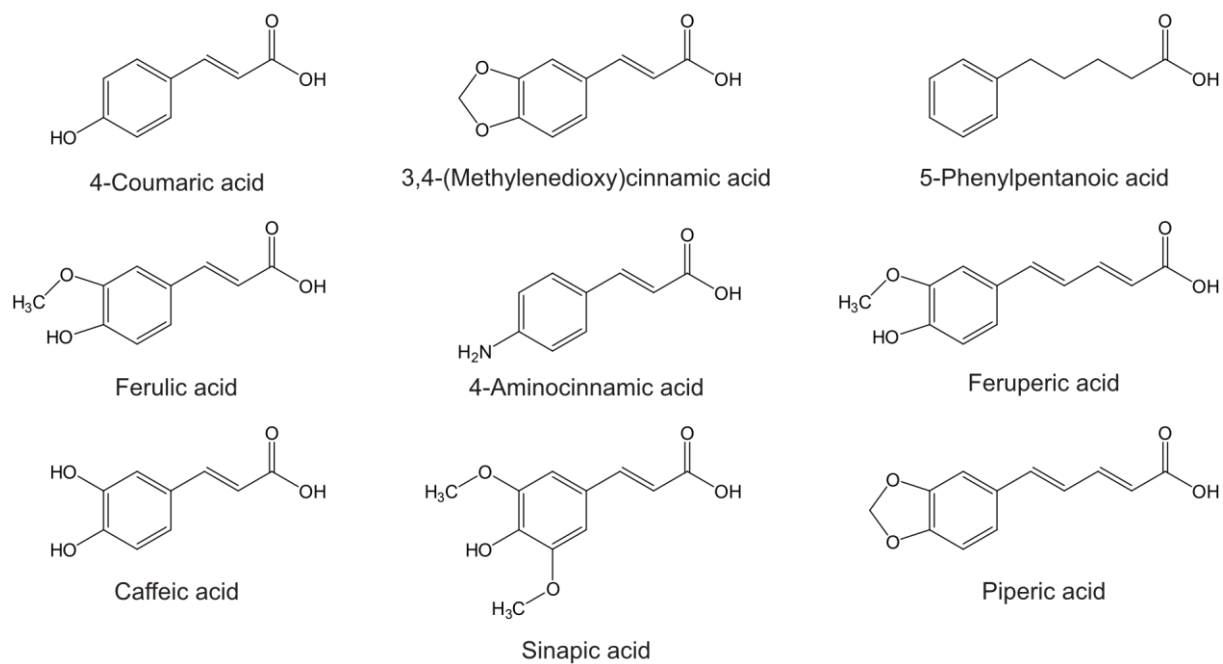


Figure 8-17: Different hydroxycinnamic acid derivatives as putative substrates for recombinant CoA ligases

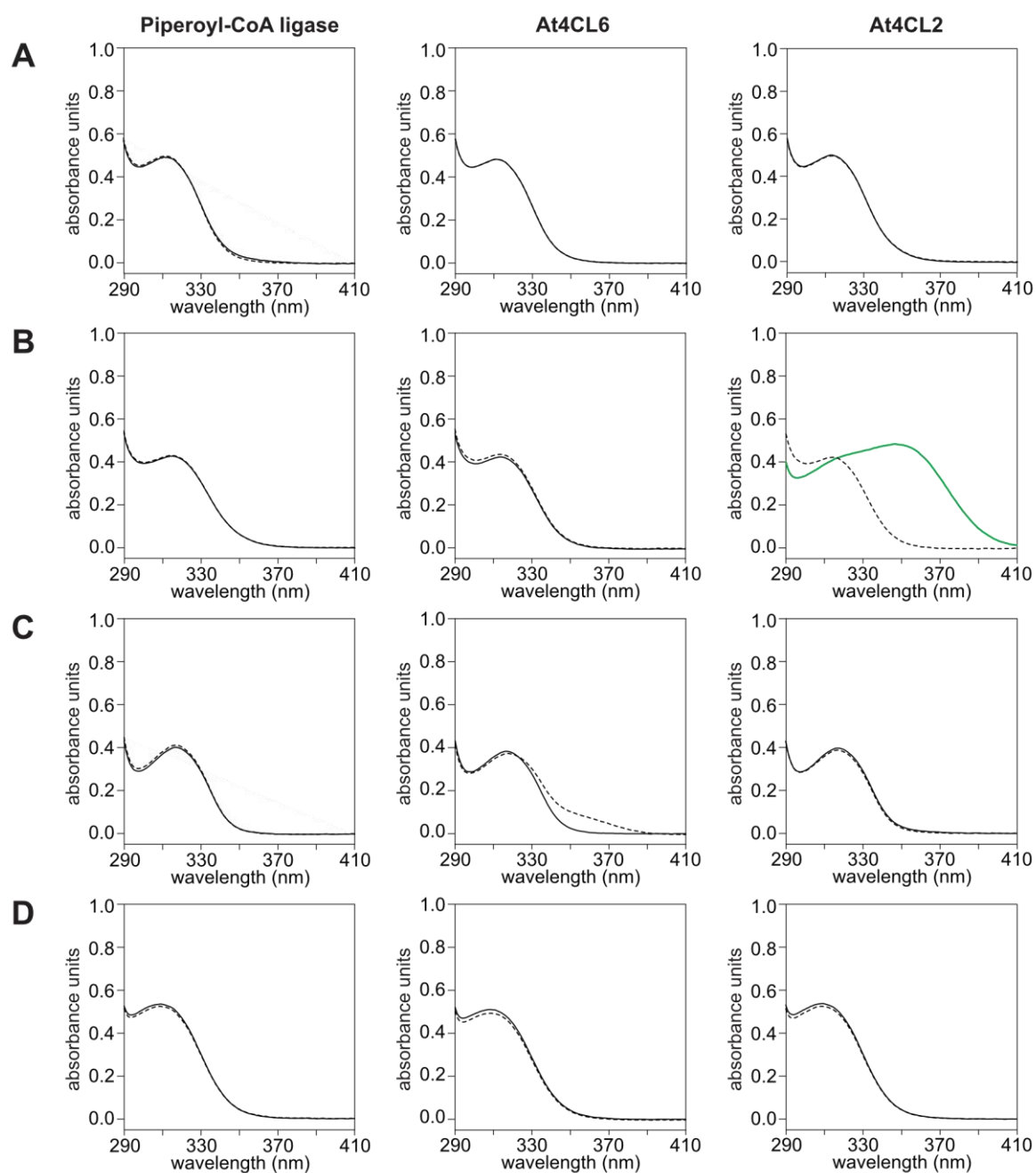


Figure 8-18: Absorbance spectra of Piperoyl-CoA ligase, At4CL6 and At4CL2 incubated with different substrates

The enzymes were incubated with different hydroxycinnamic acids (**A**) ferulic acid, (**B**) caffeic acid, (**C**) 3,4-(methylenedioxy) cinnamic acid, or (**D**) sinapic acid at 50 μ M for 1 h at 30 $^{\circ}$ C. The reactions were analyzed by a photometer recording the absorbance between 290 – 410 nm. A bathochromic shift of approximately 25 nm indicated CoA ester formation (Green). Solid line indicates active and dashed line indicates inactive enzyme.

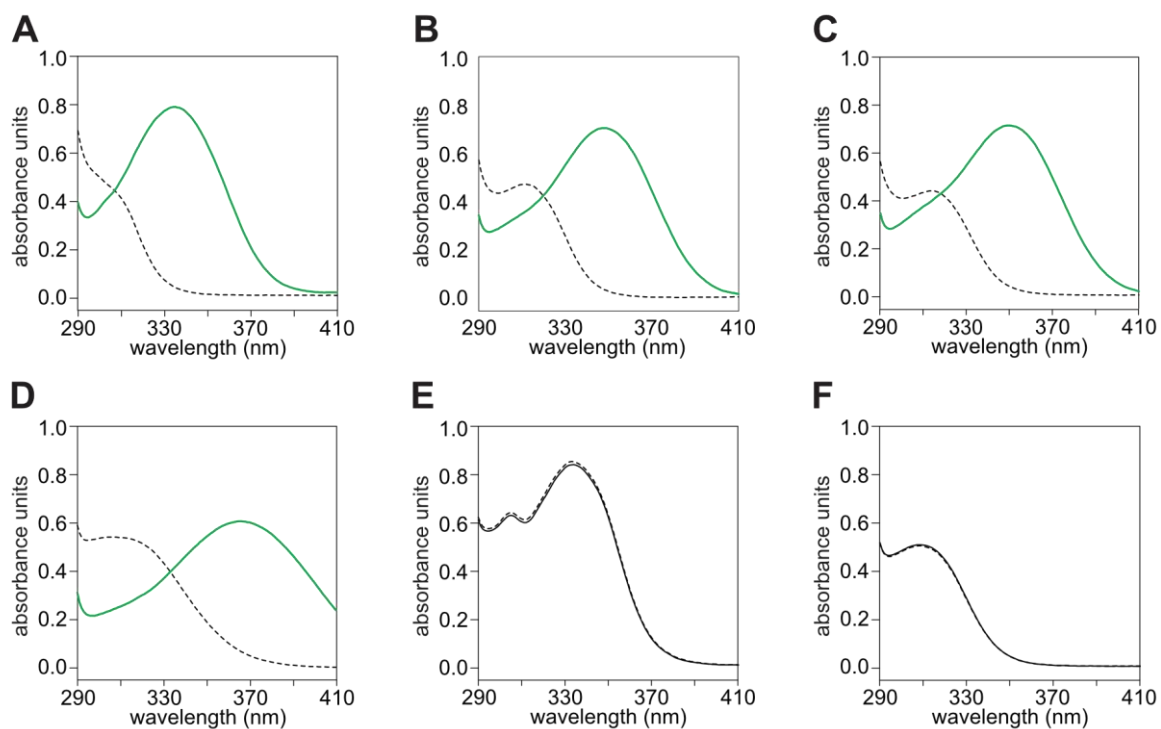


Figure 8-19: Absorbance spectra of *Piper nigrum* 4CL2 incubated with different substrates

The enzyme was incubated with different hydroxycinnamic acids (**A**) p-coumaric acid, (**B**) ferulic acid, (**C**) caffeic acid, (**D**) 4-aminocinnamic acid, (**E**) piperic acid, or (**F**) sinapic acid at 50 μ M for 1 h at 30 $^{\circ}$ C. The reactions were analyzed by a photometer recording the absorbance between 290 – 410 nm. A bathochromic shift of approximately 25 nm indicated CoA ester formation (Green). Solid line indicates active and dashed line indicates inactive enzyme. Slightly modified from a bachelor thesis by Raika Milde (IPB, 2019).

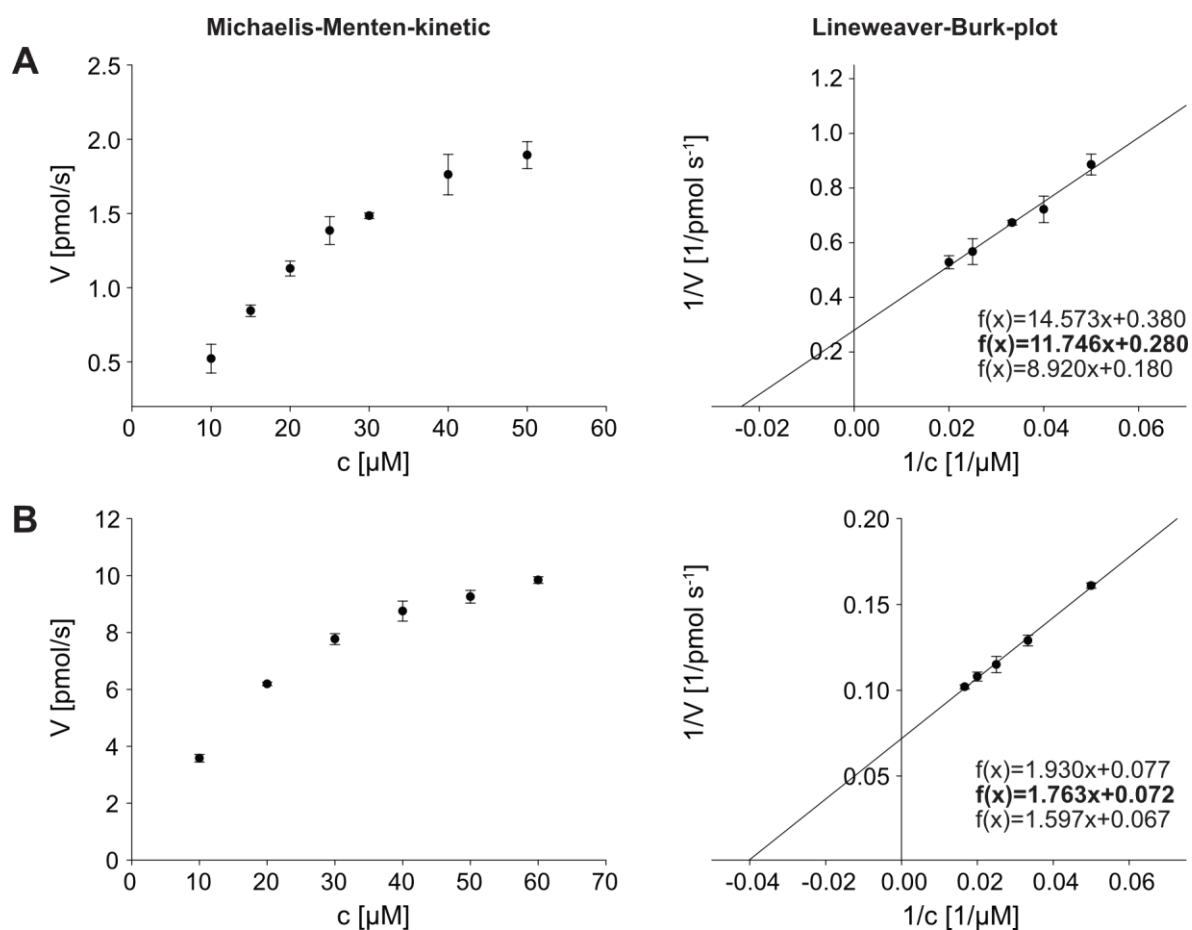


Figure 8-20: Kinetics of piperoyl-CoA with piperic acid (A) and 5-phenylpentanoic acid (B)

Apparent K_M data could be calculated for Piperoyl-CoA ligase between 10 and 60 μM of final piperic acid and 5-phenylpentanoic acid concentrations. Therefore Michaelis–Menten kinetics calculations and Lineweaver–Burk equation were used. Three independent data sets with three biological replicates were analysed.

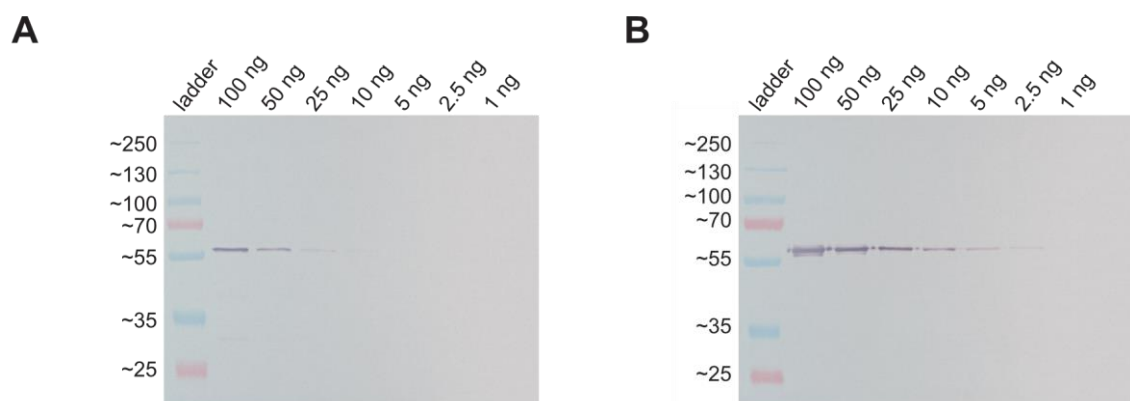


Figure 8-21: Specificity of anti-PAS-antibody against different concentrations of recombinant piperamide synthase (A) and recombinant piperine synthase (B)

9 Danksagung

"Keiner von uns ist so klug wie wir alle." – Kenneth H. Blanchard

Ich möchte mich zuallererst aus ganzem Herzen bei **Dr. Thomas Vogt** bedanken.

Insbesondere für sein herzliches Wesen, produktive Diskussionen, ein offenes Ohr gegenüber kreativen „Spinnereien“, Ideen, Rückhalt, Respekt, Vertrauen und dass er meinen Glauben an ein erfolgreiches Miteinander bestätigt hat.

Mein Dank gilt auch **Prof. Dr. Alain Tissier** und dem **Leibniz-Institut für Pflanzenbiochemie** für die Möglichkeit die Piperinbiosynthese zu bearbeiten

Der **Deutschen Forschungsgemeinschaft** möchte ich für die finanzielle Unterstützung dieses Projektes danken (VO 719/15-1 und 15-2).

Ebenfalls möchte ich **Prof. Dr. Dietrich Ober** für die Begutachtung meiner Arbeit danken.

Weiterhin bedanke Ich mich bei unseren technischen Mitarbeitern **Tim Bathe** und **Kerstin Manke** für tatkräftige Unterstützung und Zuarbeit im Labor. Tim optimierte die Expression der Piperin- und Piperamidsynthese in *E. coli*. Kerstin war von der ersten Stunde an in das Pfeffer-Projekt involviert und hat bei verschiedenen Experimenten mit Rat und Tat zur Seite gestanden. Ich bedauere sehr, dass wir dieses erfolgreiche Ende nicht mit ihr teilen können.

Meinen herzlichsten Dank geht auch an unsere begabten Nachwuchswissenschaftler, welche maßgeblich an diesem würzigen Projekt beteiligt waren oder sind: **Raika Milde**, die in ihrer Bachelorarbeit erfolgreich die Charakterisierung der Pn4CL2 vornahm, begleitet durch unser gemeinsam, täglich wachsendes Bild „Unter dem Meer“; **Luise Jäckel** – für Ihre Ausdauer und Sorgfalt bei der Lokalisation von Piperamid- und Piperinsynthese im schwarzem Pfeffer; **Sunita Shahi Khadgi** – für Ihre Arbeit zur Klonierung, Expression und ersten enzymatischen Tests der Piperin- und Piperamidsynthese sowie **Sunil Tripathee** – für die Klonierung der GGC-Konstrukte und der anfänglichen Expression der CYP719A37 in *N. benthamiana*.

Ich möchte mich auch sehr herzlich bei **Angela Schaks** und **Prof. Dr. Bernhard Westermann** für die Möglichkeit der chemischen Synthese von Piperoyl-CoA bedanken. Vor allem die Aufmerksamkeit, Geduld und Herzlichkeit beider brachte letztendlich den Erfolg in der Synthese als auch im Backen herausragender Florentiner. Gemeinsam mit **Thomas Eichhorn** und **Paul Jänicke**, beide mit hervorragenden Kenntnissen und Hilfestellungen zur organischen Chemie, wird mir auch unser erfolgreicher „Ausbruch aus Alcatraz“ noch lange im Gedächtnis bleiben. Desweiteren möchte ich auch **Andrea Porzel** für den Einblick in die NMR und ihre Hilfe bei der Auswertung der NMR-Daten danken.

Desweiteren gilt mein Dank **Prof. Dr. Fernando Cotinguiba**, der den Stein für das Projekt der Piperinbiosynthese ins Rollen brachte. Er unterstütze dieses Projekt mit der organischen Synthese von Feruperinsäure und Feruperin, welche essenzielle Substrate für einige Versuche waren.

Weiteren herzlichen Dank gilt **Prof. Dr. Milton Stubbs** und **Dr. Christoph Parthier**, welche mir für die Kristallisation der Piperamid- als auch Piperinsynthese ihre Räumlichkeiten und Geräte zur Verfügung stellten, als mich auch tatkräftig mit vielen Ideen, Hinweisen als auch Hilfestellungen unterstützten und voranbrachten. Desweiteren danke ich Prof. Dr. Milton Stubbs für die Begutachtung meiner Arbeit.

Ein besonderer Dank gilt **Frank Schumacher** vom Botanischen Garten in Wien, welcher uns an einer Raststätte in tiefster Nacht und am Bahnhof zur frühesten Morgenstunde sehr wichtige Pakete zuspielte – Pflanzenschnitte von einer blühenden und fruchtenden Pfefferpflanze aus Wien. Ohne ihn wäre das Projekt gescheitert. In diesem Zusammenhang gilt auch besonderer Dank unseren Gärtnern, vor allem **Petra Jansen**, **Sabine Voigt** und **Philipp Plato**, welche die sehr anspruchsvollen Pfefferpflanzen im wahrsten Sinne gehegt und gepflegt haben.

Desweiteren möchte ich mich bei vielen Experten bedanken, die meinen Horizont vorallem im Bereich der Methodik erweiterten und auf deren Expertise ich jeder Zeit zurückgreifen konnte: **Dr. Sylvestre Marillonnet** – Golden Gate cloning; **Dr. Gerd Hause** – Elektronenmikroskopie; **Hagen Stellmach** – allgemeine Mikroskopie, Lasermikroskopie; **Dr. Changqing Yang** – Virus induced gene silencing; **Dr. Wolfgang Brandt** – Protein modelling und **Dr. Ulschan Bathe** – Mikrosomenisolation.

Mein Dank gilt auch der gesamten Abteilung SZB für die anregenden Diskussionen, Ideen und die notwendige Zerstreuung. Besonders hervorheben möchte ich hier: **Henrikje Smits** - für die kreative Auszeit bei einem Poetry-Slam Workshop inklusive sehr erheiternden „Aggro“-stuhls, die quälenden Yoga-Stunden und mit welcher sich auch manches Pferd einfach stehen lässt; **Ramona Grützer** - welche eine wahre ARTistin, nicht allein in der Betalainbiosynthese und im GGC, ist; **Dr. Stephanie Werner** und **Kathleen Helmstedt** - für phänomenale nervenaufreibenden Tischkickerpartien, die letztendlich auch mit dem Instituts-„Meister“-Titel gekrönt wurden und **Ulrike Klauss** – welche unser Laborteam stets bereichert.

Mein herzlichster Dank gehört auch den Personen, die mich schon mein ganzes Leben auf meinem holprigen Weg unterstützt und die den Glauben an mich nie verloren haben, egal wie trüb die Sicht auch manchmal war – an **Iwona Schnabel-Thiemig**, die beste, freundlichste, stärkste und kämpferischste Mutti der Welt und an meine Großeltern **Christine** und **Christian Geithner**, die immer zu mir hielten und mir den Rücken stärken.

Ich möchte mich bei **Christin Köhler** für ihre Freundschaft und nötigen Rückhalt in vergangenen Tagen sowie für die Korrekturlesung bedanken.

Gemäß „das Beste kommt zum Schluß“ möchte ich mich bei meinem Lebensgefährten **Andreas Trummel** bedanken, dafür dass er jederzeit für mich da ist und mein Leben um so vieles bereichert. Oft waren es auch unsere „kreativen“ Gespräche über biochemischen Herausforderungen, welche unerwartet neue „Blickwinkel“ ergaben und so manches Mal einen Lösungsansatz brachten.

„Ich bin definitiv nicht so klug wie wir alle zusammen, aber sehr glücklich und stolz mit so einem großartigen Team zusammengearbeitet zu haben.“ – Arianne Schnabel

10 Eidesstattliche Erklärung

Hiermit erkläre ich, dass ich mich mit der vorliegenden wissenschaftlichen Arbeit erstmals um die Erlangung des Doktorgrades *Doctor rerum naturalium* (*Dr. rer. nat.*) bewerbe. Diese Arbeit wurde an keiner anderen Fakultät oder Universität zur Begutachtung eingereicht. Weiterhin erkläre ich, dass die Arbeit selbstständig und ohne fremde Hilfe angefertigt sowie alle Quellen und Hilfsmittel angefügt wurden. Von mir wörtlich oder inhaltlich entnommene Stellen wurden als solche gekennzeichnet. Die eingereichte schriftliche Fassung der Arbeit entspricht jener auf dem Speichermedium.

Basierend auf den Ergebnissen der vorliegenden Arbeit wurden aus Prioritätsgründen folgende Artikel bereits veröffentlicht sowie folgendes internationales Patent eingereicht:

Schnabel, A., Cotinguiba, F., Athmer, B., Yang, C., Westermann, B., Schaks, A., Porzel, A., Brandt, W., Schumacher, F., & Vogt, T. (2020). A piperic acid CoA ligase produces a putative precursor of piperine, the pungent principle from black pepper fruits. *The Plant Journal*, 102(3), 569-581. (DOI: 10.1111/tpj.14652)

Schnabel, A., Cotinguiba, F., Athmer, B., & Vogt, T. (2021). *Piper nigrum* CYP719A37 catalyzes the decisive methylenedioxy bridge formation in piperine biosynthesis. *Plants*, 10(1), 128. (DOI: 10.3390/plants10010128)

Schnabel, A., Athmer, B., Manke, K., Schumacher, F., Cotinguiba, F., & Vogt, T. (2021). Identification and characterization of piperine synthase from black pepper, *Piper nigrum* L. *Communications Biology*, 4(1), 1-10. (DOI: 10.1038/s42003-021-01967-9)

International patent application PCT/EP2020/060165 (issued 9 April 2020) with the title "Nucleic Acids, Proteins and Processes for Producing Amides" as **inventor**

Halle (Saale), den 30.06.2021



Arianne Schnabel

11 Curriculum vitae

PERSONAL INFORMATION

Birth date 22.10.1987
Maiden name Arianne Schnabel
Civil status single
Email arianne.schnabel@gmail.com

EDUCATION

PhD | 2021 (in completion)
 Leibniz Institute of Plant Biochemistry, Halle (Saale), Germany
 Thesis: Piperine biosynthesis in black pepper (*Piper nigrum*)
 Supervisor: PD Dr. Thomas Vogt

Master of Science| Sep 2014
 Biochemistry, Martin Luther University Halle-Wittenberg, Halle
 (Germany)
 Thesis: Reinigung und Charakterisierung von Proteinkomplexen mittels
 stabiler Protein-Ligand-Interaktion
 Supervisor: Prof. Dr. Milton T. Stubbs II

Bachelor of Science| Sep 2012
 Biochemistry, Martin Luther University Halle-Wittenberg, Halle
 (Germany)
 Thesis: Purification and Characterization of a component of the tripartite
 multidrug resistance transporter MdtEF-TolC from *Escherichia coli*
 Supervisor: Prof. Dr. Milton T. Stubbs II

Abitur| July 2007 Gymnasium Dresden-Cotta, Dresden (Germany)

RESEARCH EXPERIENCE

Doc. Researcher| Jan 2017 – present

Leibniz Institute of Plant Biochemistry, Halle (Germany)

Research Assistant| May 2015 – Dec 2016

Universitätsklinikum Carl Gustav Carus Dresden, Dresden (Germany)